

<b>REPORT DOCUMENTATION PAGE</b>	<b>1. REPORT NO.</b> NSF/RA-790720	<b>2.</b>	<b>3. Recipient's Accession No.</b> PB92 132101
<b>4. Title and Subtitle</b> Dynamic Response of Anisotropic Clay Soils with Applications to Soil Structure Analysis, 1979 Final Report			<b>5. Report Date</b> 1979
<b>7. Author(s)</b> A.S. Saada, PI, F. Moses, C.J. Miller, et al.			<b>6.</b> U328015
<b>9. Performing Organization Name and Address</b> Case Western Reserve University Department of Civil Engineering Cleveland, OH 44106			<b>8. Performing Organization Rept. No.</b>
<b>12. Sponsoring Organization Name and Address</b> Engineering and Applied Science (EAS) National Science Foundation 1800 G Street, N.W. Washington, DC 20550			<b>10. Project/Task/Work Unit No.</b>
<b>15. Supplementary Notes</b> Submitted by: Communications Program (OPRM) National Science Foundation Washington, DC 20550			<b>11. Contract(C) or Grant(G) No.</b> (C) (G) ENG7612332
<b>16. Abstract (Limit: 200 words)</b> Results of an investigation conducted primarily on cross anisotropic clays under small and large cyclic stresses are discussed. Experiments at small strains were conducted in the resonant column and those at large strains were conducted in a special pneumatic analog computer (SPAC) which applies to hollow cylinders of soil combinations of axial and torsional stresses. Under small strains, the effect on the moduli, represented by a modified Hardin and Black's equation, led to results which justify the use of non-linear theories in soil dynamics. Under large strains, the effects of one- and two-sided loadings were studied in axial and torsional modes. The shear modulus, its degradation, and damping were analyzed as a function of the level of stress and the cyclic number. The solution of a soil structure interaction problem was made possible by establishing a relation among the moduli of cross anisotropic saturated clays. The problem of the rigid circular plate resting on a cross anisotropic medium and subjected to sinusoidal loadings was solved in closed form. Examples using the design curves are given.			<b>13. Type of Report &amp; Period Covered</b>  Final
<b>COLOR ILLUSTRATIONS REPRODUCED IN BLACK AND WHITE</b>			
<b>17. Document Analysis a. Descriptors</b>			
Earthquakes		Torsion tests	
Determination of stress		Soil dynamics	
Cyclic loads		Clay soils	
Shear modulus			
<b>b. Identifiers/Open-Ended Terms</b>			
Special pneumatic analog computer			
SPAC			
<b>c. COSATI Field/Group</b>			
<b>18. Availability Statement</b>		<b>19. Security Class (This Report)</b>	<b>21. No. of Pages</b>
NTIS		<b>20. Security Class (This Page)</b>	<b>22. Price</b>



FINAL REPORT

THE DYNAMIC RESPONSE OF ANISOTROPIC CLAY  
SOILS WITH APPLICATIONS TO SOIL STRUCTURE  
ANALYSIS

By Adel S. Saada\*

**Any opinions, findings, conclusions  
or recommendations expressed in this  
publication are those of the author(s)  
and do not necessarily reflect the views  
of the National Science Foundation.**

\*Principal Investigator, Professor and Department Chairman  
Department of Civil Engineering  
Case Western Reserve University  
Cleveland, Ohio 44106





## PERSONNEL AND RELATED ACTIVITIES

### First Year:

Principal Investigator	Adel S. Saada
Co-Principal Investigator	Fred Moses
Graduate Students	Gary F. Bianchini David J. Kirkner
Machine Shop Technicians	

### Second Year:

Principal Investigator	Adel S. Saada
Co-Principal Investigator	Craig J. Miller
Graduate Students	Gary F. Bianchini David J. Kirkner Louise P. Shook

### Comments and Activities

- 1 - In spite of the fact that the revised proposal contained very little theoretical research goals, this aspect has been well served indeed and all of the aims of the grant reached.
- 2 - Except for computer time Mr. Kirkner did not receive any compensation from this grant.
- 3 - The Principal investigator attended an NSF/RANN meeting at the University of Texas and the International Conference on Soil Mechanics and Foundation Engineering in Japan; there he visited the Laboratories of Tokyo University, the Disaster Prevention Institute in Kyoto and the Port and Harbor Authority.



This report is in line with the modified work plan submitted with the supplement to the original proposal. Following the recommendations of the reviewers, and at the request of the National Science Foundation emphasis was to be placed on the experimental aspect of the research, with some analysis involved. All aspects have been covered, and the goals of the investigation reached.

The investigation has resulted in two doctoral dissertations and one Master's dissertation:

Doctoral Dissertation 1: "The Effect of Anisotropy and Strain on the Dynamic Properties of Clay Soils", by Gary F. Bianchini.

Master's Dissertation: "The Behavior of Clays Subjected to Slow Cyclic Loadings", by Louise P. Shook.

Doctoral Dissertation 2: "Steady State Response of a Circular Foundation on a Transverse Isotropic Medium", by David J. Kirkner.

Part I of this final report gives a "comprehensive summary" of the first doctoral dissertation. A copy of the detailed text will be forwarded to the National Science Foundation as soon as it is ready; in the very near future.

Part II is the integral text of the Master's Dissertation.

Part III is the integral text of the second Doctoral Dissertation.

Parts I and II are mostly experimental in nature and Part III analytical. The experiments in Part I were all conducted on thin long

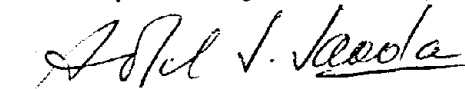
hollow cylinders in a modified Drnevich resonant column with the strains limited to the range attainable in this device. Those strains were below  $10^{-3}$ . Within the framework of the whole study those strains are referred to as small. However, within the framework of Part I, and the use of the resonant column,  $10^{-3}$  is considered a large strain compared to  $10^{-5}$  which the device is capable of measuring.

The experiments in Part II, i.e. in the Master's Dissertation, were all conducted in SPAC, a pneumatic analog computer capable of applying multidirectional states of stress in a slow cyclic way on thin long hollow cylinders.

The Doctoral Thesis in Part III is mathematical and solves the problem of the circular footing resting on a semi-infinite cross anisotropic medium and subjected to axial, torsional and rocking excitation. In this analytical study, some results obtained in the resonant column tests of Part I provided ample justification for the use of a simplifying relation which led to a closed form solution of a soil-structure interaction problem as of now unsolved. Thus, although the revised research proposal and the modified work plan did not intend to stress theoretical analysis, that aspect of the investigation has been very well served by this research.

All three parts will soon be prepared for publication in scientific and professional journals.

Respectfully submitted,



Adel S. Saada  
Principal Investigator

PART I

THE EFFECT OF ANISOTROPY AND STRAIN ON THE  
DYNAMIC PROPERTIES OF CLAY SOILS

(This is a comprehensive summary of the Thesis)

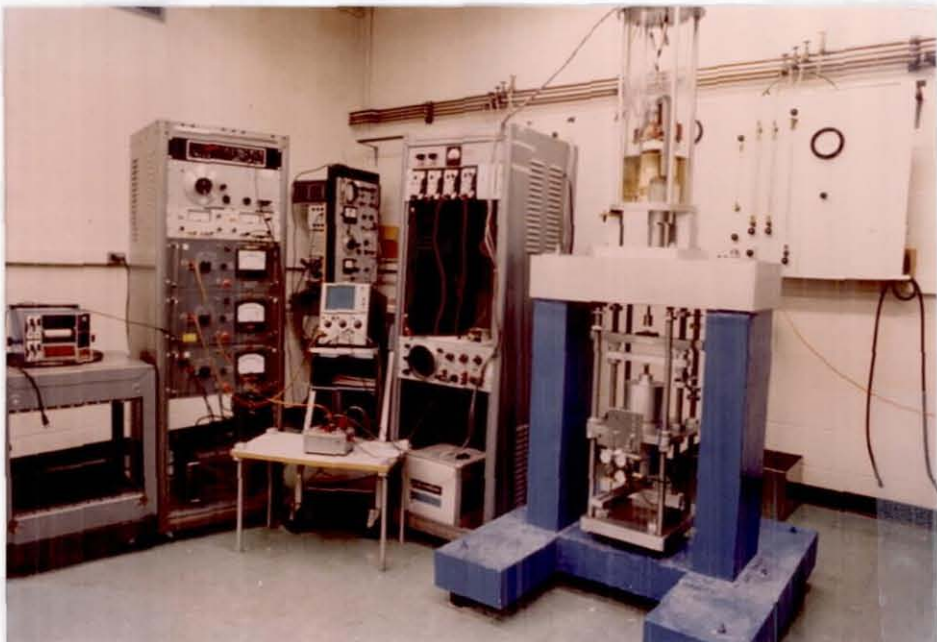


## TABLE OF CONTENTS

	Page
INTRODUCTION AND PRELIMINARY INFORMATION	1
TESTING EQUIPMENT, SAMPLES PREPARATION AND MATERIALS PROPERTIES	3
EFFECT OF THE WATER CONTENT ON THE MAXIMUM VALUE OF THE MODULI	5
EFFECT OF OVERCONSOLIDATION ON THE MAXIMUM VALUE OF THE MODULI	8
EFFECT OF LARGE DISTURBANCES ON THE MAXIMUM VALUE OF THE MODULI	10
EFFECT OF STRAIN ON THE MODUL	12
THE RAMBERG-OSGOOD REPRESENTATION	14
DAMPING	15
RELATION BETWEEN SHEAR MODULUS AND DAMPING RATIO	17
NON LINEAR BEHAVIOR	18
REPOSE CURVES	21
LAYERED SYSTEMS	22
CONCLUSIONS OF PART I	25
REFERENCES	27
FIGURES	28

## INTRODUCTION AND PRELIMINARY INFORMATION

The mechanical behavior of saturated clay soils has been intensively investigated in the last 25 years within a framework valid only for isotropic materials. It is only relatively recently that researchers have started thinking in terms of determining the mechanical properties of clays taking into account their natural structural and mechanical anisotropy. It is a well established fact that deposition, followed by one dimensional consolidation, arranges the clay particles and results in bonds such that the material acquires the property of cross anisotropy with the axis of symmetry along the direction of consolidation.

In a linearly elastic material the behavior is described by 5 constants. Following Lekhnitskii (8) the stress-strain relations are written (Fig. 1)

$$\begin{aligned}
 \epsilon_x &= \frac{1}{E} (\sigma_x - \nu \sigma_y) - \frac{\nu'}{E'} \sigma_z & \gamma_{xz} &= \frac{1}{G'} \tau_{xz} \\
 \epsilon_y &= \frac{1}{E} (\sigma_y - \nu \sigma_x) - \frac{\nu'}{E'} \sigma_z & \gamma_{yz} &= \frac{1}{G'} \tau_{yz} & \gamma_{\theta z} &= \frac{1}{G'} \tau_{\theta z} \\
 \epsilon_z &= -\frac{\nu'}{E} (\sigma_x + \sigma_y) + \frac{1}{E'} \sigma_z & \gamma_{xy} &= \frac{1}{G'} \tau_{xy} = \frac{2(1+\nu)}{E} \tau_{xy}
 \end{aligned} \tag{1}$$

$E$  and  $E'$  are the Young's moduli with respect to the direction lying in the plane of isotropy and perpendicular to it;  $\nu$  is the Poisson coefficient which characterizes the transverse reduction in the plane of isotropy for tension in the same plane;  $\nu'$  is the Poisson coefficient which characterizes the transverse reduction in the plane of isotropy for the tension in the directional normal to it;  $G'$  and  $G$  are the shear moduli for the planes normal and parallel to the plane of isotropy respectively. For a constant volume material  $\nu = 0.5$  and  $0.5 \frac{E}{E'} + \nu' = 1$ ; in this case, three measurements, namely those of  $E$ ,  $E'$  and  $G$  are

sufficient to describe the elastic response.

The Drnevich resonant column allows one to measure  $E'$  and  $G'$  on the same vertical specimen. It is of the fixed-free type and provides means to excite the specimen to resonance in the axial mode and in the torsional mode. This gives  $E'$  and  $G'$ .  $E$  is then measured on a horizontal specimen, which, in all respects, is identical to the vertical except that it is rotated 90 degrees.

Even under very small strain the response of clay involves a certain amount of material damping. This damping can be measured in the resonant column from the decay of the resonant strain amplitude or by the magnification factor method.

The resonant column can also be used to establish response curves for various levels of stress excitation. Such response curves are an excellent tool to investigate the validity of presently used models.

The theory behind the use of the resonant column and the various approximation it involves can be found in the soil dynamics literature. They will also appear in detail in the Doctoral Thesis of which this part of the report is a condensation (2).



## TESTING EQUIPMENT, SAMPLES PREPARATION AND MATERIALS PROPERTIES

The Drnevich resonant column was modified to accommodate thin, long, hollow cylinders and equipped with a central piston rod through the base plate. This rod moves along the axis of the hollow cylinder and can be fastened to the top cap with a bayonet type of lock. It is used to apply torsional and axial loads prior to the shaking of the specimen and is actuated by a pneumatic servomechanism programmed to maintain  $K_0$  consolidation conditions when desired. Axial and torsional motions at the top of the specimen are monitored by accelerometers.

To obtain cross anisotropic specimens clay slurries in a very fluid condition were consolidated in a large oedometer to a pressure high enough to allow for hollow circular cylinders to be trimmed from the resulting blocks. The vertical specimens (Fig. 1) were placed between two membranes. The cell's pressure was then slowly increased while the pneumatic servomechanism automatically applied the necessary axial force to maintain a  $K_0$  consolidation condition. After the final cell pressure was reached, enough time was allowed for complete equilibrium. The axial load was then released and the specimens allowed to rebound under the cell pressure  $\bar{\sigma}_c$ . This procedure, while resulting in a small overconsolidation in the vertical direction, gives a highly oriented clay fabric (9) and excellent reproducibility. Different final cell pressures and back pressures yielded different moisture contents.

The horizontal specimens that were tested in the resonant column were trimmed from clay blocks which had been subjected in the large oedometer to an axial pressure equal to the one indicated by the servomechanism during the one dimensional consolidations of the vertical specimens in the cell.

They were then placed in the cell and allowed to reach equilibrium under the effective pressure of the corresponding vertical specimen.

To obtain isotropic specimens the clay was hand mixed and kneaded with that amount of water which would give it the minimum stiffness compatible with the trimming and the placing of the hollow cylinders in the cells. It was stored for two weeks in a 100 percent humidity room. Trimming was followed by consolidation under the desired hydrostatic pressure and enough backpressure to insure saturation. In all cases the samples had an outer diameter of 2.8 in., and an inner diameter of 2 in. The length was approximately 5 in.

Two materials were used; a kaolinite clay known as Edgar Plastic Kaolin and an illitic clay known as Grundite. The first has a liquid limit of 56.3%, plastic limit of 37.5% and a specific gravity  $G_s$  of 2.62; the second has a liquid limit of 47.80%, a plastic limit of 24.96 and a specific gravity  $G_s$  of 2.7. A considerable amount of data on the static behavior of these clays has been published (10,11). A salient feature of  $K_0$  consolidated clays is that they behave totally differently in extension and compression. While such a behavior cannot be detected at the small strains involved in the resonant column it is very clearly seen at the larger strains reached in classical triaxial cells. Fig. 2 shows results of compression, extension and pure torsion tests on both  $K_0$  consolidated (anisotropic) clays and isotropic clays for two consolidation cell pressures (11). The anisotropic clay is more ductile in extension than in compression as well as much weaker.

EFFECT OF THE WATER CONTENT  
ON THE MAXIMUM VALUE OF THE MODULI

Each of the clays used gave a different water content for the same consolidation pressure. A straight line relation on a semi-logarithmic plot held true for all clays. This relation is represented by

$$W\% = C_1 + C_2 \log \bar{\sigma}_c, \quad (1)$$

where  $W$  is the water content,  $C_1$  and  $C_2$  constants and  $\bar{\sigma}_c$  the consolidation pressure. Each clay had its own  $C_1$  and  $C_2$ .

Similarly, each clay gives a different value of  $E$ ,  $E'$  and  $G'$  depending on the water content and the strain. Fig. 3 shows the variation of the moduli with the water content for the smallest strains obtained in this investigation. Such strains are in general close to  $2 \times 10^{-5}$  in the shear mode and  $0.15 \times 10^{-5}$  in the longitudinal mode. The relations look reasonably linear and, for the same water content, differences as high as 100 percent exist between isotropic and anisotropic clays.

In Fig. 4, the value of  $E$  for the anisotropic clay is compared to that of  $3G$ . The two should be equal for a constant volume material where  $\nu = 1/2$ . The values are practically identical. The assumptions that the volume is constant and that the clay-water acts like a single material are thus quite justified. Also plotted in Fig. 4 are the values of  $3G'$  for the two  $K_0$  consolidated clays. They lead to lines falling between those of  $E$  and  $E'$ . While for one clay the ratio  $\frac{E}{E'}$  decreases as  $W\%$  increases, it is the opposite for the other one. If one wishes to ignore anisotropy, three times the value of  $G'$  is a reasonably good approximation for  $E$  and  $E'$ .

A careful examination of the Hardin and Black equation (5) and an

analysis of its parameters in the light of the experimental data, led to the conclusion that it can adequately be used to predict the maximum values of the moduli for normally consolidated clays; provided its constant H is experimentally obtained. Thus

$$\frac{G_{\max}}{E_{\max}} = \frac{H_G}{H_E} \frac{(2.973 + e)^2}{1 + e} \left(\frac{\tau}{\sigma_c}\right)^{0.5} \quad (2)$$

where H is to be determined in the shear or the axial mode. Fig. 5 shows actual experimental data fitted with the Hardin and Black equation. The constant H is 1359 for the  $K_0$  consolidated Kaolinite and 1538 for the isotropic Kaolinite. While these values are different from the 1230 given by Hardin and Black, these differences are not as large as the one obtained with the Grundite clay; its value of H being 595 (1).

In the solution of the problem of wave propagation in elastic media, the elastic constants have often been assumed to be related to each other by the equation

$$G' = \frac{E}{\frac{E'}{4} - \frac{E}{E'}} = \frac{E'}{4 - \frac{E}{E'}} ,$$

for the constant volume materials (see Part III). The motivation for using this constraint appears to be the resulting mathematical simplifications.

From Eqs. 1 and the constant volume conditions we have

$$G = \frac{E}{4 - \frac{E}{E'}}$$

so that the assumption reduces to

$$\frac{G}{G'} = \frac{E}{E'}$$

Tabulated results in the Thesis (2) show that this relation is quite satisfactorily supported by the experimental data.

EFFECT OF OVERCONSOLIDATION  
ON THE MAXIMUM VALUE OF THE MODULI

All anisotropic specimens were prepared by  $K_0$  consolidation. Prior to testing, the vertical pressure in excess of the cell pressure was removed; so that there was a slight overconsolidation in the vertical direction compared to the lateral one. Additional overconsolidation was obtained by allowing the specimen to rebound under a reduced cell pressure. The overconsolidation ratio is defined in terms of mean (or octahedral) normal pressures.

With its overconsolidation term included, Hardin's equation is written

$$(\text{OCR})^K = \frac{G'_{\max}}{H F(e) \left(\frac{\bar{\sigma}_c}{\sigma_c}\right)^{0.5}} \quad (3)$$

For a constant  $H$  of 1359 previously obtained for  $K_0$  consolidated Kaolinite, for a plasticity index  $PI = 19\%$  ( $K=0.172$ ) and with the measured value of  $G'_{\max}$  one can compare the actual  $(\text{OCR})^K$  to that computed using the Hardin and Black equation. A large number of tests with three overconsolidation ratios and various cell pressures were conducted; the results of which appear in the following table:

OCR	$(\text{OCR})^K$ measured	$(\text{OCR})^K$ average	$(\text{OCR})^K$ from H & B
2.81	1.294 1.287 1.275	1.285	1.194
5.63	1.211 1.253 1.281	1.248	1.35
11.26	1.268	1.268	1.517

While the values obtained from the Hardin and Black equation increase, the experimental values slightly decrease or can simply be considered to be unaffected by the overconsolidation ratio.

Fig. 6 gives the relation between  $G'_{\max}$  and the water content for various overconsolidation ratios. Such curves are seen to be parallel to each other. Therefore, if one knows the relation for a normally consolidated clay and the value of  $G'_{\max}$  for another overconsolidation ratio and one water content, one can obtain the shear modulus for any other water content.

EFFECT OF LARGE DISTURBANCES  
ON THE MAXIMUM VALUE OF THE MODULI

The central piston rod through the base of the resonant column was used to apply to the top cap of the hollow cylinder axial and torsional deformations. One full cycle in either mode was usually applied with a period of approximately 30 seconds. Immediately after,  $E'_{max}$  and  $G'_{max}$  were measured and their value recorded as a function of time.

The table below shows the properties of the specimens on which the tests were conducted:

$\bar{\sigma}_c$ (Psi)	Compress. Strength $K_0$ CU	Tensile Strength $K_0$ CU	Pure Torsion $K_0$ CU
40	75.4 Psi	54.4 Psi	34.5 Psi
60	96.6 Psi	77.0 Psi	48.5 Psi
90	-	-	-

Various stress levels were applied and the moduli measured at frequent intervals. The pore water pressure increased monotonically and never dropped to zero even when the stress was removed. There always remained a residual pore pressure with the residual strain.

Fig. 7 shows  $\frac{G'_{max}}{(G'_{max})_{initial}}$  as the function of time for various values of

disturbing stresses (compare to the failure stress shown in the above table). The regain in  $G'_{max}$  is linear as a function of the logarithm of the time; but this regain did not show signs of ever becoming complete.



Fig. 8 shows similar results for  $\frac{E'_{\max}}{(E'_{\max})_{\text{initial}}}$ .

It is obvious that at least the pore water pressure and the permanent strain with the change in structure it involves are responsible for the lack of total regain of  $G'_{\max}$  and  $E'_{\max}$ . It was not possible to separate the 2 effects since opening the drainage would result in a change in the water content. Additional information and data can be found in the body of the thesis of which this is a condensed version.

## EFFECT OF STRAIN ON THE MODULI

Hardin and Drnevich (6) collected a large amount of data and suggested a hyperbolic relation between the shear modulus and the shear strain:

$$\frac{G}{G_{\max}} = \frac{1}{1 + \gamma} \quad (7)$$

where  $G$  is the secant modulus at a given strain and  $G_{\max}$  is obtained from the tangent at the origin of a stress-strain curve.  $G_{\max}$  was judged to be well represented by the values obtained in a resonant column for strains of the order of  $10^{-5}$ . Eq. 7 implies a finite negative slope at zero strain when the relation between  $\frac{G}{G_{\max}}$  and  $\gamma$  is drawn on a normal scale. Such a finite negative slope is in contradiction with the results of all the tests conducted in this investigation. The semi logarithmic representation which is very much in use results in a distortion of the graphs that makes it difficult to study their true shape at very small strain. On the other hand the Ramberg-Osgood representation allows for a zero slope at zero strain provided  $R > 2$ . Fig 9 shows the relations between the moduli  $E$ ,  $G$ ,  $E'$ ,  $G'$  for both  $K_0$  consolidation of pressures are illustrated in semi-logarithmic forms. Such graphs do not seem to contradict the general slopes published in the literature; but when the same data is plotted on normal scales, the curvatures for small strains are in the opposite direction.

Fig. 10 shows the normalized values of  $E'$  and  $G'$  versus strain on a normal scale for  $K_0$  consolidated anisotropic clay; Fig. 11 shows the normalized values of  $E$  and  $G$  for isotropic clay. Notice that in all cases the curves have a horizontal tangent near the zero strain. This as mentioned previously is in contradiction with much of the data accumulated by Hardin and Drnevich (6) and Hall (4). This point will be looked at in more detail in the section on nonlinear behavior.

It is believed that the large amount of data obtained in this investigation have reasonable weight when compared to the collection made by Hardin and Drnevich. The differences may have been caused by the differences in testing devices. The resonant column used in this investigation is a true fixed-free column and does not require assumptions or involved equipment calibration. Further comparative studies are suggested along this line.

While it is quite tempting to assume that the material behaves in the same way whether it is excited in the axial or the torsional mode, such an assumption would be totally unjustified. Figs. 9, 10, and 11 show that the strains investigated in the axial mode were about one order of magnitude smaller than those investigated in the shear mode. Cross anisotropic clay behaves totally differently in extension and in compression, and the difference becomes more noticeable (since it can be more easily measured) as the strains get larger. This will be shown very clearly in Part II of this report.

## THE RAMBERG-OSGOOD REPRESENTATION

The relation between the moduli and the strain can be expressed in terms of the Ramberg-Osgood equation. While other equations have been proposed, RO seems to be the most popular. It can be written in various forms depending on the variables to be represented. One form is

$$\frac{\gamma}{\gamma_r} = \frac{\tau}{\tau_r} \left[ 1 + \alpha \left| \frac{\tau}{\tau_r} \right|^{R-1} \right] \quad (4)$$

$\alpha$  and  $R$  are the RO constants and  $\gamma_r$  and  $\tau_r$  are reference shear strain and shear stress to be chosen in the most convenient way.  $\tau_r$  and  $\gamma_r$  have been chosen by Hardin and Drnevich as shown in Fig. 12 as  $\tau_r = \tau_{\max}$  and  $\gamma_r = \frac{\tau_{\max}}{G_{\max}}$ . Also the ratio  $\frac{\tau}{\gamma}$  can be replaced by  $G$  where  $G$  is the secant modulus, so that Eq. 4 can be written:

$$\frac{G}{G_{\max}} = \frac{1}{1 + \alpha \left| \frac{\tau}{\tau_{\max}} \right|^{R-1}} = \frac{1}{1 + \alpha \left| \frac{G}{G_{\max}} \frac{\gamma}{\gamma_r} \right|^{R-1}} \quad (5)$$

$\gamma_r$  will be chosen as  $10^{-4}$ , which means that  $\tau_{\max} = 10^{-4} G_{\max}$ .  $G$  and  $\gamma$  are experimentally obtained for various levels of excitations in the resonant column;  $G_{\max}$  corresponds to the smallest level. Equation 5 can be written:

$$\log \left[ \frac{G_{\max}}{G} - 1 \right] = \log \alpha + (R-1) \log \left| \frac{G}{G_{\max}} \frac{\gamma}{10^{-4}} \right| \quad (6)$$

Thus a plot on a double logarithmic paper yields  $\alpha$  and  $R$ . Values for  $\alpha$  and  $R$  will be given in the section on damping and its relation to the moduli. Similar equations can be written for Young's modulus  $E$ . If one deals with cross anisotropic materials, then depending on the direction of the shear and of the axial force on the specimen  $G$  and  $E$  are changed to  $G'$  and  $E'$ .

## DAMPING

Two methods are available for measuring damping in the resonant column: The logarithmic decrement method and the magnification factor method. For larger strains an average logarithmic decrement would give slightly erroneous results; the decaying amplitudes must be looked at two or three at a time. Both methods were used in this investigation with more weight given to the magnification factor method. Fig. 13 shows typical decay curves for small and large strain.

The strain in the longitudinal direction was much smaller than in the torsional direction because of the high axial rigidity of the specimen. Fig. 14 shows the damping ratio as a function of the strain, in the axial and the torsional directions, for anisotropic and isotropic materials; and for various consolidation pressure. One notices that there is practically no difference among the various consolidation pressures; i.e. the various water contents and that no significant feature differentiates the isotropic from the anisotropic clay. Dobry (3) refers to more than one mechanism coming into play and influencing the damping as the pressure varies. He refers to two private communications and presents data showing damping to first increase and then decrease as the consolidation pressure increases.

Another feature common to all the curves is the existence of a minimum damping  $\lambda_{min}$ . It is not known whether this damping is affected by the equipment or only due to the material. It varies however with the type of clay. The value for the Kaolinite varied between 1.35 and 1.6 and that for the Grundite varied between 2.08 and 2.12. Thus the total damping seems to be due to two components: one connected to the nonlinear force-displacement relations of the clay and the other, which shall be called  $\lambda_{min}$ , whose origins are not quite clear.

One way of normalizing damping data is to plot  $\frac{\lambda(\text{measured})}{\lambda_{\text{min.}}} \times \frac{\omega^2}{\omega_n^2}$

versus the strain. The ratio of the squares of the frequencies is equivalent to  $\frac{G}{G_{\text{max}}}$ . Fig. 15 shows graphs for both Kaolinite and illite clays; Graph (a), for kaolinite includes both normally consolidated and overconsolidated anisotropic material; Graph (b) for kaolinite involves normally consolidated isotropic material at various consolidation pressures; Graph (c) for illite involves normally consolidated anisotropic material. An examination of those three graphs shows that there does not seem to be much differences among normally consolidated, overconsolidated, isotropic and anisotropic clays; the values, however, vary from clay to clay; note the difference in slopes between the kaolinite and illite clays.

## RELATION BETWEEN SHEAR MODULUS AND DAMPING RATIO

Hardin and Drnevich (7) proposed a simple relation between the damping ratio and the shear modulus. Their equation is written

$$\lambda = \lambda_{\max} \left( 1 - \frac{G}{G_{\max}} \right) \quad (8)$$

If one takes into account  $\lambda_{\min}$ , a plot of a measure of the damping versus  $\left( 1 - \frac{G}{G_{\max}} \right)$  should therefore yield a straight line. Fig. 16 shows

$\left( \lambda_{\text{measured}} - \frac{\omega_n^2}{\omega^2} \lambda_{\min} \right)$  versus  $\left( 1 - \frac{G}{G_{\max}} \right)$ ; Fig. 16 (a) is a plot for anisotropic kaolinite, Fig. 16 (b) for isotropic kaolinite, Fig. 16 (c) for illite and Fig. 16 (d) for overconsolidated kaolinite. Such plots can be very adequately represented by straight lines showing that a relation of the type represented by Eq. 8 corrected for the effect of  $\lambda_{\min}$  would be quite adequate. The slope of those lines is related to  $\lambda_{\max}$ , or, as will be shown later, to the coefficient R of the Ramberg-Osgood equation.

## NONLINEAR BEHAVIOR

Clays are nonlinear materials of the strain softening type. They result in hysteresis loops whenever they are subjected to cyclic loading. Such loops seem to be independent of the rate of loading within a large range of frequencies. Tests in the resonant column result in strains falling within the nonlinear range. The strain response is not proportional to the excitation for a given frequency.

A model predicting the dynamic response "could" have in it a nonlinear spring and a dash pot whose equivalent viscosity coefficient is inversely proportional to the frequency; this characterises hysteretic damping. Static stress-strain curves are often represented by the Ramberg-Osgood equation and referred to as backbone curves. The hysteresis loops are built around those backbone curves with the loading and unloading parts following Masing's criteria.

An attempt to use nonlinear theory was made by Hall, but his data differed considerably from the predicted values. The curvature of the line expressing the variation of the resonant frequency with the strain did not fit the predictions of Pisarenko's work. Such predictions however agree reasonably well with the results obtained in this research. However, while Pisarenko used Davidenkov's formulation to express the stress-strain relations, Ramberg-Osgood's was used in this research; its flexibility has made it quite popular in recent years.

The governing differential equation is that of a material with hysteretic damping and nonlinear stiffness

$$M\ddot{x} + 2C\frac{\dot{x}}{x^y} + P(x) = F_0 \cos \omega t \quad (9)$$



which is non-dimensionalized to read (Fig. 17)

$$\frac{\ddot{x}}{x_y} + 2\lambda_{\min} \frac{\dot{x}}{x_y} + \frac{P}{P_y} \left(\frac{x}{x_y}\right) = \frac{F_o}{P_y} \cos \eta \tau \quad (10)$$

It is solved by the method of slowly varying parameters by assuming

$$\frac{x}{x_y} = \frac{x_o}{x_y} \cos(\eta \tau + \phi) \quad (11)$$

where  $\frac{x_o}{x_y}$  and  $\phi$  are the slowly varying parameters.

$P(x)$  = stress-strain loop of the Masing type

$$\eta = \frac{\omega}{\omega_n}$$

$\omega_n$  = natural frequency of small oscillations

$$\tau = \omega_n t$$

When averaged over the cycle the solution yields(7):

Response Curve

$$\eta^2 = \frac{\omega^2(x_o)}{\omega_n^2} = C(x_o) \pm \sqrt{\left(\frac{F_o}{P_y}\right)^2 \left(\frac{x_y}{x_o}\right) - \left[-S(x_o) + 2\lambda_{\min}\right]^2} \quad (12)$$

At Resonance

$$\frac{1}{2} \frac{F_o/P_y}{x_o/x_y} = \left[-\frac{1}{2} S(x_o) + \lambda_{\min}\right] \quad (13)$$

$$C(x_o) = \frac{\omega^2(x_o)}{\omega_n^2} \quad (14)$$

In the equations above,

$$\begin{aligned}
 S(x_0) &= \frac{x_y}{x_0} \frac{1}{\pi} \int_0^{2\pi} \frac{p}{p_y} \left( \frac{x_0}{x_y} \cos \theta \right) \sin \theta \, d\theta \\
 &= - \frac{\frac{4\alpha}{\pi} \left( \frac{R-1}{R+1} \right) \left( \frac{p_0}{p_y} \right)^{R+1}}{\left( \frac{x_0}{x_y} \right)^2} = - \frac{1}{2\pi} \frac{\Delta W}{\frac{1}{2} K_{\max} x_0^2} \quad (15)
 \end{aligned}$$

$$G(x_0) = \frac{x_y}{x_0} \frac{1}{\pi} \int_0^{2\pi} \frac{x_0}{x_y} (\cos \theta) \cos \theta \, d\theta \quad (16)$$

$\Delta W$  is the work done in a cycle (area of the loop),  $K_{\max}$  is the tangent modulus at the origin (Fig. 17) and  $\alpha$  and  $R$  are Ramberg-Osgood constants. For a linear system  $\alpha = 0$ ,  $S(x_0) = 0$ ,  $C(x_0) = 1$  and the equations reduce to those of the simple degree of freedom system.

Whether the above theory can be applied to clays or not can be checked by deducing the Ramberg-Osgood coefficients from the measured values of either the shear modulus or of the damping; both being functions of the strain amplitude. Therefore, one set of  $\alpha$  and  $R$  is obtained from the moduli versus strain curves at resonance and another set is obtained from the damping versus strain at resonance; the two sets should be identical if the theory applied to clay soils. Fig. 18 shows the measured and predicted values plotted as a function of strain. As one can see the differences are quite large. Additional curves for various values of the water content and different clays can be found in the thesis.

## RESPONSE CURVES

In the case of this research a response curve is a plot between the displacement and the frequency for a given excitation. It is clear from Fig. 18 that one set of  $\alpha$  and  $R$  is inadequate to fit resonance data and therefore could not predict response curves. A mixed approach was attempted and yielded good results:  $S(x_0)$  was determined using  $\alpha$  and  $R$  obtained from damping data fit and  $C(x_0)$  (in others words,  $\frac{G}{G_{max}}$ ) was determined using  $\alpha$  and  $R$  obtained from moduli data fit.

Fig. 19 shows the response for 2 low levels of excitation while Fig. 20 shows the response for levels 10 times higher.  $x_y$  is always chosen equal to  $10^{-4}$ ; the natural frequency is close to 75 Hz, and the clay is kaolinite at an effective hydrostatic pressure of 10 PSI and an overconsolidation ratio of 4. The solid lines are the predicted ones and the dots are experimental values. Agreement is quite reasonable leading to the conclusion that there is room for the theory above to be used in soil mechanics. Instability and jump phenomena were very clearly seen on the oscilloscope during the generation of the data points. It is therefore suggested that the resonant frequency be found going down along the frequency axis rather than going up since the two approaches lead to different results. Fig. 21 shows the displacement versus the excitation force for various values of the frequency; notice the instability for a frequency of 75 herz.

## LAYERED SYSTEMS

Soil masses are seldom homogeneous and layering is more the rule than the exception. Each layer may be homogeneous itself but is often cross anisotropic because of the sedimentation and  $K_0$  consolidation processes. It is of interest to study in the resonant column the variation of the natural frequency of a soil system as a function of the number of layers, their respective thickness and stiffness and the order in which they are with respect to the top mass. Can a rule of mixtures be justified and used?

Yang and Hatheway (13) tested layers of limestone and reached the conclusion that shear wave velocities determined in the laboratory were lower than those obtained in the field. However, the study does not seem to have been pursued further.

Combination of kaolinite and illite clays were used to make the layered system. Blocks of each were prepared in the large oedometer as explained at the beginning of this report. Sections of the proper dimensions were cut, fused together and hollow cylinders made. Further  $K_0$  consolidation of the hollow composite cylinders in the resonant column cell completed the fusion between the sections of the different materials. Changes in length of the elements of kaolinite and illite were simple to monitor with cathetometers since one clay is white and the other dark grey. The configurations shown in Fig. 22 were investigated. Each configuration was investigated at consolidation cell pressure of 40, 60 and 80 psi.

It happens that under the same consolidation pressure  $K_0$  the modulus of the kaolinite clay is about 60 percent larger than that of the illite clay. Thus the difference in stiffness will be well expressed by the results and not obscured by small experimental errors. The two materials have approximately the same mass density so that an average value was considered for the computations

( $2 \times 10^{-3} \text{ gr sec}^2/\text{cm}^4$ ), and of course the same polar moment of inertia ( $178 \text{ cm}^4$ ). Only very small vibrations were considered so that damping is at its minimum value and could be ignored in determining the natural frequency. This damping was about 2.1% for the illite and 1.65% for the kaolinite.

The ratio of the mass polar moments of inertia of the specimen  $I_s$  and the top cap  $I_t$  has a bearing on the determination of the resonant frequency. If  $\frac{I_t}{I_s}$  is small the relative position of the soil layers becomes unimportant. If  $\frac{I_t}{I_s}$  is large the recorded displacements are equal to those of a single degree of freedom system. Each layer is equivalent to a spring and,

$$\frac{1}{K_{eq}} = \sum_{i=1}^n \frac{1}{K_i} \quad (9)$$

where  $K_{eq}$  is the equivalent stiffness. In the present case  $\frac{I_t}{I_s} = 11$ .

The solution for finding the natural frequency of a two layer system with the boundary conditions of the resonant column can be found in the thesis. The single degree of freedom system can be applied by defining an equivalent stiffness (Eq. 9) and an equivalent moment of inertia equal to the inertia of the top cap plus one third of the inertia of the rod specimen. The natural frequency of the system would then be given by

$$\omega_n = \sqrt{\frac{K_{eq}}{I_{eq}}} \quad (10)$$

Three and multilayer systems solutions are also presented in the thesis together with cases where there is no top mass.

The approximate equations (9) and (10) were used to calculate natural frequencies of two and three layer systems knowing the properties of their components. Those natural frequencies were also measured experimentally.

Fig. 23 shows two graphs of measured versus predicted values for torsional and axial modes. Three values of  $\bar{\sigma}_c$  are involved, namely 40, 60 and 80 psi. The points fall close or within the 10% lines and the prediction appears to be quite satisfactory.

## CONCLUSIONS OF PART I

It was experimentally established that for the same water content the moduli of a cross anisotropic clay can vary very substantially (as much as 100%) from those of isotropic clay. Each can be represented by a Hardin and Black equation provided the constant  $H$  is changed from clay to clay. It is to be remembered that under the same consolidation pressure an isotropic and an anisotropic clay will yield totally different moisture contents.

Large disturbances were found to decrease the value of the moduli. While time restored some of the lost values one hundred percent recovery is not to be expected. Both the change in structure and the generation of pore water pressures are responsible for this permanent loss.

The variation of the moduli with strain can be well represented by a Ramberg-Osgood model. The hyperbolic model was found to be invalid because of the finite negative slope required for very small strains; and the fact that all the data points recorded resulted in a curve of shear modulus versus strain with a curvature in a direction opposite to that given by the hyperbola.

There was not much difference in damping characteristics between isotropic and anisotropic clays but each clay had a minimum amount of damping which varied from clay to clay. The relation between the damping and the shear modulus given by Hardin and Drnevich can be used for anisotropic as well as for isotropic clays provided it is corrected for the value of the minimum damping.

An attempt was made to use a model with a nonlinear spring and hysteretic damping to represent this clay. A backbone curve represented by a Ramberg-Osgood equation and a hysteresis loop of the Masing type were part of the solution. It was shown that the shear moduli predicted using measured values of damping differed substantially from the experimentally determined ones; and vice versa.

However, when Ramberg-Osgood coefficients were obtained from combined measurements of moduli and damping, predicted response curves agreed quite well with measured ones. The instability associated with nonlinear behavior of strain softening material was very much put in evidence.

Finally experiments on layered systems led to the conclusion that an equivalent stiffness of the layers could be defined leading to predicted natural frequencies very close to the measured ones.



## REFERENCES \*

- 1 Anderson, D. G., "Dynamic Modulus of Cohesive Soils", thesis presented to the University of Michigan, 1974, in fulfillment of the requirements for the degree of Doctor of Philosophy.
- 2 Bianchini, G. F., "Effects of Anisotropy and Strain on the Dynamic Properties of Clay Soils", thesis to be presented to Case Western Reserve University, in preparation.
- 3 Dobry, R., "Damping in Soils: Its Hysteretic Nature and the Linear Approximation", Research Report R70-15, Dept. of Civil Engineering, Massachusetts Institute of Technology, 1970.
- 4 Hall, J., "Effect of Amplitude on Damping and Wave Propagation in Granular Materials", thesis presented to the University of Florida, 1962, in partial fulfillment of the requirements for the degree of Doctor of Philosophy.
- 5 Hardin, B. O. and Black, W. L., "Vibration Modulus of Normally Consolidated Clay", Journal of the Soil Mechanics and Foundations Divisions, ASCE, Vol. 94, No. SM2, March, 1968.
- 6 Hardin, B. O. and Drnevich, V. P., "Shear Modulus and Damping in Soils; Measurement and Parameter Effects", Journal of the Soil Mechanics and Foundations Division, ASCE, Vol. 98, No. SM6, June, 1972.
- 7 Jennings, P. C., "Equivalent Damping for Yielding Structures", Journal of the Engineering Mechanics Division, ASCE, Vol. 94, No. EM1, Feb., 1968.
- 8 Leknitskii, S. G., Theory of Elasticity of an Anisotropic Elastic Body, Holden Bay, San Francisco, California, 1963.
- 9 Martin, R. T. and Ladd, C. C., "Fabric of Consolidated Kaolinite", Clays and Clay Minerals, Vol. 23, 1975, pp 17-23.
- 10 Saada, A. S. and Ou, C. D., "Strain-Stress Relations and Failure of Anisotropic Clays", Journal of the Soil Mechanics and Foundation Division ASCE, Vol. 99, No. SM12, 1973, pp 1091-1111.
- 11 Saada, A. S. and Bianchini, G. F., "Strength of One Dimensionally Consolidated Clays", Journal of the Geotechnical Engineering Division, ASCE, Vol. 101, No. GT11, pp 1151-1164, Nov., 1975.
- 12 Saada, A. S., Bianchini, G. F., and Shook, L. P., "The Dynamic Response of Normally Consolidated Anisotropic Clay", Proceedings of the 1978 ASCE Specialty Conference on Earthquake Engineering and Soil Dynamics, Pasadena, California.
- 13 Yang, Z. and Hatheway, A. W. "Dynamic Response of Tropical Marine Limestone", Journal of The Geotechnical Engineering Division, ASCE, Vol. 102, No. GT2 Feb., 1976.

\* A complete bibliography will be included in the thesis.

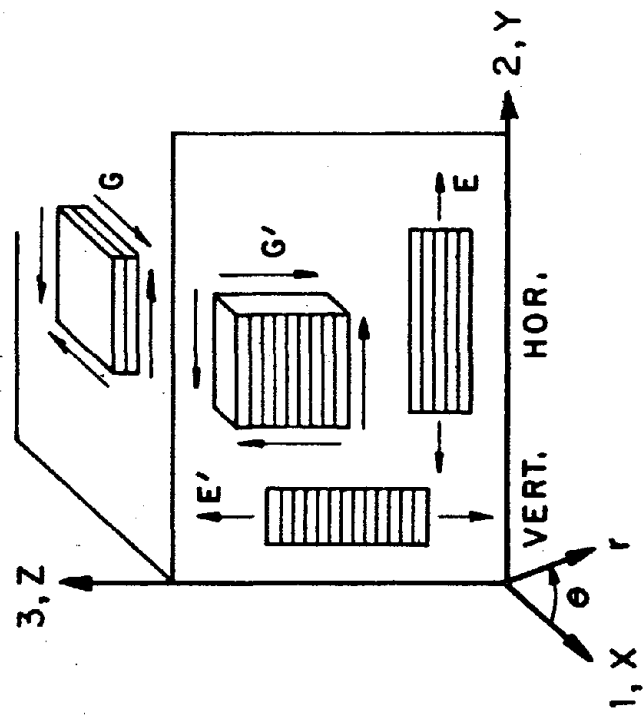


Fig. 1 System of Coordinates and Moduli

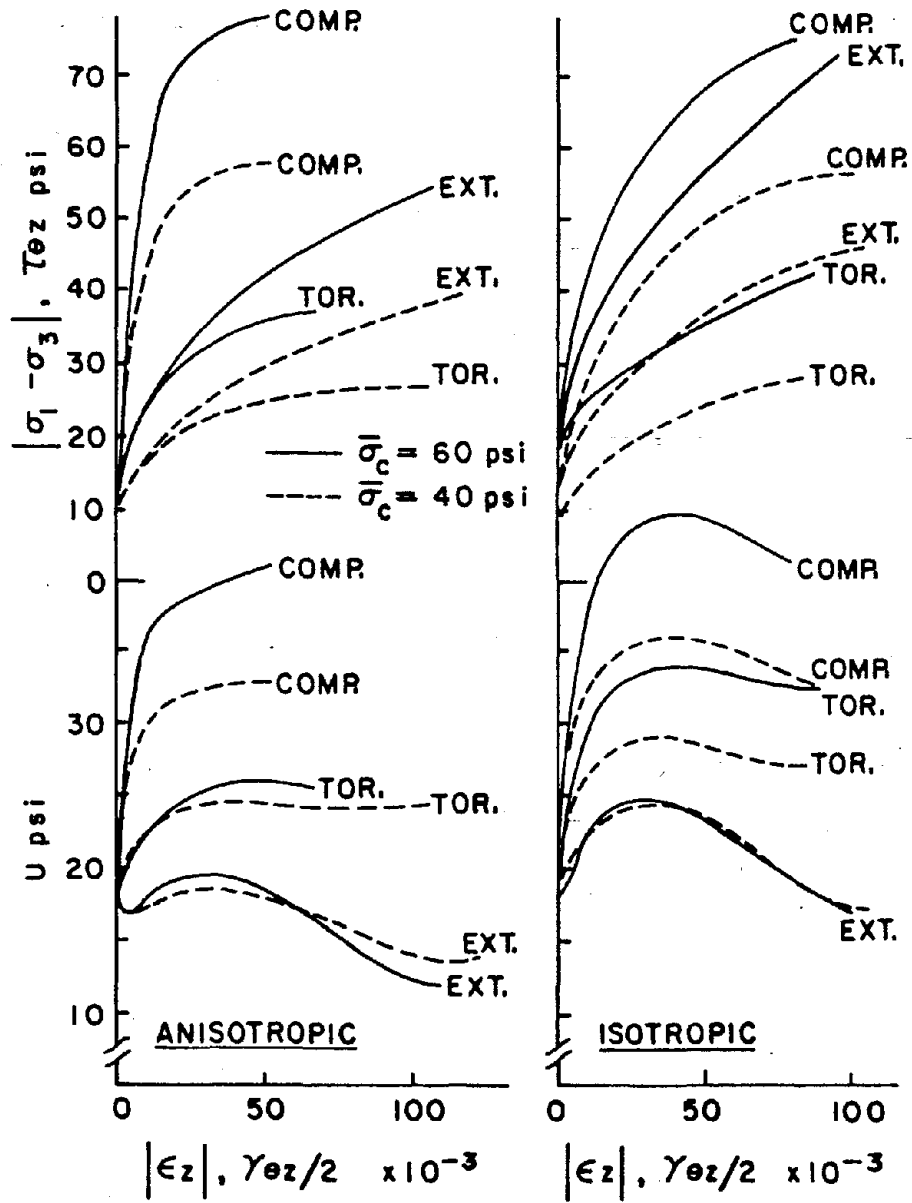


Fig. 2 Stresses, Strains and Pore Pressures from Static Tests

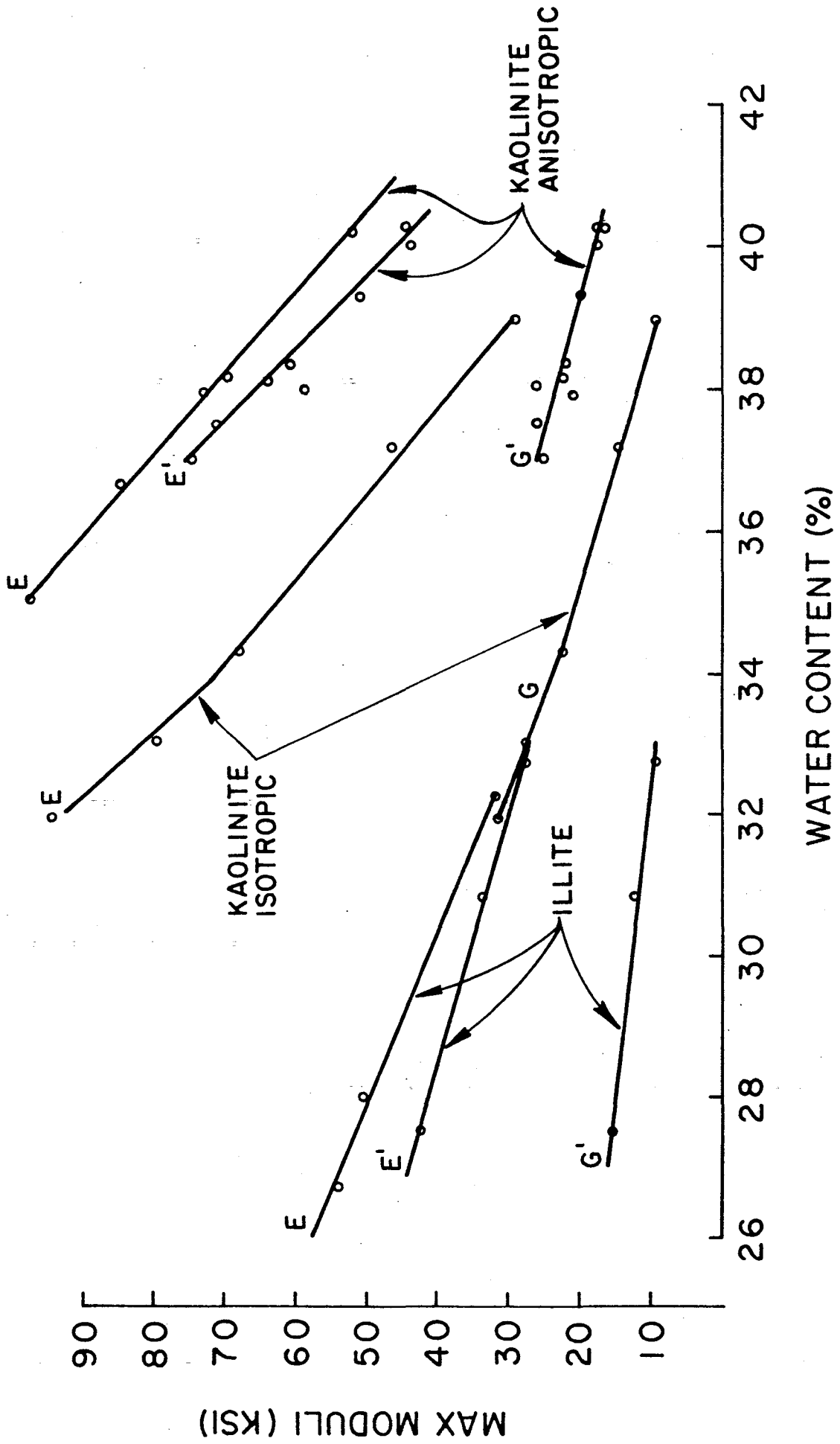


Fig. 3 Variation of the Moduli with the Water Content

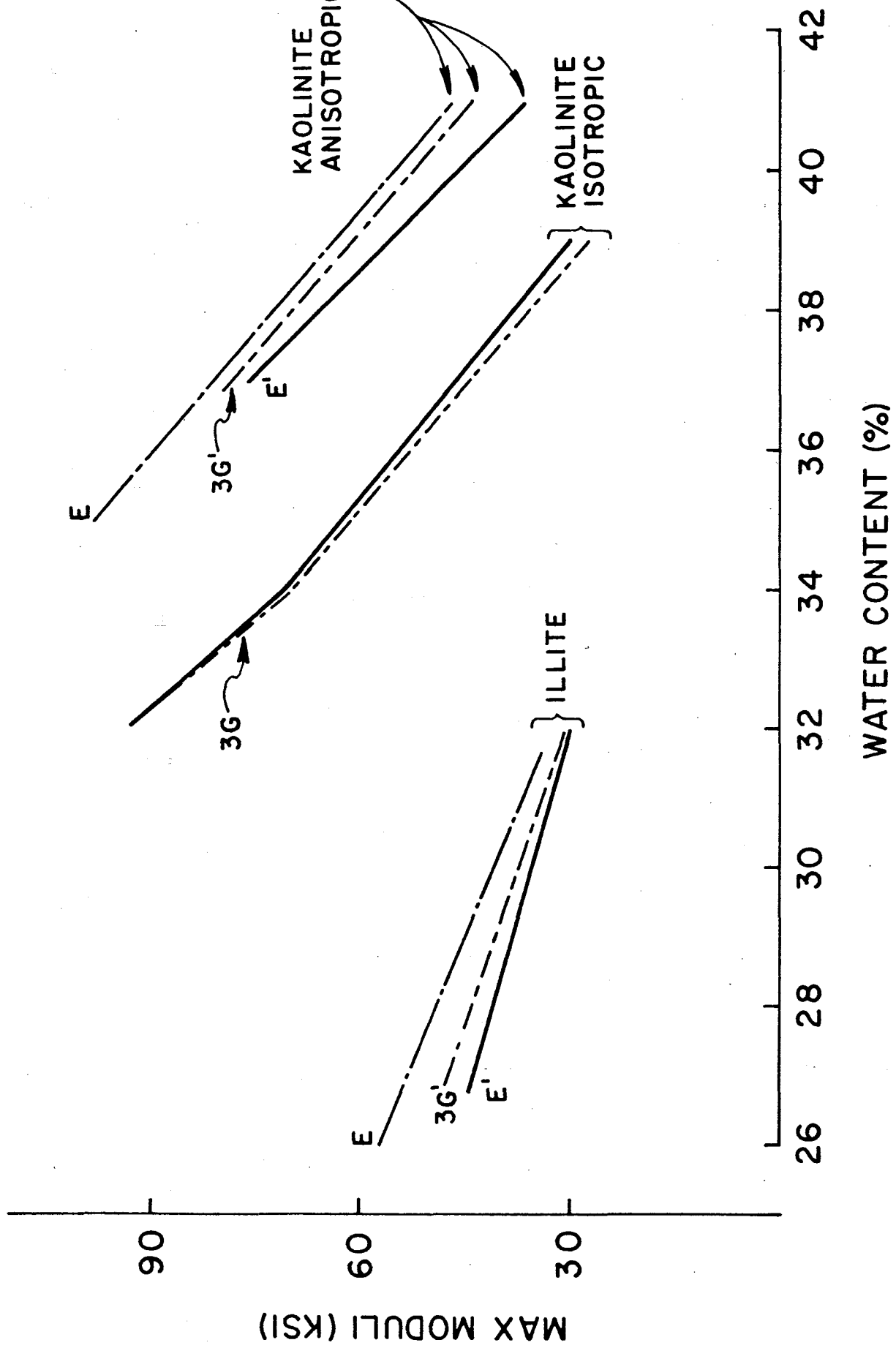


Fig. 4 Relations among Moduli for Constant Volume Clays

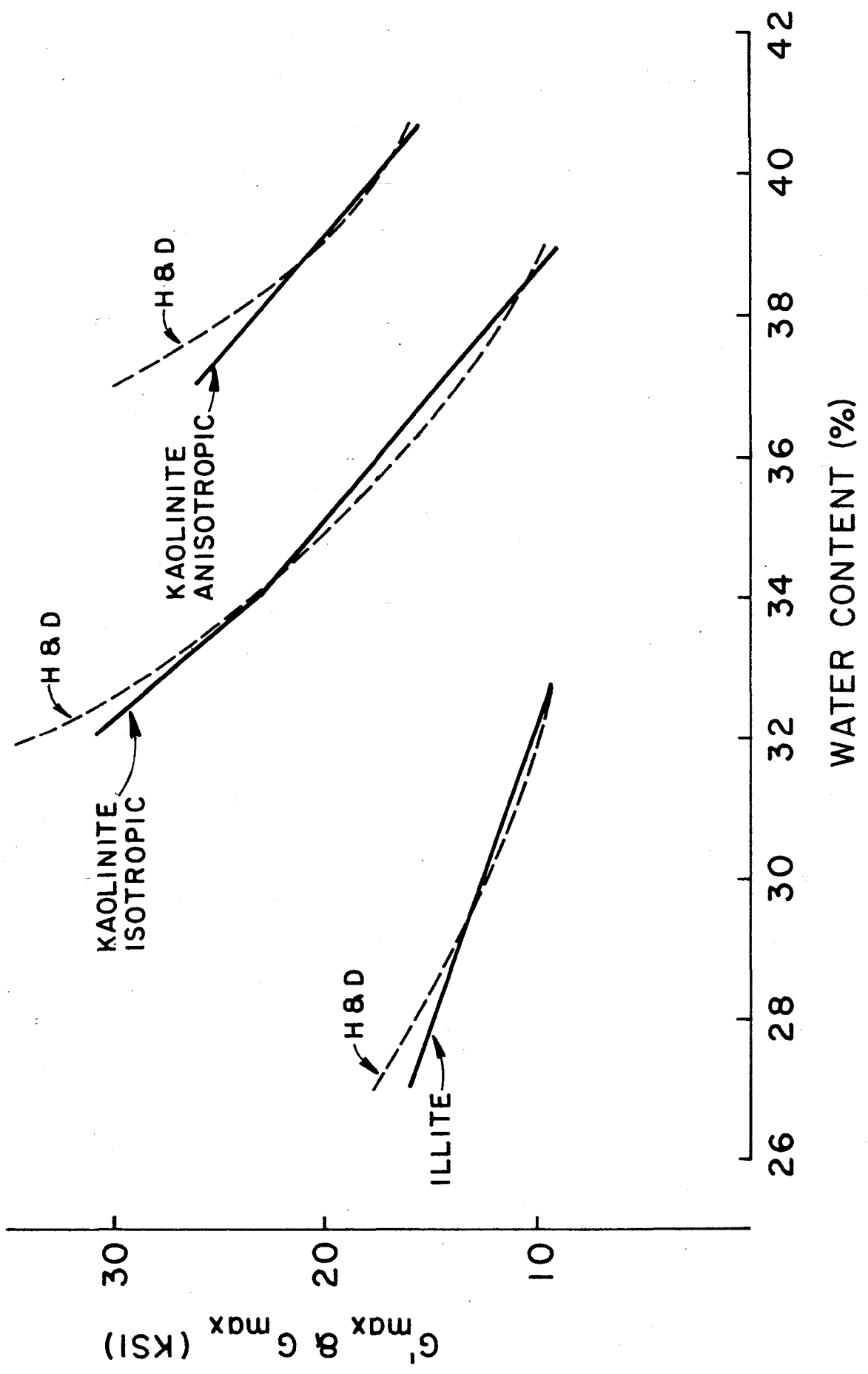


Fig. 5 Curve Fitting with Hardin and Black's Equation

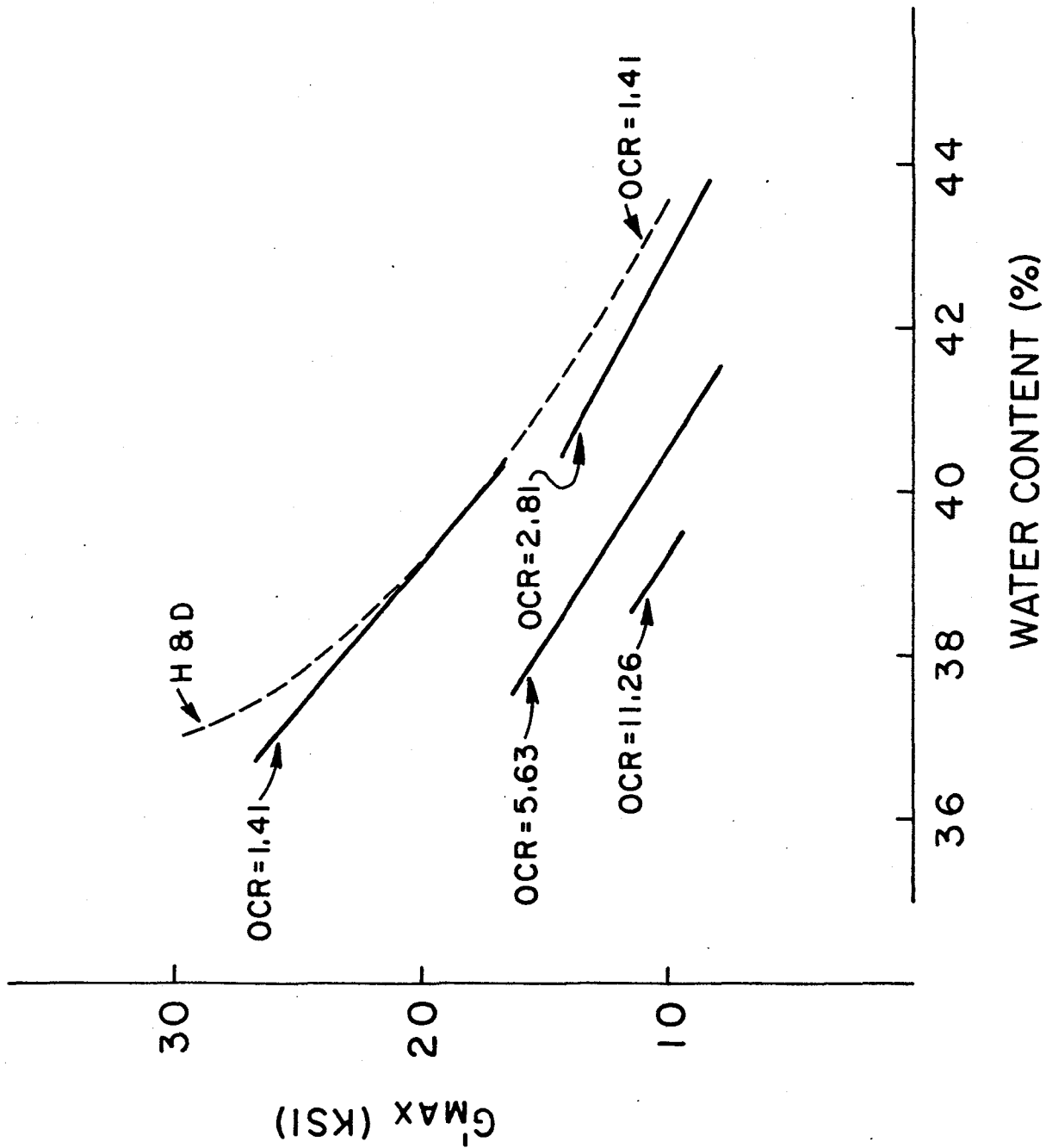


Fig. 6 Moduli versus Water Content for Overconsolidated Clay

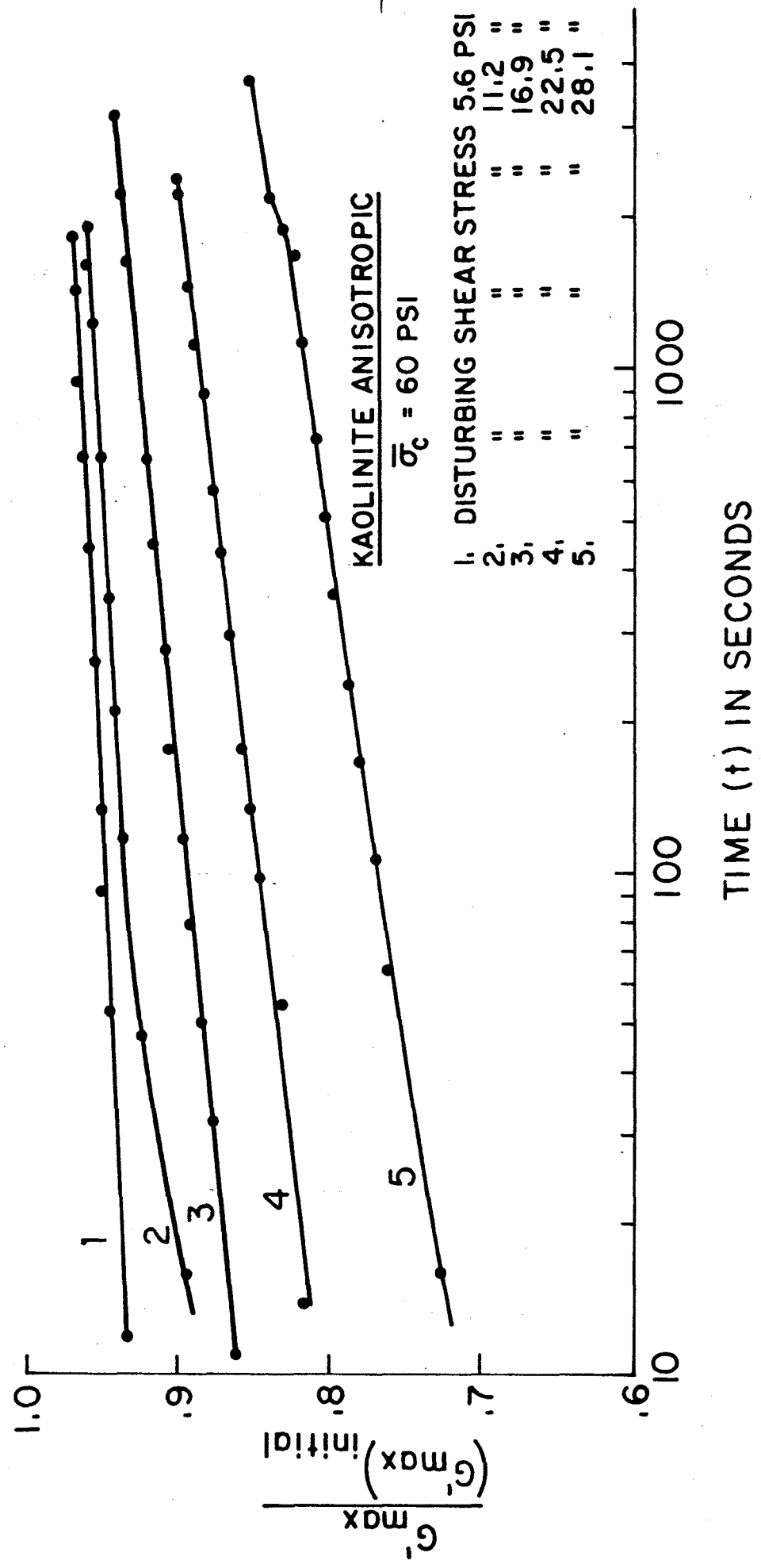


Fig. 7 Regain of Strength after Large Disturbance



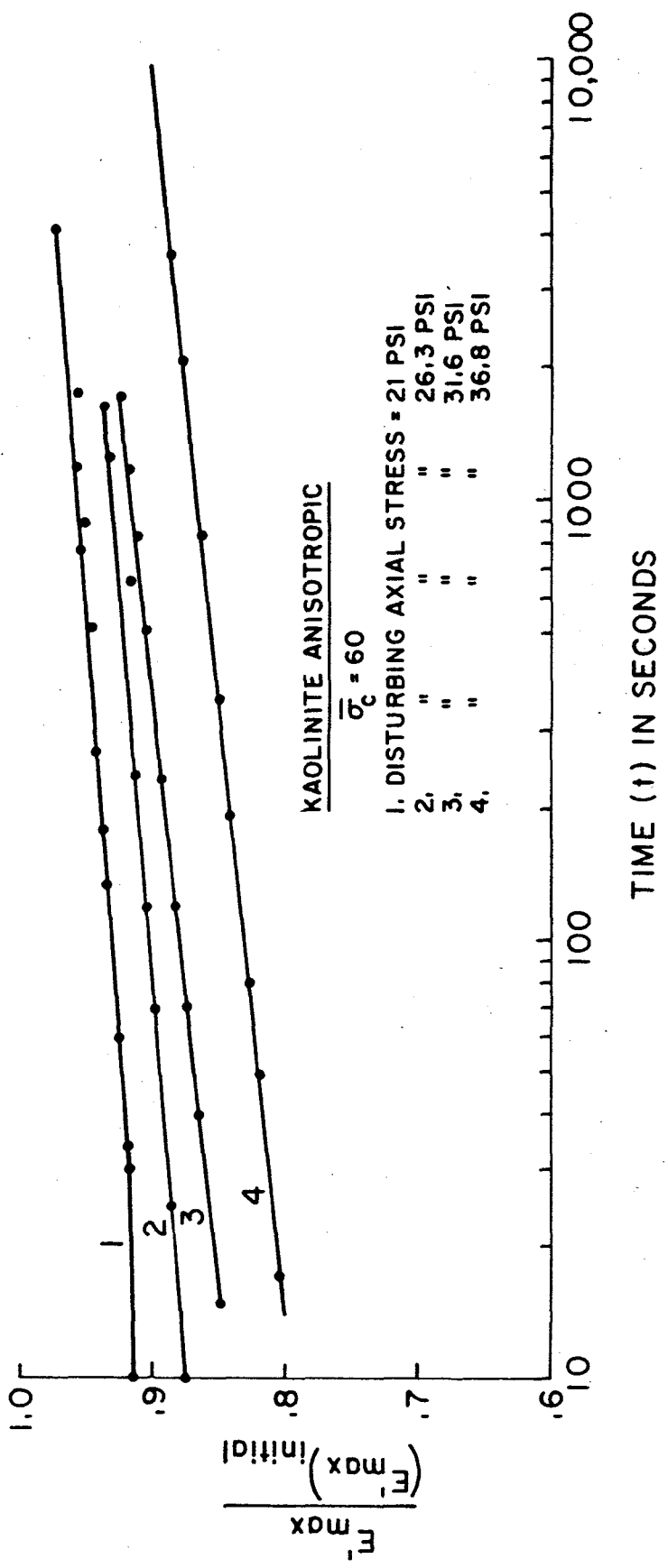


Fig. 8 Regain of Strength after Large Disturbance

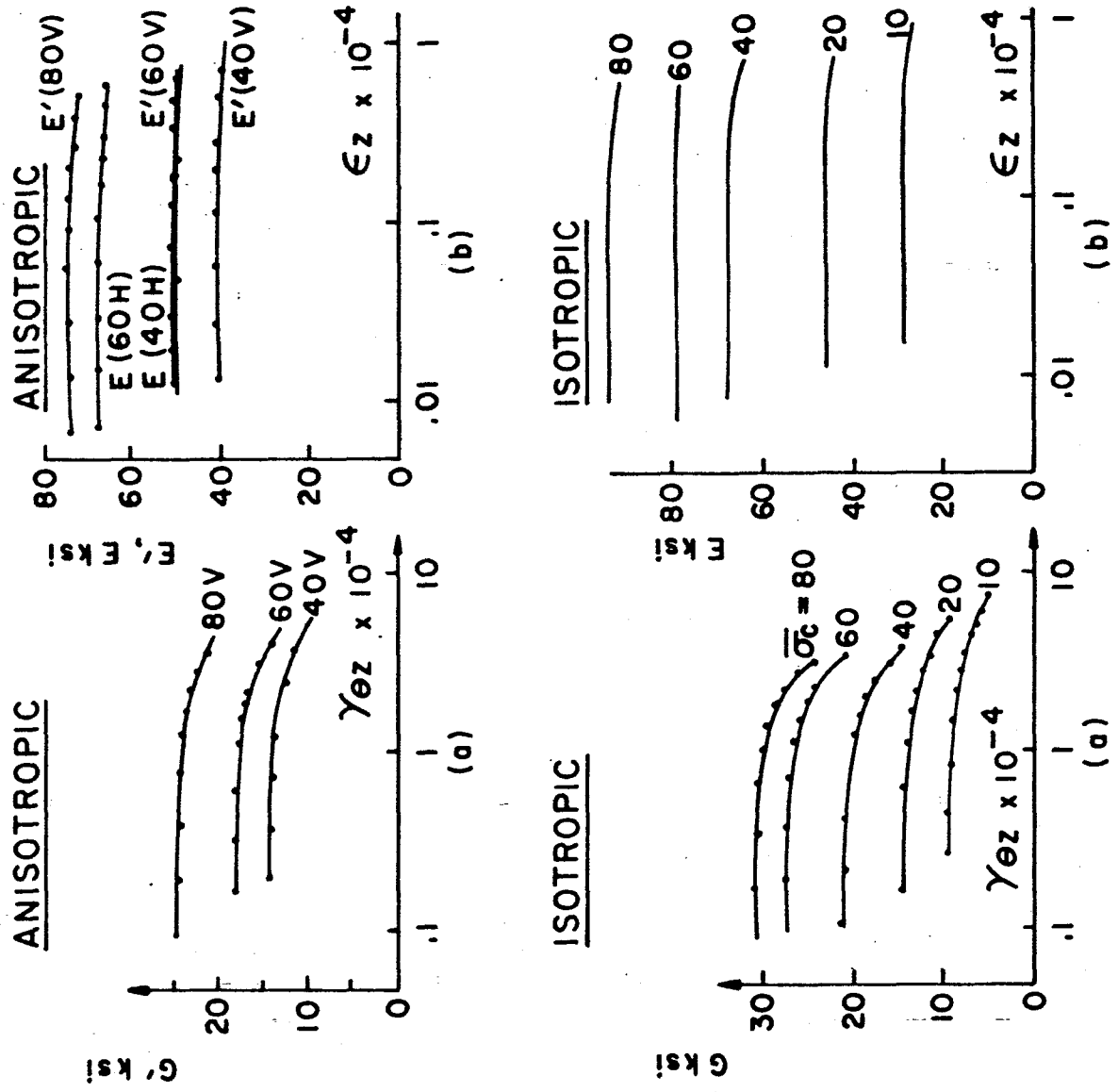


Fig. 9 Variation of Moduli with Strain (Semi-Log. Plot)

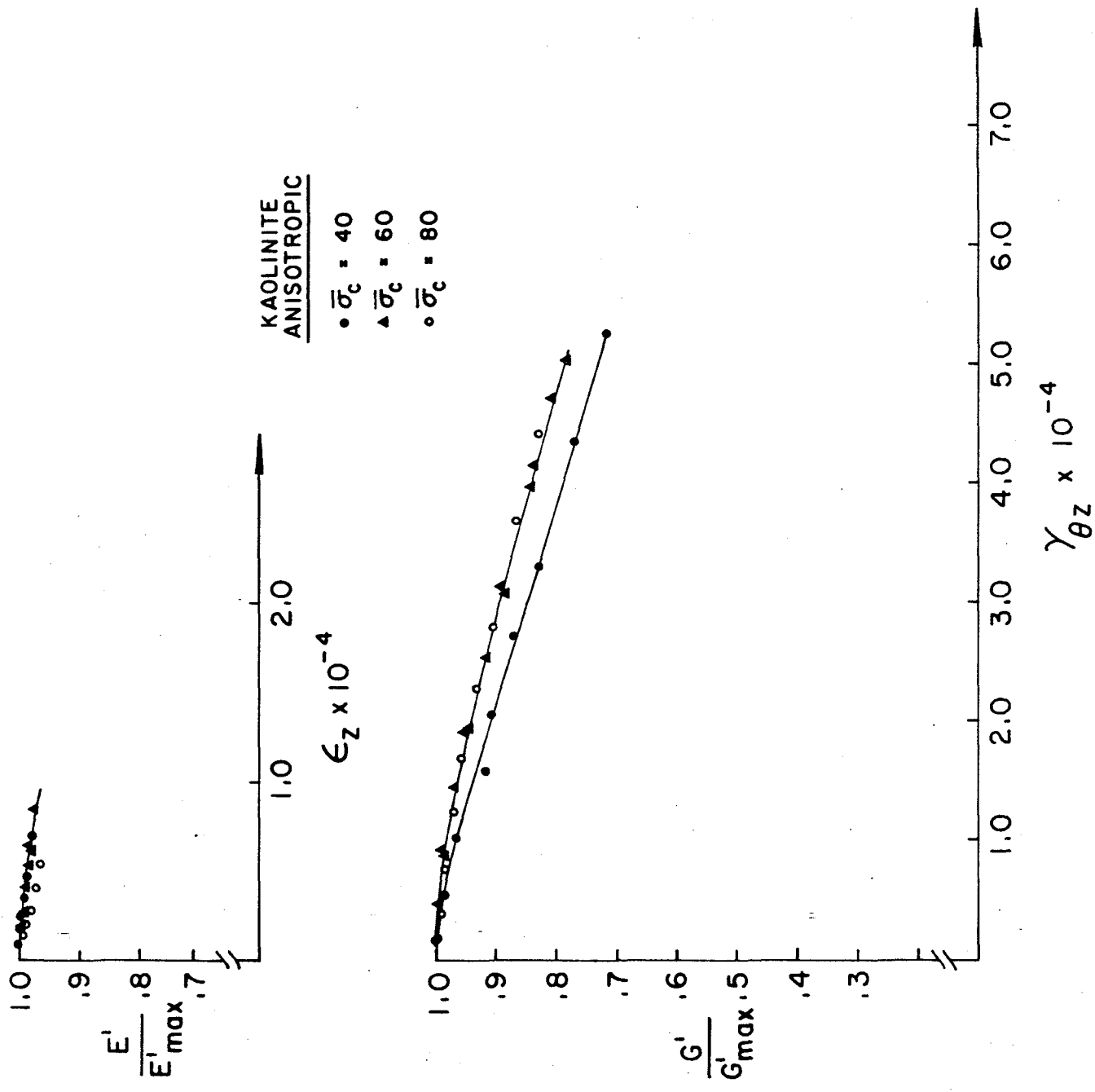


Fig. 10 Variation of Moduli with Strain for Anisotropic Clay (Normal Scales)

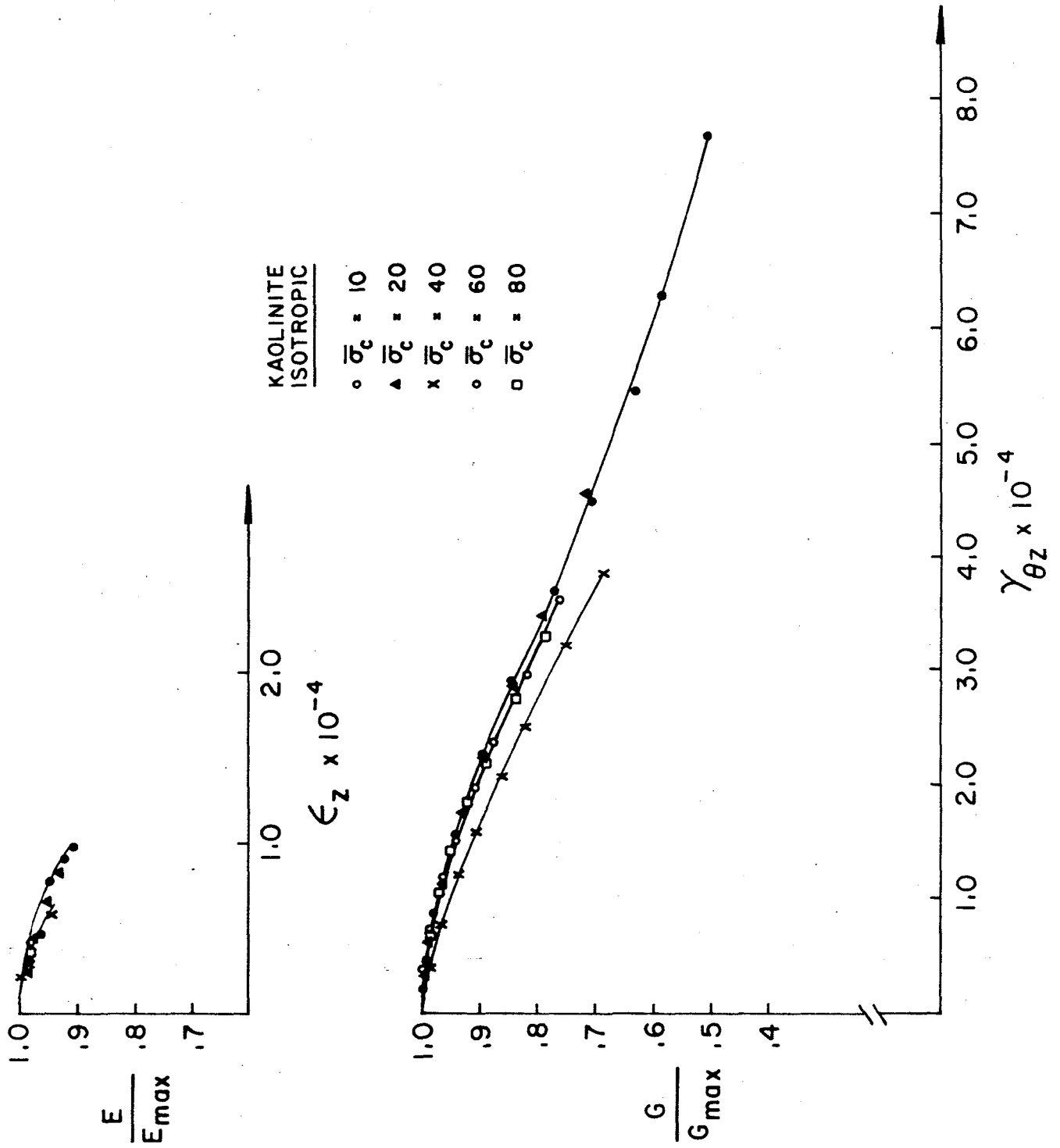


Fig. 11 Variation of Moduli with Strain for Isotropic Clay (Normal Scales)

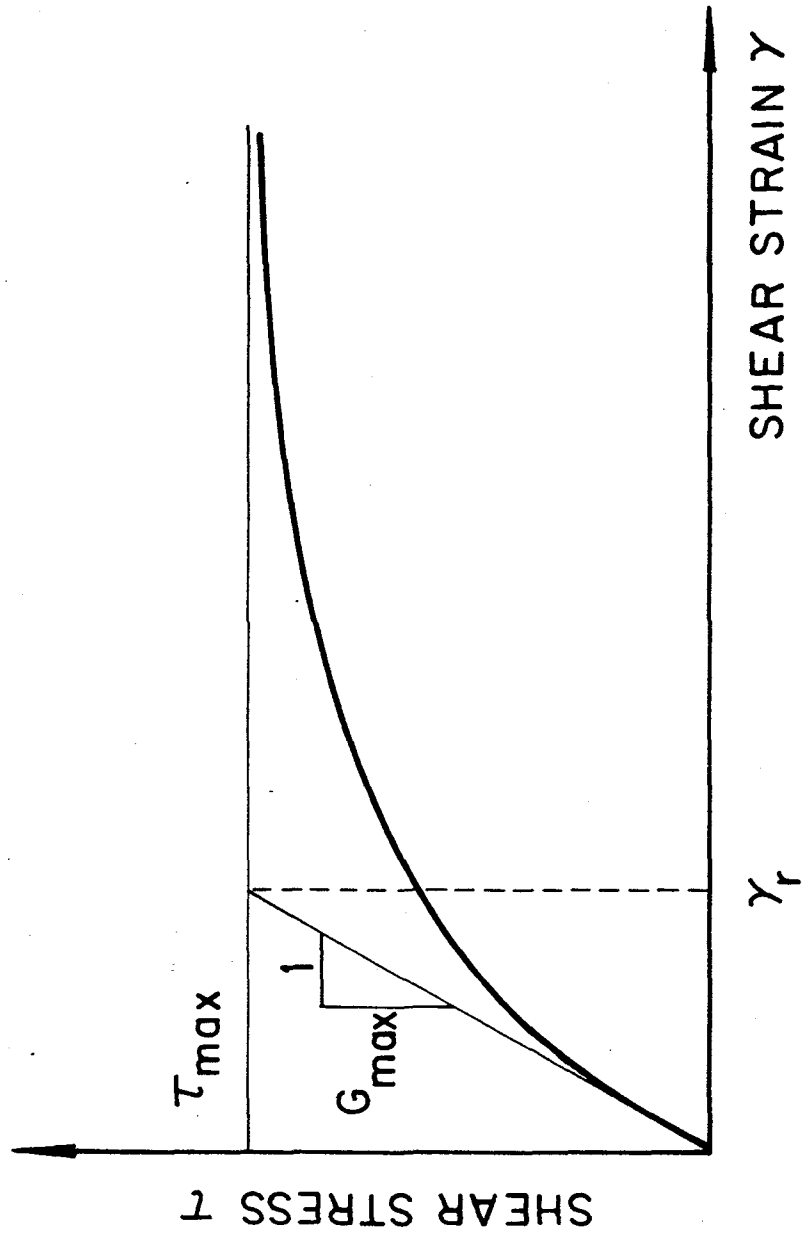


Fig. 12 Definitions of  $\tau_r$ ,  $\gamma_r$  and  $G_{\max}$  from Hardin and Drnevich

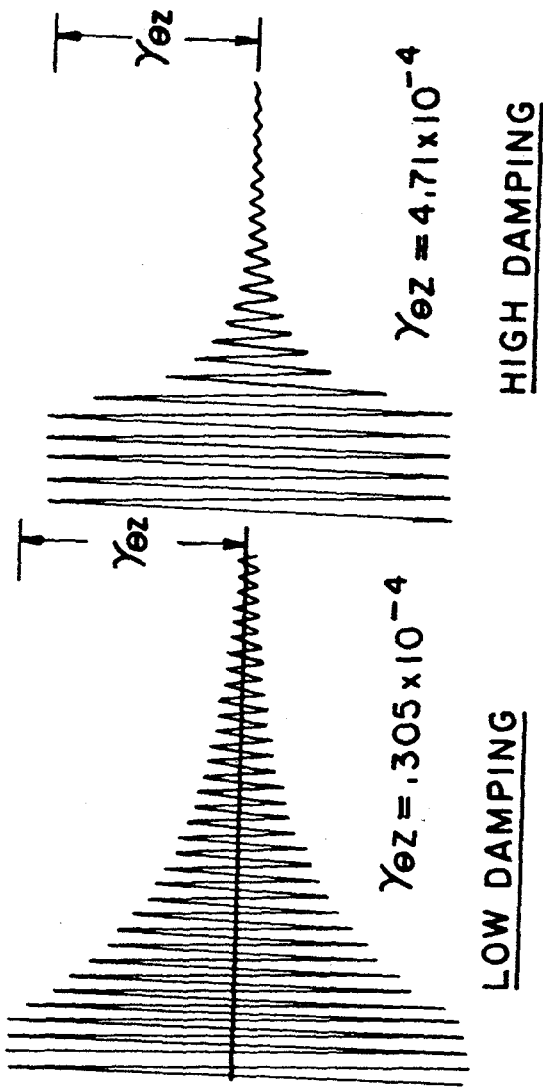


Fig. 13 Decay Curves for Small and Large Strains

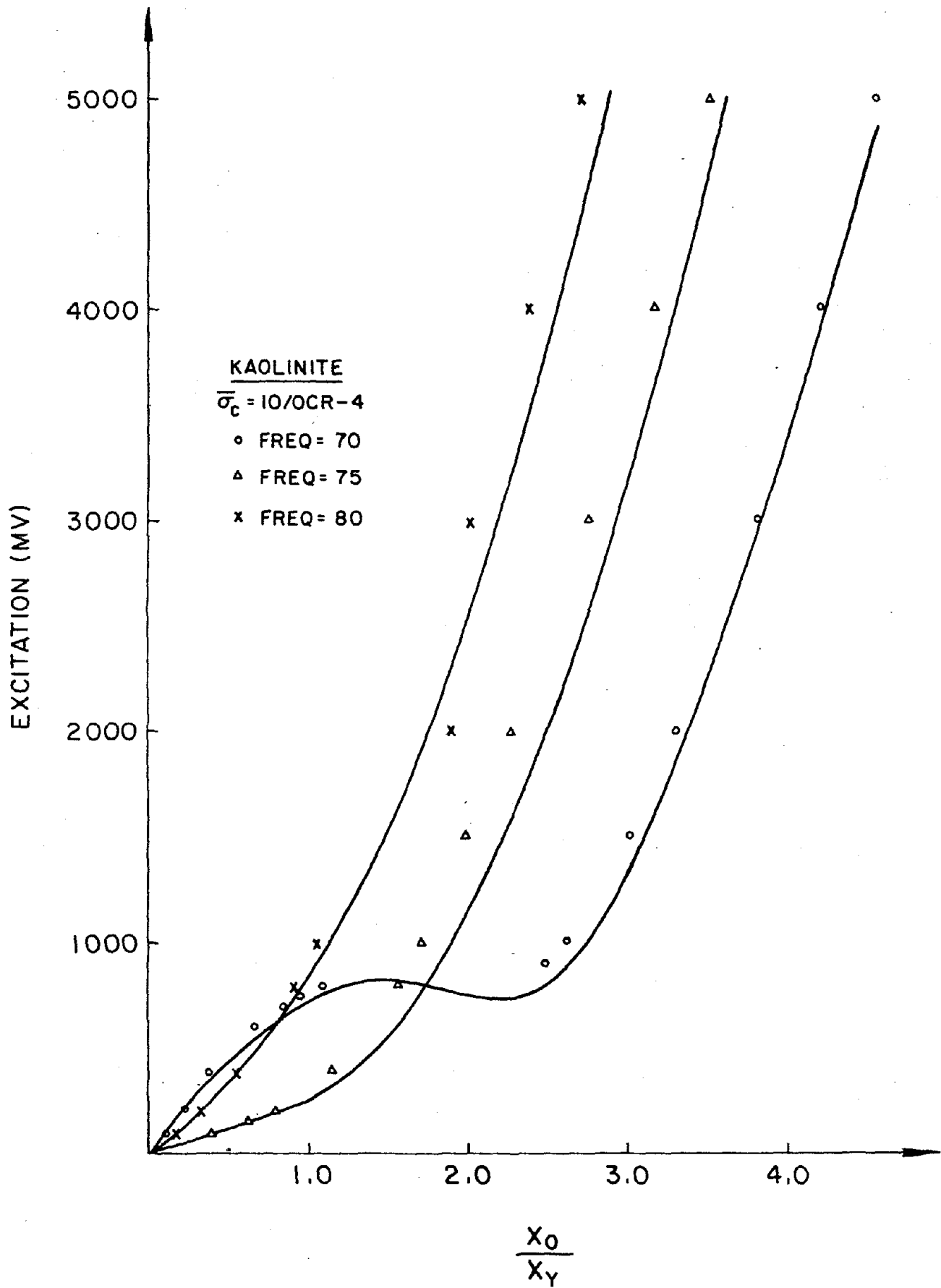


Fig. 21 Excitation versus Strain for Frequencies close to the Resonant Frequency

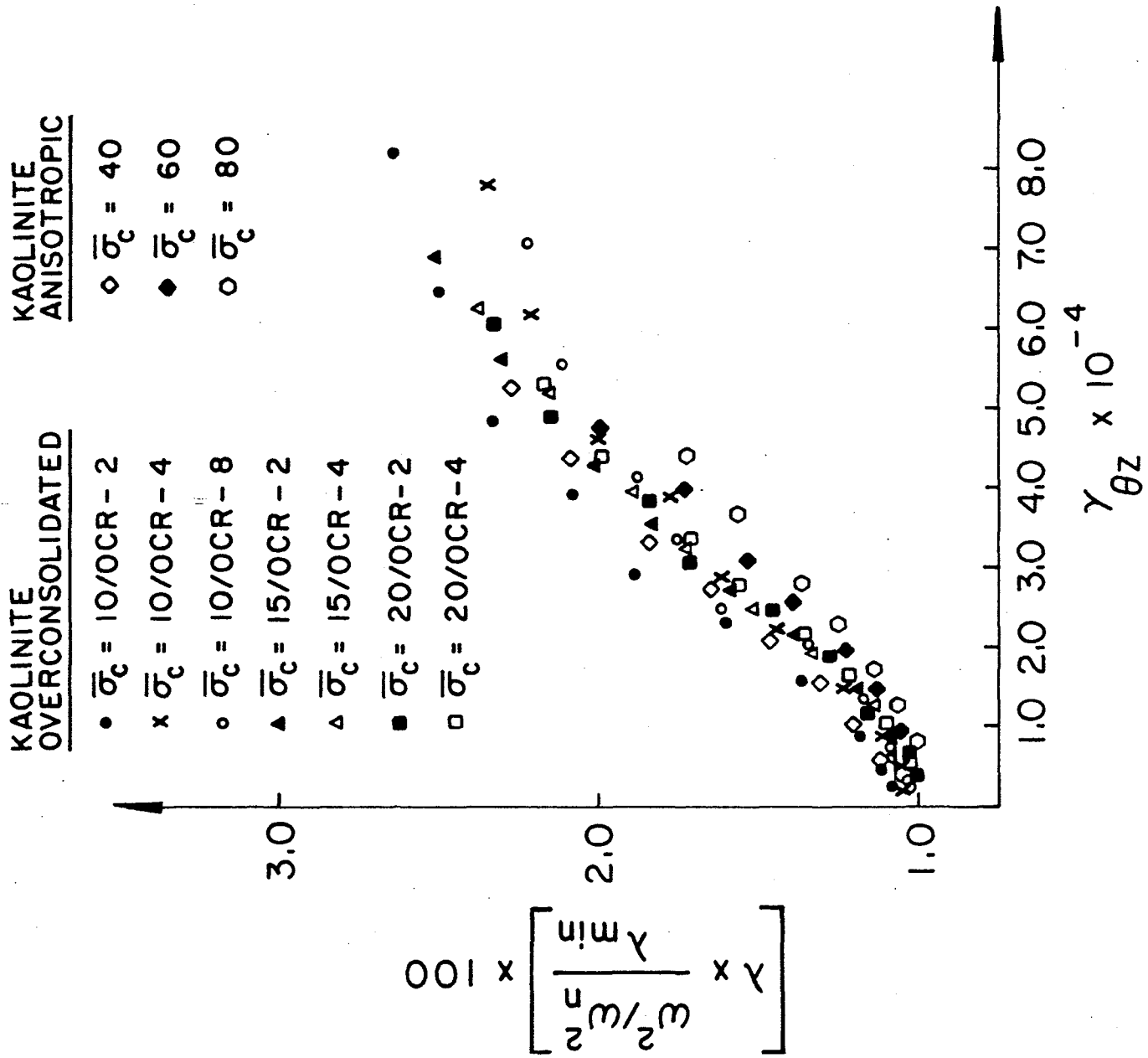


Fig. 15a Variation of Damping with Strain (Normalized)



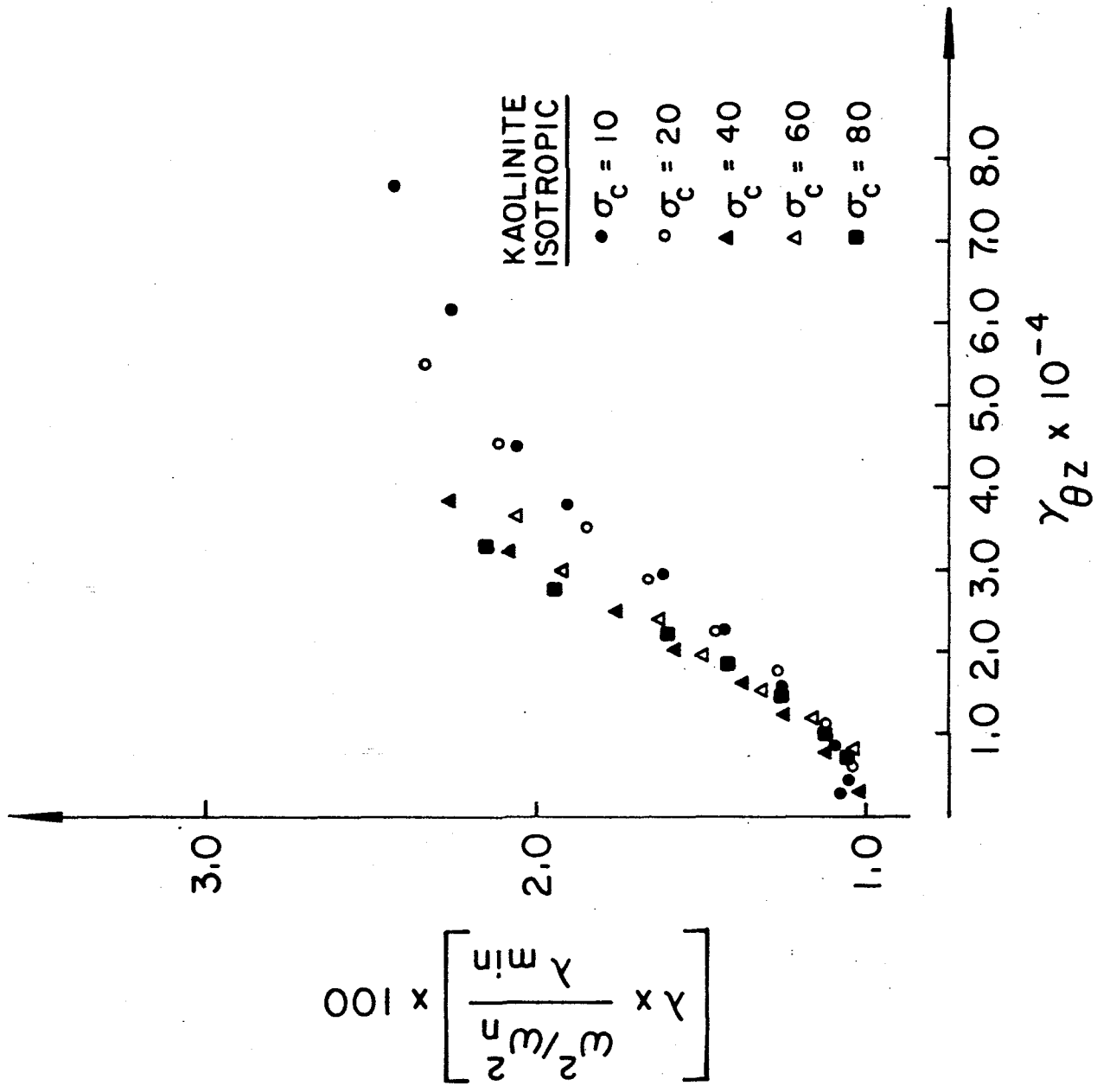


Fig. 15b Variation of Damping with Strain (Normalized)

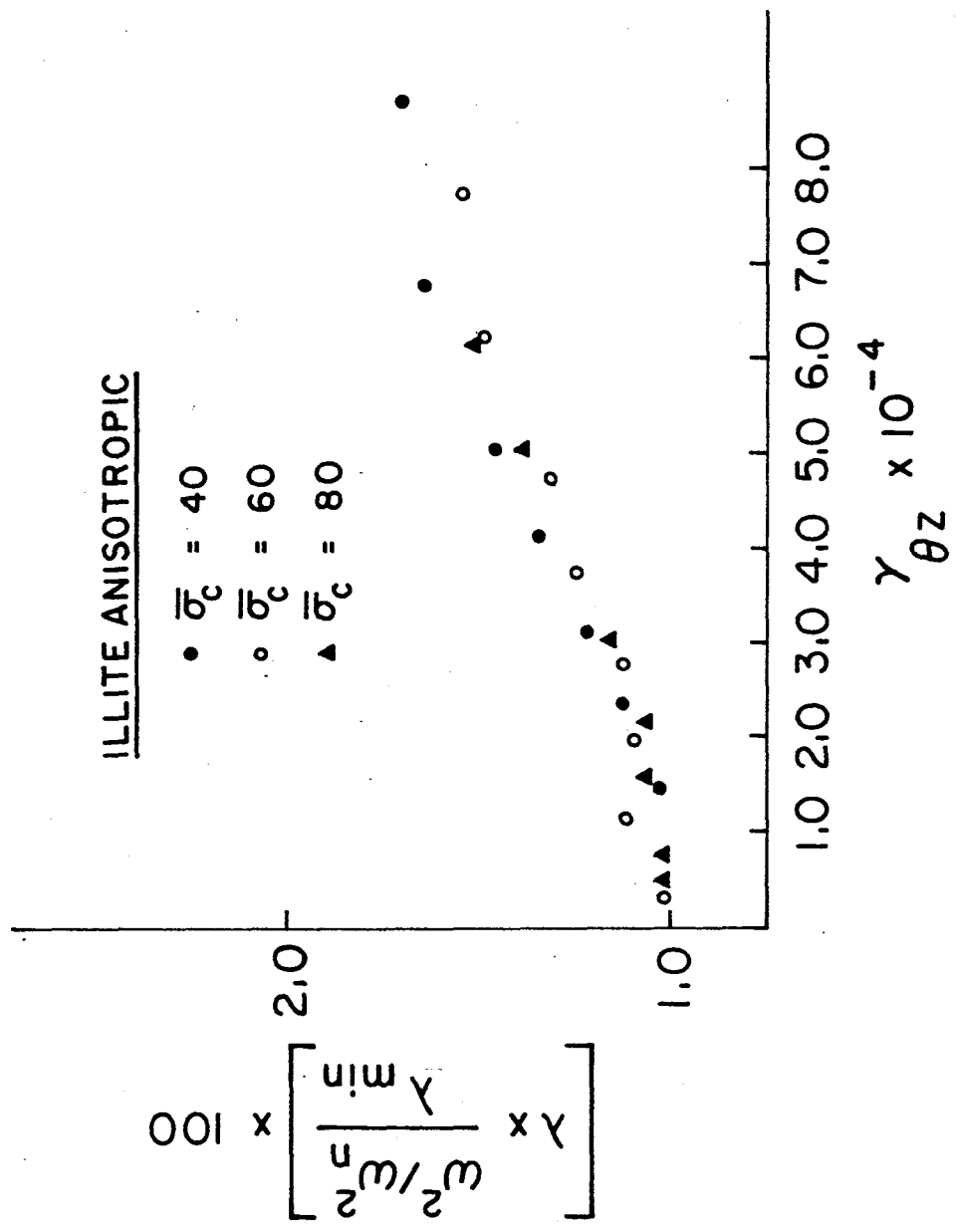


Fig. 15c Variation of Damping with Strain (Normalized)

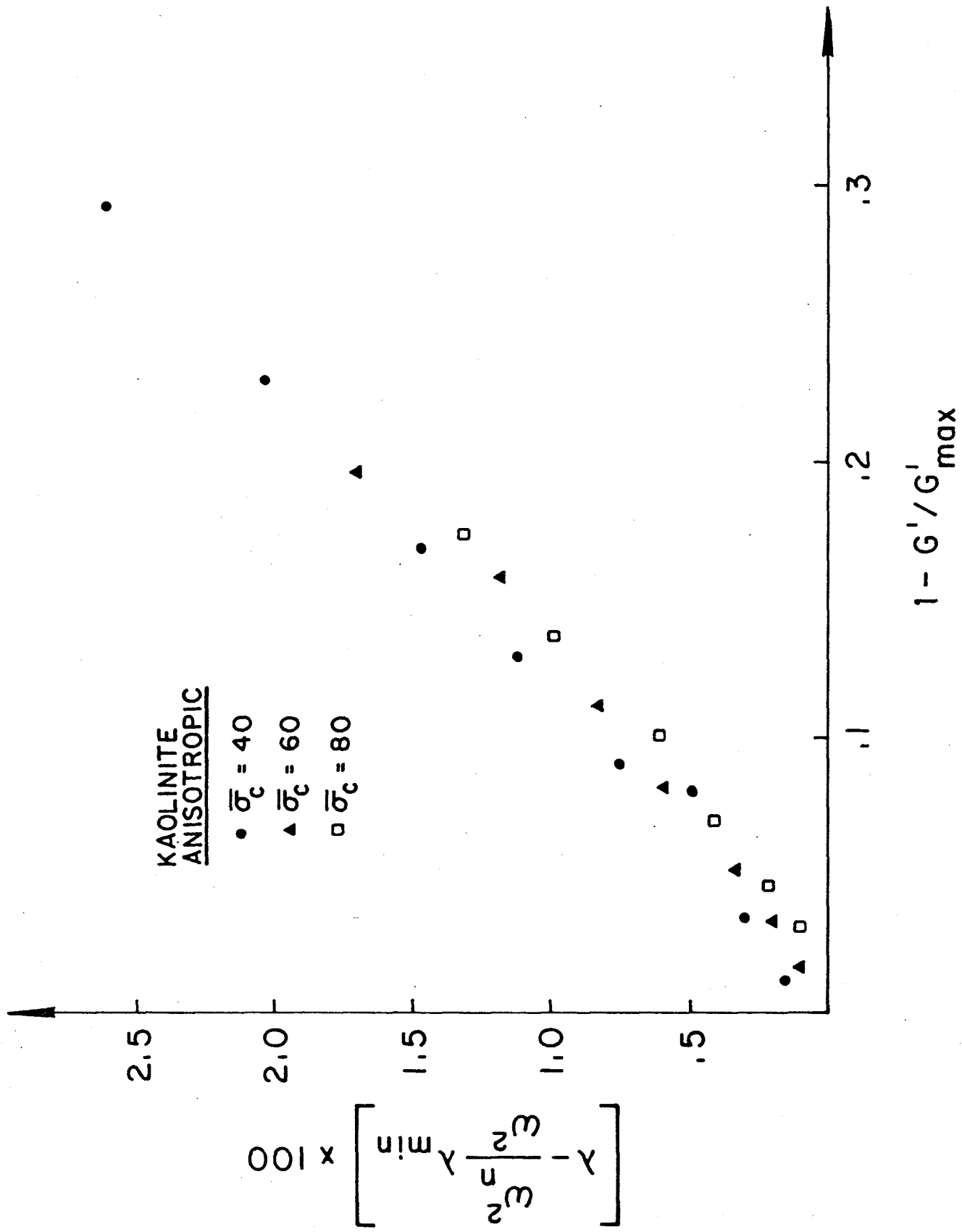


Fig. 16a Relation Between Shear Modulus and Damping

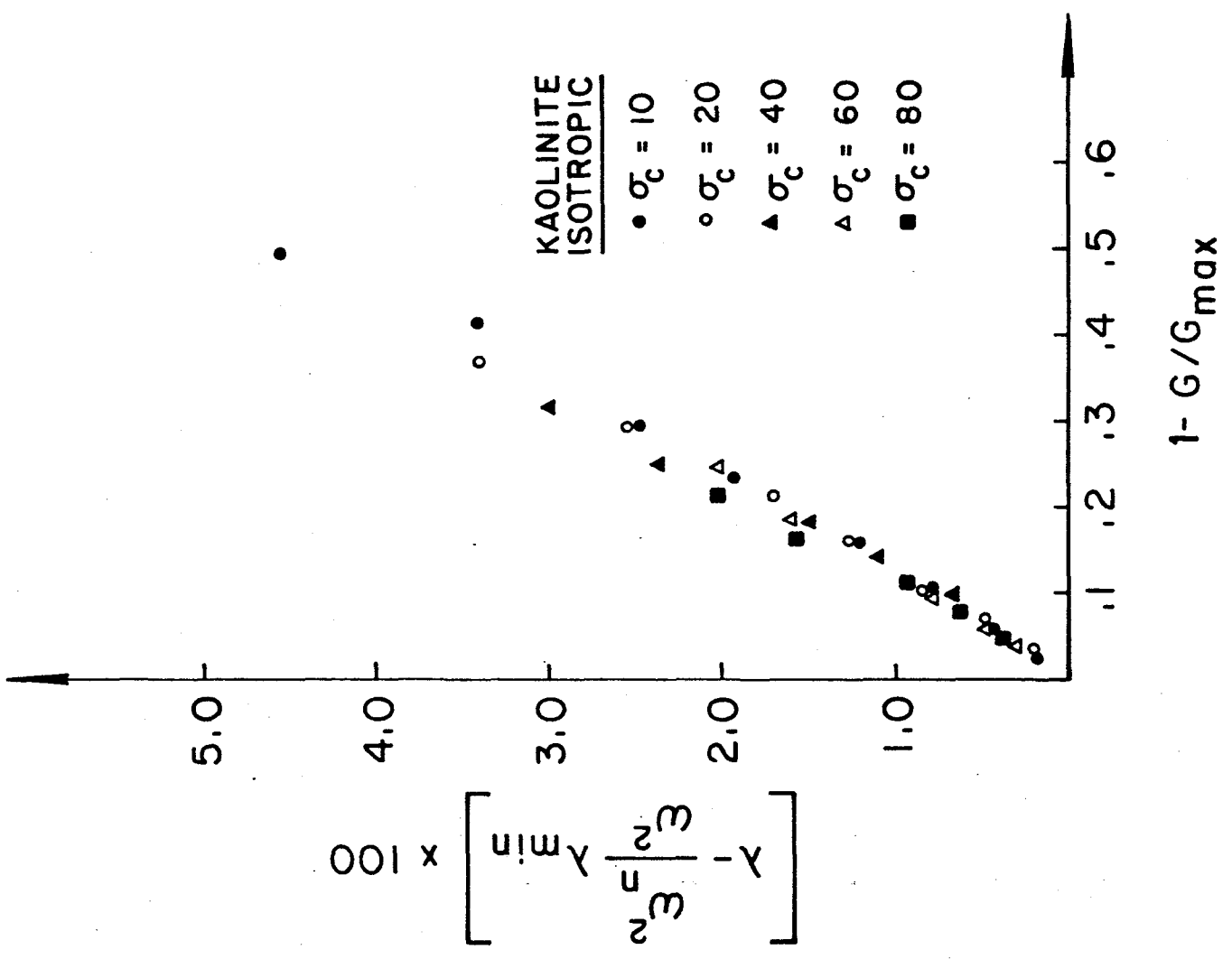


Fig. 16b Relation Between Shear Modulus and Damping

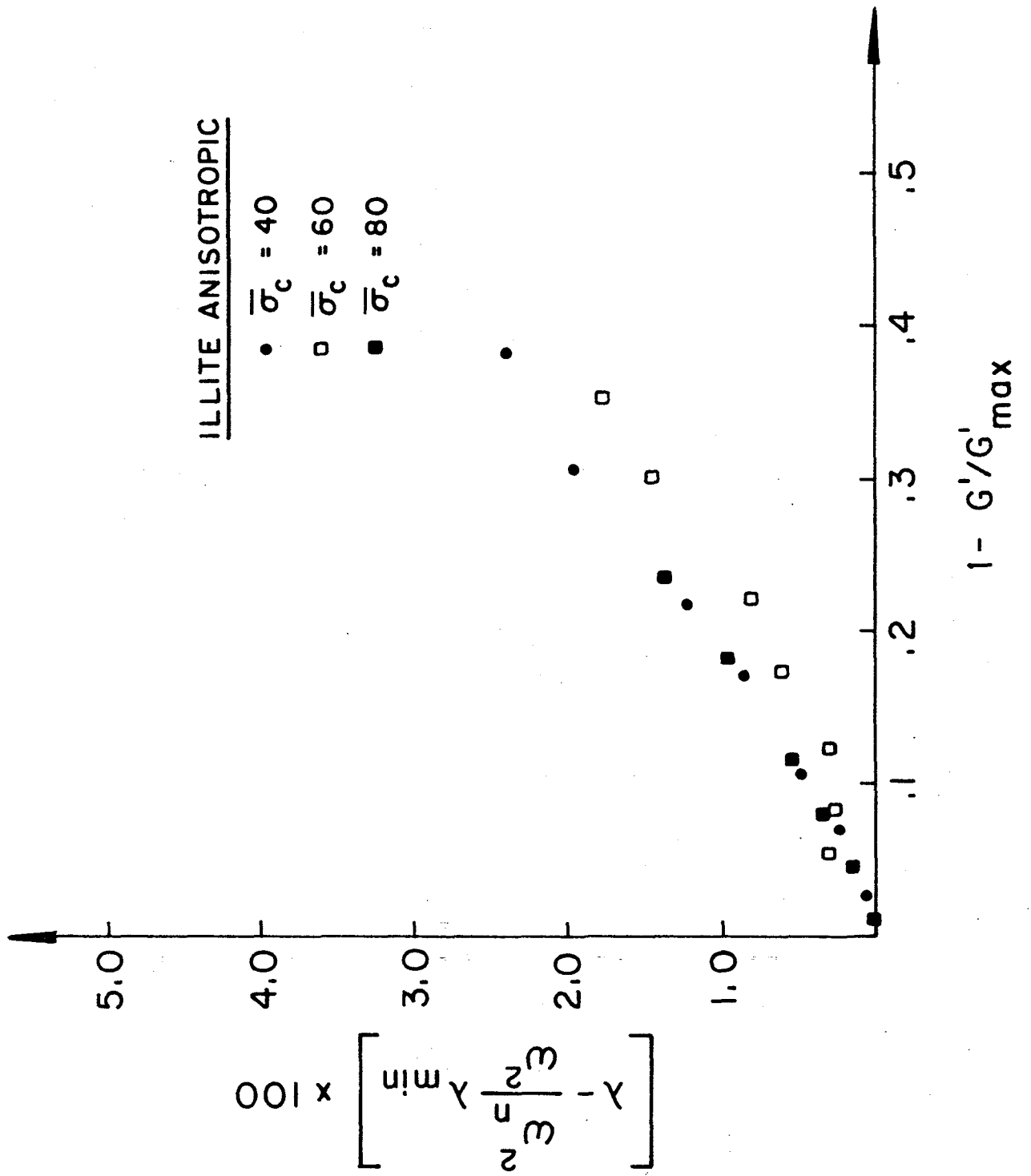


Fig. 16c Relation Between Shear Modulus and Damping

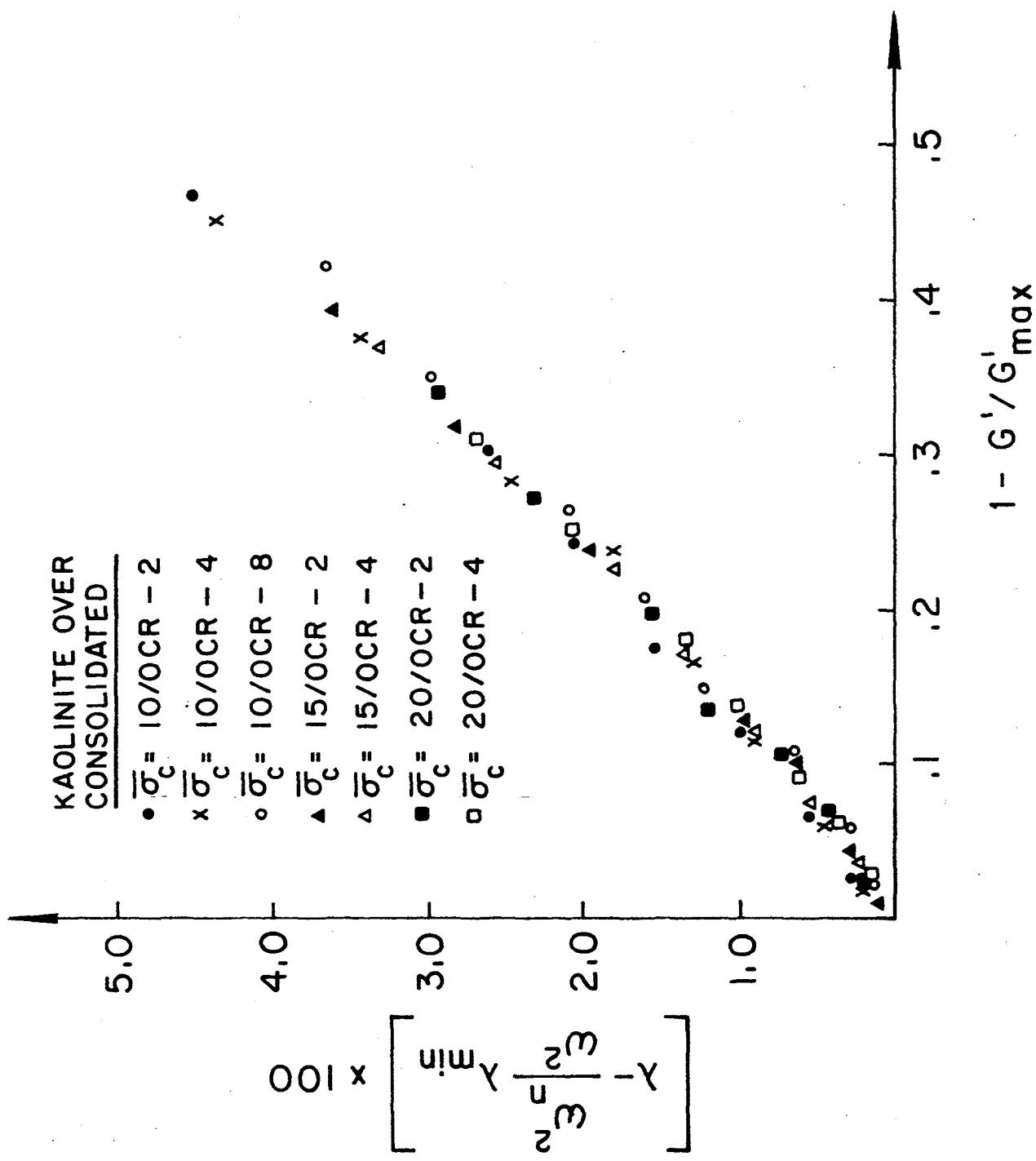


Fig. 16d Relation Between Shear Modulus and Damping

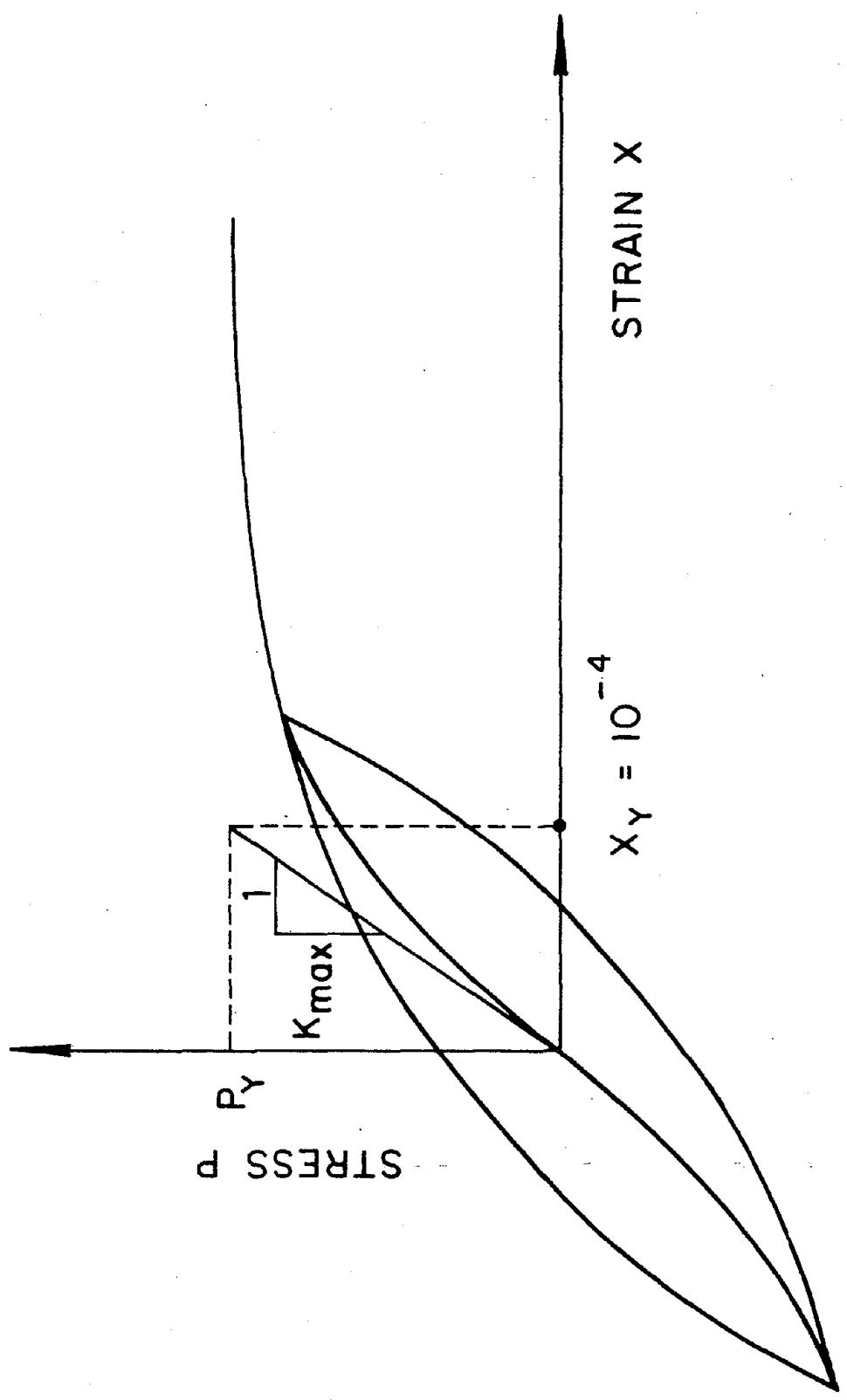


Fig. 17 Definitions used in Non-Linear Analysis

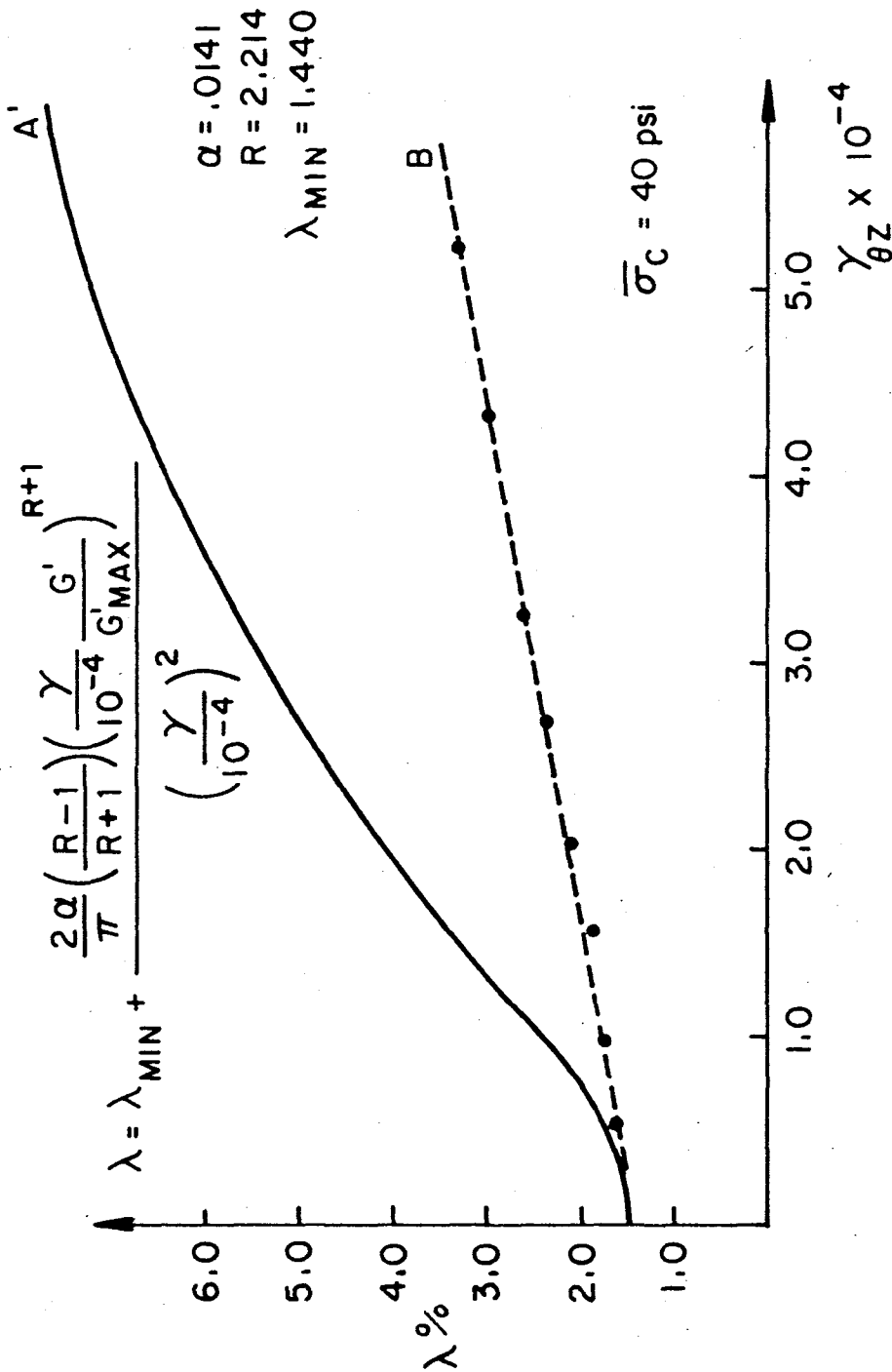
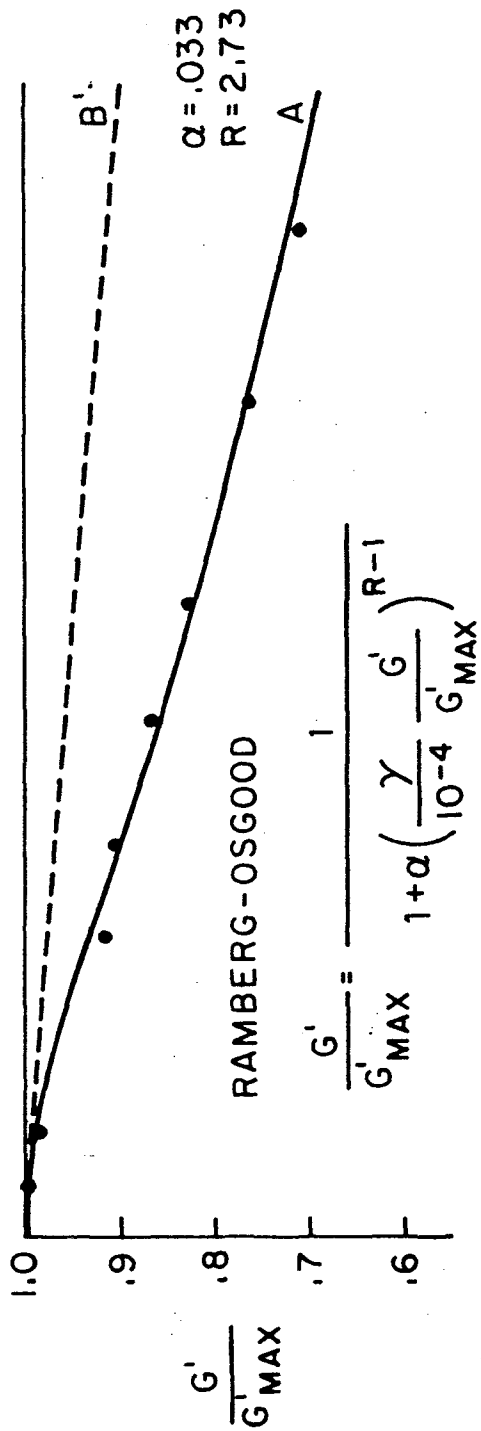


Fig. 18 Measured and Predicted  $G'/G_{MAX}$ , and  $\lambda$  using Ramberg-Osgood-Masing Model



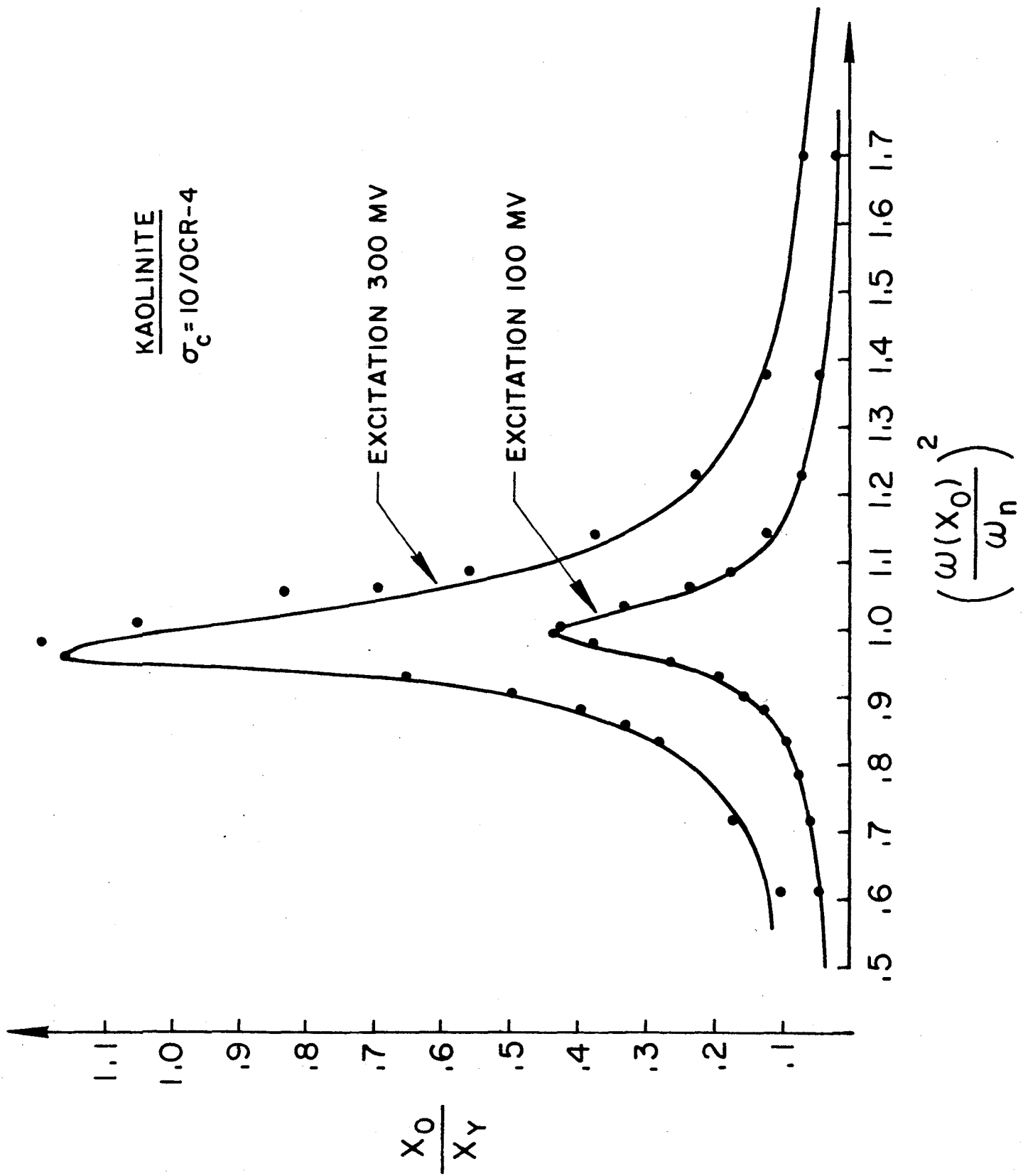


Fig. 19 Typical Response Curves under Low Excitation Levels

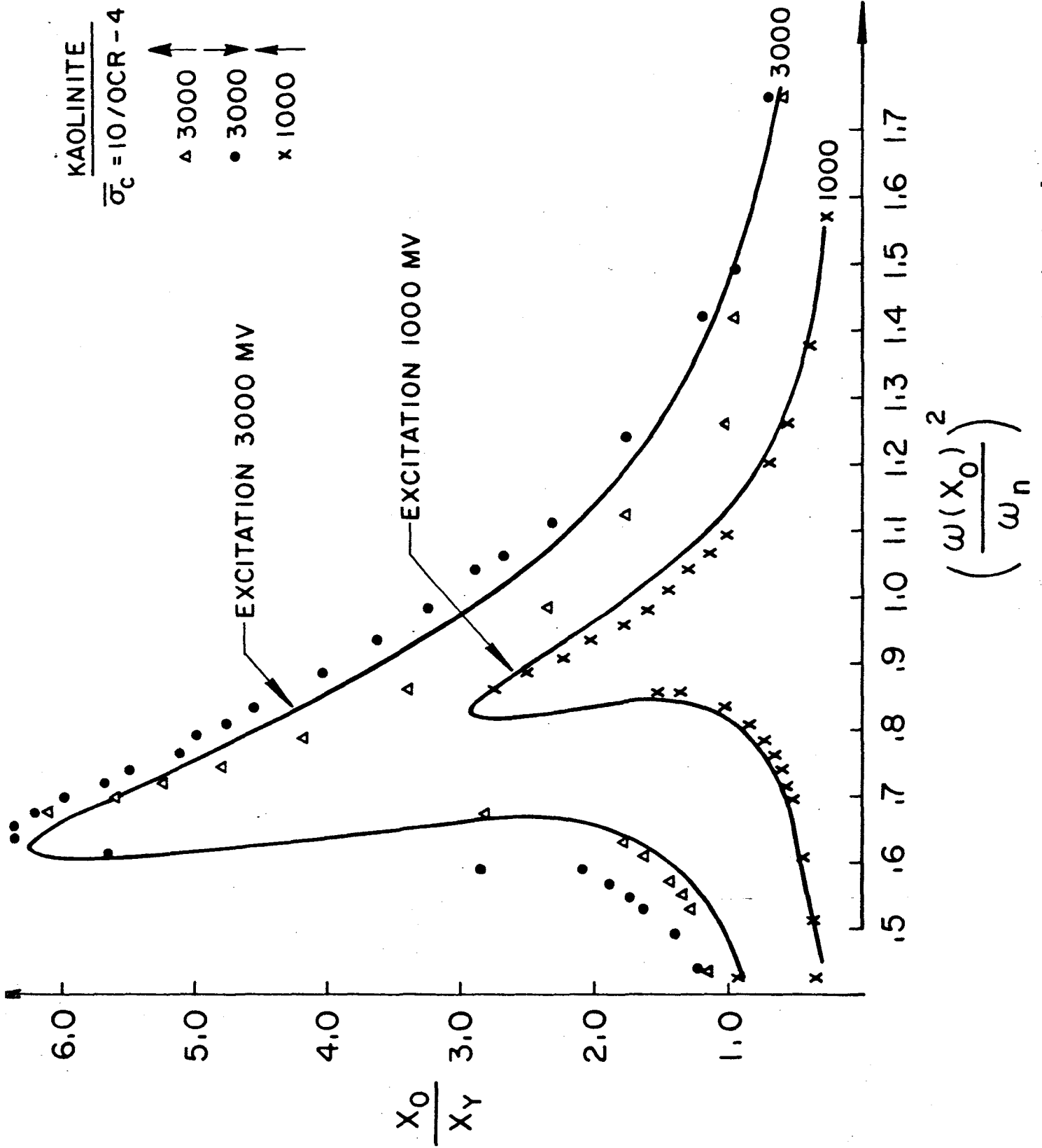


Fig. 20 Typical Response Curves under High Excitation Levels

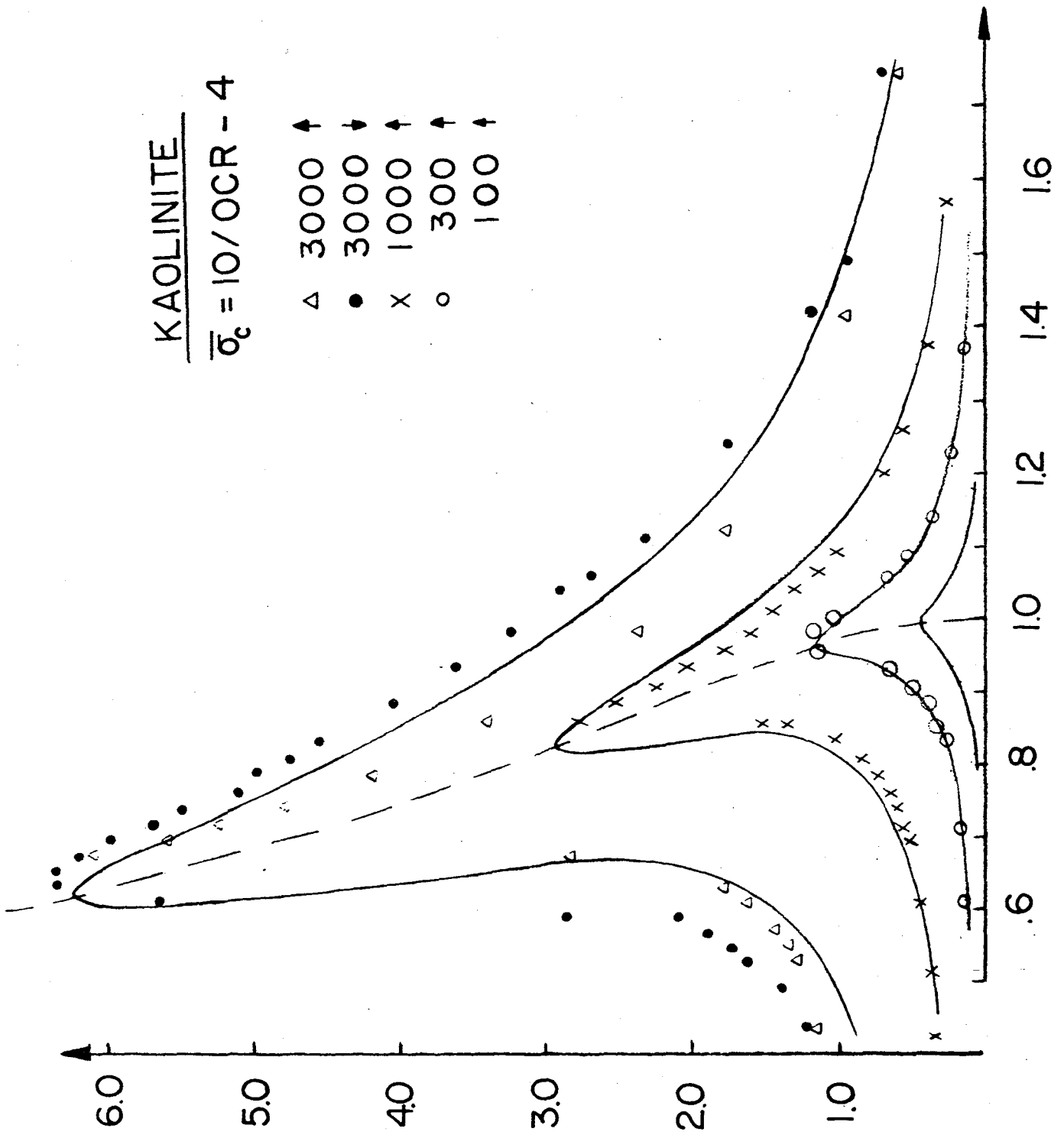
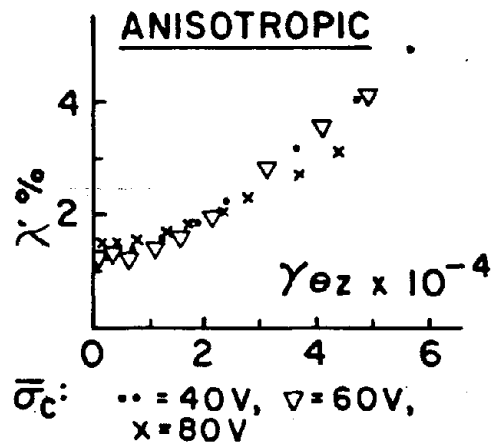
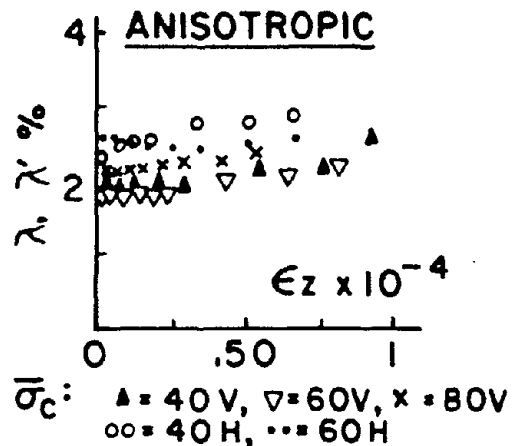


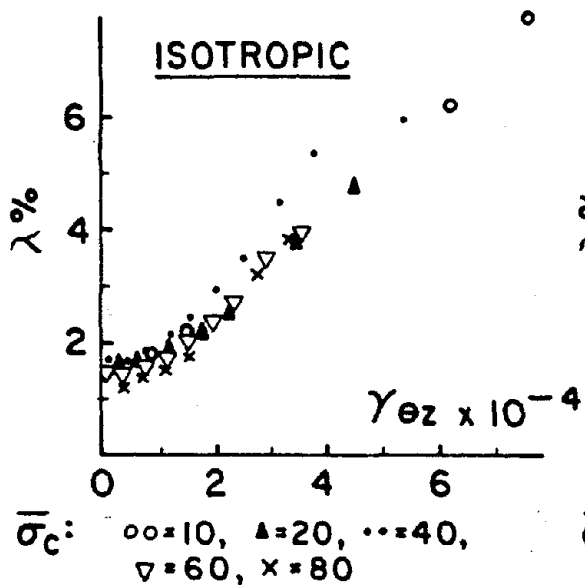
Fig. 20.1 Typical Response Curves under Low/High Excitation Levels  
Figs. 19 and 20 combined



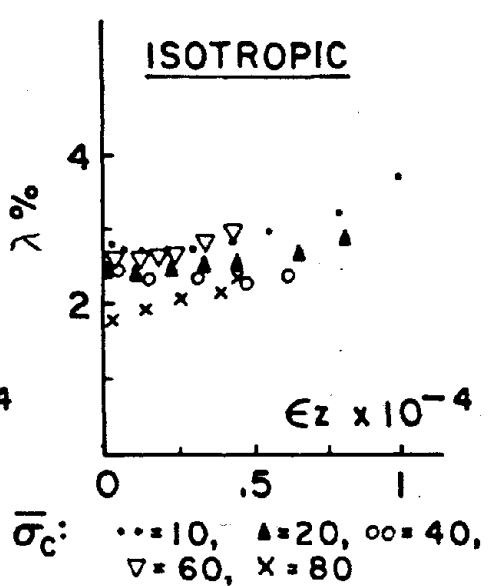
(a)



(b)

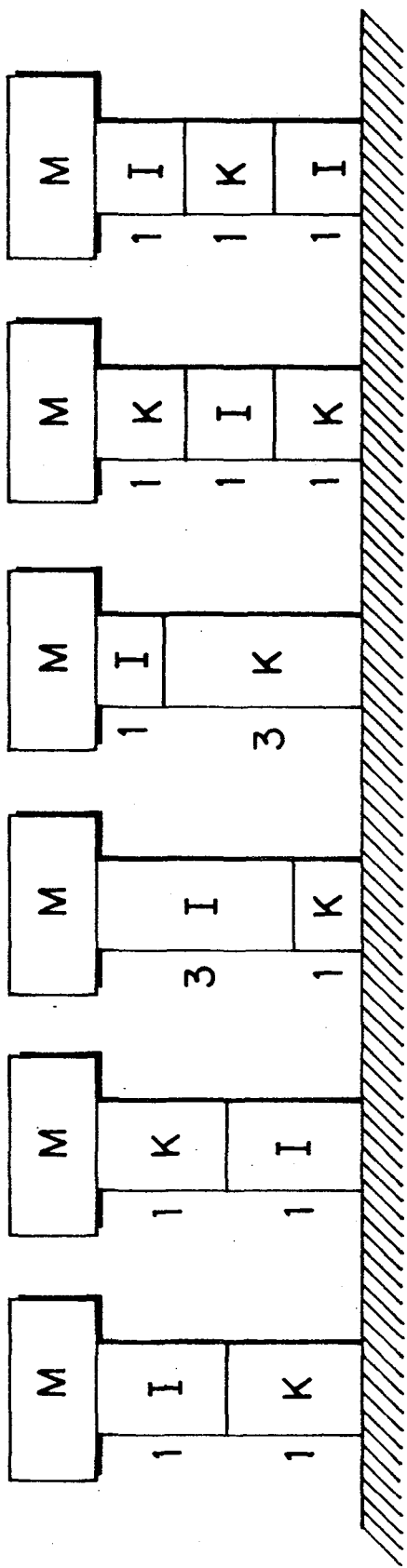


(a)



(b)

Fig. 14 Variation of Damping with Strain



K = KAOLINITE  
I = ILLITE  
M = TOP MASS

Fig. 22 Patterns of Layered Systems used

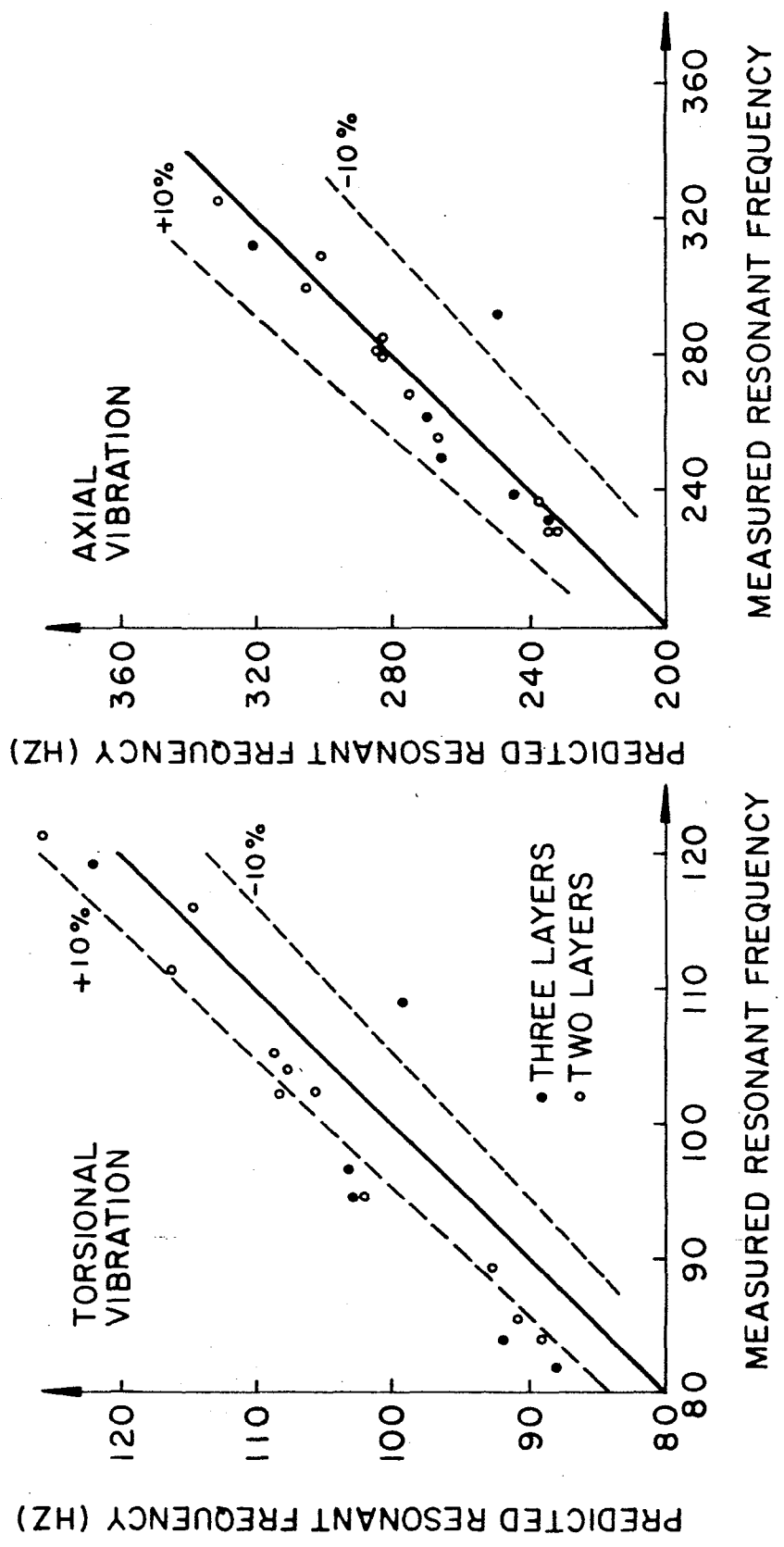


Fig. 23 Measured versus Predicted Frequencies for Layered Systems

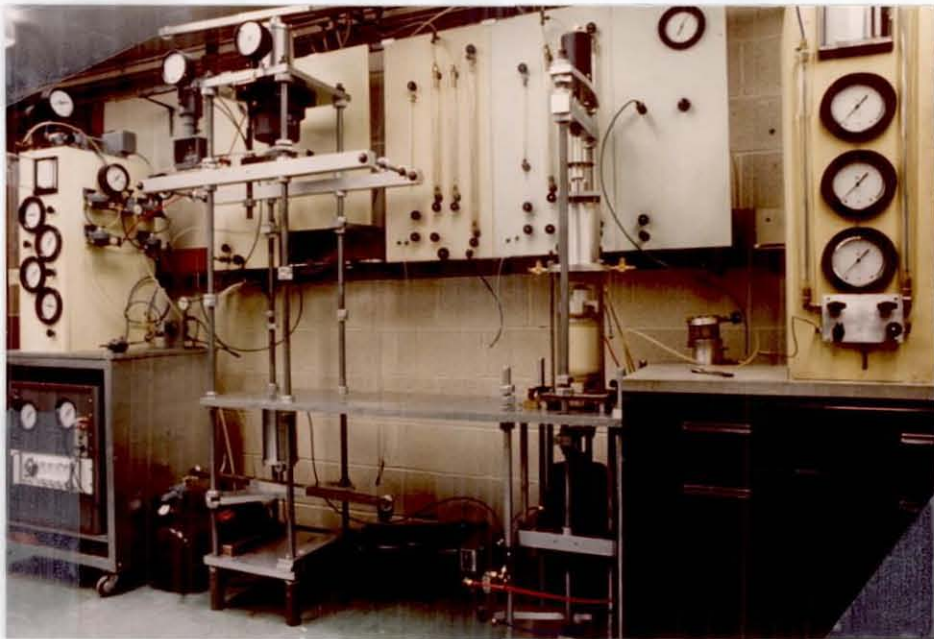
PART II

BEHAVIOR OF CLAY SUBJECTED  
TO SLOW CYCLIC LOADING

by

Louise Palmer Shook

M.SC. THESIS







BEHAVIOR OF CLAYS SUBJECTED  
TO SLOW CYCLIC LOADING

by

LOUISE PALMER SHOOK

Submitted in partial fulfillment of the requirements  
for the Degree of Master of Science

Thesis Advisor: Adel S. Saada

Department of Civil Engineering  
CASE WESTERN RESERVE UNIVERSITY

August 1979

BEHAVIOR OF CLAYS  
SUBJECTED TO SLOW CYCLIC LOADING

Abstract

by

LOUISE PALMER SHOOK

One of the major considerations of the design of offshore structures is the effect of wave action on the foundation of the structures. This involves a study of cyclic loading done at low frequencies, and the consequence such loading has on the soil properties. The anisotropic nature of the material plays an important role in the dynamic as well as the static behavior of soils.

An experimental program has been undertaken to determine the trends in behavior of clays subjected to large strain cyclic loading. Laboratory prepared clays, which are assumed to be isotropic, and normally  $K_0$ -consolidated and over consolidated clays, which have varying degrees of anisotropy and differing stress-strain characteristics have been cycled at periods of 20 to 40 seconds using different levels of stress. Damping, modulus degradation, and increasing strain values are compared with respect to overconsolidation ratio, level of applied stress, direction of applied stress, cycle number, and consolidation pressure.

The test results were fit to a mathematical model, and it was concluded that the model was not adequate to fully describe the soil response.

## ACKNOWLEDGEMENTS

I wish to extend my appreciation and gratitude to Professor Adel Saada for his extensive guidance and instruction throughout the course of this research. I am indebted to my fellow students Gary Bianchini and Richard Snyder for their assistance and suggestions during the various phases of this project. Ms. Suzanne Hazan very ably typed this dissertation.

I wish to express my gratitude to my family for their constant encouragement and support.

This research would not have been possible without the financial support of the National Science Foundation. This support is gratefully acknowledged.

## TABLE OF CONTENTS

	Page
ABSTRACT	<i>II-iii</i>
ACKNOWLEDGEMENTS	<i>II-<del>iv</del></i>
TABLE OF CONTENTS	<i>II-vi</i>
LIST OF FIGURES	<i>II-viii</i>
LIST OF TABLES	<i>II-<del>x</del></i>
CHAPTER I INTRODUCTION	<i>II-1</i>
CHAPTER II REVIEW OF THE LITERATURE	<i>II-3</i>
A. Structure of Clays	<i>II-3</i>
B. Dynamic Properties of Clays	<i>II-4</i>
CHAPTER III EQUIPMENT AND MATERIAL USED	<i>II-7</i>
CHAPTER IV RESPONSE TO MONOTONIC LOADING	<i>II-11</i>
A. Testing Procedure	<i>II-11</i>
B. Normally Consolidated Clay, Anisotropic	<i>II-12</i>
C. Isotropic or Compacted Clay	<i>II-13</i>
D. Overconsolidated Clay	<i>II-15</i>
CHAPTER V ONE SIDED LOADING	<i>II-17</i>
A. Testing Procedure	<i>II-17</i>
B. Strain Behavior	<i>II-18</i>
C. Pore Pressure Development	<i>II-19</i>
D. Secant Moduli	<i>II-19</i>
E. Equivalent Damping Ratio	<i>II-20</i>
CHAPTER VI TWO SIDED LOADING	<i>II-21</i>
A. Testing Procedure	<i>II-21</i>

	B. Strain Behavior	<i>II-23</i>
	C. Secant Modulus	<i>II-25</i>
	D. Damping	<i>II-27</i>
CHAPTER VII	Ramberg-Osgood Model	<i>II-31</i>
	A. Backbone Curve	<i>II-31</i>
	B. Ramberg-Osgood Equation	<i>II-32</i>
	C. Degradation	<i>II-35</i>
	D. Overconsolidated Clay	<i>II-42</i>
APPENDIX I	EXTENSION TESTS ON REDUCED AREA SPECIMENS	<i>II-44</i>
APPENDIX 2	REFERENCES	<i>II-45</i>
APPENDIX 3	NOTATION	<i>II-48</i>
FIGURES		<i>II-50</i>
TABLES		<i>II-80</i>

## LIST OF FIGURES

Figure		Page
2-1	Schematic Representation of Possible Material Structure	<u>II</u> - 50
4-1	Stresses, Strains, and Pore Pressures from Static Tests	<u>II</u> - 51
4-2	Stresses, Strains, and Pore Pressures from Static Tests	<u>II</u> - 51
4-3	Typical Stress-Strain and Pore Pressure Development Curves for Overconsolidated Clays	<u>II</u> - 52
5-1	Typical Stress Pattern for One Sided Loading	<u>II</u> - 53
5-2	Maximum, Minimum and Average Strain for One Sided Loading	<u>II</u> - 53
5-3	Strain vs. N Envelopes for One Sided Loading	<u>II</u> - 54
5-4	Pore Pressure Development for One Sided Loading	<u>II</u> - 55
5-5	Secant Modulus vs. Cycle Number for One Sided Loading	<u>II</u> - 56
5-6	Equivalent Damping Ratio vs. Cycle Number for One Sided Loading	<u>II</u> - 57
6-1	Typical Stress-Strain Loops for Torsional Tests	<u>II</u> - 58
6-2	Typical Stress-Strain Loops for Axial Tests	<u>II</u> - 58
6-3	Strain Envelopes for Two Sided Loading	<u>II</u> - 59
6-4	Typical Secant Modulus for Two Sided Loading	<u>II</u> - 60
6-5	Degradation Index for Anisotropic Clay	<u>II</u> - 61
6-6	Degradation Parameter $t$ vs. Stress Level	<u>II</u> - 62
6-7	Damping Energy vs. Cycle Number	<u>II</u> - 63
6-8	Potential Energy for Lehr's Damping	<u>II</u> - 64
6-9	Potential Energy for Roelig's Damping	<u>II</u> - 64
6-10	Equivalent Damping Ratio for Two Sided Loading	<u>II</u> - 65

## LIST OF FIGURES

6-11	Damping Ratio vs. Strain Envelope	<i>II-67</i>
6-12	Typical Damping Ratios for Overconsolidated Clay	<i>II-68</i>
7-1	Shear Modulus vs. Measured and Calculated Damping Ratios	<i>II-69</i>
7-2	Degradation of Backbone Curve	<i>II-70</i>
7-3	Ramberg-Osgood Coefficients for Normally Consolidated Clay	<i>II-71</i>
7-4	Secant Modulus Derived from Eq. (7-11)	<i>II-72</i>
7-5	Secant Modulus vs. Damping Ratio for Normally Consolidated Clay	<i>II-73</i>
7-6	Ramberg-Osgood Coefficients for Overconsolidated Clay	<i>II-74</i>
7-7	Secant Modulus vs. Damping Ratio for Overconsolidated Clay	<i>II-75</i>
A-1	Specimen with Reduced Area	<i>II-76</i>
A-2	Standard Triaxial Specimen Tested in Extension	<i>II-77</i>
A-3	Stress-Strain and Stress Ratios for Reduced Area Specimens	<i>II-78</i>



## LIST OF TABLES

Table		Page
Table I	Ramberg-Osgood Coefficients for Undegraded Backbone and Damping Curves	II-80
Table II	Ramberg-Osgood Coefficients for Curves Using $\delta = N^{-t}$	II-81
Table III	Ramberg-Osgood Coefficients for Degraded Backbone Curve - Eq. (7-11)	II-82



## CHAPTER I

### INTRODUCTION

One of the major considerations of the design of offshore structures is the effect of wave action on the foundation of the structures. This involves a study of cyclic loading done at low frequencies, and the consequence such loading has on the soil properties. The anisotropic nature of the material plays an important rôle in the dynamic as well as the static behavior of soils (18,21).

Many of the proposed models deal with soils at small strains where the soil is more or less linearly elastic. The response to large strain cycling (greater than  $\pm 10\%$ ) has not been so thoroughly researched. An experimental program has been undertaken to determine the trends in behavior of clays subjected to such loadings. Laboratory prepared clays, which are assumed to be isotropic, and normally  $K_0$ -consolidated and overconsolidated clays, which have varying degrees of anisotropy and differing stress-strain characteristics, have been cycled at periods of 20 to 40 seconds using different levels of stress. A triaxial cell using applied stress (17) on long thin hollow circular cylinders was used. The response was recorded as deformation and pore pressure changes. Damping, modulus degradation, and increasing strain values are shown to vary with overconsolidation ratio, level of applied stress, mode of applied stress, cycle number, and consolidation pressure. An attempt

was made to fit the test results to a mathematical model, incorporating the effect of increasing strain as the test progressed.

## CHAPTER II

### REVIEW OF THE LITERATURE

Much effort has been spent over the years to try to describe the behavior of soils. It has been necessary to classify the material into its constituent components to help distinguish the obvious differences between sands, silts, and clays. This study concerns clay soils.

#### A. Structure of Clays

As in all materials, the structure of the clay plays a very important role in describing it. This structure depends on a number of things, among which are the electrochemical properties of the particles and pore fluid, and the method of deposit of the particles.

Yong and Warkentin (30) describe the basic structural units of clays as examined by electron microscopy. Domains are made up of a few platelets, which are usually stacked in a parallel arrangement. Fabric units, or peds, are relatively large groups of domains. The particles within a fabric unit may be randomly or orderly arranged, and the peds themselves may be randomly or preferentially oriented. Fig. 2-1 describes four combinations of order ranging from total isotropy (random domain positions) within random ped positions) to total anisotropy (peds and domains all parallel.)

An ideal condition to study the effects of anisotropy would be compare total fabric isotropy to total fabric anisotropy. The

nearest to totally isotropic that could be developed was a clay compacted with continually changing axis of compaction. Seed and Chan (23) suggested that clays compacted at a moisture content lower than the optimum water content would have a flocculated arrangement of particles, and that those compacted higher than optimum would have a dispersed arrangement. Diamond (4) showed that the relative positions of the groups of particles, or domains, did not differ much between the wet or dry sides of the optimum, but the size of the voids were larger on the dry side. He also found only a small degree of preferential orientation normal to the axis of compaction for both wet and dry samples.

The natural sedimentation process of clay particles in fresh water results in a fabric whose properties are cross-anisotropic. One dimensional consolidation further emphasizes the ordered structure of the material. The mechanical properties of such a material have been investigated by Saada and Ou (21) and Saada and Bianchini (18). Stress-strain relationships were found to vary depending on the direction of applied stresses. Coefficients of anisotropy were described to compare stress-strain curves for different angles of principal stress.

#### B. Dynamic Properties of Clays

It has been maintained (11,29) that cycling a sensitive normally consolidated clay breaks down the sensitivity of the material and reorients the fabric until it acts like a remolded clay. This has encouraged researchers to believe that their laboratory

compacted clay represents that found in the field when considering dynamic loading. The wide range of values normally found for cyclic loading from various different researchers make it difficult to compare results with respect to clay structure.

The wide interest in liquifaction of sand due to earthquakes has generated a lot of research involving the dynamic response of soil. While clays have not shown the liquifaction phenomena, they have been known to suffer loss of strength when dynamically stressed. The analysis of pavement subgrade reaction to transient or cyclic loading was one of the first investigations into the dynamic properties of clay. One sided compressive loading was used by a number of investigators (3,5,9,22,24,26,29), some using pulse loading and others with sine or triangle waves.

Lee and Focht (11) presented a comprehensive survey of the research done on dynamic loading of clay up to 1975. They concluded that "reversing cyclic stress is more detrimental than one-directional cyclic stress." It was thought that the large excess pore pressures caused the decrease in soil strength encountered after cycling.

When applying two sided loading, for strain-controlled tests the stress typically decreased with cycle number, and for stress-controlled tests the strain increased as the test progressed. This notion has been identified as a degradation, or decrease in cyclic strength. There has appeared a level of loading in which this degradation does not show up; it has been termed the "threshold

stress" (5,9,22).

Some models have been proposed to describe cyclic stress-strain response. The two that are most commonly used are the Hardin-Drnevich hyperbolic stress-strain model (6):

$$\tau = \frac{\gamma}{\frac{1}{G'_{\max}} + \frac{\gamma}{\tau_{\max}}}$$

and the Ramberg-Osgood model (7,15):

$$\gamma = \gamma_r \frac{\tau}{G'_{\max} \gamma_r} \left\{ 1 + \alpha \left| \frac{\tau}{G'_{\max} \gamma_r} \right|^{R-1} \right\}$$

in which  $G'_{\max}$  = shear modulus at strains less than  $10^{-4}\%$ .

$\gamma_r$  = a reference strain

$\tau_{\max}$  = maximum static shear stress

$\tau, \gamma$  = cyclic amplitudes of stress and strain

$\alpha, R$  = Ramberg-Osgood coefficients

Shibata et al. (27) introduced a four-parameter relation to take into account the degradation of  $G'_{\max}$  and  $\tau_{\max}$  in the hyperbolic equation. Idriss et al(7) did the same with the Ramberg-Osgood model.

With dynamic testing, numerous failure criteria have been adopted. Some define failure in terms of pore pressure buildup or effective stress criteria (19,22), while many others involve strain amplitude or rate (13,19,28).



CHAPTER III  
EQUIPMENT AND MATERIAL USED

The material used in this research project was a frequently used commercially available clay, Edgar Plastic Kaolin from Florida. Its plastic and liquid limits are 37.5% and 56.3%, respectively, with specific gravity  $G_s$  of 2.62. A hydrometer analysis showed 76% clay content.

For purposes of comparison, the clay was prepared by two methods designed to impose either a flocculated structure or a dispersed structure to the clay.

The dispersed structure was achieved by a one-dimensional consolidation process. A slurry was prepared at 125% water content, using de-aired de-ionized water. It was consolidated in a 8" diameter oedometer for 5-6 days until reaching a 40 psi axial pressure. The final water content was approximately 50%. This clay was called the anisotropic clay. (The anisotropy was later emphasized through additional  $K_0$  consolidation in the cell prior to shearing.)

An attempt was made to prepare the flocculated clay by compaction at a water content comparable to the consolidated clay; it proved to be too soft for the compaction rod. An average water content of 40% was then used, and the clay was kneaded manually. Considerable force was used to achieve a high saturation. The clay had particles which were of a more random orientation. The material properties were assumed equivalent in all directions. This clay was

called the isotropic clay. (Isotropy was maintained by further isotropic consolidation in the cell prior to shearing.)

Both types of clay were stored for at least a week in a humid room. They were cut into hollow cylinders with an outside diameter of 2.8" and an inside diameter of 2.0". The lengths ranged from 5.5" to 6".

A modified triaxial cell was used for testing. The static testing and the one-sided testing were done in a cell in which the piston was attached to the top cap of the specimen with a bayonet type connection. This connection allowed an axial tension or compression force to be applied in combination with a torque. The magnitudes of these forces were controlled by SPAC (17), a pneumatic analog computer which applies shear and/or axial stresses in any designated ratio.

The two-sided loading used a triaxial cell with air bearings in the bushings to eliminate the effects of piston friction. The confining fluid was silicon oil with a short layer of air at the top of the cell.

One-dimensional consolidation before testing was applied to all anisotropic specimens. This was achieved by applying an axial displacement proportional to the amount of water expelled, such that lateral strain was kept at zero (16). Confining pressure was increased at 14.4 psi/hr until the desired cell pressure was reached. This procedure simulates field conditions for naturally deposited clay.

After primary consolidation was completed, the excess axial load was lifted and the clay was allowed to rebound hydrostatically so that testing could start from a deviator stress of zero. The amount of area change during this rebound phase was minimal. The isotropic clay was consolidated hydrostatically.

One-sided loading was controlled with pressure switches. The two-sided loading cycles were applied by a voltage output signal generator. A Fairchild current-pressure transducer converted the signal to air pressure, and SPAC was used to apply axial forces and torque. Axial force, torque, pore pressure, and axial and rotational displacements were all measured by transducers and recorded on a Gould chart recorder and two Hewlett-Packard X-Y recorders.

Three basic types of tests were run: static, one-sided cyclic, and two-sided cyclic. Slow monotonic loading was done to get the static strengths for normally  $K_0$ -consolidated, isotropically consolidated, and overconsolidated clays. A total of thirty-five static tests were run.

Normally  $K_0$ -consolidated and isotropic clays were tested using one-sided loading, in which the stresses never changed direction (Fig. 5-1). Twelve of these tests were carried out and evaluated to examine the differences between the two clay structures.

Two sided cyclic loading was done on normally  $K_0$ -consolidated, isotropically consolidated, and overconsolidated clay. Of the normally consolidated specimens, eleven had a single stress level for the duration of the test and four were cycled using increasingly

greater stresses. The overconsolidated specimens were all tested with a minimum of three stress levels.

CHAPTER IV  
RESPONSE TO MONOTONIC LOADING

Monotonic loading was done primarily to compare static behavior of one-dimensionally consolidated clays to the compacted, isotropic clay. The failure strengths obtained were used as parameters for the subsequent cyclic loading.

A. Testing Procedure

Kaolinite clays, consolidated from a slurry, were cut into hollow cylinders and further consolidated one-dimensionally in the triaxial cell. The final cell pressure was reached in two to four hours. After eight hours the axial load was reduced to hydrostatic permitting the specimen to rebound axially for eight hours minimum. This resulted in an overconsolidation ratio of  $1/K_0$  in the vertical direction and 1.0 in the lateral directions, or an approximate average of 1.3 overall. These specimens were called the normally  $K_0$ -consolidated specimens.

For tests done on overconsolidated clays the same consolidation procedure was followed until rebound, when the hydrostatic pressure was reduced by the overconsolidation ratio. This left an overconsolidation ratio for the vertical direction twice as high as that for the radial direction, or an actual average overconsolidation ratio 1.3 times higher than the overconsolidation ratio.

The isotropic clays were consolidated hydrostatically, with the final cell pressure being reached in two to four hours. The

specimen was left to stabilize for at least eight hours after primary consolidation.

The testing was done using SPAC, with the stresses being applied at a constant rate, 0.2 psi/min. for axial loading and 0.1 psi/min. for torsional loading. Failure was noted for brittle materials with sudden deformation. Overconsolidated clays tested in torsion were defined to reach failure condition when the axial deformations reached a maximum. This usually occurred at shear strains of 6 to 9%.

Static tests were run on normally and hydrostatically consolidated clays at effective confining pressures of 40 psi and 60 psi in the extension, compression, and torsional loading directions. The overconsolidated clays were tested in the three directions at effective cell pressures of 10, 15, and 20 psi with lateral overconsolidation ratios of 2 and 4. An additional trio of tests were run at an effective cell pressure of 10 psi with an overconsolidation ratio of 8.

#### B. Normally Consolidated Clay, Anisotropic

Examination of the stress-strain curves and pore-pressure curves in Fig. 4-1 shows that the clay is always stronger in compression than extension, although more brittle. The failure strain for compression is about half that for extension, while the failure strength,  $(\sigma_1 - \sigma_3)$ , is about 1.4 times higher.

The pore pressure created in compression is always positive and always increasing. It levels off only at failure. In the

extension mode, though, the pore pressure changes such that the ultimate decrease in pore pressure is one-fourth the pore pressure developed in compression. The stress-strain curves in the pure torsional loading are similar in shape to the extension mode, and the pore pressure increases gradually, then levels off.

In the extension mode, for the tests done at confining pressures of 40 psi, the minor principal effective stress,  $\bar{\sigma}_3$ , decreased below zero and continued into suction for a short time until failure. The Mohr's circle at failure covered the origin of the  $\tau$ - $\bar{\sigma}$  axes, creating a situation in which it was impossible to define a friction angle. [The fact that the clay itself was in tension has also been shown by Bishop and Garga (2)].

This strength in pure tension was further shown with small cylindrical specimens tested in a triaxial Geonor Cell.<sup>1</sup> It was found that for both one-dimensionally consolidated and compacted Kaolinite the minor principal effective stress became less than zero before failure had occurred. This indicates that the Kaolinite clay particles themselves maintain a tensile force, possible due to what has often been called the true cohesion of the clay.

### C. Isotropic or Compacted Clay

The effect of the clay fabric becomes very evident when the compacted clay, which has particles of more random orientation than the one-dimensionally consolidated clay, is compared to the more

---

<sup>1</sup>Tests run by R. Snyder, See Appendix 1

ordered structure of the  $K_0$ -consolidated clay. It was noticed that the strength of the compacted clay was less than the strength of the anisotropic clay for the respective confining pressures. This occurred even though the compacted clays had water contents in the range 30-35%, and the  $K_0$ -consolidated ones 39-43%. If it had been possible to test a  $K_0$ -consolidated saturated sample at 30% water content, the static strength would have been greater than either of the clays actually tested. So the strength difference cannot be accounted for by the difference in water contents alone, and therefore is highly influenced by differences in clay structure and bonds.

As seen in Fig. 4-2, the shapes of the monotonic loading curves were not always similar to those curves for anisotropic material. The compacted material in compression was much more ductile than the anisotropic clay, with a consistently lower tangent modulus until failure. The extension and torsion tests had the same shaped curves for both clay fabrics; however, the extension strength was much closer to the compression strength for compacted clay. Due to the increased ductility and lower strength in compression, the failure strains were comparable for extension and compression, while the failure strains for  $K_0$ -consolidated clay were twice as high for extension than compression.

The pore pressures also show different behavior for the compacted clay. For all three directions of loading, the pore pressure development was positive until it reached a maximum value



near one-third of the failure strain, and then it gradually decreased. This resulted in a change in the effective stress paths for the extension and torsional loading, even though the shapes of the stress-strain curves were similar.

#### D. Overconsolidated Clay

Normally consolidated clay may be considered to be overconsolidated with an overconsolidation ratio of one. Therefore, there should be a smooth transition in stress-strain behavior as overconsolidation ratio increases. A trend was observed along these lines in the compression and torsional directions of loading, with static strength continuing to increase with overconsolidation ratio. The compression curves became more brittle with higher values for the tangent modulus as overconsolidation ratio increased. Higher failure stresses were observed with increased overconsolidation ratio. Typical stress-strain curves and pore pressure development curves are presented in Fig. 4-3.

The failure stresses in the extension and torsion directions also were greater as overconsolidation ratio rose. The torsion stress-strain curve resembled the normally  $K_0$ -consolidated curve, with a shape similar to the first part of the extension curve.

Extension behavior displayed the greatest difference between normally consolidated and overconsolidated clay. Ductility was increased tremendously. Many times, 18% strain was exceeded without indicating a failure condition. The height limitations of the testing cell prevented some of the tests from stressing until a

failure condition was noted. In all cases, extension strength was greater than compression strength for overconsolidation ratios of two or more.

The stress-strain curves in the extension direction initially followed curved paths very similar to those of the normally consolidated extension tests. However, near 2-3% strain, the curves became linear, and remained so. These straight line portions had slopes ranging from 200 to 300 psi/unit strain, with no dependence on consolidation pressure or overconsolidation ratio. During this linear behavior the minor principal effective stress decreased to zero and continued in the negative direction. In over 70% of the cases, the minor principal total stress decreased past zero and held a suction force without showing failure.

It was noted that the minor principal effective stress became less than zero for all extension tests. This also happened for torsional tests with low consolidation pressures and low overconsolidation ratios. Negative pore pressure development was maintained for extension and torsional loading. The compression loading initially had a positive pore pressure development, eventually decreasing to less than 15% of the peak and crossing zero in 85% of the tests.

CHAPTER V  
ONE SIDED LOADING

Loading is defined as one sided when the deviator stress is always positive or always negative. Low frequency triangle waves were applied to both  $K_0$ -consolidated and isotropically consolidated clays to examine the differences in response.

A. Testing Procedure

Consolidation for the two types of clay was carried out as explained in the previous chapter. Both isotropic and  $K_0$ -consolidated clays were tested at 40 and 60 psi effective confining pressures. Three loading directions were evaluated: axial compression, axial extension, and pure torsion. The maximum deviator stress per cycle was 85% of the failure stress in static loading<sup>1</sup> for each direction while the minimum stress per cycle was 3 psi, as illustrated in Fig. 5-1.

Stress application was done by a motorized pressure regulator. Electro-pneumatic switches reversed direction of the motor at the maximum desired stress, thus producing a triangular stress input. All tests were run at periods from 20 to 40 seconds. Force, torque, axial deformation, rotational deformation, and pore pressure response were measured by various transducers and recorded. Each specimen was cycled for a minimum of 200 cycles or until failure. Failure was noted as a sudden increase either in average deformation or in strain amplitude.

---

<sup>1</sup> For  $K_0$ -consolidated clay, static strengths were determined by  $Q_u$  (2).

## B. Strain Behavior

Stress-strain loops were open at the beginning of each test. As the number of cycles,  $N$ , increased, the loops closed while migrating in the direction of positive strain. The average strain, defined as  $\frac{1}{2}(\epsilon_{\max} - \epsilon_{\min})$ , (Fig. 5-2), continued to increase slowly, while the strain amplitude remained fairly constant, until failure.

A comparison of the isotropic and the  $K_0$ -consolidated clay strain behavior plotted versus  $N$  indicated different responses. As can be seen from Fig. 5-3, the average strain for  $K_0$ -consolidated Kaolinite increased at a lower rate than the isotropically formed clay for the three loading directions. Extension and torsion tests had equivalent envelope shapes for both clay structures, but isotropic specimens were much less brittle in the compression mode. This tendency parallels that noted in the monotonic loading. Although an 85% stress level ( $\frac{\sigma_d}{\sigma_{d \max, \text{static}}}$ ) was used for all tests, failure was observed more often and at fewer cycles for compacted clays than the one-dimensionally consolidated clays. The randomly oriented clays lost their strength much more rapidly than the orderly clays.

The differences in strain behavior which were noted in the monotonic loading were also present in this cyclic, one sided loading. Both the relative ductility of the compressive specimens and the average strains at failure distinguished between isotropic and  $K_0$ -consolidated specimens. Although the  $K_0$ -consolidated specimens had achieved a substantial disturbance, they still retained many properties of their initial structure. So while it is

acknowledged that disturbance will greatly affect cyclic properties, the clay fabric is also an important factor in behavior.

C. Pore Pressure Development

Pore pressure was measured from the base of the specimen. The cyclic amplitude of the pore pressure was not fully transmitted to the transducer although both the outside and the inside of the cylindrical specimen were covered with filter paper. It was expected that the measured pore pressure fluctuations gave a relative indication of the effect of the clay anisotropy.

The shapes of the pore pressure development curves for monotonic compression loading compared to the cyclic pore pressure curves presented in Fig. 5-4 indicate that the average pore pressure increases for the anisotropic clay. The isotropic clay showed a levelling off of the pore pressure development curve, and then a decrease, as in the static case. The extension and the torsion modes appear to have no difference in pore pressure for isotropic or anisotropic clay.

D. Secant Moduli

The secant modulus,  $G'$  or  $E'$ , defined as the slope of the line connecting the tips of the hysteresis loops,  $\frac{\tau_{\max} - \tau_{\min}}{\gamma_{\max} - \gamma_{\min}}$ , or  $\frac{\sigma_{\max} - \sigma_{\min}}{\epsilon_{\max} - \epsilon_{\min}}$ , could only be measured when the loops finally closed. An increase in secant modulus indicates a decrease in strain amplitude, which is often called a strengthening effect.

As seen in Fig. 5-5, the anisotropic extension and torsion specimens appeared to have constant secant moduli as  $N$  increased

until relatively high values of N were reached, when secant moduli rose slightly. In the isotropic specimens the increase in G and E occurred almost immediately. The relationship between secant modulus and cycle number is discussed in Chapter 6.

#### E. Equivalent Damping Ratio

Equivalent damping ratio is defined as  $\frac{1}{4\pi} \frac{\Delta W}{\frac{1}{2} G \gamma^2}$ , where  $\Delta W$  is the area of the hysteresis loop (total energy lost per unit volume) and  $\gamma$  is one-half the cyclic strain difference,  $\frac{1}{2}(\gamma_{\max} - \gamma_{\min})$ . To fit the definition, this had to be measured after the loops had closed, so damping for the initial cycles was not accurately evaluated.

The damping ratio showed no dependence on direction of loading or on initial consolidation pressure, Fig. 5-6. For controlled stress tests the strain increased with each cycle, yet the damping showed very little dependence on strain. In fact, there was a slight decrease of damping as cycle number increased for both the anisotropically and isotropically consolidated specimens. Overall, the equivalent damping ratios for the  $K_0$ -consolidated clays were 20% to 30%, and for isotropically consolidated clay 25% to 35%.

CHAPTER VI  
TWO SIDED LOADING

The bulk of the experimental program involved two sided loading of hydrostatically and one-dimensionally consolidated clay. Both normally consolidated and overconsolidated cases were studied. The main area of concern was the strain response, involving total deformation as well as secant moduli and damping. A comparison was made of these properties that showed a definite degrading behavior as the number of cycles increased. The data was fit with a Ramberg-Osgood model, to be discussed in Chapter 7.

A. Testing Procedure

The consolidation procedure was as described in Chapter 3. After consolidation the clay was allowed to rebound for a minimum of eight hours so that a hydrostatic stress condition existed at the start of loading. Deviator stresses for some tests were applied with the triangular loading system used for one-sided loading. A wave generator provided sine waves for other tests. An inspection of the response showed that strain amplitude differed little between the two wave types, and the shape of the cyclic deformation was very similar for both triangle and sine waves. This is probably due to the high level of damping associated with the clay at the given stresses.

Loading was always symmetrical with respect to the hydrostatic stress condition. Stress amplitude depended on the failure stress obtained in the monotonic loading. For the torsional loading

the stress level was simply the ratio of single amplitude deviator stress to static strength. Since the loading was in a direction normal to the material's axis of symmetry (for anisotropic clay), there was no distinction between positive and negative shear.

For the axial loading, one half of each cycle was in compression and one half in extension. To determine the stress level the lower failure stress of the two directions was taken as the reference. Thus for the normally consolidated specimen the stress level was the percentage of deviator stress to extension strength, and for overconsolidated clay it was the percentage of the compression strength. This results because for overconsolidated clay the failure stress in extension is higher than in compression - Fig. 4-4.

Some specimens were tested with a constant stress level until failure was noted by rapidly increasing strain amplitude. If no failure had developed they were cycled at least 100 times. No stress level was maintained for more than 1000 cycles. On other specimens loading was incremented at increasingly greater stresses with each stress level being applied for 100 or more cycles.<sup>1</sup> An increment began from a hydrostatic stress state after an interval of 10 to 20 minutes. In the event local buildups occurred during the previous loading, the drainage remained closed during this interval but the pore pressure was believed to have equalized itself.

---

<sup>1</sup> For a few of the extremely low stress levels when deformation was too small to be detected, loading was stopped before 100 cycles.



The possible change in strength and maximum shear modulus which may have occurred during the previous loading period was assumed negligible when compared to the disturbance caused by the first few cycles of the next larger stress level.

Changes in pore pressure, axial and rotational deformations, and forces were recorded on strip charts. Force-deformation loops were recorded on X-Y recorders. Damping was measured from these loops, and secant modulus from the chart recordings.

#### B. Strain Behavior

Clay responds with the same strain magnitude when shear stresses are applied in either the positive or negative directions. Therefore, the stress-strain loops maintain symmetric strain for symmetrically applied stress. Fig. 6-1 shows stress-strain loops for a torsional test in which the average strain,  $|\gamma_{\text{pos}}| - |\gamma_{\text{neg}}|$ , is nearly zero for all cycles.

An examination of the static stress-strain behavior for clays in compression and extension always indicates a strain for a given stress which is greater in the extension direction. It follows that the strain on the extension side of the cyclic loading is larger than the compressive strain, and that the average strain will be an extension strain. The  $K_0$ -consolidated clay maintained an extension strain from the start of each test. Fig. 6-2 shows typical behavior for axial loading on this clay, with the loops completely on the extension side of the stress axis.

A simple model to describe this behavior is the kinematic hardening model. A typical stress-strain curve in the axial

direction has a weaker, more ductile extension curve, while the compression side has a higher tangent modulus. If a loop is imposed on the clay with equal stresses in extension and compression, the loop will migrate to a steady position with strains being mostly extension strains. If the clay is subjected to equal strains in compression and extension, the loop will shift to show mostly compressive stresses. Thus the model predicts a shift from the origin whenever a material has properties which differ in opposing directions. (20)

The extent of this shift in average strain is significant for the  $K_0$ -consolidated clay when compared to the isotropic, compacted clay. The isotropic clay had a more ductile static compression curve, with tangent modulus being much closer to the extension curve for that material. The cyclic loading in the axial direction produced an average strain still on the extension side, but much closer to zero, Fig. 6-3. This average strain behavior was changed little by the number of cycles, except at failure. So by looking at the strains produced in the Nth cycle, it was easily determined whether the clay was anisotropic or isotropic by noticing the position of the average strain relative to the strain amplitude. It is concluded that the distinctive behavior of isotropically and anisotropically formed clays prevents them from being substituted for each other in any testing program.

Failure was noted with a sharp increase in strain amplitude. The isotropic clay typically failed much sooner than the

anisotropic when cycled at the same stress level. The strain amplitude consistently was greater for isotropic than anisotropic material.

As with the one-sided loading tests in Chapter 5, the two-sided cyclic tests displayed a steady increase in pore pressure such that the effective stress became zero or negative on the extension side of loading. This usually occurred several cycles before failure was noted, which may have been a result of the change in sign of the effective stresses.

### C. Secant Modulus

The hysteresis loop of the Kaolinite tested was such that maximum strain occurred at the instant of maximum stress, and minimum strain at the instant of minimum stress. Secant modulus is defined as the slope of the line connecting the tips of the hysteresis loop. This line becomes equal to the shear or elastic modulus,  $G'_{max}$  or  $E'_{max}$ , as strain becomes very small. The quantities  $G'_{max}$  and  $E'_{max}$  were measured in the resonant column device (1) for each of the consolidation methods and water contents used in the testing program. Secant moduli measured in the slow cyclic loading tests were usually normalized by dividing by  $G'_{max}$  or  $E'_{max}$  for comparison purposes.

For a controlled stress test the stress amplitude was kept constant and the corresponding strains were recorded. Each loop was assumed to be centered at the origin of the stress-strain axes, even though it is acknowledged that loop migration took place. So as strain amplitude increased,  $G' = \frac{\tau}{\gamma}$  or  $E' = \frac{\sigma_d}{\epsilon_z}$  decreased. This

reduction in secant modulus is called degradation, and indicates the difference between the first cycle loop and the Nth cycle loop, or the first cycle strain and the Nth cycle strain.

Two things must be emphasized before any further discussion:

1) The strain behavior for a constant stress amplitude may be characterized by average strain migration and by strain amplitude, both of which depend on N. 2) The initial cycle presents a loop which has a large strain before the first stress reversal, and upon return of the stress to the initial position the strain does not come close to its original position. Loop O-A-B-C in Fig. 6-2 is not closed, so the secant modulus is undefined in this 'loop'. Therefore, the 'first' cycle response must be determined from extrapolation of subsequent cycles. This extrapolated first cycle secant modulus in some cases coincided quite well with the measured modulus, especially for low stress levels. On the other hand, when it did not represent the measured conditions, the extrapolated value differed as much as 30% from the measured modulus. In any case, all analyses were made with the extrapolated value for the first loop instead of the measured data.

A plot of  $\log \frac{E'_1}{E'_{max}}$  vs  $\log N$ , Fig. 6-4, shows typical degradation behavior. The values of  $\frac{E'_1}{E'_{max}}$  are extended to  $N=1$ , and this is taken as  $\frac{E'_1}{E'_{max}}$ . The secant modulus for the Nth cycle,  $G'_n$  or  $E'_n$  is related to the initial secant modulus by the degradation index(17)

$$\delta = \frac{G'_n}{G'_1} \quad \text{or} \quad \frac{E'_n}{E'_1} \quad (6-1)$$

For small levels of stress the degradation index (which can also be defined as  $\frac{\gamma_1}{\gamma_n}$  for a constant stress amplitude, or as  $\frac{\tau_n}{\tau_1}$  for a constant strain amplitude) forms a line which has a linear plot with  $N$  on log-log scales (7). The slope of this line is defined as  $t$ , the degradation parameter.

$$\delta = N^{-t} \quad (6-2)$$

Stress levels greater than 30% usually produced a non-linear degradation curve, mostly with slope increasing with  $N$ . Degradation index is plotted versus  $N$  for several loads on anisotropic clay in Fig. 6-5.

Other investigators (7) using constant strain amplitude tests and the linear relation  $\delta = N^{-t}$ , obtained a smooth curve relating the parameter  $t$  with strain amplitude. With constant stress amplitude tests, when degradation parameter  $t$  was obtained by a power fit least squares method, most  $t$ 's were found within a band which increased with stress level. The range of values of  $t$  within this band was too wide to be used for prediction purposes. Fig. 6-6 shows little correlation between  $t$  and stress level for isotropic clay, and small dependence of  $t$  on stress level for anisotropic clay.

#### D. Damping

Damping energy is defined as work done during a cycle of loading, (10,26). This is measured as the area within the force-deformation loop divided by the specimen volume. Fig. 6-7 shows

that as N increases, the energy lost increases for a constant stress amplitude.

Specific damping capacity is the ratio of the energy lost per unit volume,  $\frac{\Delta W}{V_0}$ , to the maximum potential energy stored during the cycle. The maximum potential energy can be defined as the average of the potential energy from the positive loading direction and that from the negative direction, or as  $\frac{1}{2}(A_a + A_b)$  on Fig. 6-8. These areas can be equated by moving the  $\gamma=0$  position to midway between  $\gamma_a$  and  $\gamma_b$ . Thus the maximum potential energy is  $\frac{1}{2}\tau\gamma$ , in which  $\gamma$  is one half the double amplitude strain response. In terms of shear stresses and strains, P.E.<sub>max</sub> =  $\frac{1}{2}\tau\gamma$  or  $\frac{1}{2}G'\gamma^2$

$$\text{specific damping capacity} = \frac{\Delta W/V_0}{\frac{1}{2}G'\gamma^2} \quad (6-3)$$

Equivalent damping ratio, or equivalent damping, is simply  $\frac{1}{4\pi}$  times the specific damping capacity. This is Lehr's definition of damping ratio. Various definitions determine the amount of potential energy used in the equivalent damping relation. Roelig(25) damping is defined as

$$D_{\text{Roelig}} = \frac{1}{4\pi} \frac{\Delta W}{W_i} \quad (6-4)$$

where  $W_i$  is the area of energy under the loading half of the loop, shaded in Fig. 6-9. If it is assumed that the secant modulus line divides the loop in half, then

$$W_i = \frac{1}{2}\Delta W + 4\left(\frac{1}{2}G'\gamma^2\right) \quad (6-5)$$

From Lehr's definition of damping,

$$\Delta W = 4\pi \left( \frac{1}{2} G' \gamma^2 \right) D_{Lehr} \quad (6-6)$$

Combining Eq. 6-5 and Eq. 6-6 into Roelig's definition of damping,

$$D_{Roelig} = \frac{D_{Lehr}}{4+2\pi D_{Lehr}} \quad (6-7)$$

Most of the measured values of  $D_{Lehr}$  were in the range of 20-30%, so Roelig damping was one-fifth to one-sixth Lehr damping. To be consistent with the literature, the Lehr definition was used on all damping ratio evaluations.

In most tests, damping remained relatively constant throughout the entire test. The isotropically consolidated clays presented a trend of slightly decreasing damping ratio as  $N$  increased. Normally, the area of the loop grew with  $N$  as cyclic strain grew. The stored potential energy, however, grew by at least the same amount so the effects of increasing strain were not evident in the damping ratio. The  $K_0$ -consolidated clays displayed a very slight decreasing damping behavior with  $N$ . Typical damping vs  $N$  data is shown in Fig. 6-10. This condition has been noted by Idriss, et al. (7) using controlled strain amplitude testing.

It is interesting to note that there appeared a small dependence of damping ratio on stress level. Naturally, the strain amplitude for any given  $N$  increased as stress level increased. Traditionally it has been indicated that damping ratio rises with strain, so it should rise with stress level since damping shows

little dependence on  $N$ . The effect of the stress level is seen particularly for low stress levels; for stress levels higher than 30% this effect is negligible. An envelope may be described when damping ratio vs strain is plotted for each test, Fig. 6-11, showing the general trend towards higher damping ratios with higher strain amplitudes.

Overconsolidated clay reacted very similarly to the normally  $K_0$ -consolidated clay. The overconsolidation ratio had no effect on the magnitude of the damping ratio. There was a definite decrease with  $N$  in damping ratio for all the axial loading. Most of the torsional tests ( $\bar{\sigma}_c = 10$  and  $\bar{\sigma}_c = 20$  psi) showed a small but steady increase in damping. As expected, there occurred an increase in damping ratio with stress level. Fig. 6-12 shows typical damping ratios for overconsolidated clays.



## CHAPTER VII

### RAMBERG-OSGOOD MODEL

In this study, we need to know three things about any particular stress-strain loop. The first is the position of the center of the loop. This may be determined from a relationship between the average strain expected for a certain stress level and a given cycle number; it depends on the amount of non-symmetry between the two loading directions. The second is strain amplitude, given by the amount of secant modulus degradation involved and the estimate of the first loop's strain amplitude. The third is the damping ratio, which can be reasonably estimated within the range of stress levels used in this testing program. The second and third items here may be described by a mathematical model for two sided loading. Such a model would be the Ramberg-Osgood model (14).

#### A. Backbone Curve

For a material cycled under a constant stress amplitude, the hysteresis loop defines two strain extremes. The magnitude of strain measured between these extremes is the peak-to-peak strain, and the strain amplitude is defined as one-half of this magnitude. Different stress levels result in loops with different strain amplitudes. A plot of the stress levels versus the strain amplitudes yields what is called the backbone curve.

If a material has the same behavior in extension and compression and does not degrade during cycling then the backbone curve coincides with the stress-strain curves. If a material, such as most soils, has different behaviors in extension and compression then the hysteresis loops will shift away from the origin of a stress-strain diagram. The backbone curve will still describe the strain amplitude, but will have no bearing on the position of the loop. In this case the backbone curve will not concur with the stress-strain curves.

B. Ramberg-Osgood Equation

Most static stress-strain curves for clay can be well represented by a Ramberg-Osgood (14) type of equation. Since in most cases the backbone curve shows similarity to the monotonic loading curve, it will be assumed that the Ramberg-Osgood equation adequately describes the backbone curve.

The Ramberg-Osgood equation is stated as:

$$\gamma = \gamma_r \frac{\tau}{G'_{\max} \gamma_r} \left\{ 1 + \alpha \left| \frac{\tau}{G'_{\max} \gamma_r} \right|^{R-1} \right\} \quad (7-1)$$

in which

- $\gamma$  = strain amplitude
- $\tau$  = stress amplitude
- $\gamma_r$  = reference strain
- $G'_{\max}$  = secant modulus at strains lower than  $10^{-6}$
- $\alpha, R$  = Ramberg-Osgood parameters

$\gamma_r$  is often arbitrarily chosen as a small strain such as  $10^{-4}$  and then  $\alpha$  will depend on this reference strain. In this study the reference strain was a constant relating to the material

properties of the clay,  $\gamma_r = \frac{\tau_{\max}}{G'_{\max}}$ .  $\tau_{\max}$  and  $G'_{\max}$  primarily depend on the consolidation pressure, water content, and degree of anisotropy (6).

The backbone curve is now described by

$$\gamma = \frac{\tau}{G'_{\max}} \left\{ 1 + \alpha \left| \frac{\tau}{\tau_{\max}} \right|^{R-1} \right\} \quad (7-2)$$

or

$$\frac{G'_{\max}}{G'} = 1 + \alpha |SL|^{R-1} \quad (7-3)$$

where  $G' = \frac{\tau}{\gamma}$  and  $SL = \text{stress level} = \frac{\tau}{\tau_{\max}}$ .

For the axial loading the Ramberg-Osgood equation becomes

$$\frac{E'_{\max}}{E'} = 1 + \alpha |SL|^{R-1}$$

One can see that as SL approaches zero,  $E'$  becomes  $E'_{\max}$ .

The clay tested had all been previously tested in static loading, so  $\tau_{\max}$  and  $\sigma_{\max}$  were known. They were also tested in the resonant column to get  $G'_{\max}$  and  $E'_{\max}$ , so the only unknowns in the model were  $\alpha$  and  $R$ .

Since the first cycle of loading imposed total strains on the specimen, it is incorrect to describe the backbone curve and all subsequent behavior with the constants obtained for the first cycle. It is common in the literature to find the tenth cycle used to describe the backbone curve for the purpose of predicting

earthquake responses. This is reasonable because any single earthquake is not expected to create more than ten cycles of a certain amplitude. As mentioned previously, the end points of the tenth cycle loop define the strain amplitude used in constructing the backbone curve for the cycle.

Using Eq. (7-3) and fitting the tenth cycle data from the  $K_0$ -consolidated clay, the axial tests for  $\bar{\sigma}_c = 40$  psi gave coefficients of 4.09 for R and 123.0 for  $\alpha$ .

The Masing criterion (12) is used to describe loading and unloading. It is assumed that the loading branch of the loop is twice the ordinates of the backbone curve, and that the unloading branch is symmetrical about zero. Having the mathematical expression for the loop enables one to determine the area within the loop, and thus get a relation for damping ratio. Jennings (8) expressed damping ratio using the Masing criterion with a Ramberg-Osgood backbone curve as

$$\lambda = \frac{2\alpha}{\pi} \frac{\left(\frac{\tau}{G'_{\max} \gamma_r}\right)^R}{\gamma/\gamma_r} \frac{R-1}{R+1} \quad (7-4)$$

which can be simply expressed as

$$\lambda = \frac{2}{\pi} \frac{R-1}{R+1} \left(1 - \frac{G'}{G'_{\max}}\right). \quad (7-5)$$

It is advantageous to use this form of the equation because there is only one coefficient to find. After the R has been found the data is put back into Eq. (7-3) to find  $\alpha$ .

As was seen in Chapter VI, the damping ratios were all within the range 20-30%, while the secant moduli had large differences between stress levels.

Using Eq. (7-5) R can be evaluated for each loop measured at each stress level. For the tenth cycle, each stress level predicted a different R which in all cases was lower than the R obtained by linear regression of the backbone curve. The  $\alpha$ 's in all cases were lower than the  $\alpha$  predicted by the backbone curve.

In Table I Ramberg-Osgood coefficients are obtained using eqs. (7-5) and (7-3). Thus the combination of the Masing criterion with this version of the Ramberg-Osgood backbone curve does not represent the actual data. Masing predicts a loop of larger area than that which actually happens, which indicates that the loading and unloading sides of the loop generally don't follow the backbone curve or its slope. The last column in Table I gives  $\lambda$  predicted by Eq. (7-5) using the R value from the fourth column. These  $\lambda$ 's are always higher than those measured. The calculated and the measured  $\lambda$ 's are shown in Fig. 7-1, plotted with the measured  $\frac{E'}{E'_{\max}}$  or  $\frac{G'}{G'_{\max}}$ .

### C. Degradation

It has been shown that as the number of cycles increases, the secant moduli decrease. A plot of the backbone curve for various cycle numbers indicates that the curve itself degrades, Fig. 7-2. Previous investigation (5, 9, 22) suggests a threshold stress or strain before degradation can occur, so it is presumed that  $G'_{\max}$  itself does not degrade. Idriss, et al. (7) introduced the degradation

idea into the Ramberg-Osgood equation by multiplying  $\tau$  by  $1/\delta$ , where  $\delta$  is the degradation index. Their revised expression for the backbone curve is:

$$\gamma = \gamma_r \frac{\tau}{\delta G'_{\max} \gamma_r} \left\{ 1 + \alpha \left| \frac{\tau}{\delta G'_{\max} \gamma_r} \right|^{R-1} \right\}$$

or

$$\frac{\delta G'_{\max}}{G'} = 1 + \alpha \left| \frac{SL}{\delta} \right|^{R-1} \quad (7-6)$$

Following this lead, Jennings' expression for damping ratio based on Eq. (7-4) is

$$\lambda = \frac{2\alpha}{\pi} \left( \frac{\tau/\delta}{G'_{\max} \gamma_r} \right)^R \frac{1}{\gamma/\gamma_r} \frac{R-1}{R+1}$$

which becomes

$$\lambda = \frac{2}{\pi} \frac{R-1}{R+1} \left( 1 - \frac{G'}{\delta G'_{\max}} \right) \quad (7-7)$$

Contending that  $\delta = N^{-t}$  with  $t$  depending on stress level,

$$\frac{G'_{\max}}{G'} N^{-t} = 1 + \alpha |SL \times N^t|^{R-1} \quad (7-8)$$

and

$$\lambda = \frac{2}{\pi} \frac{R-1}{R+1} \left( 1 - \frac{G'}{G'_{\max}} N^t \right). \quad (7-9)$$

The  $\alpha$  and  $R$  calculated by linear regression for the tenth cycle with the computed  $t$ ,  $G'$ , and  $SL$  for the axial mode at  $\bar{\sigma}_c = 40$  psi are  $\alpha = 4.45$  and  $R = 2.30$ . These are much closer to the original  $\alpha$  and  $R$  obtained from the first cycle compression and extension tests, but a little lower. Table II lists the Ramberg-Osgood coefficients

for this form of the backbone curve.

The damping expression, Eq. (7-9), when used to predict the coefficient R, gives more consistent results when the degradation is taken into account. The axial case presented a higher R when evaluated by the backbone curve than from the damping curve, while the opposite happened for the torsional mode. An examination of the damping ratios predicted from Eq. (7-9) using the R obtained from the backbone curve shows underestimation of the actual damping. However, the damping ratios do not vary quite as much with stress level as when evaluated using Eq. (7-5), and this follows the trend found in the data.

Eq. (7-8) may be very useful for predicting  $\frac{G'}{G'_{\max}}$  if the degradation index  $\delta$  follows the form  $N^{-t}$ . Stress levels in excess of 20% usually do not have such a simple relationship, and therefore this expression is not representative of what actually happens. For the bulk of the stress levels tested, an expression was not found which described the degradation index in terms of N, so the definition  $\delta = \frac{G'}{G'_1}$  was used. A look back at Eqs. (7-6) and (7-7) bring

$$\frac{G'}{G'_1} \frac{G'_{\max}}{G'} = 1 + \alpha \left| \frac{G'_1}{G'} SL \right|^{R-1} \quad (7-10)$$

or

$$\frac{G'_{\max}}{G'_1} = 1 + \alpha \left| \frac{G'_1}{G'} SL \right|^{R-1} \quad (7-11)$$

and

$$\lambda = \frac{2}{\pi} \frac{R-1}{R+1} \left( 1 - \frac{G'_1}{G'} \frac{G'}{G'_{\max}} \right)$$

or

$$\lambda = \frac{2}{\pi} \frac{R-1}{R+1} \left( 1 - \frac{G'_1}{G'_{\max}} \right) \quad (7-12)$$

It is recommended to use these forms of the Ramberg-Osgood and damping equations when the relation  $\delta = N^{-t}$  does not apply, especially for large strain responses.

Using Eq. (7-12), the damping ratio becomes independent of the cycle number if the Ramberg-Osgood coefficient  $R$  is assumed independent. This fits the damping data much more closely than the other formulations of the damping ratio. However, it does not explain the slight decrease in damping ratio with increasing cycle number.

Eq. (7-11) may be stated

$$\frac{G'_{\max}}{G'_1} = 1 + \alpha \left| \frac{G'_1}{\tau_{\max}} \gamma \right|^{R-1}.$$

If the cyclic strain remains constant then it is evident that for all cycles the coefficients  $\alpha$  and  $R$  remain constant. However, for constant stress amplitude tests the strain increases with cycle number and therefore  $\alpha$  and/or  $R$  must be functions of  $N$ . Therefore, the idea of Ramberg-Osgood 'constants' does not apply when degradation is introduced into the Ramberg-Osgood equation. Assuming a unique backbone curve for each cycle  $N$ , and solving the backbone curve for  $\alpha$  and  $R$ , the values in Table III are obtained. When plotted on log-log scales, the  $\alpha$  and  $R$  coefficients form smooth curves of approximately consistent shapes, Fig. 7-3. For torsional loading, the higher consolidation pressure had higher values of  $\alpha$  and  $R$  than the lower consolidation pressure. However, the opposite is true for the axial cyclic loading. The  $\alpha$  and  $R$  curves seem to



level out as the cycle number increases, and may reach a constant value for non-failure behavior. It is suspected that tests run at other consolidation pressures would result in  $\alpha$  and  $R$  following the same trends.

Given specific  $R$  vs and  $\alpha$  vs  $N$  curves for a consolidation pressure, Eq. (7-11) may be solved for secant modulus:

$$\frac{G'_n}{G'_{\max}} = \frac{G'_1}{G'_{\max}} \frac{SL}{\left[ \frac{1}{\alpha_n} \left( \frac{G'_{\max}}{G'_1} - 1 \right) \right]^{R_n - 1}} \quad (7-13)$$

$\frac{G'_1}{G'_{\max}}$  is found using the expression for the backbone curve with  $\alpha_n = \alpha_1$  and  $R_n = R_1$ . Substituting Eq. (7-3) into Eq. (7-13), an expression involving  $\alpha$ ,  $R$ , and  $SL$  is obtained:

$$\frac{G'_n}{G'_{\max}} = \frac{\left[ \frac{\alpha_1}{\alpha_n} |SL|^{(R_1 - R_n)} \right]^{\frac{1}{1 - R_n}}}{1 + \alpha_1 |SL|^{R_1 - 1}} \quad (7-14)$$

It is imperative that the stress level be constant for this equation.

Eq. (7-14) enables one to determine  $\frac{G'_n}{G'_{\max}}$  without having to compute  $G'_1$ . Its accuracy depends on the accuracy of the previously determined relationship between  $R_1$ ,  $\alpha_1$ ,  $R_n$ , and  $\alpha_n$ . Note that if  $\alpha$  and  $R$  are assumed to be constants (ie.,  $\alpha_1 = \alpha_n$  and  $R_1 = R_n$ ) then

$$\frac{G'_n}{G'_{\max}} = \frac{1}{1 + \alpha_1 |SL|^{R_1 - 1}} = \frac{G'_1}{G'_{\max}}$$

and there has been no degradation.

The dependence of  $G'_n$  in Eq. (7-13) on  $G'_1$  creates much room for error because of the uncertainty in determining  $G'_1$ .  $\alpha_1$  and  $R_1$  may be obtained from Eq. (7-3), which uses an extrapolated value of  $G'_1$ , or it may be extrapolated from the  $\alpha$  vs  $N$  and  $R$  vs  $N$  curves. In either way, it is not usually obtained directly from experimental data. The consequences of this show up when the secant modulus is predicted from Eqs. (7-13) or (7-14).

Eq. (7-13) was used to predict  $\frac{G'_n}{G'_{max}}$  using the  $\alpha_n$  and  $R_n$  from Fig. 7-3. Stress levels greater than 40% showed good agreement with the measured secant modulus values. For stress levels approaching zero the predicted secant moduli had very poor agreement with the measured ones. As indicated in Fig. 7-4, the secant modulus for  $N=1$  approaches  $E'_{max}$ , as expected. However, the predicted modulus for small stress levels increased as  $N$  increased, and became greater than  $E'_{max}$ . This has been proven otherwise in the resonant column device. Consequently, it is concluded that this form of the Ramberg-Osgood model does not represent well the backbone curve for small stress levels.

Re-examining Eq. (7-12),

$$\lambda = \frac{2}{\pi} \frac{R-1}{R+1} \left( 1 - \frac{G'_1}{G'_{max}} \right),$$

it is evident that as  $R$  decreases the damping ratio will decrease also. The change in damping ratio predicted by this equation exceeds the slight change in damping actually observed. Conversely, if this equation is to be used to predict the Ramberg-Osgood  $R$ , then the

variation in R vs N will be quite small when compared to the R's obtained from the backbone curve.

A comparison of the secant modulus and damping values predicted from Eqs. (7-11) and (7-12) is illustrated in Fig. 7-5. The solid lines represent both the measured modulus and measured damping. The measured secant modulus is used in the backbone curve, Eq. (7-11), to derive Ramberg-Osgood coefficients  $\alpha$  and R. This R then is used in Eq. (7-12) to calculate the damping ratio predicted by the Masing criterion.

The dashed line in Fig. 7-5 plots the measured secant modulus vs the calculated damping ratio. These calculated damping ratios differ from the measured values by as much as 40%. The predicted damping ratios were generally less than the measured ratios for stress levels less than 40%, and higher for higher stress levels.

The measured damping ratios were used in Eq. (7-12) to determine the Ramberg-Osgood R. This R was then used in Eq. (7-11) to predict secant modulus. The predicted values differed by up to 60%, and in most cases were lower than the measured moduli. The dotted line in Fig. 7-5 shows the predicted modulus plotted with the measured damping data.

These results show that the Ramberg-Osgood model used in conjunction with the Masing criterion does not adequately describe the behavior of Kaolinite when loaded with large amplitude stress cycles.

#### D. Overconsolidated Clay

The secant modulus degradation for overconsolidated clay appears to be independent of overconsolidation ratio. The damping ratios also show no dependence on the overconsolidation ratio, so it is assumed that the backbone curve will have the same form as for normally consolidated clay.

The Ramberg-Osgood coefficients  $\alpha$  and  $R$ , when determined from the backbone curve, were found to vary in the same manner with the cycle number  $N$  as with the normally  $K_0$  consolidated clay. Smooth curves were plotted to show that in all but one case,  $\alpha$  and  $R$  decreased as  $N$  increased. Fig. 7-6 shows  $\alpha$  and  $R$  for  $\bar{\sigma}_c = 10$  psi. There appeared no dependence on either the consolidation pressure or the overconsolidation ratio.

The secant modulus and damping ratios for the fifth cycle in the torsional mode are presented in Fig. 7-7. The solid line represents the measured modulus and damping. The measured moduli were used in the backbone curve, Eq. (7-11), to find the Ramberg-Osgood  $R$ . This  $R$  was then used in the damping equation, Eq. (7-12), to determine a damping ratio. This damping, plotted as a dashed line in Fig. 7-7, was in most cases greater than that measured, i.e. it predicted more energy lost per cycle than actually happened.

Eq. (7-12) with the measured damping ratios were used to obtain an  $R$  value. The  $R$  was then placed in the backbone curve to predict a secant modulus, plotted as a dotted line in Fig. 7-7. Most of the derived moduli were lower than those measured, with

greater differences at higher stress levels.

These results reinforce the conclusion that the Masing criterion does not fit well with anisotropic clay loaded with a constant stress amplitude.

## APPENDIX 1

### EXTENSION TESTS ON REDUCED AREA SPECIMENS

A series of four extension tests were carried out in a Norwegian Triaxial Cell. Isotropically formed and anisotropically formed samples were each tested at effective consolidation pressures of 40 and 60 psi. The samples had reduced diameters in the center portion of their height, as shown in Fig. A-1. Due to the reduced area, the tension stress in the center of the specimen is greater than the stress existing near the caps. A conventionally-shaped specimen, Fig. A-2, necks when the minor principal effective stress approaches zero due to the cap's inability to apply an actual tension force to the specimen.

All four tests created minor principal stresses (axial) which were negative. The isotropic specimens showed minor principal effective stress of zero at 58% and 78% of their failure strains, while the two anisotropic specimens reached it at 37% and 42% of their failure strains. This is relatively early in the test.

Fig. A-3 shows the stress-strain curves for the anisotropic and the isotropic specimens at  $\bar{\sigma}_c = 60$  psi. Plots of  $\bar{\sigma}_1/\bar{\sigma}_3$  are also shown on these graphs.

A discontinuity exists at the point where  $\bar{\sigma}_3 = 0$ . Attempts to describe a failure criterion using this effective stress ratio are therefore meaningless.

## APPENDIX 2

### REFERENCES

1. Bianchini, G. F., "Effects of Anisotropy and Strain on the Dynamic Properties of Clay Soils", Ph.D. thesis, in preparation.
2. Bishop, A. W. and Garga, V. K., "Drained Tension Tests on London Clay", Geotechnique, Vol. 19, 1969.
3. Brown, S. F., Lashine, A. K. F., and Hyde, A. F. L., "Repeated Load Triaxial Testing of a Silty Clay," Geotechnique, Vol. 25, No. 1, March, 1975.
4. Diamond, S., "Microstructure and Pore Structure of Impact-Compacted Clays", Clays and Clay Minerals, Vol. 19, 1971, pp. 239-249.
5. Glynn, T. E. and Kirwan, R. W., "A Stress-Strain Relationship for Clays Subjected to Repeated Loading", Proceedings, Seventh International Conference on Soil Mechanics and Foundation Engineering, Mexico City, Mexico, 1969.
6. Hardin, B. O. and Drnevich, V. P., "Shear Modulus and Damping in Soils: Design Equations and Curves", Journal of the Soil Mechanics and Foundations Division, ASCE, Vol 98, No. SM7, July, 1972.
7. Idriss, I. M., Dobry, R., and Singh, R. D., "Nonlinear Behavior of Soft Clays during Cyclic Loading", Journal of the Geotechnical Engineering Division, ASCE, Vol. 104, No. GT12, Dec., 1978.
8. Jennings, P. C., "Response of Simple Yielding Structures to Earthquake Excitation", Report by Earthquake Engineering Research Laboratory, California Institute of Technology, Pasadena, CA., 1963.
9. Larew, H. G. and Leonards, G. A., "A Strength Criterion for Repeated Loads", Proceedings, Highway Research Board, Bull. 41, 1962.
10. Lazan, B. J., Damping of Materials and Members in Structural Mechanics, Pergamon Press, New York, 1968.
11. Lee, K. E. and Focht, J. A., "Strength of Clay Subjected to Cyclic Loading," Marine Geotechnology, Vol. I, No. 3, 1976.

## REFERENCES

12. Masing, G., "Eigenspannungen und Verfestigung beim Messing", Proceedings of the Second International Congress of Applied Mechanics, 1926.
13. Ogawa, S., Shibayama, T., Yamaguchi, H., "Dynamic Strength of Saturated Cohesive Soil", Proceedings, Ninth International Conference on Soil Mechanics and Foundation Engineering, Tokyo, Vol. 2, 1977.
14. Ramberg, W. and Osgood, W. R., "Description of Stress-Strain Curves by Three Parameters", Technical Note 902, National Advisory Committee for Aeronautics, Washington, D.C., 1943.
15. Richart, F. E., "Some Effects of Dynamic Soil Properties on Soil-Structure Interaction", Journal of the Geotechnical Engineering Division, ASCE, Vol. 101, No. GT12, Dec., 1975.
16. Saada, A. S., "One Dimensional Consolidation in Triaxial Cell", Journal of the Soil Mechanics and Foundations Division, ASCE, Vol. 96, No. SM3, May, 1970.
17. Saada, A. S., "Testing of Anisotropic Clay Soils", Journal of the Soil Mechanics and Foundations Division, ASCE. Vol. 96, No. SM5, Sept., 1970.
18. Saada, A. S. and Bianchini, G. F., "Strength of One-Dimensionally Consolidated Clays", Journal of the Geotechnical Engineering Division, ASCE, Vol. 101, No. GT11, 1975, pp 1151-1164.
19. Saada, A. S., Bianchini, G. F., and Shook, L.P., "The Dynamic Response of Anisotropic Clay", Proceedings, Geotechnical Engineering Division Specialty Conference on Earthquake Engineering and Soil Dynamics, Vol. II, ASCE, Pasadena, CA, June, 1978.
20. Saada, A. S. Bianchini, G. F., and Shook. L. P., Discussion of "Nonlinear Behavior of Soft Clays During Cyclic Loading", to be published.
21. Saada, A. S. and Ou, C. D., "Stress-Strain Relations and Failure of Anisotropic Clays", Journal of the Soil Mechanics and Foundations Division, ASCE, Vol 99, No. SM12, 1973, pp. 1091-1111.
22. Sangrey, D. A., Henkel, D. J. and Esrig, M. I., "The Effective Stress Response of a Saturated Clay Soil to Repeated Loading", Canadian Geotechnical Journal, Vol. 6, 1969.



## REFERENCES

23. Seed, H. B. and Chan, C. K., "Structure and Strength Characteristics of Compacted Clays", Journal of the Soil Mechanics and Foundations Division, ASCE, Vol 85, No. SM5, 1959, pp. 87-128.
24. Seed, H. B., Chan, C. K., and Monismith, C. L., "Effects of Repeated Loading on the Strength and Deformation of Compacted Clay", Proceedings, Highway Research Board, Bull. 34, 1955.
25. Shackel, B., "Damping Characteristics of Soils", Journal of Australian Road Research Board, Vol 4, Part 2, 1968.
26. Shackel, B., "Measurement of Soil Damping Characteristics Using Cyclic Triaxial Equipment", Proceedings, 4th Asian Regional Conference on Soil Mechanics and Foundations, Bangkok, Thailand, 1971.
27. Shibata, T., Sato, T., Soelarno, D. S., "Dyanmic Behavior of Soils and Sub-Surface Ground", Proceedings, Ninth International Conference on Soil Mechanics and Foundation Engineering, Tokyo, 1977.
28. Thiers, G. R. and Seed, H. B., "Strength and Stress-Stain Characteristics of Clays Subjected to Seismic Loading Conditions", Vibration Effects of Earthquakes on Soils and Foundations, ASTM STP 450, 1968.
29. Wilson, N. E. and Greenwood, J. R., "Pore Pressures and Strains After Repeated Loading of Saturated Clay", Canadian Geotechnical Journal, Vol. II, 1974.
30. Yong, R. N. and Warkentin, B. P., Soil Properties and Behavior, Elsevier, 1975.

### APPENDIX 3

#### NOTATION

$A_a, A_b$	areas located on Fig. 6-8
$D_{Lehr}$	Lehr damping
$D_{Roelig}$	Roelig damping
$E'_{max}$	Young's modulus for strains less than $10^{-6}$
$G', E'$	secant moduli
$G'_1, E'_1$	secant moduli for first cycle
$G'_n, E'_n$	secant moduli for nth cycle
$G'_{max}$	shear modulus for strains less than $10^{-6}$
$G_s$	specific gravity
$K_o$	coefficient of lateral earth pressure at rest
$N$	cycle number
OCR	overconsolidation ratio
$P.E._{max}$	maximum potential energy in one cycle
$R$	Ramberg-Osgood coefficient
SL	stress level
SPAC	Saada Pneumatic Analog Computer
$t$	degradation parameter
$W_i$	area under loading portion of loop
$\alpha$	Ramberg-Osgood coefficient
$\alpha_1, R_1$	Ramberg-Osgood coefficients for first cycle

NOTATION

$\alpha_n, R_n$	Ramberg-Osgood coefficients for nth cycle
$\gamma$	shear strain; shear strain amplitude
$\gamma_{max}, \gamma_{min}$	shear strain limits for one sided loading
$\gamma_n$	shear strain amplitude for nth cycle
$\gamma_r$	reference strain
$\gamma_{pos}, \gamma_{neg}$	shear strain limits for two sided loading
$\delta$	degradation index
$\Delta u$	pore pressure development
$\Delta W$	energy lost per unit volume
$\epsilon_{max}, \epsilon_{min}$	axial strain limits for one sided loading
$\lambda$	equivalent damping ratio
$\bar{\sigma}_c$	effective confining pressure at start of test
$\sigma_d$	deviator stress
$\sigma_{max}, \sigma_{min}$	axial stress limits for one sided loading
$\bar{\sigma}_1, \bar{\sigma}_3$	major and minor principal effective stresses
$\tau$	shear stress; shear stress amplitude
$\tau_{max}$	static shear strength
$\tau_{max}, \tau_{min}$	shear stress limits for one sided loading

Reproduced from  
best available copy.

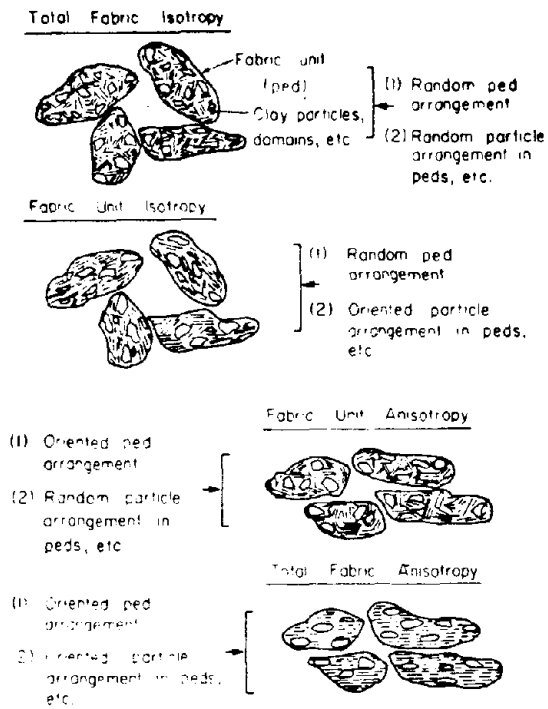


Fig. 2-7 Schematic Representation of Possible Material Structure  
(from Yong and Warkentin, 1975)

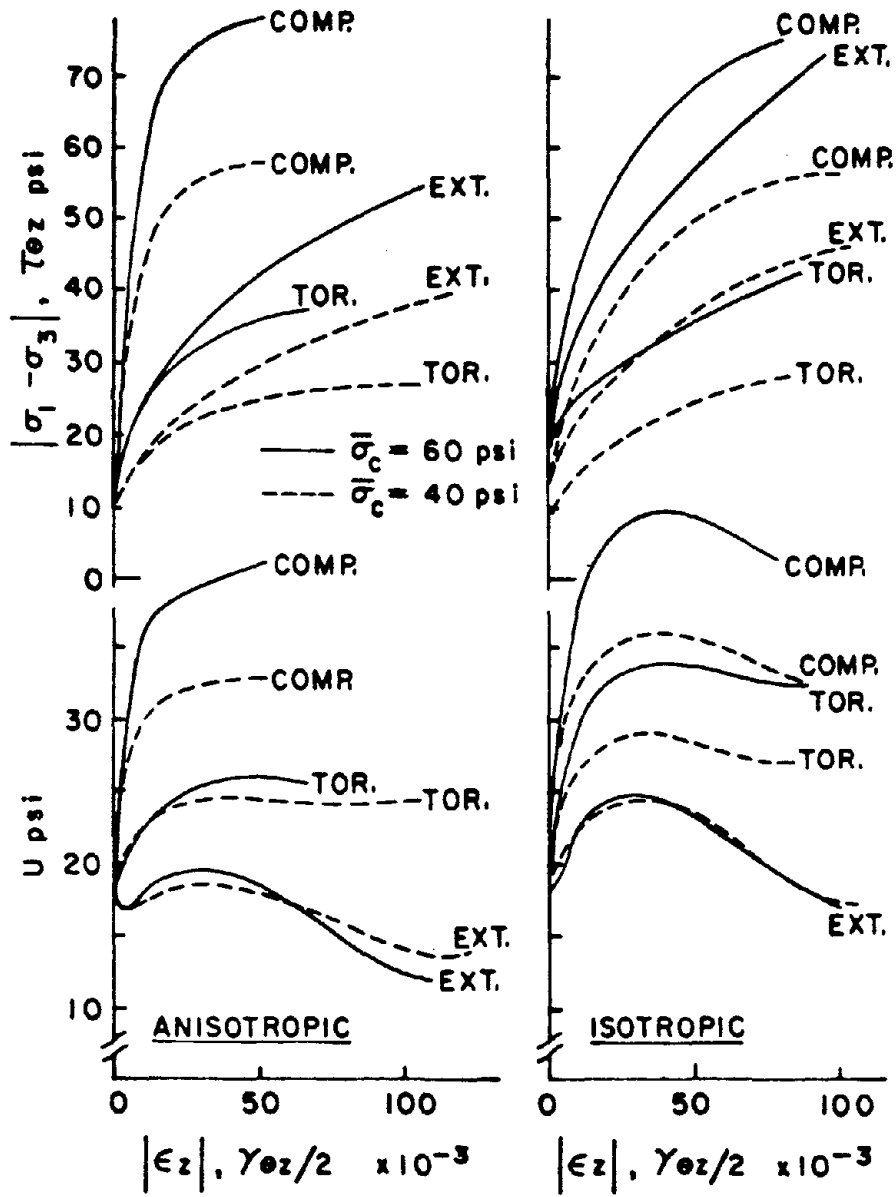


Fig. 4-1

Fig. 4-2

Stresses, Strains, and Pore Pressures from Static Tests

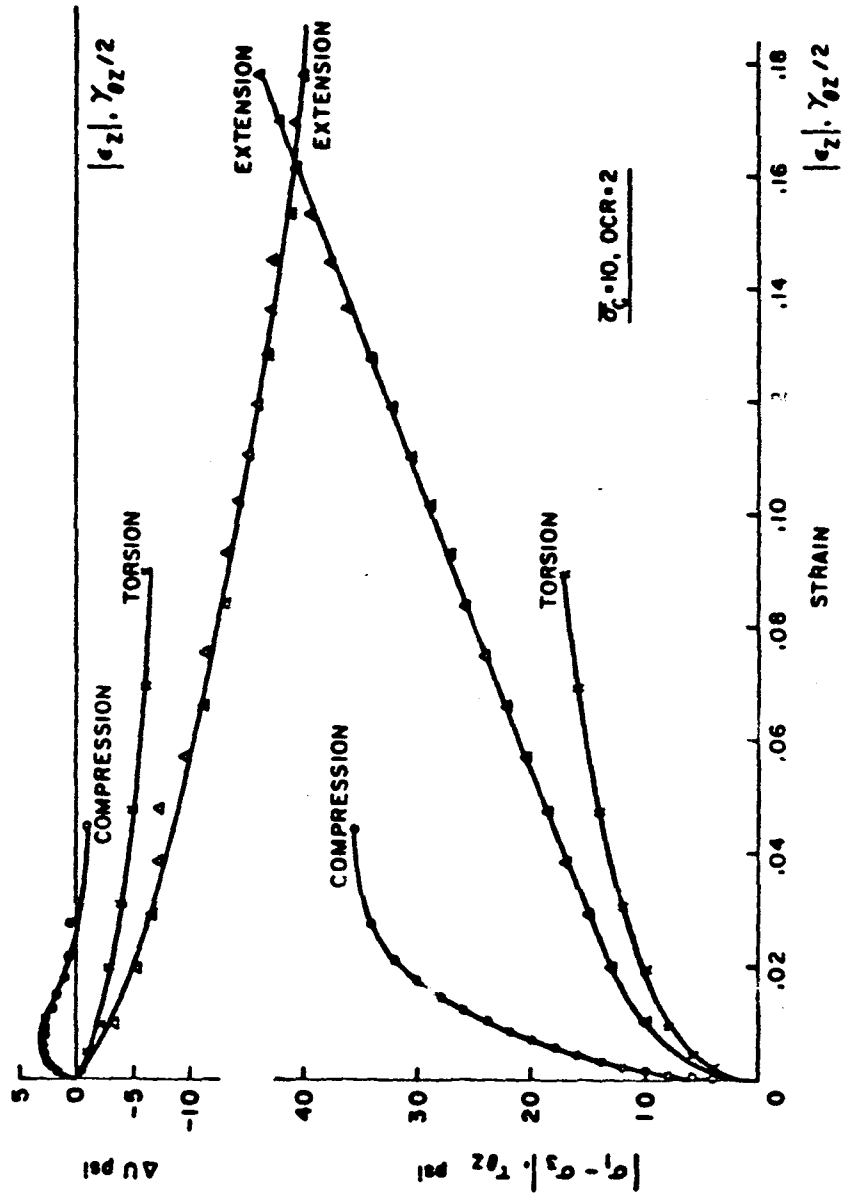


Fig. 4-3 Typical Stress-Strain and Pore Pressure Development Curves for Overconsolidated Clays

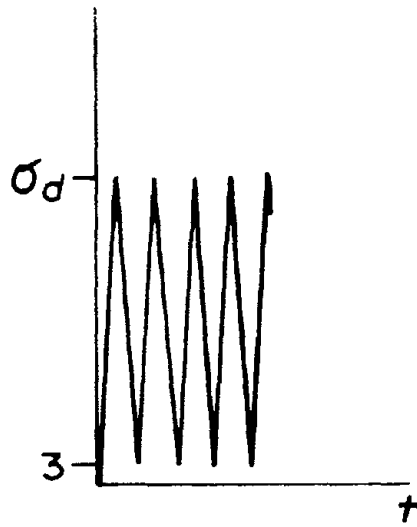


Fig. 5-1 Typical Stress Pattern for One Sided Loading

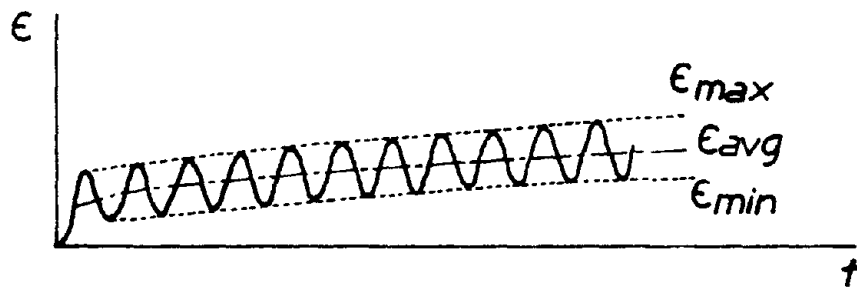


Fig. 5-2 Maximum, Minimum, and Average Strain for One Sided Loading

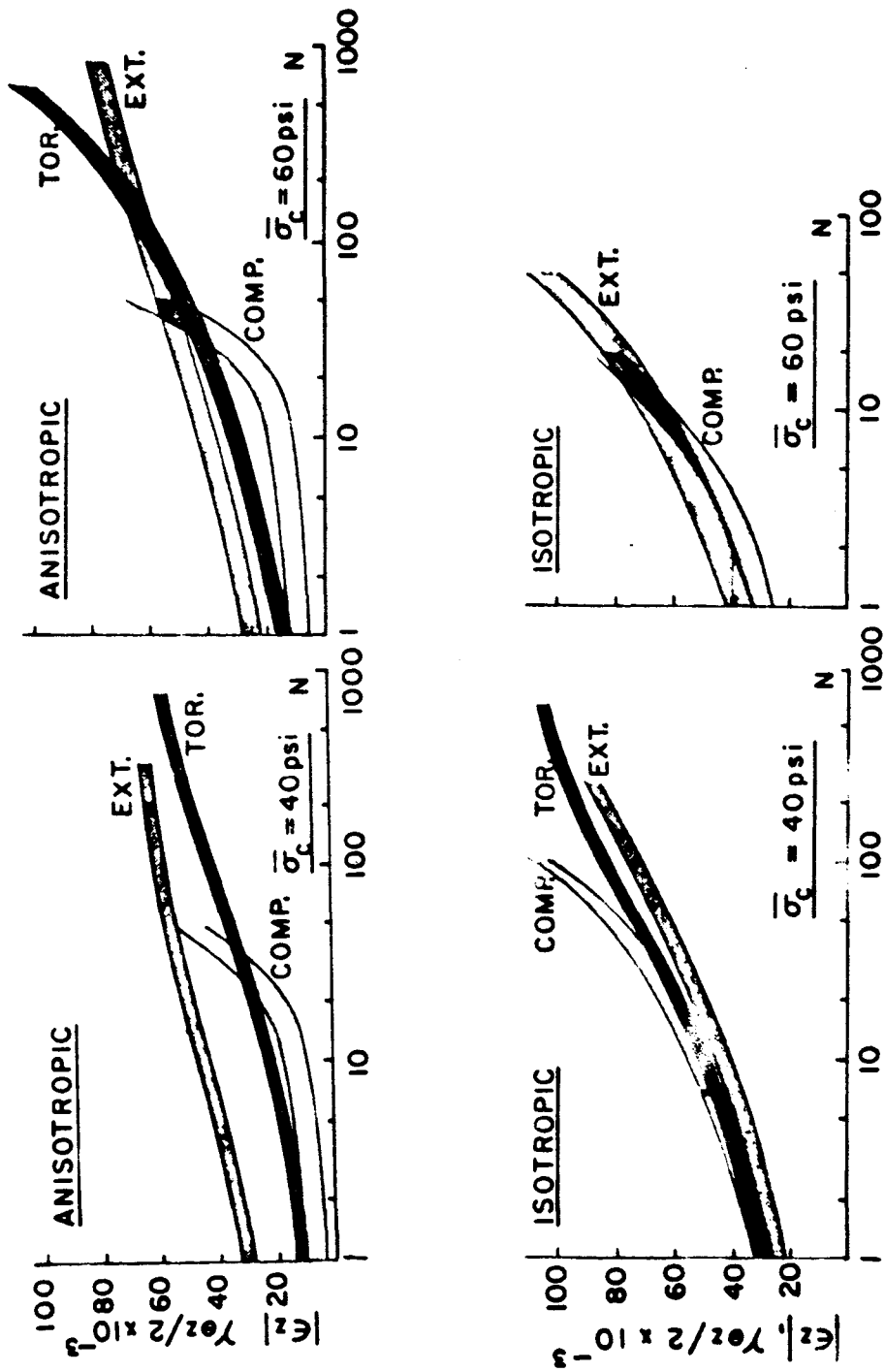
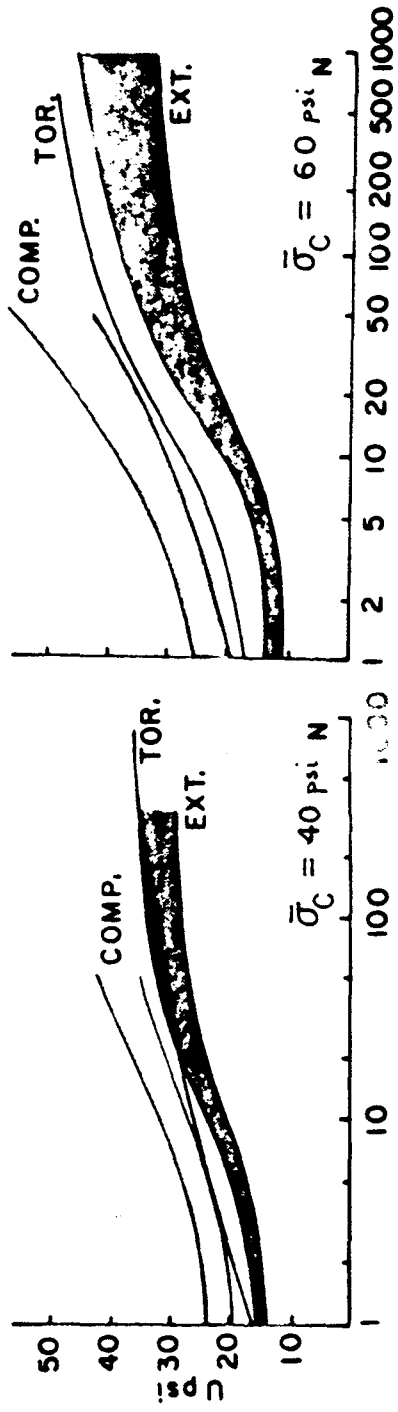
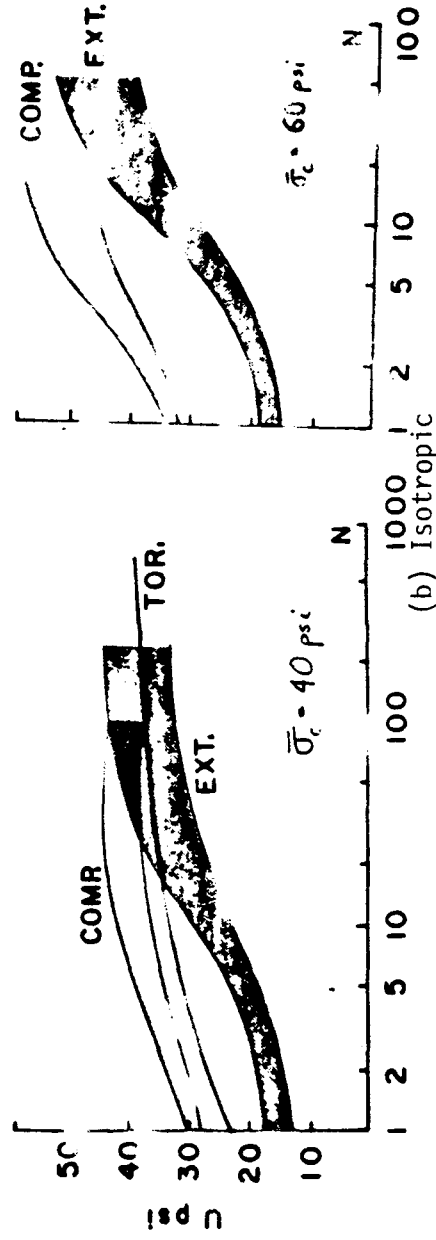


Fig. 5-3 Strain vs. N Envelopes for One Sided Loading

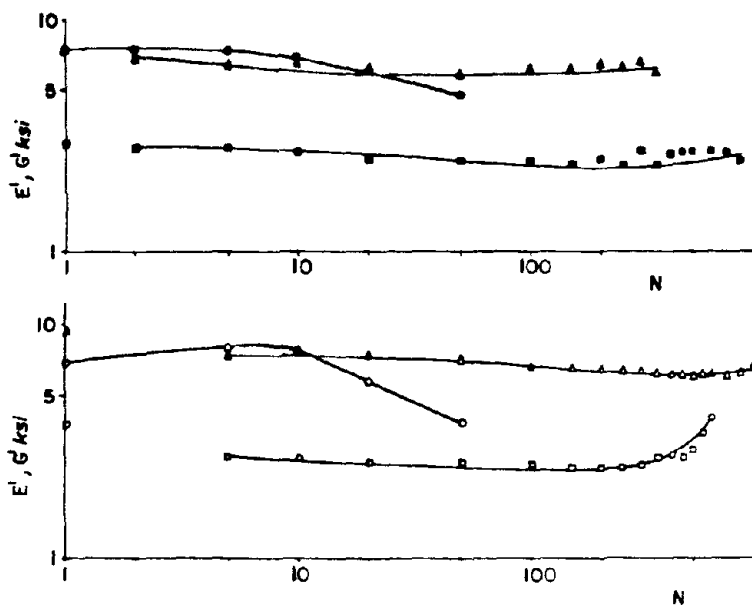




(a) Anisotropic

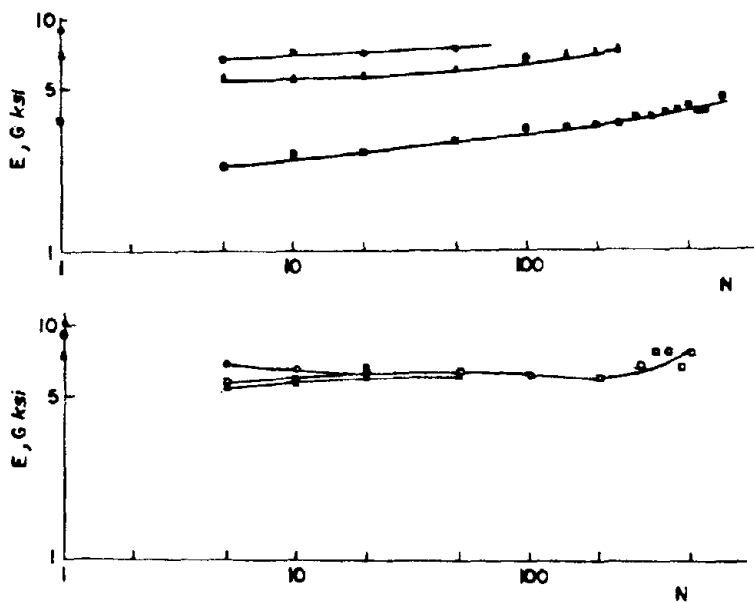


(b) Isotropic  
 Fig. 5-4 Pore Pressure Development for One Sided Loading



(a) Anisotropic

- COMPRESSION  $\bar{\sigma}_c = 40 \text{ psi}$
- ▲ EXTENSION  $\bar{\sigma}_c = 40 \text{ psi}$
- TORSION  $\bar{\sigma}_c = 40 \text{ psi}$
- COMPRESSION  $\bar{\sigma}_c = 60 \text{ psi}$
- ▲ EXTENSION  $\bar{\sigma}_c = 60 \text{ psi}$
- ◻ TORSION  $\bar{\sigma}_c = 60 \text{ psi}$



(b) Isotropic

Fig. 5-5 Secant Modulus vs. Cycle Number for One Sided Loading

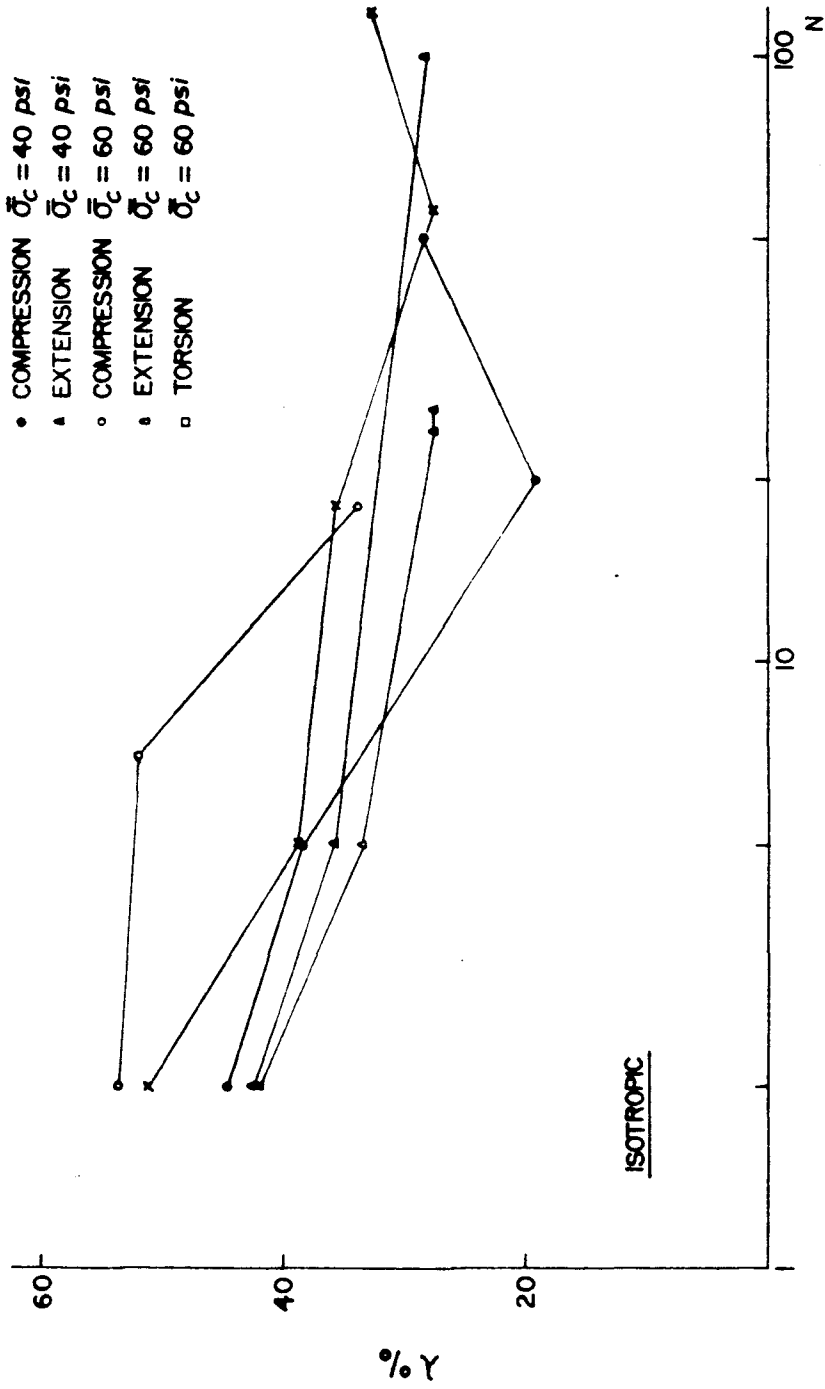


Fig. 5-6 Equivalent Damping Ratio vs. Cycle Number for One Sided Loading

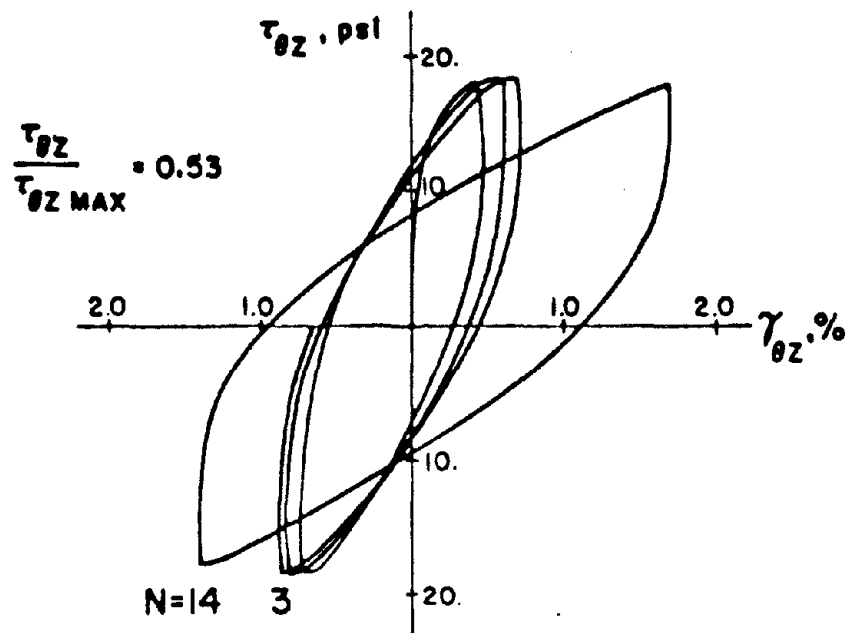


Fig. 6-1 Typical Stress-Strain Loops for Torsional Tests

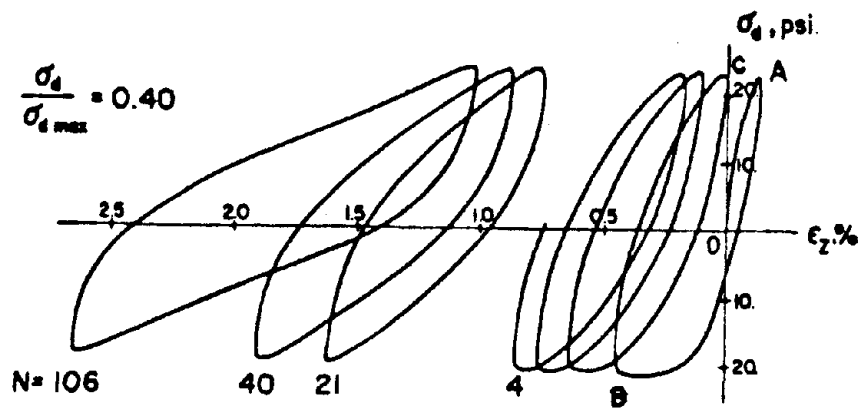


Fig. 6-2 Typical Stress-Strain Loops for Axial Tests

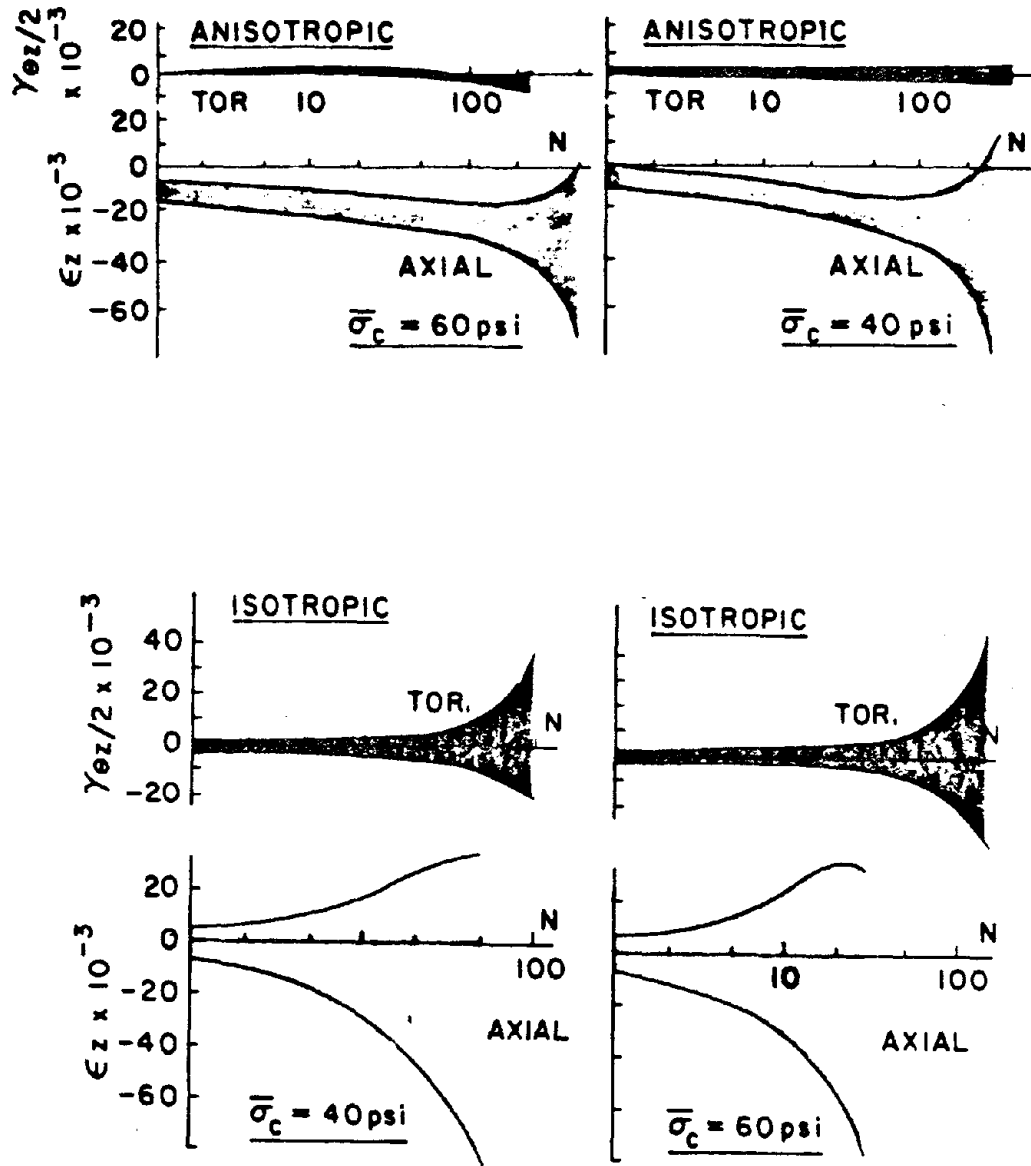


Fig. 6-3 Strain Envelopes for Two Sided Loading

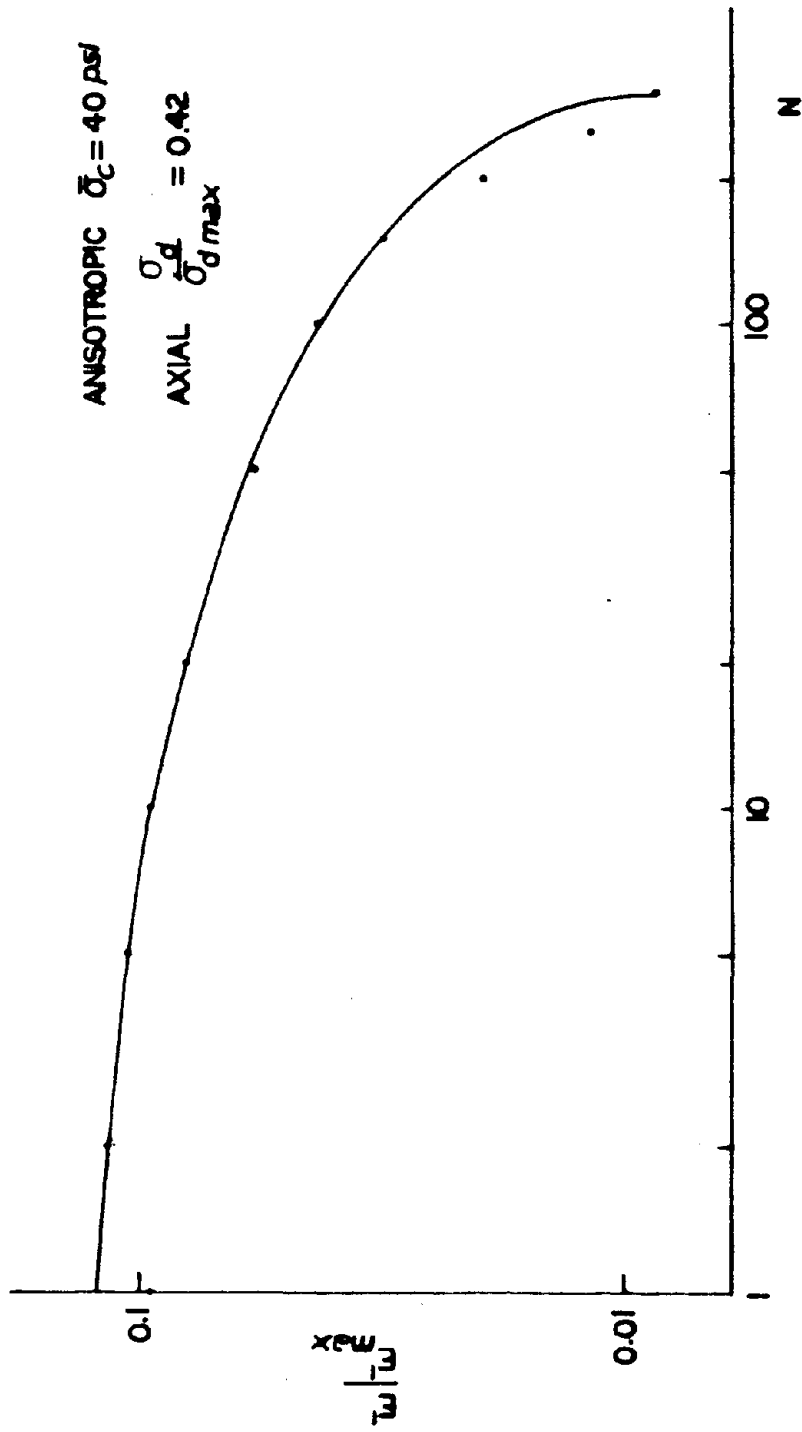


Fig. 6-4 Typical Secant Modulus for Two Sided Loading

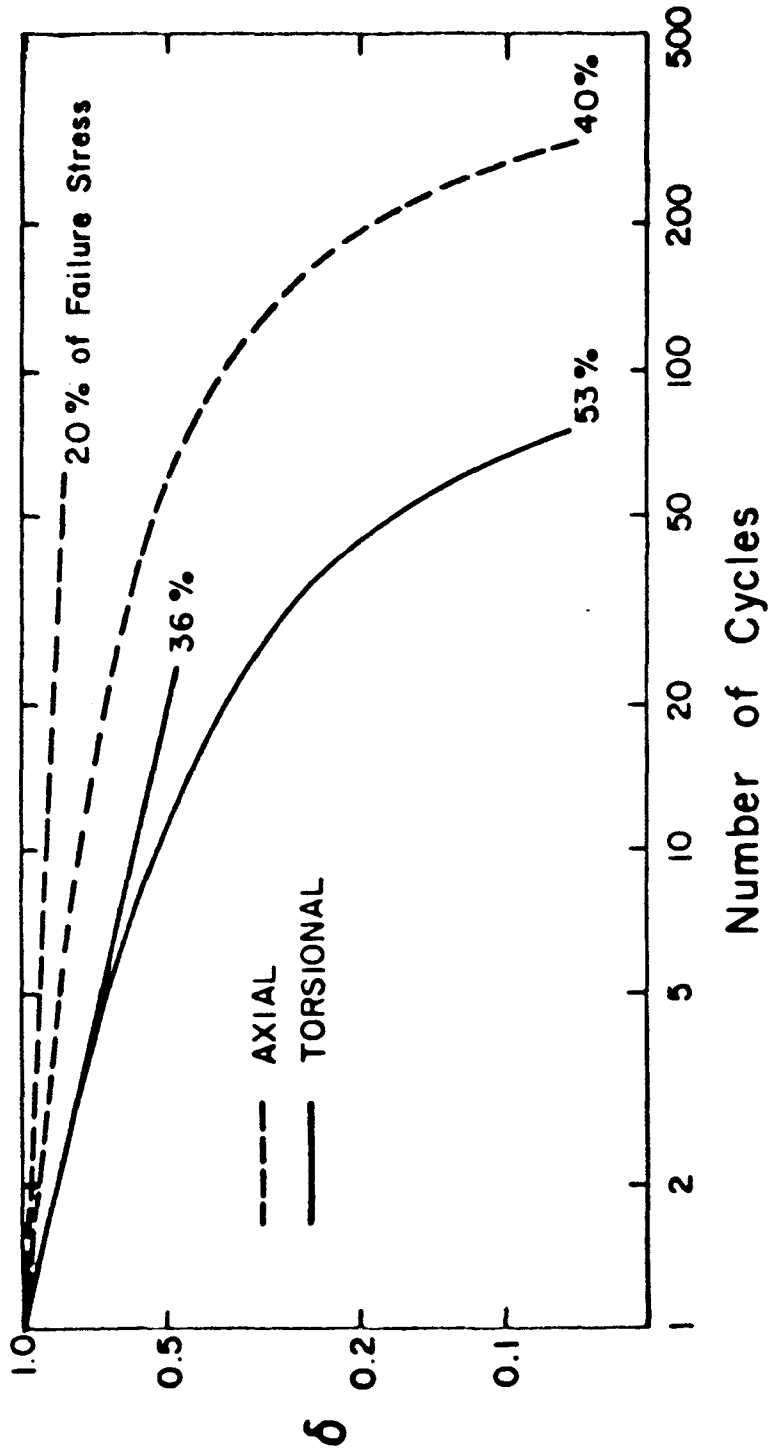


Fig. 6-5 Degradation Index for Anisotropic Clay

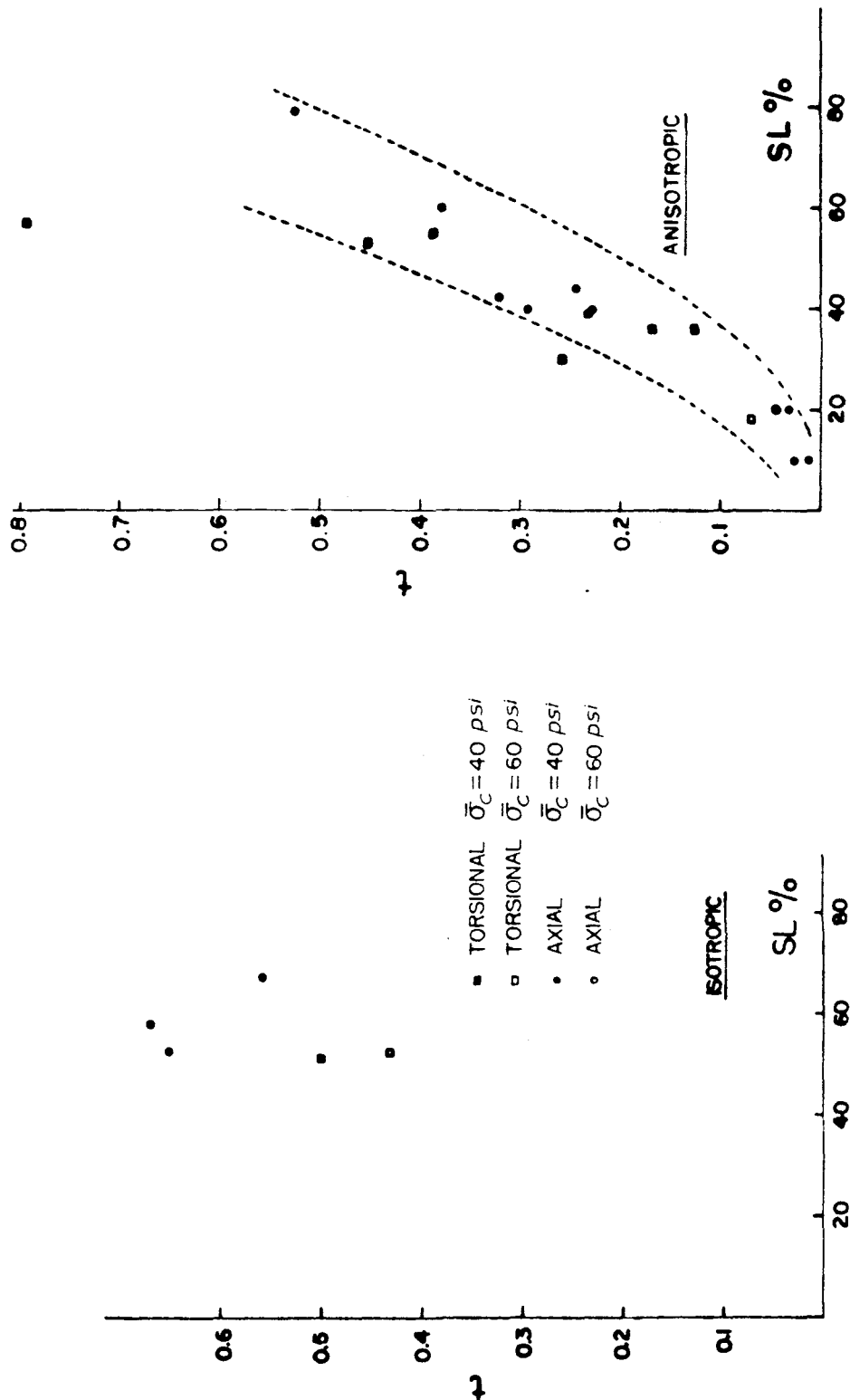


Fig. 6-6 Degradation Parameter t vs. Stress Level



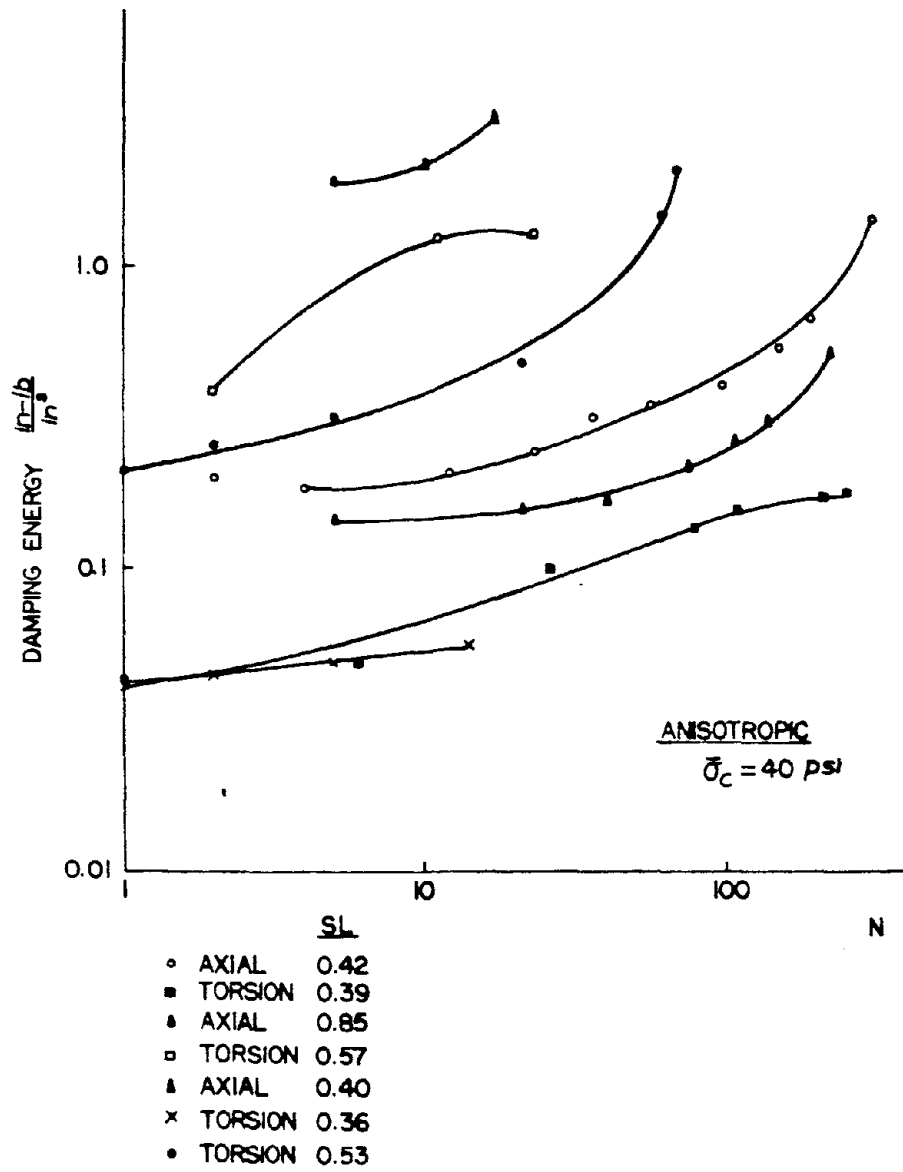


Fig. 6-7 Damping Energy vs. Cycle Number

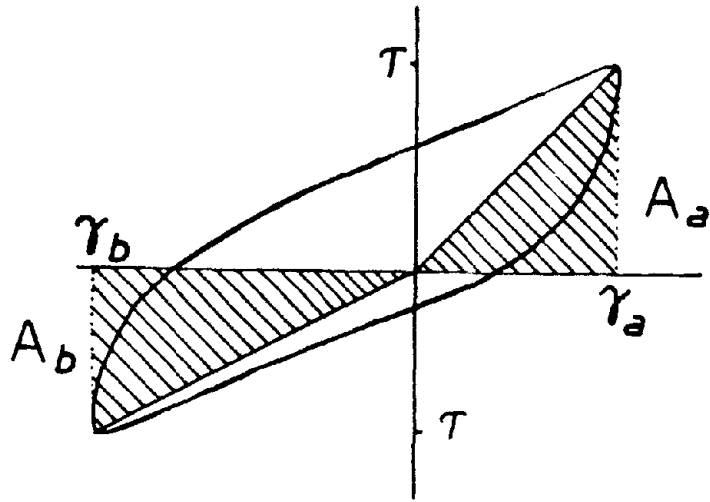


Fig. 6-8 Potential Energy for Lehr's Damping

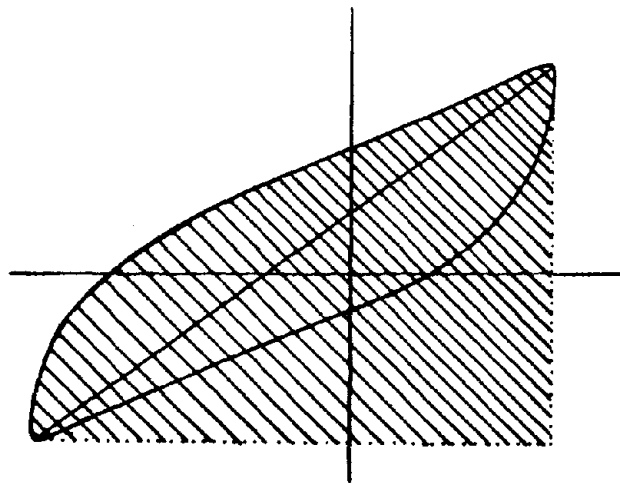


Fig. 6-9 Potential Energy for Roelig's Damping

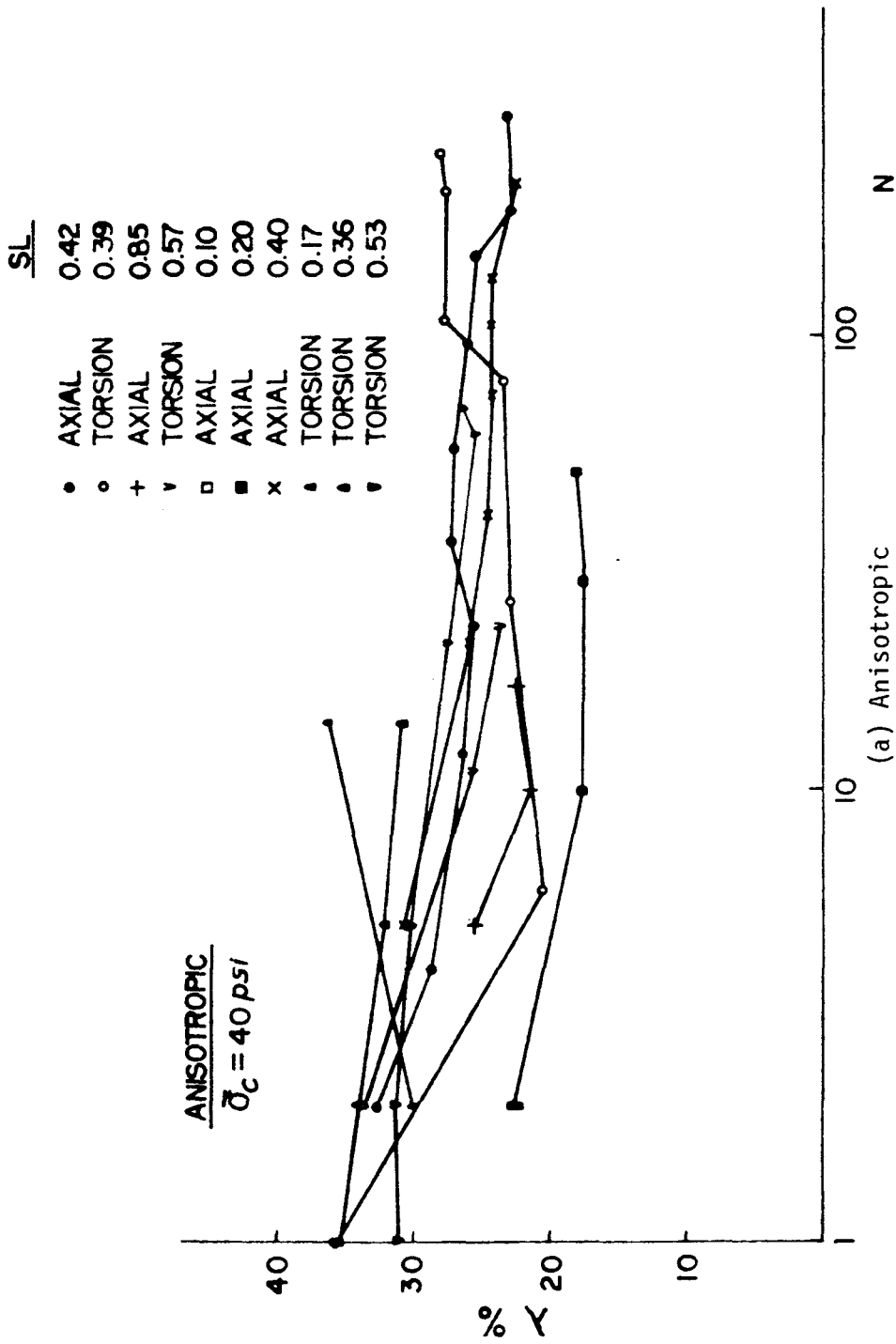
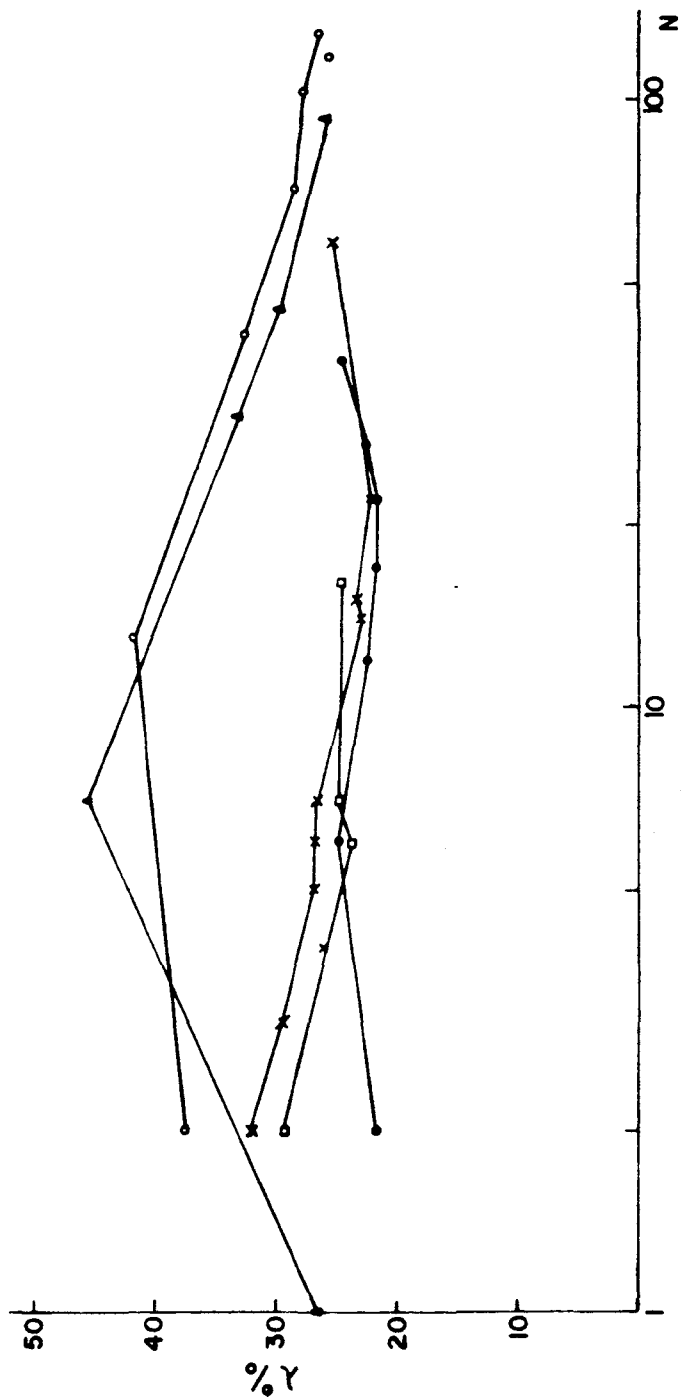


Fig. 6-10 Equivalent Damping Ratio for Two Sided Loading

	$\frac{SL}{\bar{\sigma}_c, psi}$
x	0.60
•	0.51
◻	0.70
●	0.60
○	0.60

ISOTROPIC



(b) Isotropic

Fig. 6-10 Equivalent Damping Ratio for Two Sided Loading

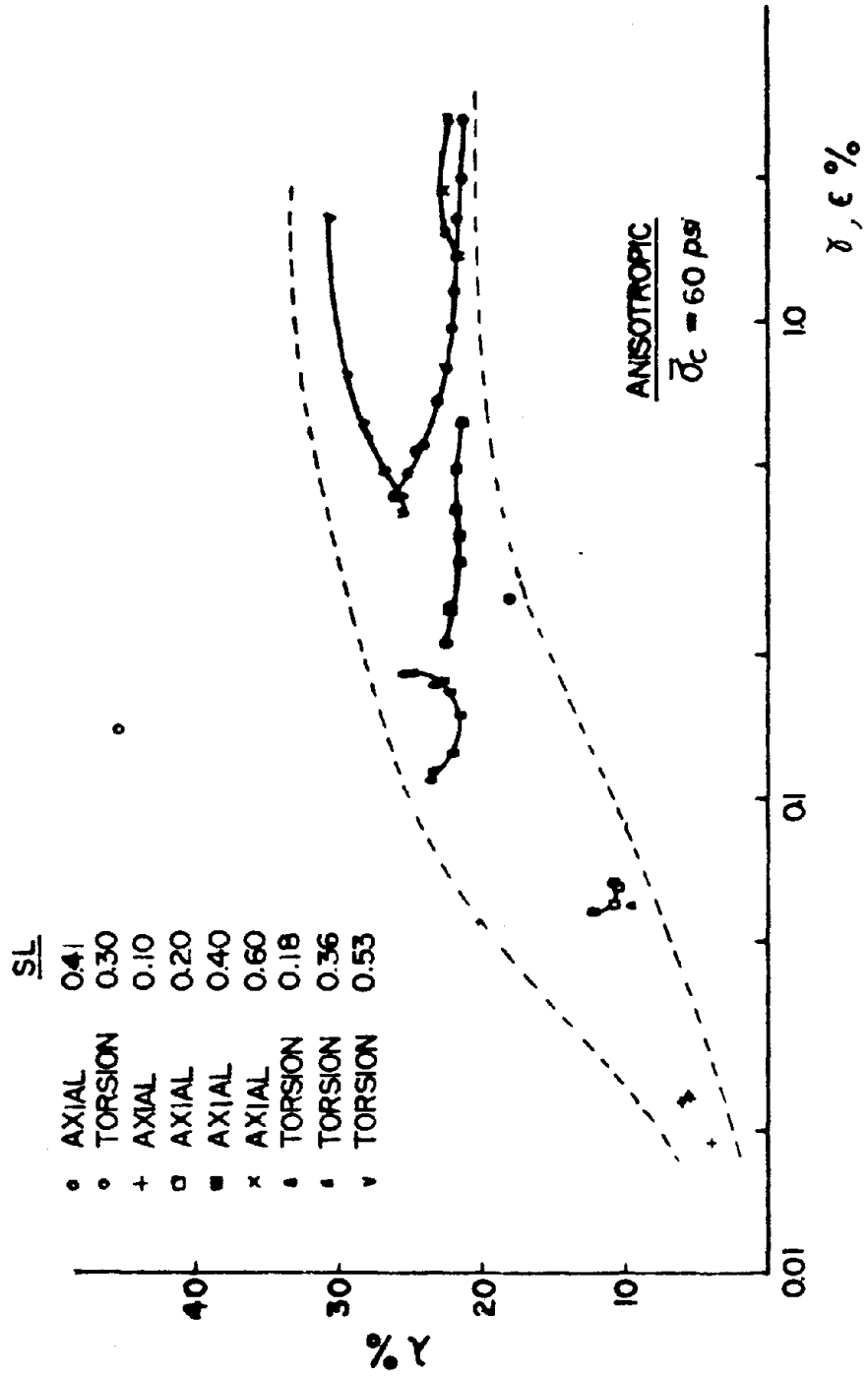


Fig. 6-11 Damping Ratio vs. Strain Envelope

OCR	SL
•	2 0.11
•	2 0.20
+	2 0.38
x	4 0.10
•	4 0.19
•	4 0.38
▲	4 0.53
▲	8 0.20
▽	8 0.38

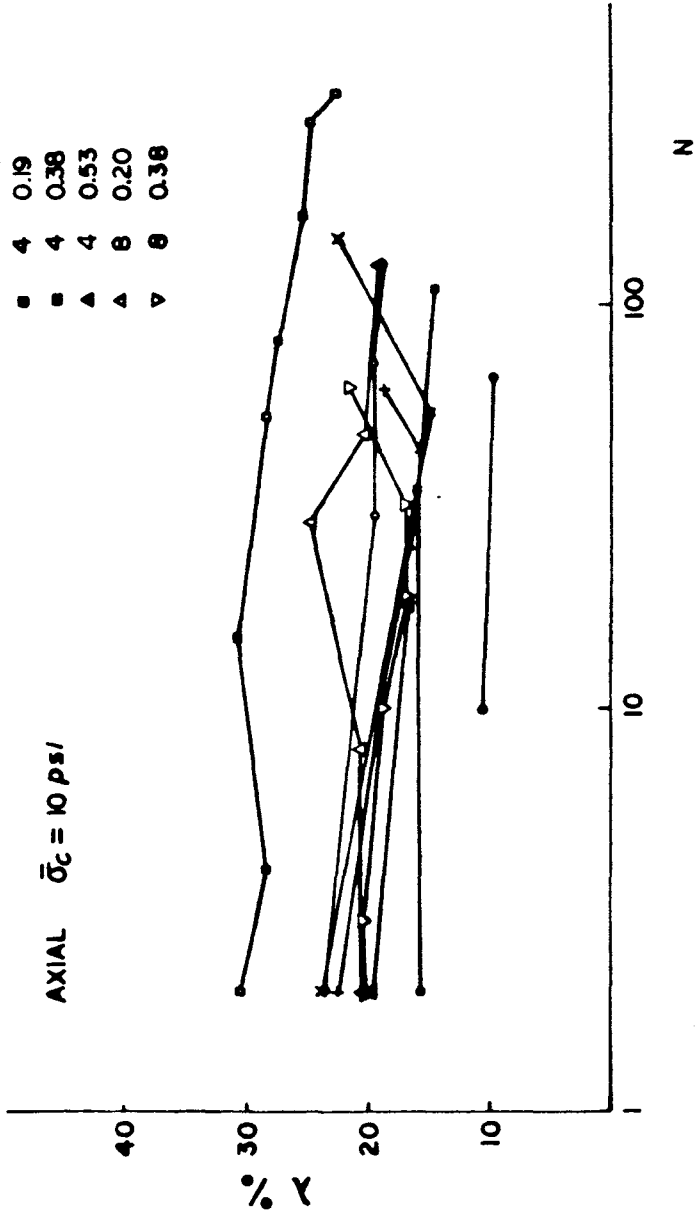


Fig. 6-12 Typical Damping Ratios for Overconsolidated Clay

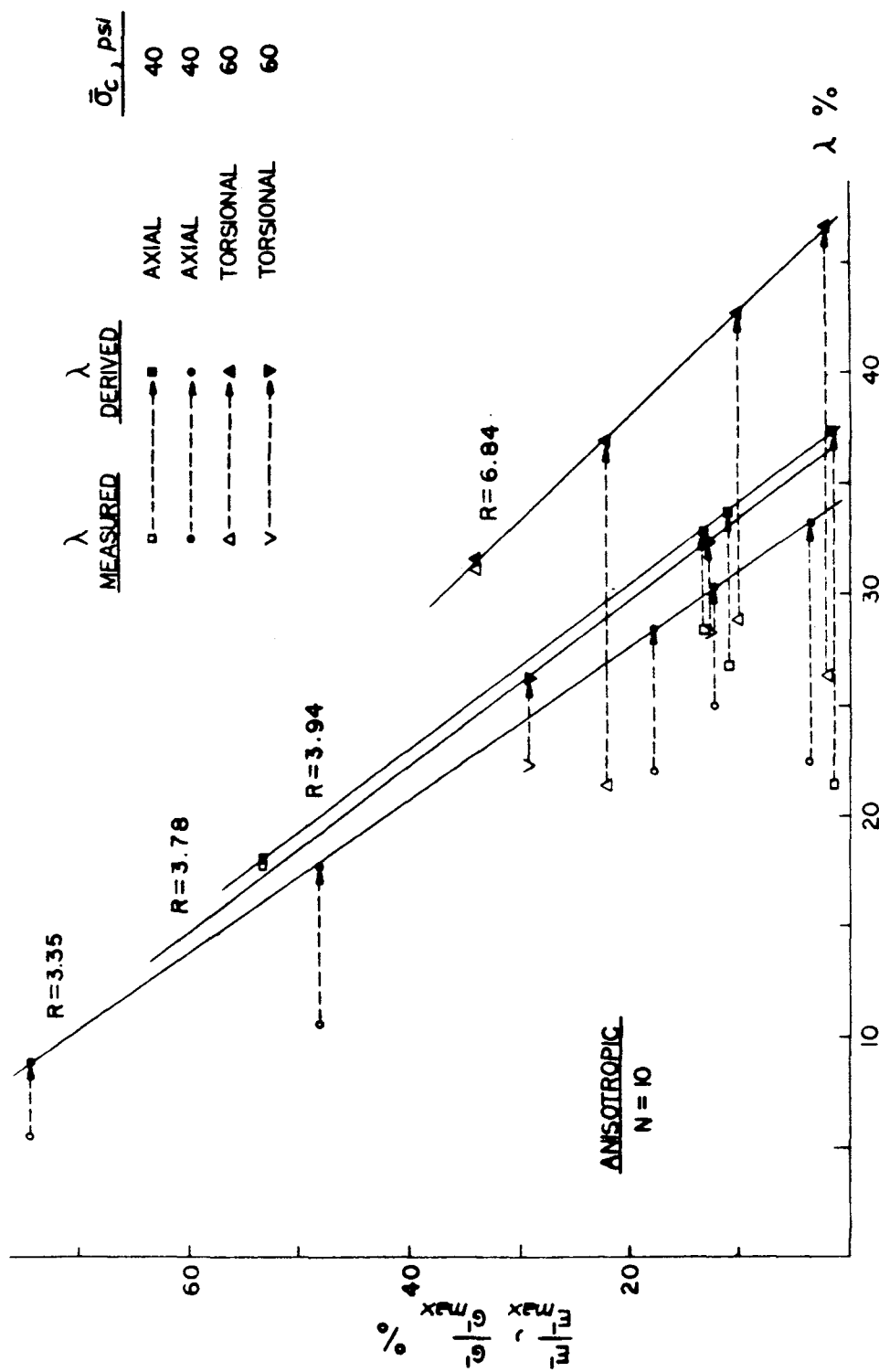


Fig. 7-1 Shear Modulus vs. Measured and Calculated Damping Ratios

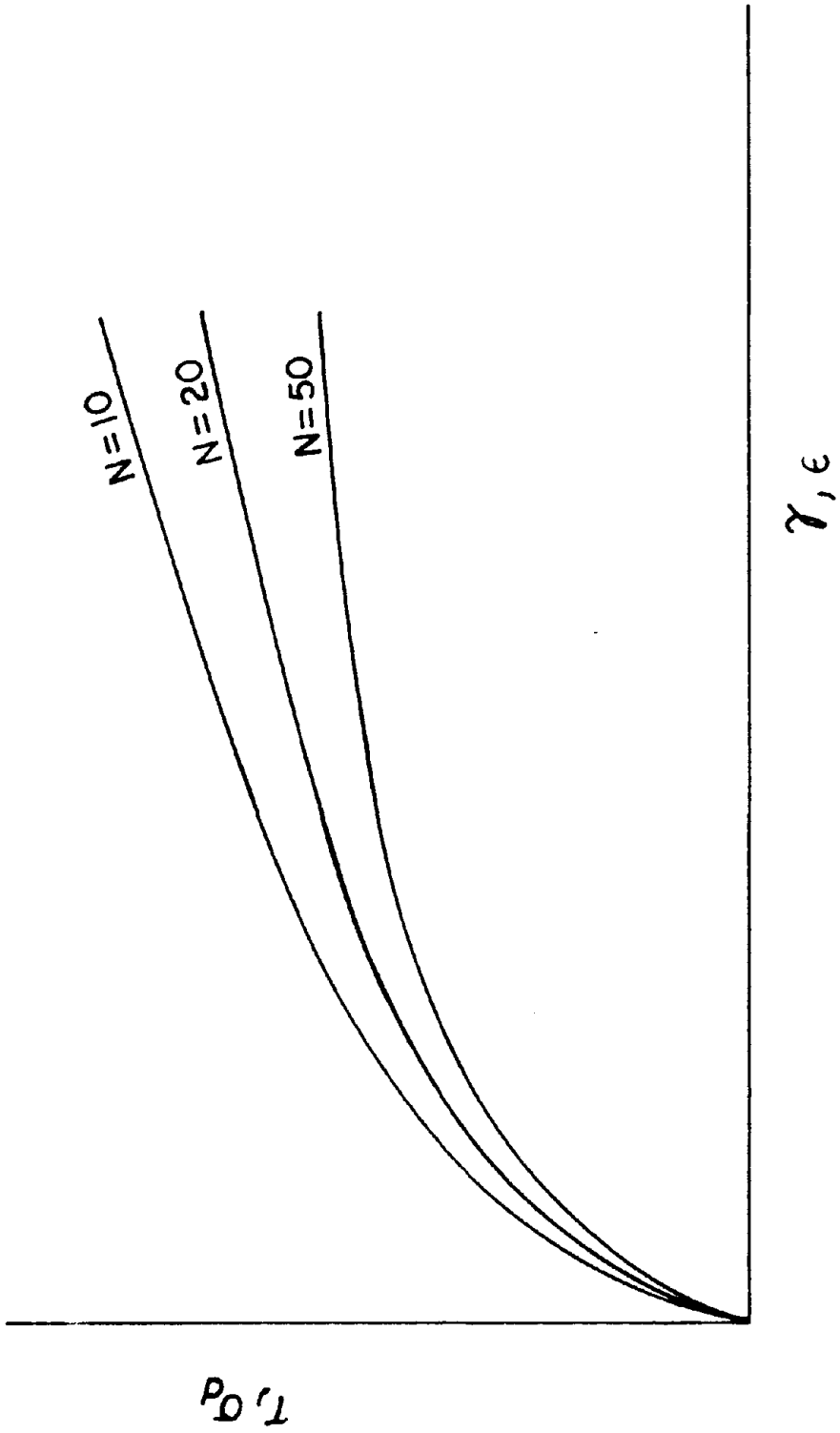


Fig. 7-2 Degradation of Backbone Curve



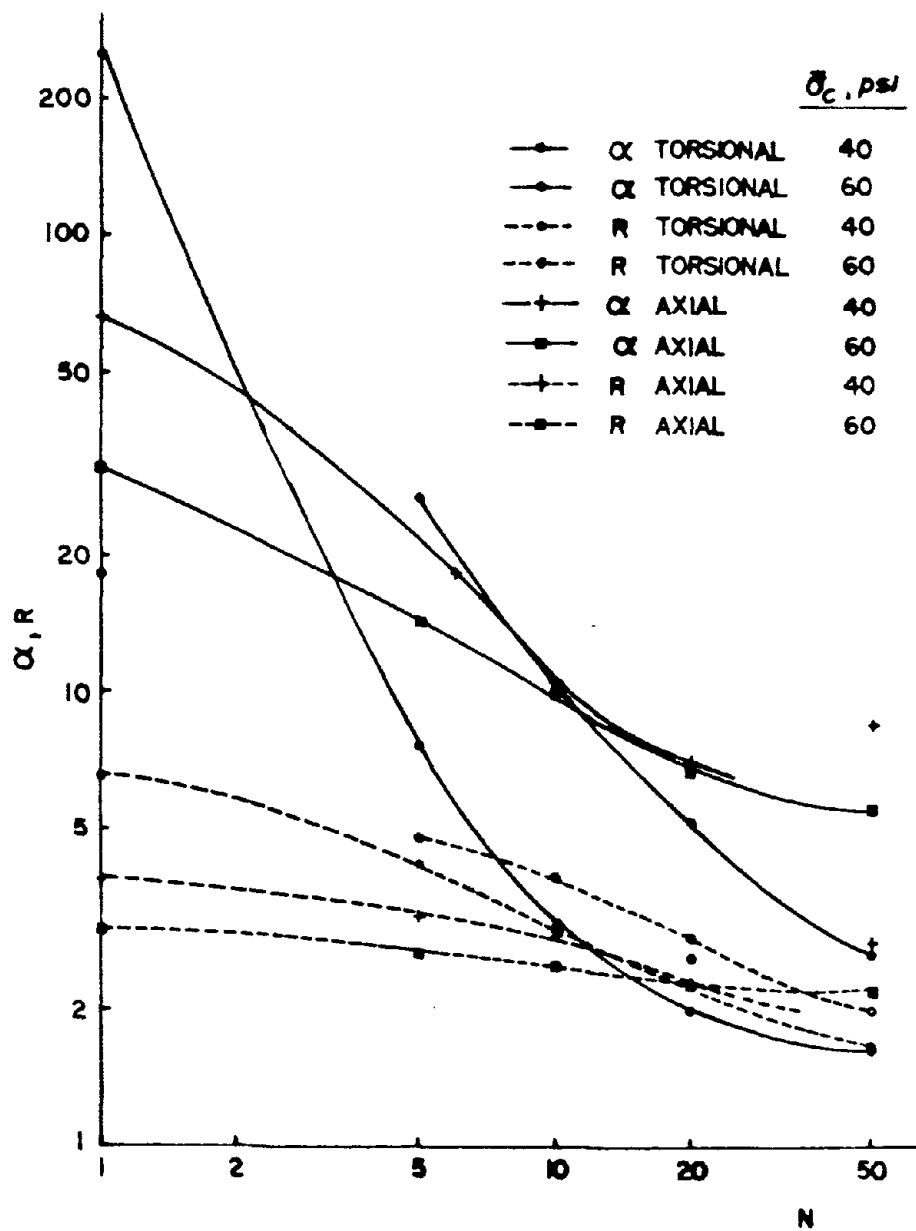


Fig. 7-3 Ramberg-Osgood Coefficients for Normally Consolidated Clay

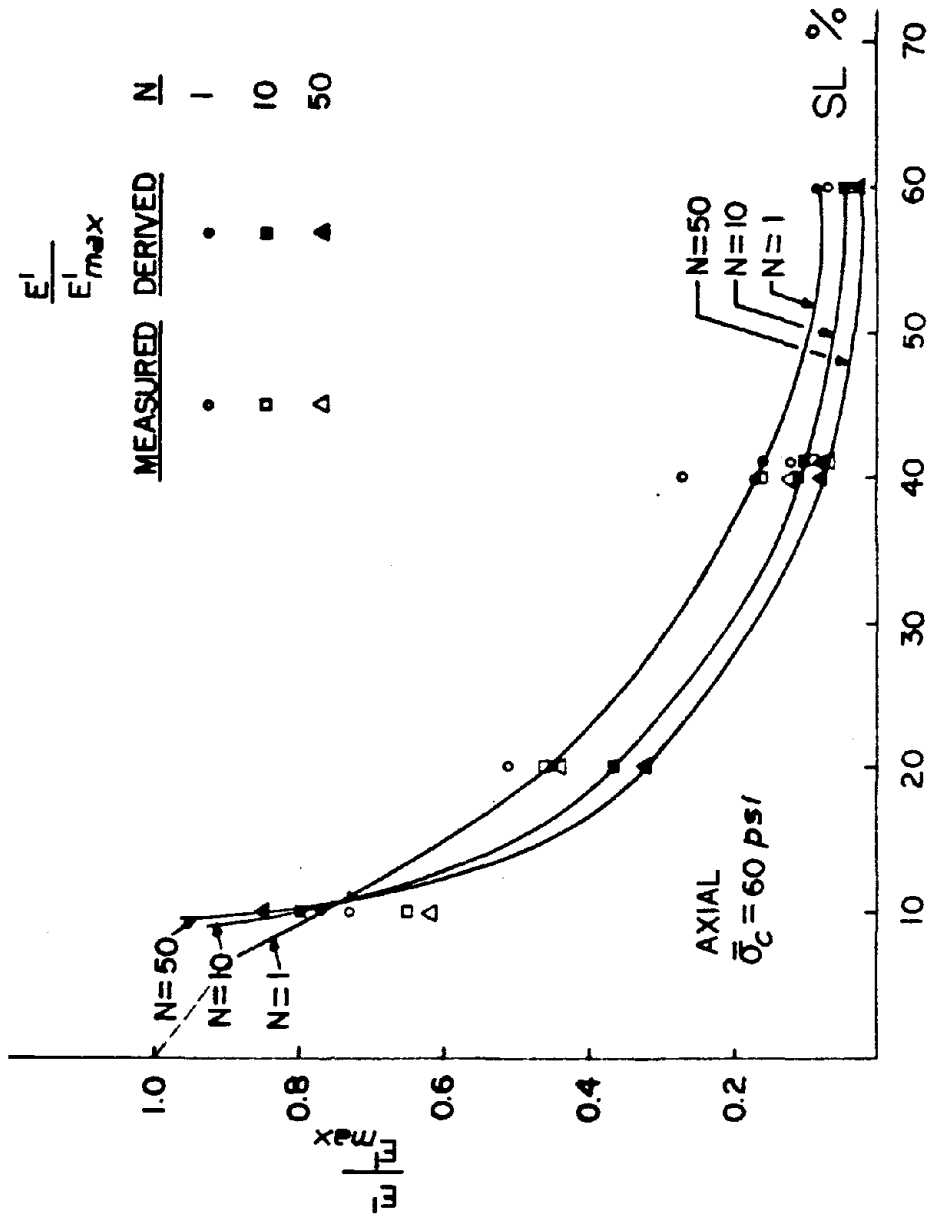


Fig. 7-4 Secant Modulus Derived from Eq. (7-11)

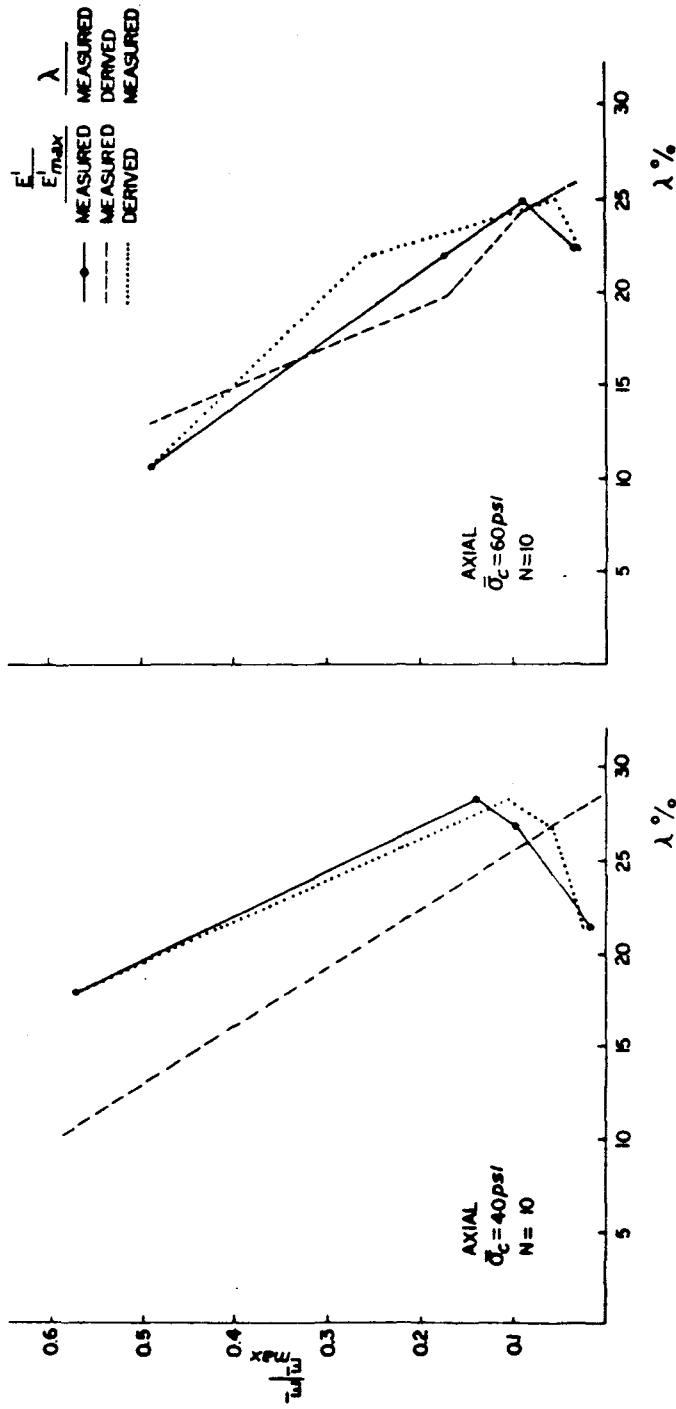


Fig. 7-5 Secant Modulus vs. Damping Ratio for Normally Consolidated Clay

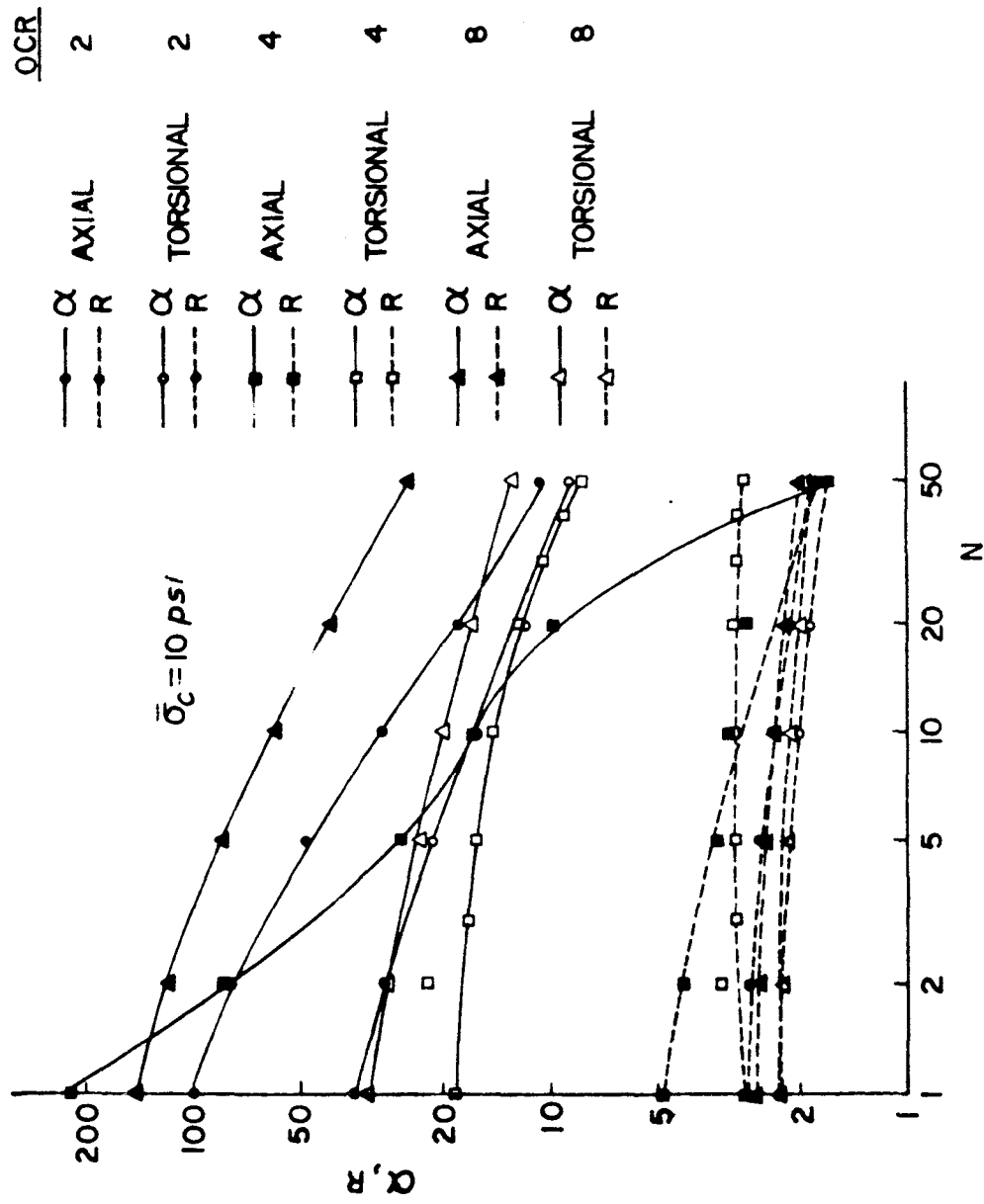


Fig. 7-6 Ramberg-Osgood Coefficients for Overconsolidated Clay

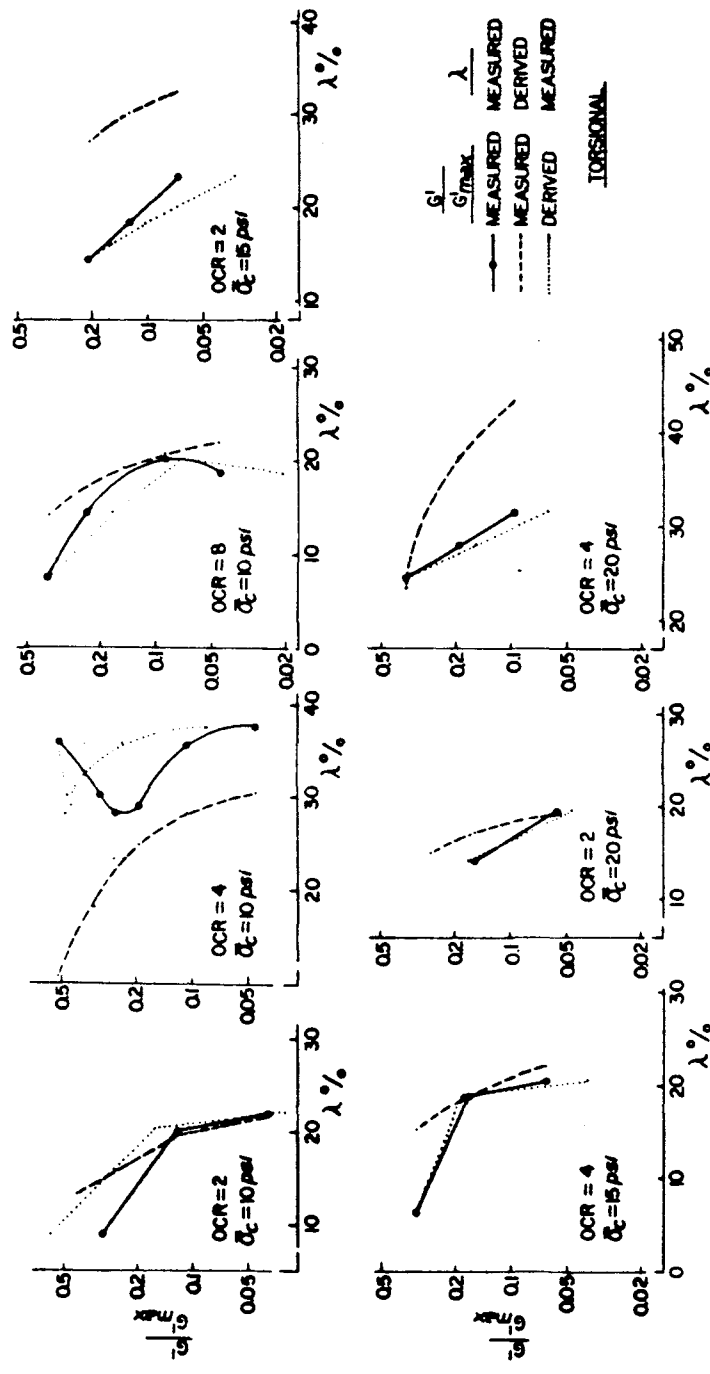


Fig. 7-7 Secant Modulus vs. Damping Ratio for Overconsolidated Clay

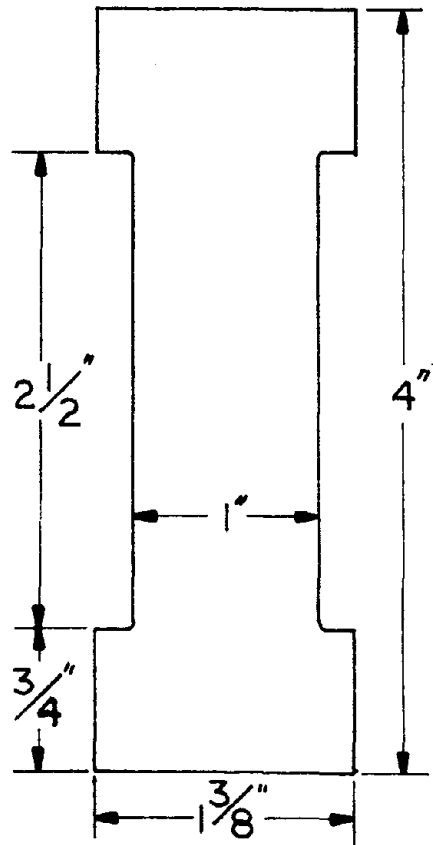


Fig. A-1 Specimen with Reduced Area

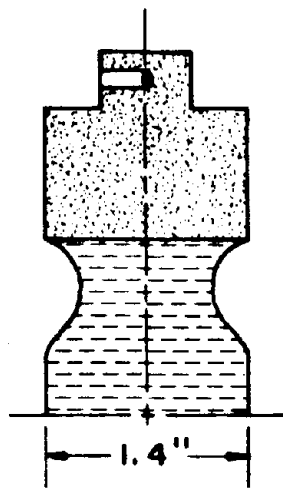
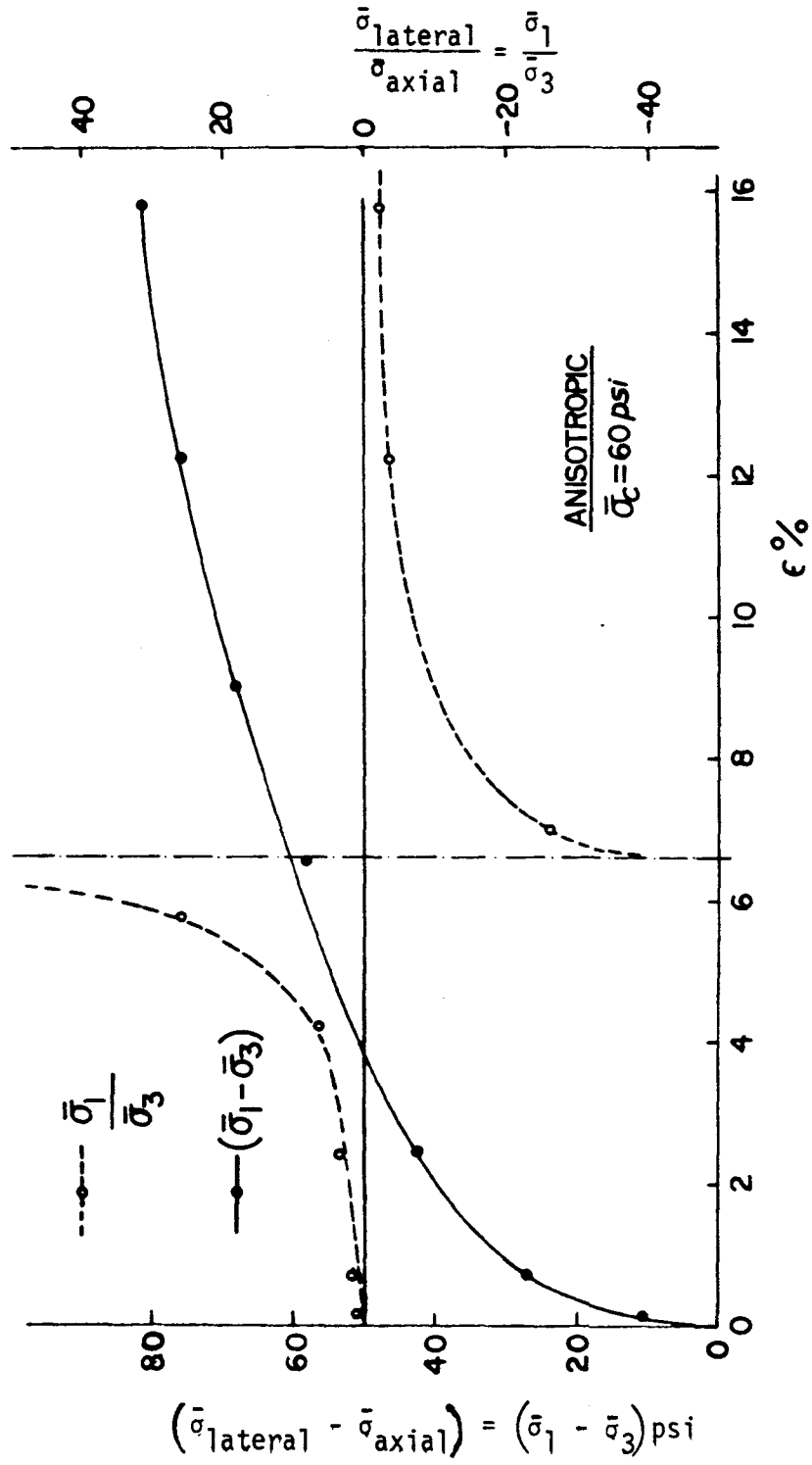


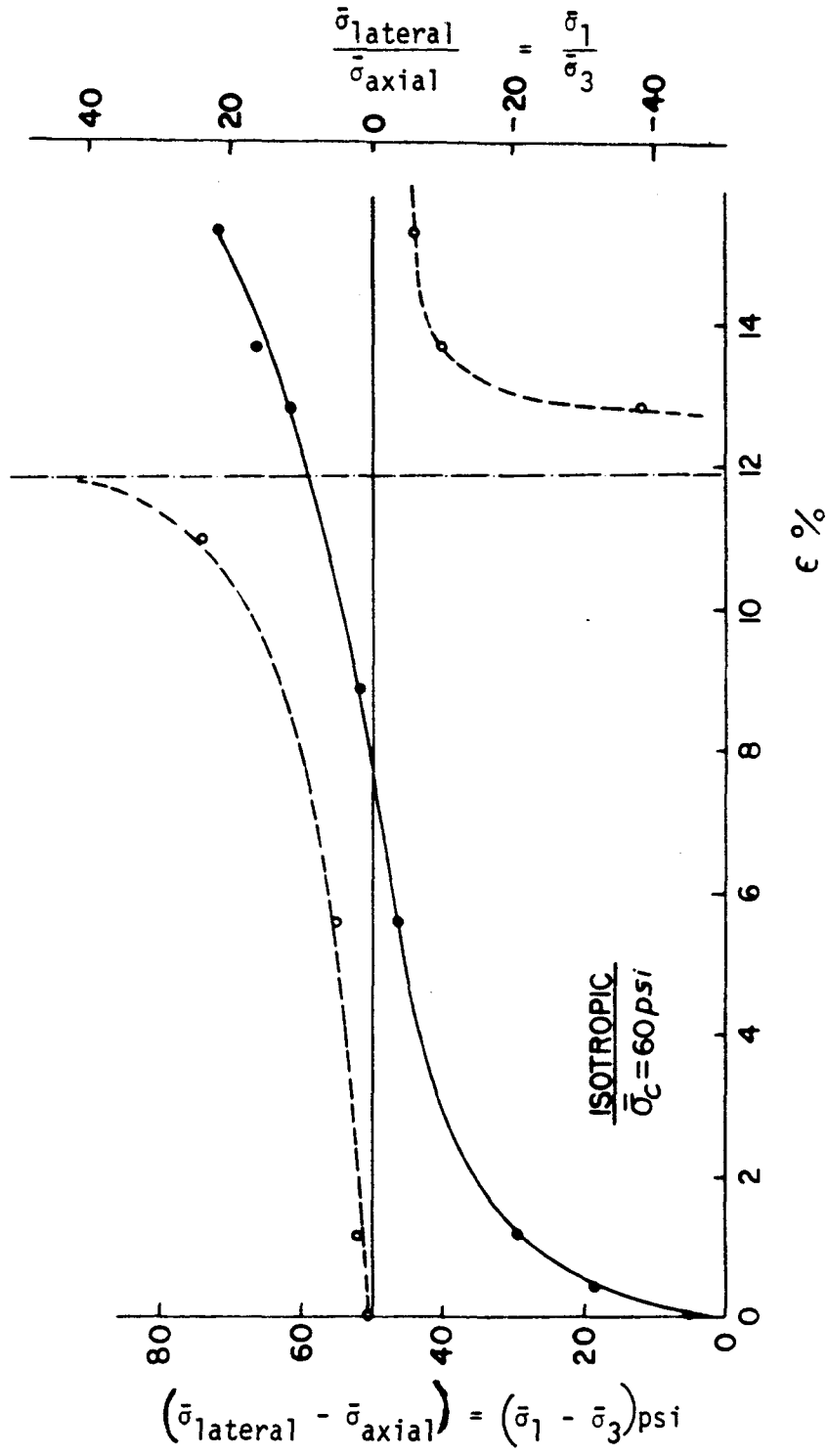
Fig. A-2 Standard Triaxial Specimen Tested in Extension



(a) Anisotropic

Fig. A-3 Stress-Strain and Stress Ratios for Reduced Area Specimens Tested in Extension





(b) Isotropic

Fig. A-3 Stress-Strain and Stress Ratios for Reduced Area Specimens

Tested in Extension

TABLE I  
 RAMBERG-OSGOOD COEFFICIENTS FOR  
 UNDEGRADED BACKBONE AND DAMPING CURVES

10th Cycle

	SL	$\lambda$	Measured $\frac{E'}{E'_{max}}, \frac{G'}{G'_{max}}$		From Eq. (7-3)		From Eq.(7-5)		From Eq. (7-5)
			$\frac{E'}{E'_{max}}$	$\frac{G'}{G'_{max}}$	R	$\alpha$	R	$\alpha$	$\lambda$
AXIAL $\bar{\sigma}_c = 40$ psi	.20	.178	.529		4.09	122.57	3.92	98.11	.182
	.40	.283	.131				3.09	45.21	.336
	.42	.268	.110				2.80	38.40	.334
	.79	.214	.0157				2.04	80.06	.381
TORSIONAL $\bar{\sigma}_c = 40$ psi	.36	.312	.335		6.84	766.42	6.60	608.4	.315
	.39	.213	.221				2.51	14.55	.369
	.53	.289	.099				3.03	33.04	.427
	.57	.262	.019				2.45	16.35	.350
AXIAL $\bar{\sigma}_c = 60$ psi	.10	.055	.742		3.35	61.04	2.01	3.53	.089
	.20	.106	.481				1.94	4.94	.178
	.40	.219	.176				2.43	17.41	.283
	.41	.248	.123				2.60	29.65	.302
	.60	.223	.0336				2.14	51.41	.332
TORSIONAL $\bar{\sigma}_c = 60$ psi	.36	.222	.289		3.78	41.91	2.93	17.58	.263
	.53	.283	.122				3.05	26.46	.325

TABLE II  
 RAMBERG-OSGOOD COEFFICIENTS FOR CURVES  
 USING  $\delta = N^{-t}$

10th Cycle

	SL	t	From Eq. (7-6)		From Eq. (7-9)		Eq. (7-9)
			$\alpha$	R	$\alpha$	R	$\lambda^*$
AXIAL $\bar{\sigma}_c = 40$ psi	.20	.045	4.45	2.30	383.8	5.18	.104
	.40	.293			5.93	3.98	.186
	.42	.322			4.52	3.42	.193
	.79	.526			6.15	2.10	.237
TORSIONAL $\bar{\sigma}_c = 40$ psi	.36	.233	2.00	1.96	$4 \times 10^{-4}$	-14.57	.088
	.39	.169			6.14	2.97	.140
	.53	.453			0.632	4.43	.149
	.57	.794			0.813	2.75	.183
AXIAL $\bar{\sigma}_c = 60$ psi	.10	.026	5.72	2.34	5.86	2.37	.054
	.20	.033			4.70	2.06	.123
	.40	.228			5.00	2.92	.179
	.41	.245			6.92	2.98	.200
	.60	.379			7.33	2.23	.235
TORSIONAL $\bar{\sigma}_c = 60$ psi	.36	.127	2.13	1.41	10.86	3.64	.066
	.53	.387			0.977	4.45	.076

\* Compare to measured  $\lambda$  in Table I.

TABLE III  
 RAMBERG-OSGOOD COEFFICIENTS FOR  
 DEGRADED BACKBONE CURVE-EQ. (7-11)

	N	AXIAL		TORSIONAL	
		$\alpha$	R	$\alpha$	R
$\bar{\sigma}_c = 40$ psi	1	65.45	3.87	253.03	6.53
	5	18.34	3.22	7.60	4.20
	10	10.54	2.91	3.12	3.00
	20	7.01	2.29	2.01	2.61
	50	8.45	2.82	1.64	1.66
$\bar{\sigma}_c = 60$ psi	1	30.96	3.01	18.32	3.07
	5	14.37	2.68	26.63	4.74
	10	9.85	2.49	10.15	3.91
	20	6.66	2.28	5.21	2.88
	50	5.56	2.21	2.64	1.99

PART III

STEADY RESPONSE OF A CIRCULAR FOUNDATION

ON A TRANSVERSELY ISOTROPIC MEDIUM

by

David John Kirkner

PH.D. THESIS

STEADY STATE RESPONSE OF A CIRCULAR FOUNDATION  
ON A TRANSVERSELY ISOTROPIC MEDIUM

by  
DAVID JOHN KIRKNER

Submitted in partial fulfillment of the requirements  
for the Degree of Doctor of Philosophy

Department of Civil Engineering  
CASE WESTERN RESERVE UNIVERSITY  
August 1979

STEADY STATE RESPONSE OF A CIRCULAR FOUNDATION  
ON A TRANSVERSELY ISOTROPIC MEDIUM

Abstract

by

DAVID JOHN KIRKNER

The steady state response of a circular foundation vibrating harmonically on a transversely isotropic elastic half space is investigated. The analytical solution to the massless disc problem requires the elastic constants to satisfy a certain constraint equation. Typical values of the elastic constants for actual soils are shown to agree well in many instances with this constraint equation.

Dimensionless parameters which are functions of the elastic constants are utilized to define the degree of anisotropy when the foundation is undergoing vertical, rocking or translational vibrations. Impedance and compliance coefficients are presented in tables and curves for a wide range of a dimensionless frequency parameter.

Approximate impedance and compliance coefficients are also obtained for a visco-elastic soil.

The effect of the mass of the foundation on the amplitude of vibration is also studied. A principal

result is that for massive foundations undergoing harmonic vibrations the dimensionless part of the isotropic impedance function may be used with the expression for the anisotropic static stiffness to obtain the amplitude of vibration. A dimensionless parameter determines the Poisson's ratio of the equivalent isotropic soil. The result is important for the design of machine foundations since it allows for an approximate analysis by using the available isotropic solutions.



## ACKNOWLEDGEMENTS

The author would like to thank the National Science Foundation, Grant Number ENV-76-12332, for partial support of this work. He would also like to thank his committee, Drs. C. Miller, Chairman, A. Saada, G. Gazetas and T. Kicher for reviewing this work.

Finally, he must thank his wife Carol, whose constant support made his graduate education possible.

## TABLE OF CONTENTS

CHAPTER		PAGE
I.	INTRODUCTION.....	<u>III-1</u>
	1.1 Object of Study.....	<u>III-1</u>
	1.2 Historical Review.....	<u>III-4</u>
	1.3 Scope of Study.....	<u>III-7</u>
II.	WAVE PROPAGATION IN A CONSTRAINED TRANSVERSELY ISOTROPIC ELASTIC MATERIAL.	<u>III-8</u>
	2.1 General.....	<u>III-8</u>
	2.2 Basic Equations.....	<u>III-8</u>
	2.3 Body Wave Propagation.....	<u>III-12</u>
	2.4 Surface Wave Propagation.....	<u>III-24</u>
	2.5 Range of Dimensionless Elastic Constants.....	<u>III-28</u>
III.	SOLUTION OF THE HOMOGENEOUS ELASTIC HALF SPACE PROBLEM .....	<u>III-32</u>
	3.1 General.....	<u>III-32</u>
	3.2 General Solution of the Equations of Motion.....	<u>III-33</u>
	3.3 Stiffness and Flexibility coefficients.....	<u>III-38</u>
	3.4 Reduction to Dimensionless Form.	<u>III-53</u>
	3.5 Numerical Solution.....	<u>III-57</u>
	3.6 Results.....	<u>III-62</u>
IV.	APPROXIMATE SOLUTION OF THE VISCOELASTIC PROBLEM.....	<u>III-66</u>
	4.1 General.....	<u>III-66</u>
	4.2 Viscoelastic Models.....	<u>III-67</u>
	4.3 Viscoelastic Impedance Functions	<u>III-72</u>

CHAPTER	PAGE
4.4 RESULTS.....	<i>III</i> -74
V. MASSIVE FOUNDATIONS.....	<i>III</i> -76
5.1 GENERAL.....	<i>III</i> -76
5.2 EQUIVALENT SINGLE DEGREE OF FREEDOM REPRESENTATION.....	<i>III</i> -76
5.3 RESULTS.....	<i>III</i> -80
VI. SUMMARY & CONCLUSIONS.....	<i>III</i> -86
FIGURES.....	<i>III</i> -89
TABLES.....	<i>III</i> -104
APPENDIX A.....	<i>III</i> -166
APPENDIX B.....	<i>III</i> -170
APPENDIX C.....	<i>III</i> -205
REFERENCES.....	<i>III</i> -217

## NOTATION

$\alpha$	-	$\rho\omega^2/C_{rr}$	
$\beta$	-	$\rho\omega^2/G$	
	-	Damping ratio	
$\beta_H$	-	$\rho\omega^2/G_H$	
$\gamma$	-	$c_2/\bar{c}_1 = G/C_{xx}, G/C_{rr}$	
$\gamma_{12}, \gamma_{13}, \gamma_{23}$	}		- shear strain
$\gamma_{xy}, \gamma_{xz}, \gamma_{yz}$			
$\gamma_{r\theta}, \gamma_{rz}, \gamma_{\theta z}$			
$\delta$	-	Prescribed angle of rotation	
$\epsilon_{ij}$	-	Strain tensor	
$\zeta$	-	Voigt loss factor = $\frac{C_z G'}{r_o \bar{G}}$	
$\eta$	-	Scalar potential	
$\lambda_1$	-	$C_{xx}/C_{zz}, C_{rr}/C_{zz}$	
$\lambda_2$	-	$G_H/G$	

## NOTATION

$\nu_\alpha$	-	$\sqrt{\xi^2 - \alpha^2}$
$\nu_\beta$	-	$\sqrt{\xi^2 - \beta^2}$
$\nu_{\beta_H}$	-	$\sqrt{\xi^2 - \beta_H^2}$
$\nu_{vH}, \nu_{Hv}, \nu_H$	-	Poisson's ratios
$\xi$	-	Hankel transform parameter
$\rho$	-	mass density
$\tau_{ij}$	-	Stress tensor
$\phi$	-	scalar potential
$\chi$	-	scalar potential
$\omega$	-	circular frequency

## NOTATION

$\Delta_H$	- Prescribed horizontal displacement
$\Delta_V$	- Prescribed vertical displacement
$\Sigma$	- $\frac{C_{xz} + C_{zz}}{C_{zz} - G}$ , $\frac{C_{rz} + C_{zz}}{C_{zz} - G}$
$\Phi$	- $\frac{C_{xz} + C_{zz}}{C_{zz} - G}$ , $\frac{C_{rz} + C_{zz}}{C_{zz} - G}$
$\Psi_H$	- $\left[ \frac{1}{\lambda_2} - \frac{\Phi - 2}{\Phi(1 - \lambda_2)} \right]$
$\Psi_V$	- $\left[ \frac{-\lambda_1(\Phi - 2)}{\Phi(1 - \lambda_1)} \right]$
$a_0$	- Dimensionless frequency = $\frac{\omega r_0}{c_2}$
$\bar{c}_1$	- $C_{xx}/\rho$ $C_{rr}/\rho$
$\bar{c}_2$	- $G_H/\rho$
$c_2$	- $G/\rho$
$f(\xi)$	- Surface wave equation = $\left[ (\Phi \xi^2 - \beta^2) - \xi^2 \Phi^2 \lambda_1 \nu_\alpha \nu_\beta \right]$

## NOTATION

$g(\xi)$	-	$[\phi \xi^2 (\phi - 2) + \beta^2]$	
$k$	-	$\xi/\beta$	
$n$	-	$E_H/E_V$	
$r_0$	-	Radius of disc	
$\tan \delta$	-	Hysteretic loss coefficient	
$B_V$	-	Vertical mass ratio = $\frac{\Psi_V}{4} \frac{M}{\rho r_0^3}$	
$B_R$	-	Rocking mass ratio = $\frac{3\Psi_V}{8} \frac{I}{\rho r_0^5}$	
$B_H$	-	Horizontal mass ratio = $\frac{\Psi_H}{8} \frac{M}{\rho r_0^3}$	
$C_{11}, C_{12}, C_{13}, C_{33}$	}	$C_{xx}, C_{xy}, C_{xz}, C_{zz}$	- Elastic constants
$C_{rr}, C_{r\theta}, C_{rz}, C_{zz}$			
$E_H$	-	Horizontal modulus of elasticity	
$E_V$	-	Vertical modulus of elasticity	
$F(k)$	-	$[(\phi k^2 - 1)^2 - k^2 \phi^2 \lambda_1 \nu_\alpha \nu_\beta]$	

## NOTATION

$G$	- Shear modulus
$G_H$	- Shear modulus = $1/2(C_{rr} - C_{r\theta})$
$K_H$	- Horizontal static stiffness = $\frac{8Gr_0}{\psi_H}$
$K_R$	- Rocking static stiffness = $\frac{8Gr_0^3}{3\psi_V}$
$K_V$	- Vertical static stiffness = $\frac{8Gr_0}{\psi_V}$
$M$	- Total resisting moment under disc
$P_H$	- Total horizontal force under disc
$P_V$	- Total vertical force under disc
$V_\alpha$	- $\sqrt{k^2 - \gamma^2}$
$V_\beta$	- $\sqrt{k^2 - 1}$
$V_{\beta H}$	- $\sqrt{k^2 - 1/\lambda_2^2}$
$\bar{X}$	- $r/r_0$



# CHAPTER I

## INTRODUCTION

### 1.1 Object of Study

Recent years have seen considerable research activity in the dynamic response of structures founded on soils. Requirements for nuclear power plant structural safety in the event of an earthquake have given great impetus to this activity (1). The problem also has direct application in the design of machine foundations.

To date, this research activity has been directed toward the response of machines or structures founded on isotropic soils. It is the intent of this study to determine the effect that material anisotropy has on the dynamic response of structures.

It has been observed that the process of sedimentation followed by one-dimensional consolidation results in a material possessing cross anisotropic or transversely isotropic mechanical properties (2). Also, it can be shown (3), (4), (5) that a mass of material consisting of an alternating system of individual homogeneous layers is equivalent to a single mass of a cross anisotropic material, provided the thickness of the layers is small compared to the other dimensions of the problem. Varved clays are an example of this type of medium. Thus the study of soil structure interaction effects considering soil anisotropy is of considerable practical interest.

There are numerous analytical techniques available in the literature for obtaining the dynamic response of structures including the effects of ground interaction. Probably the most widely used in practice today is the finite element method, (1), (6). A major drawback to the finite element method is its inability to model infinite regions. Unless a significant amount of material damping is present, energy which should radiate to infinity is reflected back into the soil mass. This difficulty was partially overcome by the development of the so-called transmitting boundary (7), (8). This enabled the lateral boundaries of the finite element grid to be placed almost at the edge of the foundation. However, a rigid lower boundary is still required at some finite depth, whether one actually exists or not. The method has some obvious advantages for this problem. It easily handles embedded foundations, layered media and even anisotropic materials.

There are techniques which are not entirely numerical, but utilize a continuum solution along with numerical procedures (9), (10), (11). The foundation of these techniques is usually the solution to some basic problem such as a uniform stress, harmonic in time, distributed over a rectangular region on the surface of an elastic half space. A number of these rectangular regions are then assembled to give the desired foundation configuration. The

amplitude of the uniform stress over each subregion is adjusted to yield the overall specified foundation displacement<sup>(10)</sup>. Techniques such as this account properly for the radiation of energy to infinity. The main advantage is the ability to model foundations of arbitrary shape. Solutions have also been presented for foundations on layered media<sup>(9)</sup>.

A third method is to solve the governing differential equations of motion, usually for a simple foundation geometry (12),(13),(14),(15),(16),(17),(18). The problem is difficult, however, because it involves mixed boundary conditions. The standard procedure is to reduce the equations of motion and boundary conditions to one or two integral equations. The integral equation(s) may then be solved numerically to any desired degree of accuracy. The results, usually presented in dimensionless form, include the total force under a rigid, massless footing undergoing unit harmonic vibrations, i.e., the dynamic stiffness or impedance. The equations of motion for a given structure can be written to include the dynamic stiffness of the soil.

Analytical solutions offer distinct advantages over other methods especially for half space problems. Besides the relatively low cost, they are inherently more accurate.

The purpose of this study is to assess the effect of soil anisotropy. This will obviously entail

a large number of analyses and so an analytical solution is economically attractive. Also, the effect of the anisotropy is most easily assessed if the least number of parameters other than the soil anisotropy are introduced. A basic problem which is amendable to an analytical solution and which fits this requirement is the circular foundation supported on the surface of an elastic half space. This will be the problem studied herein.

## 1.2 Historical Review

The first attempt at the solution of the harmonically vibrating footing was made by Reissner in 1936 (19). He solved the problem by integrating the solution to a harmonically vibrating point load on an elastic half space (previously determined by Lamb (20) ) over a circular area. He thus approximated the rigid footing with a uniform pressure distribution.

Several years later Sung (21) and Quinlan(22) examined other assumed stress distributions and presented results for low values of a dimensionless frequency parameter ( $a_0 = \omega r_0 / c_s$ ) first introduced by Reissner. In this expression  $\omega$  is the circular frequency,  $r_0$  is the radius of the disc and  $c_s$  is the shear wave velocity of the soil. Bycroft (23) assumed the static stress distribution existed under the footing and examined all modes of vibration. He also attempted an approximate solution

to the coupling motions between rocking and sliding. Again solutions were presented only for low values of the dimensionless frequency. The results of Bycroft were used in the early soil-structure analyses (24).

It will be noted that in all the above solutions, the actual mixed boundary value problem was converted to a first boundary value problem by assuming a stress distribution under the footing. Lysmer (25) attempted to circumvent this by replacing the footing with a set of concentric rings each with a uniform stress. By adjusting the value of the stress on each ring he was able to get a uniform displacement and thus approximate the behaviour of a rigid footing. Lysmer noted, as did Reissner, that the equation of motion of the circular footing was analogous to that of a single degree of freedom oscillator with the impedance or dynamic stiffness of the soil acting as a spring and a dashpot. Of course this "spring and dashpot" were frequency dependent. By adjusting the equivalent spring and dashpot to values which were independent of  $\omega$ , he arrived at an approximate equation of motion for the mass which was truly analogous to a single degree of freedom oscillator. This has been dubbed "Lysmer's analog" (25).

The first attack on the problem as a true mixed boundary value problem was by Robertson(26). Since the vertical oscillation problem is axially symmetric he was

able to reduce the equations of motion and boundary conditions to a pair of dual integral equations, via Hankel transforms. The dual integral equations were of the type possessing a Hankel kernel and an arbitrary weight function and were reduced to a single Fredholm equation of the second kind by methods as described in Sneddon (27). Robertson expanded the kernel of the integral equation in a power series allowing him to present results valid only for low dimensionless frequencies.

Gladwell (28), beginning with the general solution to the isotropic equations of motion expressed in circular coordinates (due to Sezawa (29) ), was able to follow a method similar to Robertson and give results for the rocking and translational problem; again only valid for low dimensionless frequencies.

Shah (30), by a different technique obtained the same integral equation as Robertson which he solved numerically yielding results over a wide range of frequencies. At approximately this same time, Luco and Westmann(12) using Gladwell's technique recapped the integral equations for all modes of vibration and presented extensive results including contact stresses and far field surface displacements.

In (14), (15), and (16) the solutions were extended to layered media, by methods similar to the half space problem. Luco in (17) replaced the elastic constants

with complex moduli and solved the viscoelastic problem for the half space and for a single layer overlying a half space.

### 1.3 Scope of Study

There are three main areas to this study. The first is the determination of the harmonic force-displacement relationship of a massless, rigid, circular disc supported on a transversely isotropic elastic half space. This relationship will be determined at discrete values of the dimensionless frequency parameter and for a practical range of soil properties. The second area is the approximate solution to the same problem for a linear viscoelastic soil. This simulates the losses due to hysteresis which occur in a true soil. Finally, the effect of foundation mass will be studied over a frequency range determined to be of practical interest.

## CHAPTER II

### WAVE PROPAGATION IN A CONSTRAINED TRANSVERSELY ISOTROPIC ELASTIC MATERIAL

#### 2.1 General

In this chapter the phenomena of body and surface wave propagation in transversely isotropic materials will be discussed. The results presented should provide insight into the nature of the problem to be addressed in the next chapter.

Primarily for mathematical simplification a certain constraint equation is assumed to hold between some of the elastic constants. The practical use of such a "constrained" material is discussed.

#### 2.2 Basic Equations

Primarily to define notation, the stress-strain equations for a transversely isotropic linear elastic material are given below:

$$\sigma_{11} = C_{11}\epsilon_{11} + C_{12}\epsilon_{22} + C_{13}\epsilon_{33} \quad (2.1a)$$

$$\sigma_{22} = C_{12}\epsilon_{11} + C_{11}\epsilon_{22} + C_{13}\epsilon_{33} \quad (2.1b)$$

$$\sigma_{33} = C_{13}\epsilon_{11} + C_{13}\epsilon_{22} + C_{33}\epsilon_{33} \quad (2.1c)$$

$$\sigma_{12} = \frac{1}{2}(C_{11} - C_{12})\gamma_{12} = G_H\gamma_{12} \quad (2.1d)$$

$$\sigma_{13} = G\gamma_{13} \quad (2.1e)$$

$$\sigma_{23} = G\gamma_{23} \quad (2.1f)$$



The "3" axis is the axis of symmetry, and the equations are valid in cartesian or circular cylindrical coordinates replacing the subscripts (1, 2, 3) with (x,y,z) or (r,θ,z) respectively.

The strains can be expressed in terms of the stresses by the following relations

$$\epsilon_{11} = \frac{\sigma_{11}}{E_H} - \frac{\nu_H}{E_H} \sigma_{22} - \frac{\nu_{VH}}{E_V} \sigma_{33} \quad (2.2a)$$

$$\epsilon_{22} = -\frac{\nu_H}{E_H} \sigma_{11} + \frac{\sigma_{22}}{E_H} - \frac{\nu_{VH}}{E_V} \sigma_{33} \quad (2.2b)$$

$$\epsilon_{33} = -\frac{\nu_{HV}}{E_H} \sigma_{11} - \frac{\nu_{HV}}{E_H} \sigma_{22} + \frac{\sigma_{33}}{E_V} \quad (2.2c)$$

$$\gamma_{12} = \frac{\sigma_{12}}{G_H} \quad (2.2d)$$

$$\gamma_{13} = \frac{\sigma_{13}}{G} \quad (2.2e)$$

$$\gamma_{23} = \frac{\sigma_{23}}{G} \quad (2.2f)$$

From equations (2.1) and (2.2) the following relationships can be determined between the elastic parameters

$$C_{11} = \frac{E_H(1-n \nu_{VH}^2)}{(1+\nu_H)(1-\nu_H-2n \nu_{VH}^2)} \quad (2.3a)$$

$$C_{12} = \frac{E_H(\nu_H+n \nu_{VH}^2)}{(1+\nu_H)(1-\nu_H-2n \nu_{VH}^2)} \quad (2.3b)$$

$$C_{13} = \frac{E_H \nu_{VH}}{1-\nu_H-2n \nu_{VH}^2} \quad (2.3c)$$

$$C_{33} = \frac{E_H(1-\nu_H)}{n(1-\nu_H-2n \nu_{VH}^2)} \quad (2.3d)$$

$$G_H = \frac{E_H}{2(1+\nu_H)} \quad (2.3e)$$

$$n = \frac{E_H}{E_V} = \frac{\nu_{HV}}{\nu_{VH}} \quad (2.3f)$$

In equation (2.3)  $E_H$  is the modulus of elasticity in the horizontal direction,  $E_V$  is the modulus of elasticity in the vertical direction,  $\nu_H$  is Poisson's ratio measuring the effect of horizontal strain on complimentary horizontal strain,  $\nu_{HV}$  is Poisson's ratio measuring the effect of horizontal strain on vertical strain,  $\nu_{VH}$  is Poisson's ratio

measuring the effect of vertical strain on horizontal strain and  $n$  is by definition the degree of anisotropy. This notation is similar to Gerrard, reference (40).

Substituting equations (2.1) along with the strain displacement relations into the equations of equilibrium yields the equations of motion in terms of the displacement components. In cartesian coordinates they are

$$C_{xx}u_{x,xx} + G_H u_{x,yy} + G u_{x,zz} + (C_{xx} - G_H)u_{y,xy} + (C_{xz} + G) u_{z,xz} = \rho \ddot{u}_x \quad (2.4a)$$

$$(C_{xx} - G_H)u_{x,xy} + C_{xx}u_{y,yy} + G_H u_{y,xx} + G u_{y,zz} + (C_{xz} + G)u_{z,yz} = \rho \ddot{u}_y \quad (2.4b)$$

$$G(u_{z,xx} + u_{z,yy}) + C_{zz} u_{z,zz} + (C_{xz} + G)(u_{x,xz} + u_{y,yz}) = \rho \ddot{u}_z \quad (2.4c)$$

In equations (2.4) the displacements in the  $x$ ,  $y$ ,  $z$  directions are  $u_x$ ,  $u_y$ ,  $u_z$  respectively.  $\rho$  is the mass density, and the convention for differenti-

ation is

$$u_{x,xy} = \frac{\partial^2 u_x}{\partial x \partial y}$$

$$\ddot{u}_x = \frac{\partial^2 u_x}{\partial t^2}$$

For future reference the equations of motion in circular cylindrical coordinates are

$$C_{rr} \left( \frac{1}{r} (ru_r)_{,r} \right) + \frac{1}{r^2} G_H u_{r,\theta\theta} + G u_{r,zz} + \frac{1}{r} (C_{rr} - G_H) u_{\theta,r\theta} - (C_{rr} + G_H) \frac{1}{r^2} u_{\theta,\theta} + (C_{rz} + G) u_{z,rz} = \rho \ddot{u}_r \quad (2.5a)$$

$$(C_{rr} + G_H) \frac{1}{r^2} u_{r,\theta} + \frac{1}{r} (C_{rr} - G_H) u_{r,r\theta} + \frac{1}{r^2} C_{rr} u_{\theta,\theta\theta} + G_H \left( \frac{1}{r} (ru_\theta)_{,r} \right)_{,r} + G u_{\theta,zz} + \frac{1}{r} (C_{rz} + G) u_{z,\theta z} = \rho \ddot{u}_\theta \quad (2.5b)$$

$$\frac{1}{r} (C_{rz} + G) [(r u_{r,z})_{,r} + u_{\theta,\theta z}] + \frac{1}{r} G (ru_{z,r})_{,r} + \frac{1}{r^2} G u_{z,\theta\theta} + C_{zz} u_{z,zz} = \rho \ddot{u}_z \quad (2.5c)$$

### 2.3 Body Wave Propagation

If it is assumed that a plane harmonic wave is propagating in some direction given by direction cosines  $l, m, n$  with respect to the  $x, y, z$  axes, the displacement components may be expressed as

$$u_x = A_1 \exp \left[ i \frac{2\pi}{L} (\ell x + m y + n z \pm ct) \right] \quad (2.6a)$$

$$u_y = A_2 \exp \left[ i \frac{2\pi}{L} (\ell x + m y + n z \pm ct) \right] \quad (2.6b)$$

$$u_z = A_3 \exp \left[ i \frac{2\pi}{L} (\ell x + m y + n z \pm ct) \right] \quad (2.6c)$$

In equations (2.6)  $c$  is the wave speed,  $L$  is the wavelength and the  $A_i$  are amplitudes. Substituting equations (2.6) into (2.4) yields the following homogeneous equations given in matrix form

$$\begin{bmatrix} (B_1 - \Lambda) & B_6 & B_5 \\ B_6 & (B_2 - \Lambda) & B_4 \\ B_5 & B_4 & (B_3 - \Lambda) \end{bmatrix} \begin{Bmatrix} A_1 \\ A_2 \\ A_3 \end{Bmatrix} = \begin{Bmatrix} 0 \\ 0 \\ 0 \end{Bmatrix} \quad (2.7)$$

where

$$B_1 = C_{xx} \ell^2 + G_H m^2 + G n^2$$

$$B_2 = G_H \ell^2 + C_{xx} m^2 + G n^2$$

$$B_3 = G \ell^2 + G m^2 + C_{zz} n^2$$

$$B_4 = (C_{xz} + G) m n$$

$$B_5 = (C_{xx} - G_H) \ell m$$

$$B_6 = (C_{xx} - G_H) \Lambda$$

$$\Lambda = \rho c^2$$

In order that there be motion, the determinant of the coefficients in equations (2.7) must vanish. This condition gives a cubic equation in  $\Lambda$ , the solution of which yields three real wave speeds. In fact, this is the case even for a completely general anisotropic material-see ref. (31). For the simple case of an isotropic material solution of the cubic yields wave speeds independent of the direction of propagation. One root corresponds to a dilatational wave and the two repeated roots correspond to shear waves.

The determinant resulting from equation (2.7) does not yield roots independent of the direction of propagation and in fact they cannot be expressed in a simple form. However, if the elastic constants are constrained to satisfy the following relation

$$(C_{13} + G)^2 = (C_{11} - G)(C_{33} - G) \quad (2.8a)$$

or

$$G = \frac{C_{11} C_{33} - C_{13}^2}{C_{11} + 2C_{13} + C_{33}} \quad (2.8b)$$

the roots of the determinantal equation become

$$\Lambda_1 = \rho c_1^2 = C_{xx}(l^2 + m^2) + C_{zz} n^2 \quad (2.9a)$$

$$\Lambda_2 = \rho c_2^2 = G_H(l^2 + m^2) + G n^2 \quad (2.9b)$$

$$\Lambda_3 = \rho c_3^2 = G(l^2 + m^2 + n^2) = G \quad (2.9c)$$

In essence this constraint defines a subset of all transversely isotropic materials by making the shear modulus,  $G$  a function of the other elastic parameters. This type of material appears first to have been investigated by Carrier (32). Particular applications have been made in refs. (33), (34), and (35). Henceforth, use of the phrase constrained transversely isotropic medium will mean a transversely isotropic material whose elastic constants satisfy equation (2.8).

The motivation for using this constrained transversely isotropic material is not simply that the wave speed appears in a convenient form, but that the equations of motions can be uncoupled in terms of potential functions as will be shown subsequently. Payton (34) states, "the value of such a constraint relation lies not in its approximation to any particular material, but rather in the mathematical simplification of the problem while still preserving some of the qualitative features of wave propagation in transversely isotropic media".

A set of eigenvectors corresponding to the eigenvalues, equation (2.9) is

$$\begin{bmatrix} A_{11} & A_{12} & A_{13} \\ A_{21} & A_{22} & A_{23} \\ A_{31} & A_{32} & A_{33} \end{bmatrix} = \begin{bmatrix} 1 & -m & -1 \\ m & 1 & -m \\ n/\Sigma & 0 & \Sigma(1^2+m^2)/n \end{bmatrix} \quad (2.10)$$

where

$$\Sigma = \frac{C_{xz} + G}{C_{zz} - G} \quad (2.11)$$

For the limiting case of an isotropic material equations (2.9) become

$$\begin{aligned} \Lambda_1 &= (\lambda + 2\mu) \\ \Lambda_2 &= \Lambda_3 = \mu \end{aligned}$$

where  $\lambda$  and  $\mu$  are Lamé's constants and  $\Sigma$  becomes identically one. The wave associated with  $\Lambda_1 = \lambda + 2\mu$  is of course the dilatational wave. This is easily shown by taking the first eigenvector from (2.10) (with  $\Sigma=1$ ) substituting into (2.6) and utilizing the strain displacement relations to show that the components of the rotation vector are identically zero. For  $\Sigma$  not equal to one a similar result can be obtained by defining an artificial  $z$ -axis as



$$\bar{z} = \Sigma z \quad (2.12)$$

Equations (2.6) now become

$$u_i = A_i \exp\left\{i \frac{2\pi}{L} \left(1x+my+\frac{n\bar{z}}{\Sigma} \pm ct\right)\right\} \quad (2.13)$$

Again using the first eigenvector of (2.10) in (2.13) along with the strain displacement relations it is easily shown that the components of the rotation vector vanish. Thus, referred to this distorted coordinate system, the wave speed (2.9a) corresponds to a dilatational wave. Following this same procedure the wave speeds (2.9b) and (2.9c) correspond to shear waves with respect to the distorted coordinate system, i.e. the volumetric strain is zero.

This property of equation (2.12) hints at a method for uncoupling the equations of motion. With isotropic materials a standard procedure is to define the displacement vector in terms of two potential functions according to Helmholtz's Theorem as

$$\underline{u} = \underline{\nabla}\phi + \underline{\nabla}\times\underline{\psi}$$

Substitution into the equations of motion yields a scalar wave equation in  $\phi$  and a vector wave equation

in  $\psi$ . In the analysis of the transversely isotropic material above, the distortion of the z-axis was equivalent to replacing the operator  $\partial/\partial z$  with  $(1/\Sigma)(\partial/\partial z)$ . Therefore, define the following modified operators<sup>(32)</sup>

$$\nabla_{\Sigma}^* = (\partial/\partial x) a_{\Sigma x} + (\partial/\partial y) a_{\Sigma y} + (\partial/\partial z)(1/\Sigma) a_{\Sigma z}$$

$$\begin{aligned} \nabla_{\Sigma}^* \times \psi &= \left( \frac{\partial \psi_3}{\partial y} - \frac{1}{\Sigma} \left( \frac{\partial \psi_2}{\partial z} \right) \right) a_{\Sigma x} \\ &+ \left( \frac{1}{\Sigma} \left( \frac{\partial \psi_1}{\partial z} \right) - \frac{\partial \psi_3}{\partial x} \right) a_{\Sigma y} \\ &+ \left( \frac{\partial \psi_2}{\partial x} - \frac{\partial \psi_1}{\partial y} \right) a_{\Sigma z} \end{aligned}$$

and let

$$u = \nabla_{\Sigma}^* \phi - \nabla_{\Sigma}^* \times \psi \tag{2.14}$$

Substitution of (2.14) into the equations of motion along with the additional restriction

$$\frac{\partial \psi_1}{\partial x} + \frac{\partial \psi_2}{\partial y} = 0 \tag{2.15}$$

yields the following uncoupled equations

$$C_{xx} \phi_{,xx} + C_{yy} \phi_{,yy} + C_{zz} \phi_{,zz} - \rho \ddot{\phi} = 0 \quad (2.16a)$$

$$G(\psi_{1,xx} + \psi_{1,yy} + \psi_{1,zz}) - \rho \ddot{\psi}_1 = 0 \quad (2.16b)$$

$$G(\psi_{2,xx} + \psi_{2,yy} + \psi_{2,zz}) - \rho \ddot{\psi}_2 = 0 \quad (2.16c)$$

$$G_H (\psi_{3,xx} + \psi_{3,yy}) + G \psi_{3,zz} - \rho \ddot{\psi}_3 = 0 \quad (2.16d)$$

Equations 2.16a, d could be transformed to a standard Poisson form by again distorting the z- axis. Then 2.16a becomes

$$\nabla^2 \phi - \frac{1}{c_1} \ddot{\phi} = 0$$

where

$$\nabla^2 = \frac{\partial^2}{\partial x^2} + \frac{\partial^2}{\partial y^2} + \frac{\partial^2}{\partial z^2}$$

$$\bar{z} = z/\lambda_1$$

$$\lambda_1 = (C_{xx}/C_{zz})^{1/2}$$

$$\bar{c}_1^2 = C_{xx}/\rho$$

Note in general that  $\bar{c}_1$  is not the wave speed of (2.9a). The physical relationship between the two can be inferred from Fig. 2.1 and equation 2.9a, (where for convenience  $m$  is taken as zero).

Dividing (2.9a) on both sides by  $C_{xx}$

$$\frac{\rho c_1^2}{C_{xx}} = l^2 + \frac{n^2}{\lambda_1^2} \equiv p^2$$

or

$$\frac{\rho c_1^2}{p^2 C_{xx}} = 1$$

Define  $\bar{c}_1^2 = c_1^2 / p^2$  where in general

$$p^2 = l^2 + m^2 + n^2/\lambda_1^2$$

Then  $\bar{c}_1^2 = C_{xx}/\rho$  as given above and the direction of propagation is defined by the unit vector

$$\hat{a} = (l/p) \hat{a}_x + (m/p) \hat{a}_y + (n/p\lambda_1) \hat{a}_z$$

Similarly for equation (2.16d)

$$\nabla^2 \psi_3 - \frac{1}{\bar{c}_2^2} \ddot{\psi}_3 = 0$$

$$\nabla^2 = \frac{\partial^2}{\partial x^2} + \frac{\partial^2}{\partial y^2} + \frac{\partial^2}{\partial z^2}$$

$$\bar{z} = z/\lambda_2$$

$$\lambda_2^2 = G_H/G$$

$$\bar{c}_2^2 = G_H/\rho$$

For use in the next chapter, the preceding results are required in circular cylindrical coordinates

$$\underline{u} = u_r \underline{a}_r + u_\theta \underline{a}_\theta + u_z \underline{a}_z$$

$$\nabla^* \phi = \phi_{,r} \underline{a}_r + \frac{1}{r} \phi_{,\theta} \underline{a}_\theta + \frac{1}{\Sigma} \phi_{,z} \underline{a}_z$$

$$\begin{aligned} \nabla^* \times \underline{\psi} &= \left( \frac{1}{r} \psi_{3,\theta} - \frac{1}{\Sigma} \psi_{z,z} \right) \underline{a}_r \\ &+ \left( \frac{1}{\Sigma} \psi_{1,z} - \psi_{3,r} \right) \underline{a}_\theta \\ &+ \frac{1}{r} \left( (r \psi_2)_{,r} - \psi_{1,} \right) \underline{a}_z \end{aligned}$$

Eqn. (2.15) becomes

$$\psi_{1,r} + \frac{1}{r} \psi_{2,\theta} = 0$$

Eqn. (2.16) becomes

$$C_{rr} \frac{1}{r} (r\phi_{,r})_{,r} + C_{rr} \frac{1}{r^2} \phi_{,\theta\theta} + C_{zz} \phi_{,zz} - \rho \ddot{\phi} = 0$$

$$G \left( \frac{1}{r} (r\psi_{1,r})_{,r} + \frac{1}{r^2} \psi_{1,\theta\theta} + \psi_{1,zz} \right) - \rho \ddot{\psi}_1 = 0$$

$$G_H \left( \frac{1}{r} (r\psi_{3,r})_{,r} + \frac{1}{r^2} \psi_{3,\theta\theta} \right) + G \psi_{3,zz} - \rho \ddot{\psi}_3 = 0$$

$$G \left( \frac{1}{r} (r\psi_{2,r})_{,r} + \frac{1}{r^2} \psi_{2,\theta\theta} + \psi_{2,zz} \right) - \rho \ddot{\psi}_2 = 0$$

Notice that the Helmholtz theorem introduces four functions, i.e. a scalar potential and the three components of the vector potential, whereas, there are only three independent components of the displacement vector. The additional equation to make this relationship unique is given in this case by

$$\psi_{1,r} + \frac{1}{r} \psi_{2,\theta} = 0$$

When attempting to fit boundary conditions in terms of potential functions, it would seem more convenient to work with only three independent quantities. This can be accomplished by replacing the curl of the vector potential with two vectors fields, each derived from a separate scalar, such that one vector is tangential to the surface of the boundary and the other is normal to the surface. This is detailed in Chapter 13 of Morse and Feshbach (36). This technique was used by Wei (14) in analyzing the isotropic problem. When the boundary is a plane perpendicular to the z- axis, the decomposition becomes

$$\tilde{u} = \nabla^* \phi + \tilde{M} + \tilde{N} \quad (2.17)$$

$$\tilde{M} = (\nabla^* \eta) \times \hat{a}_z$$

$$\tilde{N} = (\nabla^* \times \nabla^* \times (\chi \hat{a}_z))$$

or expanding

$$\tilde{M} = -\eta_{,r} \hat{a}_\theta + \frac{1}{r} \eta_{,\theta} \hat{a}_r$$

$$\tilde{N} = \frac{1}{\beta \Sigma} \chi_{,rz} \hat{a}_r + \frac{1}{r\beta \Sigma} \chi_{,\theta z} \hat{a}_\theta$$

$$+ \left( \frac{1}{\beta \Sigma^2} \chi_{,zz} + \beta \chi \right) \hat{a}_z$$

where  $\beta^2 = \omega_0/G$  has been introduced for convenience.

Substitution of (2.17) into (2.5) yields

$$C_{rr} \left[ \frac{1}{r} (r\phi_{,r})_{,r} + \frac{1}{r^2} \phi_{,\theta\theta} \right] + C_{zz} \phi_{,zz} - \rho \ddot{\phi} = 0 \quad (2.18a)$$

$$G_H \left[ \frac{1}{r} (r\eta_{,r})_{,r} + \frac{1}{r^2} \eta_{,\theta\theta} \right] + G \eta_{,zz} - \rho \ddot{\eta} = 0 \quad (2.18b)$$

$$G \left[ \frac{1}{r} (r\chi_{,r})_{,r} + \frac{1}{r^2} \chi_{,\theta\theta} + \chi_{,zz} \right] - \rho \ddot{\chi} = 0 \quad (2.18c)$$

Again, these equations can all be put in the standard Poisson form by distorting the  $z$ -axis.

Thus, it has been shown by a careful examination of the wave propagation characteristics of a constrained transversely isotropic material that the governing equations of motion can be expressed in terms of three independent pseudo wave equations.

#### 2.4 Surface Wave Propagation

The phenomena of surface waves in anisotropic media has been addressed by numerous investigators, for instance, see ref. (37), (38), (39). In (39), Stonely solves the problem of surface waves in a transversely isotropic medium.

The difficulty in solving any elastodynamic problem in an anisotropic medium arises in general because the equations of motion do not uncouple in terms of potential functions, which is the starting point for most isotropic problems. Since for the constrained transversely isotropic material considered herein the uncoupling may be performed, the surface wave problem should be solved more directly by using potential functions. The solution using potentials is presented below and the result compared to Stonley (39).

Assume without loss of generality, a plane wave propagating in the x- direction. The potential representation (2.14) becomes



$$u_x = \phi_{,x} + \frac{1}{\Sigma} \psi_{,z} \quad (2.19a)$$

$$u_z = \frac{1}{\Sigma} \phi_{,z} - \psi_{,x} \quad (2.19b)$$

The pseudo wave equations (2.16) become

$$\phi_{,xx} + \frac{1}{\lambda_1^2} \phi_{,zz} + \frac{\rho\omega^2}{C_{xx}} \phi = 0 \quad (2.20a)$$

$$\psi_{,xx} + \psi_{,zz} + \frac{\rho\omega^2}{G} \psi = 0 \quad (2.20b)$$

The assumption of a plane wave propagating in the x- direction leads to

$$\phi(x,z) = F(z) \exp \left[ i \frac{2\pi}{L} (ct-x) \right] \quad (2.21a)$$

$$\psi(x,z) = H(z) \exp \left[ i \frac{2\pi}{L} (ct-x) \right] \quad (2.21b)$$

Substituting (2.21) into (2.20) and solving yields

$$\phi(x,z) = A \exp \left[ i \frac{2\pi}{L} (ct - x + \lambda_1 R_1 z) \right] \quad (2.22a)$$

$$\psi(x,z) = B \exp \left[ i \frac{2\pi}{L} (ct-x + R_2 z) \right] \quad (2.22b)$$

$$R_1^2 = (c/\bar{c}_1)^2 - 1 \quad (2.22c)$$

$$R_2^2 = (c/c_2)^2 - 1 \quad (2.22d)$$

The stress boundary conditions to be satisfied for a half space are

$$\sigma_{zz} = C_{xz} u_{x,x} + C_{zz} u_{z,z} = 0 \quad \text{on } z = 0 \quad (2.23a)$$

$$\sigma_{xz} = G(u_{x,z} + u_{z,x}) = 0 \quad \text{on } z = 0 \quad (2.23b)$$

Substituting (2.22) into (2.23) yields the following homogeneous equations

$$- [C_{xz} + \frac{C_{zz} \lambda_1^2 R_1^2}{\Sigma}] A + [ \frac{C_{xz} R_2}{\Sigma} - C_{zz} R_2 ] B = 0$$

$$\lambda_1 (1 + \frac{1}{\Sigma}) R_1 A - [ \frac{R_2^2}{\Sigma} - 1 ] B = 0$$

Setting the determinant of the coefficients to zero yields the following characteristic equation for the surface wave velocities

$$(\phi - q)^2 - \phi^2 \lambda_1 \sqrt{1 - \gamma^2 q} \sqrt{1 - q} = 0 \quad (2.24)$$

where  $\phi = \Sigma + 1 = \frac{C_{xz} + C_{zz}}{C_{zz} - G}$

$$q = (c/\bar{c}_2)^2$$

$$\gamma^2 = (c_2/\bar{c}_1)^2 = G/C_{xx}$$

Rationalizing equation 2.24 gives the following quartic

$$q^4 - 4\phi q^3 + \phi^2 (6 - \gamma^2 \lambda_1^2 \phi^2) q^2 - \phi^3 (4 - (1 + \gamma^2) \lambda_1^2 \phi) q + \phi^4 (1 - \lambda_1^2) = 0$$

This equation can be factored as follows

$$\left( q - \frac{1 - \lambda_1^2}{1 - \lambda_1^2 \gamma^2} \right) \left( q^3 (1 - \gamma^2 \lambda_1^2) - q^2 (1 - \lambda_1^2 + 2f) + qf(f+2) = f^2 \right) = 0 \quad (2.25)$$

where  $f = \frac{1}{G} \left( C_{xx} - \frac{C_{xz}^2}{C_{zz}} \right)$

The root  $q = \frac{1 - \lambda_1^2}{1 - \lambda_1^2 \gamma^2}$  leads to zero displacement and thus the cubic remains for determining physical surface wave speeds.

Stonely's result is

$$q = \frac{(q-1)^{1/2}}{(\gamma^2-1)^{1/2}} \left[ \frac{C_{xx} C_{zz} (\gamma^2-1) + C_{xz}^2}{G(C_{xx} C_{zz})^{1/2}} \right]$$

(Note: there are sign errors in eqn. 13 of ref. (39) )  
 Rationalizing this equation yields the cubic of eqn.  
 (2.25).

Therefore, the surface wave velocity for the  
 constrained transversely isotropic material considered  
 herein is identical to that of a general transversely  
 isotropic material.

### 2.5 Range of Dimensionless Elastic Constants

It can be seen from the preceding two sections that  
 the phenomena of body and surface wave propagation in a  
 constrained transversely isotropic medium can be expressed  
 in terms of the dimensionless constants  $\lambda_1, \lambda_2, \gamma, \phi$ .  
 It will be shown that the constraint equation (2.8) places  
 certain restrictions on the values these parameters may  
 assume. Recall

$$\lambda_1^2 = \frac{C_{rr}}{C_{zz}}, \quad \lambda_2^2 = \frac{G_H}{G}, \quad \gamma = \frac{G}{C_{rr}}$$

$$\phi = \frac{C_{rz} + C_{zz}}{C_{zz} - G} = \frac{\left(\frac{C_{rz}}{C_{zz}}\right) + 1}{1 - \left(\frac{G}{C_{zz}}\right)}$$

or

$$\phi = \frac{\left(\frac{C_{rz}}{C_{zz}}\right) + 1}{1 - \lambda_1^2 \gamma^2} \quad (2.26)$$

From (2.8)

$$G = \frac{C_{rr} C_{zz} - C_{rz}^2}{C_{rr} + 2C_{rz} + C_{zz}}$$

or

$$\frac{G}{C_{zz}} = \lambda_1^2 \gamma^2 = \frac{\lambda_1^2 - \left(\frac{C_{rz}}{C_{zz}}\right)^2}{\lambda_1^2 + 2\left(\frac{C_{rz}}{C_{zz}}\right) + 1} \quad (2.27)$$

Solve equation (2.26) for  $(C_{rr}/C_{zz})$  and substitute into (2.27) and solve for  $\phi$  yielding

$$\phi = 1 + \sqrt{\frac{\lambda_1^2(1-\gamma^2)}{1-\gamma^2\lambda_1^2}} \quad (2.28)$$

For a given set of elastic constants, satisfying equation (2.8), the value of  $\phi$  calculated from its definition (2.26) will automatically satisfy (2.28). However, if we wish to choose a range of values for the dimensionless parameters such that the constraint equation (2.8) is satisfied,  $\lambda_1$ , and  $\gamma$  may be chosen arbitrarily while  $\phi$  must be calculated from (2.28). It was not necessary to express  $\phi$  in terms of  $\lambda_1$ , and  $\gamma$ .  $\lambda_1$ , or  $\gamma$  could have been expressed in terms of the other two. However, because of the more physically meaningful definitions of  $\lambda_1$ , and  $\gamma$  it would seem desirable to

vary these independently.

From (2.27) a bound on  $\lambda_1^2 \gamma^2$  can also be obtained.

Assume  $\lambda_1^2 \gamma^2 > 1$ . From (2.27)

$$\frac{\lambda_1^2 - (C_{rz}/C_{zz})^2}{\lambda_1^2 + 2(C_{rz}/C_{zz}) + 1} > 1$$

or

$$\left(\frac{C_{rz}}{C_{zz}}\right)^2 + 2\left(\frac{C_{rz}}{C_{zz}}\right) + 1 < 0$$

$$\left(\left(\frac{C_{rz}}{C_{zz}}\right) + 1\right)^2 < 0$$

Since the square of a number must be positive or zero,

$\lambda_1^2 \gamma^2 < 1$  by contradiction.

The elastic constant  $G_H$  does not appear in the constraint equation and so the value of  $\lambda_2$  may be varied independently.

To properly assess the effect of soil anisotropy on the response of a structure, a suitable range of the elastic parameters  $\lambda_1$ ,  $\lambda_2$ , and  $\gamma$  must be chosen. Chapter eight of reference (40) presents static solutions for various distributions of stress or displacement over a circular area on a transversely isotropic elastic half space. The different sets of elastic constants used in their investigation along with the resulting dimensionless constants are presented in Table 2.1 as cases one through eight.

Saada, et al. in reference (2) have determined from dynamic tests the values of the elastic constants for

incompressible transversely isotropic clays. For an incompressible material the constraint equation (2.8) becomes

$$G = \frac{E_H}{n(4-n)} \quad (2.29a)$$

and the dimensionless constants are  $\lambda_1^2=1, \lambda_2^2=n, \gamma^2=0$

Results are reported in reference (2) for various peak strain levels. Values of  $E_H$ ,  $E_V$ , and  $G$  at similar levels were used to obtain the properties shown as cases nine and ten of Table 2.1.

The last column of Table 2.1 gives the value of  $G/E_H$  calculated from the constraint equation (2.8). It can be seen that for most cases the comparison with the actual value of  $G/E_H$  is quite favorable, leading to the conclusion that equation (2.8) is a reasonable assumption for soils.

Based on Table 2.1, a suitable range for the dimensionless constants was chosen for use in subsequent parameter studies. The cases chosen are given in Table 2.2. The surface or Rayleigh wave velocity required later is also given. This is determined by solving equation (2.25).

CHAPTER III  
SOLUTION OF THE HOMOGENEOUS ELASTIC  
HALFSPACE PROBLEM

3.1 General

A key step in the dynamic analysis of a structure-soil system is the determination of the force-displacement relationship between the foundation and the soil assuming the foundation to be massless. Given this relationship, the equations of motion for the structure can be written to include the stiffness of the soil media. In the case of machine foundations, the motion is usually harmonic. For seismic problems, the analysis is often performed in the frequency domain (1). Thus, the force displacement relationship of harmonically vibrating foundations is of considerable importance.

In this chapter the harmonic force-displacement relationship for a rigid circular disc supported on a constrained transversely isotropic elastic halfspace will be presented. The system considered is depicted in Figure 3.1.

The so-called relaxed boundary conditions at the disc-soil interface are assumed. This means that for vertical and rotational oscillations, the shear stress under the disc is zero, while for lateral motion the normal stress under the disc is zero. This allows the rocking and translational problems to be treated separately.



Also, it has been noticed (12) (for the isotropic problem) that the shear stress component perpendicular to the direction of motion is very small compared to the component parallel to the direction of motion for translational vibrations. In fact, for static loading it is exactly zero. The assumption that this smaller component is zero was made by Luco (16), (17) to greatly reduce the computational effort. This further relaxation of the boundary conditions is also made herein.

The mathematical procedure employed to find the dynamic stiffness or impedance is similar to that utilized by Gladwell (28). The starting point in Gladwell's analysis was the general solution to the isotropic equations of motion, first obtained by Sezawa (29). The general solution for a constrained transversely isotropic material is presented in the next section.

### 3.2 General Solution of the Equations of Motion

The governing equations of motion (2.5) were uncoupled through the use of the modified Helmholtz theorem (2.17). The result was the pseudo wave equations (2.18), repeated here for convenience

$$C_{rr} \left[ \frac{1}{r} (r\phi, r), r + \frac{1}{r^2} \phi, \theta\theta \right] + C_{zz} \phi,_{zz} - \rho \ddot{\phi} = 0 \quad (2.18a)$$

$$G_H \left[ \frac{1}{r} (rn, r), r + \frac{1}{r^2} n, \theta\theta \right] + G_n,_{zz} - \rho \ddot{n} = 0 \quad (2.18b)$$

$$G \left[ \frac{1}{r} (r x_{,r})_{,r} + \frac{1}{r^2} x_{,\theta\theta} + x_{,zz} \right] - \rho \ddot{x} = 0 \quad (2.18c)$$

If the motions are assumed to be harmonic, the solutions of (2.18) satisfying the radiation condition at infinity obtained via Hankel transforms are

$$\begin{aligned} \phi(r, \theta, z, \omega) = & \sum_{n=0}^{\infty} \cos(n\theta) \int_0^{\infty} \xi A_C^n e^{-\lambda_1 v_\alpha z} J_n(\xi r) d\xi \\ & + \sum_{n=0}^{\infty} \sin(n\theta) \int_0^{\infty} \xi A_S^n e^{-\lambda_1 v_\alpha z} J_n(\xi r) d\xi \end{aligned} \quad (3.1a)$$

$$\begin{aligned} \eta(r, \theta, z, \omega) = & \sum_{n=0}^{\infty} \cos(n\theta) \int_0^{\infty} \xi B_C^n e^{-\lambda_2 v_{\beta H} z} J_n(\xi r) d\xi \\ & + \sum_{n=0}^{\infty} \sin(n\theta) \int_0^{\infty} \xi B_S^n e^{-\lambda_2 v_{\beta H} z} J_n(\xi r) d\xi \end{aligned} \quad (3.1b)$$

$$\begin{aligned} \chi(r, \theta, z, \omega) = & \sum_{n=0}^{\beta} \cos(n\theta) \int_0^{\infty} \xi C_C^n e^{-v_\beta z} J_n(\xi r) d\xi \\ & \sum_{n=0}^{\infty} \sin(n\theta) \int_0^{\infty} \xi C_S^n e^{-v_\beta z} J_n(\xi r) d\xi \end{aligned}$$

where

$$v_\alpha^2 = \xi^2 - \alpha^2 \quad (3.2a)$$

$$\alpha^2 = \rho \omega^2 / C_{rr} \quad (3.2b)$$

$$v_{\beta H}^2 = \xi^2 - \beta_H^2 \quad (3.2c)$$

$$\beta_H^2 = \rho \omega^2 / G_H \quad (3.2d)$$

$$v_\beta^2 = \xi^2 - \beta^2 \quad (3.2e)$$

$$\beta^2 = \rho \omega^2 / G \quad (3.2f)$$

$A_c^n, A_s^n, B_s^n, C_c^n, C_s^n$  are constants,

$J_n(\xi r)$  is the Bessel function of the first kind of order  $n$  and  $\omega$  is the frequency of vibration.

The modified Helmholtz theorem is given below in expanded form.

$$u_r = \phi_{,r} + \frac{1}{r} n_{, \theta} + \frac{1}{\beta \Sigma} \chi_{, rz} \quad (3.3a)$$

$$u_{\theta} = \frac{1}{r} \phi_{, \theta} - n_{, r} + \frac{1}{r \beta \Sigma} \chi_{, \theta z} \quad (3.3b)$$

$$u_z = \frac{1}{\Sigma} \phi_{, z} + \frac{1}{\beta} \chi_{, zz} + \beta \chi \quad (3.3c)$$

Substitution of (3.2) into (3.3) yields the general solution for the displacements. For the axially symmetric vertical vibrations, the solution for  $n = 0$  is required.

$$u_r = - \int_0^{\infty} \xi^2 [A_c^0 e^{-\lambda_1 v_{\alpha} z} - C_c^0 \frac{v_{\beta}}{\beta \Sigma} e^{-v_{\beta} z}] J_1(\xi r) d\xi \quad (3.4a)$$

$$u_{\theta} = \int_0^{\infty} \xi^2 B_c^0 e^{-\lambda_2 v_{\beta} z} J_1(\xi r) d\xi \quad (3.4b)$$

$$u_z = \int_0^{\infty} \xi [A_c^0 \frac{\lambda_1 v_{\alpha}}{\Sigma} e^{-\lambda_1 v_{\alpha} z} - C_c^0 \frac{\xi^2}{\beta} e^{-v_{\beta} z}] J_0(\xi r) d\xi \quad (3.4c)$$

Using the strain displacement relations and the stress strain equations, the stress components of interest are obtained

$$\sigma_{rz} = \frac{G}{\Sigma} \int_0^{\infty} \xi^2 [A_c^0 \phi \lambda_1 v_\alpha e^{-\lambda_1 v_\alpha z} - \frac{C_c^0 (\phi \xi^2 - \beta^2)}{\beta} e^{-v_\beta z}] J_1(\xi r) d\xi \quad (3.5a)$$

$$\sigma_{\theta z} = -G \int_0^{\infty} \xi^2 \lambda_2 v_{\beta H} B_c^0 e^{-\lambda_2 v_{\beta H} z} J_1(\xi r) d\xi \quad (3.5b)$$

$$\sigma_{zz} = \frac{G}{\Sigma} \int_0^{\infty} \xi [(\phi \xi^2 - \beta^2) A_c^0 e^{-\lambda_1 v_\alpha z} - \frac{\xi^2 v_\beta \phi e^{-v_\beta z}}{\beta} C_c^0] J_0(\xi r) d\xi \quad (3.5c)$$

For rocking and translational motions, the solutions for  $n = 1$  are required

$$u_r = \int_0^{\infty} [\xi A_c' e^{-\lambda_1 v_\alpha z} \frac{dJ_1(\xi r)}{dr} + \frac{1}{r} \xi B_s' e^{-\lambda_2 v_{\beta H} z} J_1(\xi r) - \frac{\xi v_\beta}{\beta \Sigma} C_c' e^{-v_\beta z} \frac{dJ_1(\xi r)}{dr}] d\xi \cos(\theta) \quad (3.6a)$$

$$u_\theta = \int_0^{\infty} [A_c' e^{-\lambda_1 v_\alpha z} J_1(\xi r) - \xi B_s' e^{-\lambda_2 v_{\beta H} z} \frac{dJ_1(\xi r)}{dr} + \frac{\xi v_\beta}{r \beta \Sigma} C_s' e^{-v_\beta z} J_1(\xi r)] d\xi \sin(\theta) \quad (3.6b)$$

$$u_z = \int_0^{\infty} [-\frac{\xi \lambda_1 v_\alpha}{\Sigma} A_c' e^{-\lambda_1 v_\alpha z} J_1(\xi r) + \frac{\xi^3}{\beta} C_c' e^{-v_\beta z} J_1(\xi r)] d\xi \cos(\theta) \quad (3.6c)$$

The required stress components are

$$\begin{aligned} \sigma_{rz} = G \int_0^\infty & \left[ -\frac{\phi \xi \lambda_1 \nu_\alpha}{\Sigma} A'_c e^{-\lambda_1 \nu_\alpha z} \frac{dJ_1(\xi r)}{dr} - \frac{\lambda_2 \nu_{\beta H}}{r} \xi B'_s e^{-\lambda_2 \nu_{\beta H} z} J_1(\xi r) \right. \\ & \left. + \frac{(\phi \xi^2 - \beta^2)}{\beta \Sigma} C'_c e^{-\nu_{\beta} z} \frac{dJ_1(\xi r)}{dr} \right] d\xi \cos(\theta) \end{aligned} \quad (3.7a)$$

$$\begin{aligned} \sigma_{\theta z} = G \int_0^\infty & \left[ \frac{\xi \lambda_1 \nu_\alpha \phi}{r \Sigma} A'_c J_1(\xi r) + \xi \lambda_2 \nu_{\beta H} B'_s e^{-\lambda_2 \nu_{\beta H} z} \frac{dJ_1(\xi r)}{dr} \right. \\ & \left. - \frac{\xi(\phi \xi^2 - \beta^2)}{r \beta \Sigma} C'_c e^{-\nu_{\beta} z} J_1(\xi r) \right] d\xi \sin(\theta) \end{aligned} \quad (3.7b)$$

$$\begin{aligned} \sigma_{zz} = \frac{G}{\Sigma} \int_0^\infty & \xi [(\phi \xi^2 - \beta^2) A'_c e^{-\lambda_1 \nu_\alpha z} - \frac{\xi^2 \phi \nu_{\beta}}{\beta} C'_c e^{-\nu_{\beta} z}] J_1(\xi r) d\xi \cos(\theta) \end{aligned} \quad (3.7c)$$

For vertical vibrations, equations (3.4) and (3.5) along with the boundary conditions reduce the problem to the solution of two dual integral equations which may be further reduced to a single Fredholm integral equation of the second kind by the methods detailed in Sneddon, (27). Using equations (3.6) and (3.7) the rocking and translational problems are handled similarly. For each mode of vibration, integration of the unknown in the Fredholm equation over the radius of the disc yields a quantity proportional to the total force under the disc undergoing unit harmonic displacement, i.e. the dynamic stiffness or impedance.

### 3.3 Stiffness and Flexibility Coefficients

#### 3.3a Vertical Vibrations

Consider a transversely isotropic elastic half space subject to the following boundary conditions

$$u_z(r, \theta, 0) = \Delta_v \quad , \quad r \leq r_0 \quad (3.8a)$$

$$\sigma_{rz}(r, 0) = 0 \quad , \quad r > 0 \quad (3.8b)$$

$$\sigma_{zz}(r, 0) = 0 \quad , \quad r > r_0 \quad (3.8c)$$

Since the motions are symmetric about the z -axis, the solutions to the equations of motion given in equations (3.4) and (3.5) are used. Substitute (3.4) and (3.5) into (3.8) evaluating at  $z=0$  . Because of the axial symmetry, take  $B_c^0=0$  . Equation (3.8b) is satisfied identically by taking

$$A_c^0 = \frac{(\Phi \xi^2 - \beta^2)}{\Phi \lambda_1 \nu_\alpha \beta} C_c^0$$

Equations (3.8a) and (3.8c) can be simplified by defining a new parameter

$$B(\xi) = \frac{\xi f(\xi)}{\Phi \lambda_1 \nu_\alpha \beta} C_c^0$$

$$\text{where } f(\xi) = (\phi\xi^2 - \beta^2) - \xi^2 \phi^2 \lambda_1 v_\alpha v_\beta \quad (3.9)$$

Recall that  $f(\xi)$  is the equation for the surface wave velocity as derived in Chapter 2. With these definitions (3.8 a,c) become

$$\int_0^\infty \left[ \frac{\lambda_1 v_\alpha (\phi\xi^2 (\phi-2) + \beta^2)}{f(\xi)} \right] B(\xi) J_0(\xi r) d\xi = \Sigma \Delta_V, \quad r < r_0 \quad (3.10a)$$

$$\int_0^\infty B(\xi) J_0(\xi r) d\xi = 0, \quad r > r_0 \quad (3.10b)$$

Notice that

$$\left[ \frac{\lambda_1 v_\alpha (\phi\xi^2 (\phi-2) + \beta^2)}{f(\xi)} \right]_{\omega=0} = \frac{\lambda_1 (\phi-2)}{\xi\phi(1-\lambda_1)}$$

To simplify the computations later define

$$\Psi_V = - \frac{\lambda_1 (\phi-2)}{\phi(1-\lambda_1)} \quad (3.11)$$

and

$$H_1(\xi) = - \frac{\xi \lambda_1 v_\alpha [\phi\xi^2 (\phi-2) + \beta^2]}{\Psi_V f(\xi)} - 1 \quad (3.12)$$

Note that  $H_1(\xi) \Big|_{\omega=0} = 0$

and that  $H_1(\xi) \rightarrow 0$  as  $\xi \rightarrow \infty$

Equations (3.10 a,b) may now be rewritten

$$\int_0^{\infty} \frac{1}{\xi} [1 + H_1(\xi)] B(\xi) J_0(\xi r) d\xi = \frac{\Sigma \Delta_v}{\Psi_v}, \quad r \leq r_0 \quad (3.13a)$$

$$\int_0^{\infty} B(\xi) J_0(\xi r) d\xi = 0, \quad r > r_0 \quad (3.13b)$$

Equations (3.13) are a pair of dual integral equations with Hankel weighting function as considered by Sneddon, ref. (27). They are identical in form to the isotropic problem.

Let

$$B(\xi) = \frac{2\xi \Sigma \Delta_v}{\pi \Psi_v} \int_0^{r_0} h_1(x) \cos(\xi x) dx \quad (3.14)$$

Equation (3.13b) is then automatically satisfied and (3.13a) is equivalent to the following Fredholm integral equation of the second kind

$$h_1(x) + \frac{1}{\pi} \int_0^{r_0} L_1(x,u) h_1(u) du = 1 \quad (3.15)$$

where

$$L_1(x,u) = 2 \int_0^{\infty} H_1(\xi) \cos(\xi x) \cos(\xi u) d\xi \quad (3.16)$$



The dynamic stiffness or impedance can now be expressed in terms of the unknown in the Fredholm integral equation,  $h_1(x)$ . The total force under the disc is

$$P_v = \int_0^{2\pi} \int_0^{r_0} \sigma_{zz} r dr d\theta$$

For  $r < r_0$

$$\sigma_{zz} = \frac{G}{\Sigma} \int_0^{\infty} B(\xi) J_0(\xi r) d\xi$$

Using this expression and equation (3.14) yields

$$P_v = \frac{2G\Delta_v}{\pi \Psi_v} \int_0^{2\pi} \int_0^{r_0} \int_0^{\infty} \int_0^{r_0} \xi h_1(x) \cos(\xi x) J_0(\xi r) dx d\xi r dr d\theta$$

Making use of a Weber-Schafheitlin type integral (see Appendix A) reduces this to

$$P_v = \frac{4G\Delta_v}{\Psi_v} \int_0^{r_0} h_1(x) dx \quad (3.17)$$

The dynamic stiffness or impedance is defined as

$$\bar{K}_v = \frac{P_v}{\Delta_v} = \frac{4G}{\Psi_v} \int_0^{r_0} h_1(x) dx \quad (3.18)$$

at  $\omega=0, L_1(x,u)=0$  and therefore  $h_1(x)=1$ .

Thus for the static case

$$K_v = \frac{4G}{\Psi_v} \int_0^{r_0} dx = \frac{4Gr_0}{\Psi_v} \quad (3.19)$$

### 3.3.a.1 Verification of Static Solution

The static problem has been considered previously by Gerrard (40) who obtained for the stiffness

$$K_V = \frac{4Gr_0 (C_{rz} + C_{zz}\rho_1^2)(C_{rz} + C_{zz}\phi_1^2)}{\rho_1\phi_1 C_{zz} (C_{rz} + G)(\rho_1 + \phi_1)}$$

where

$$\rho_1 = \alpha_1 + \beta_1 \quad \phi_1 = \alpha_1 - \beta_1$$

and

$$\alpha_1^2 = \frac{[C_{rr}C_{zz} - C_{rz}^2 - 2C_{rz}G + 2G(C_{rr}C_{zz})^{1/2}]}{4G C_{zz}} \quad (3.21a)$$

$$\beta_1^2 = \frac{[C_{rr}C_{zz} - C_{rz}^2 + 2C_{rz}G + 2G(C_{rr}C_{zz})^{1/2}]}{4G C_{zz}} \quad (3.21b)$$

Recall the constraint eqn. (2.8a) in expanded form

$$C_{rr}C_{zz} - C_{rz}^2 - 2C_{rz}G - G(C_{rr} + C_{zz}) = 0$$

Using this expression in (3.21) leaves

$$\alpha_1^2 = \left(\frac{\lambda_1 + 1}{4}\right)^2 \quad \beta_1^2 = \left(\frac{\lambda_1 - 1}{4}\right)^2 \quad (3.22)$$

Gerrard presents solutions for three conditions

$$(A.) \quad \alpha_1^2 > 0 \quad , \quad \beta_1^2 > 0$$

$$(B.) \quad \alpha_1^2 > 0 \quad , \quad \beta_1^2 < 0$$

$$(C.) \quad \alpha_1^2 > 0 \quad , \quad \beta_1^2 = 0$$

The quantity  $\alpha_1^2$  must be greater than zero for positive strain energy. It can be seen from (3.22) that the constraint used herein forces  $\beta_1$  to also be greater than or equal to zero, thus eliminating case B.

Using (3.22) in (3.20) yields Gerrard's result specialized for the constrained material

$$K_V = \frac{4Gr_o(C_{rz}+C_{rr})(C_{rz}+C_{zz})}{(C_{rz}+G)(1+\lambda_1)C_{zz}\lambda_1} \quad (3.23)$$

It will now be shown that (3.19) agrees with (3.23). Substituting for  $\Psi_V$  from (3.11) into (3.19) yields after some manipulation

$$K_V = -\frac{4Gr_o(C_{rz}+C_{zz})(C_{rz}+C_{rr})}{\left[ \frac{(C_{rz}-C_{zz}+2G)(C_{rz}+C_{rr})}{(C_{zz}-C_{rr})} \right] C_{zz}\lambda_1(1+\lambda_1)}$$

Using the constraint eqn. (2.8) the expression in the brackets is easily shown to be  $-(C_{rz}+G)$  which then yields equation (3.23).

### 3.3.b Rocking Vibrations

Consider now the transversely isotropic elastic halfspace subject to the following boundary conditions

$$u_z(r,\theta,0) = \delta r \cos(\theta) \quad , \quad r \leq r_o \quad (3.24a)$$

$$\sigma_{zz}(r,\theta,0) = 0 \quad , \quad r \geq r_o \quad (3.24b)$$

$$\sigma_{rz}(r,\theta,0) = \sigma_{\theta z}(r,\theta,0) = 0 \quad , \quad r > 0 \quad (3.24c)$$

(3.24c) may be satisfied by taking  $B_s' = 0$  in eqns.

(3.6) and (3.7). Following a procedure identical to the vertical problem 3.24 a,b become

$$\int_0^{\infty} \frac{1}{\xi} [1 + H_1(\xi)] B(\xi) J_1(\xi r) d\xi = \frac{r \Sigma \delta}{\Psi_V} \quad , \quad r \leq r_0 \quad (3.25a)$$

$$\int_0^{\infty} B(\xi) J_1(\xi r) d\xi = 0 \quad , \quad r > r_0 \quad (3.25b)$$

In this case let

$$B(\xi) = \frac{4 \delta \Sigma \xi}{\pi \Psi_V} \int_0^{r_0} h_2(x) \sin(\xi x) dx \quad (3.26)$$

Equation (3.25b) is satisfied identically and (3.25a) becomes

$$h_2(x) + \frac{1}{\pi} \int_0^{r_0} L_2(x,u) h_2(u) du = x \quad (3.27)$$

$$\text{where } L_2(x,u) = 2 \int_0^{\infty} H_1(\xi) \sin(\xi x) \sin(\xi u) d\xi \quad (3.28)$$

The total moment under the disc is

$$M = \int_0^{2\pi} \int_0^{r_0} r^2 \sigma_{zz} \cos(\theta) dr d\theta$$

but

$$\sigma_{zz} = \frac{G}{z} \int_0^{\infty} B(\xi) J_1(\xi r) d\xi \cos(\theta) \quad , \quad r \leq r_0$$

and  $B(\xi)$  is given by (3.26), thus

$$M = \frac{4G\delta}{\pi\Psi_V} \int_0^{2\pi} \int_0^{r_0} \int_0^{\infty} \int_0^{r_0} \xi r^2 J_1(\xi r) h_2(x) \sin(\xi x) \cos^2(\theta) dx d\xi dr d\theta$$

again using the Weber-Schafheitlin integral yields

$$M = \frac{8G\delta}{\Psi_V} \int_0^{r_0} x h_2(x) dx$$

The impedance is therefore

$$\bar{K}_R = \frac{M}{\delta} \frac{8G}{\Psi_V} \int_0^{r_0} x h_2(x) dx \tag{3.29}$$

In the static case  $h_2(x) = x$  and therefore

$$K_R = \frac{8Gr_0^3}{3\Psi_V} \tag{3.30}$$

The factor  $\Psi_V$  is the same one which appears in the vertical solution. In Gerrard's static rocking solution the factor multiplying  $8Gr_0^3/3$  is the same factor that multiplied  $4Gr_0$  in his vertical solution, thus the static solution is verified from Section 3.3.a.1.

### 3.3.c Horizontal Vibrations

Now consider a transversely isotropic elastic halfspace subject to the following boundary conditions

$$u_r(r, \theta, 0) = \Delta_H \cos(\theta) \quad , \quad r \leq r_0 \quad (3.31a)$$

$$u_\theta(r, \theta, 0) = -\Delta_H \sin(\theta) \quad , \quad r \leq r_0 \quad (3.31b)$$

$$\sigma_{r\theta}(r, \theta, 0) = \sigma_{rz}(r, \theta, 0) = 0 \quad , \quad r > r_0 \quad (3.31c)$$

$$\sigma_{zz}(r, \theta, 0) = 0 \quad , \quad r > 0 \quad (3.31d)$$

From equations (3.7) we can make the following representation

$$\sigma_{rz}(r, \theta, 0) = \sigma_{rz}^*(r) \cos(\theta) \quad (3.32a)$$

$$\sigma_{\theta z}(r, \theta, 0) = \sigma_{\theta z}^*(r) \sin(\theta) \quad (3.32b)$$

Equation (3.31d) is satisfied identically by taking

$$A'_c = \frac{\phi \xi^2 v_\beta}{(\phi \xi^2 - \beta^2) \beta} C'_c$$

in equation (3.7c).

Equations 3.31a,b,c then become

$$u_r = \int_0^\infty \xi \left[ v_\beta \left( \frac{\phi \xi^2 (\phi - 2) + \beta^2}{(\phi \xi^2 - \beta^2) \beta \xi} \right) C'_c \frac{d J_1(\xi r)}{dr} + B'_s \frac{J_1(\xi r)}{r} \right] d\xi = \Delta_H \quad , \quad r \leq r_0$$

$$u_{\theta} = \int_0^{\infty} \xi \left[ -v_{\beta} \left( \frac{\phi \xi^2 (\phi-2) + \beta^2}{(\phi \xi^2 - \beta^2) \beta \Sigma} \right) C_c' \frac{J_1(\xi r)}{r} \right. \\ \left. - B_s' \frac{dJ_1(\xi r)}{dr} \right] d\xi = -\Delta_H, \quad r \leq r_0$$

$$\sigma_{rz}^* = G \int_0^{\infty} \xi \left[ \frac{f(\xi) C_c'}{\beta \Sigma (\phi \xi^2 - \beta^2)} \frac{dJ_1(\xi r)}{dr} \right. \\ \left. - \lambda_2 v_{\beta_H} B_s' \frac{J_1(\xi r)}{r} \right] d\xi = 0, \quad r > r_0$$

$$\sigma_{\theta z}^* = G \int_0^{\infty} \xi \left[ \frac{-f(\xi) C_c'}{\beta \Sigma (\phi \xi^2 - \beta^2)} \frac{J_1(\xi r)}{r} \right. \\ \left. + \lambda_2 v_{\beta_H} B_s' \frac{dJ_1(\xi r)}{dr} \right] d\xi = 0, \quad r > r_0$$

Using these Bessel function relationships

$$\frac{dJ_1(\xi r)}{dr} + \frac{J_1(\xi r)}{r} = \xi J_0(\xi r)$$

$$\frac{dJ_1(\xi r)}{dr} - \frac{J_1(\xi r)}{r} = \xi J_2(\xi r)$$

and defining

$$D(\xi) = \frac{\xi^2 f(\xi)}{\beta \Sigma (\phi \xi^2 - \beta^2)} C_c'$$

$$g(\xi) = \phi \xi^2 (\phi-2) + \beta^2$$

leads to the following

$$u_r + u_\theta = \int_0^\infty \left[ \frac{-v_\beta g(\xi)}{f(\xi)} D(\xi) J_2(\xi r) + \xi^2 B'_s J_2(\xi r) \right] d\xi = 0 \quad (3.33a)$$

$$u_r - u_\theta = \int_0^\infty \left[ \frac{v_\beta g(\xi)}{f(\xi)} D(\xi) J_0(\xi r) + \xi^2 B'_s J_0(\xi r) \right] d\xi = 0 \quad (3.33b)$$

$$\sigma_{rz}^* + \sigma_{\theta z}^* = \int_0^\infty \left[ -D(\xi) J_2(\xi r) - \xi^2 \lambda_2 v_{\beta H} B'_s J_2(\xi r) \right] d\xi = 0 \quad (3.33c)$$

$$\sigma_{rz}^* - \sigma_{\theta z}^* = \int_0^\infty \left[ D(\xi) J_0(\xi r) - \xi^2 \lambda_2 v_{\beta H} B'_s J_0(\xi r) \right] ds = 0 \quad (3.33d)$$

Defining

$$E(\xi) = D(\xi) - \xi^2 \lambda_2 v_{\beta H} B'_s$$

$$F(\xi) = D(\xi) + \xi^2 \lambda_2 v_{\beta H} B'_s$$

equations (3.33) can be rewritten

$$\int_0^\infty \left[ \frac{v_\beta g(\xi)}{f(\xi)} - \frac{1}{\lambda_2 v_{\beta H}} \right] F(\xi) J_2(\xi r) d\xi =$$

$$- \int_0^\infty \left[ \frac{v_\beta g(\xi)}{f(\xi)} + \frac{1}{\lambda_2 v_{\beta H}} \right] E(\xi) J_2(\xi r) d\xi \quad (3.34a)$$

$$\int_0^\infty \left[ \frac{v_\beta g(\xi)}{f(\xi)} - \frac{1}{\lambda_2 v_{\beta H}} \right] E(\xi) J_0(\xi r) d\xi = 4\Delta_H$$

$$- \int_0^\infty \left[ \frac{v_\beta g(\xi)}{f(\xi)} + \frac{1}{\lambda_2 v_{\beta H}} \right] F(\xi) J_0(\xi r) d\xi \quad (3.34b)$$



$$\sigma_{rz}^* + \sigma_{\theta z}^* = \int_0^\infty F(\xi) J_2(\xi r) d\xi = 0 \quad (3.34c)$$

$$\sigma_{rz}^* - \sigma_{\theta z}^* = \int_0^\infty E(\xi) J_0(\xi r) d\xi = 0 \quad (3.34d)$$

Note that

$$\left| \frac{\nu_\beta g(\xi)}{f(\xi)} - \frac{1}{\lambda_2 \nu_{\beta H}} \right|_{\omega=0} = \frac{1}{\xi} \left| \frac{\phi-2}{\phi(1-\lambda_1)} - \frac{1}{\lambda_1} \right|$$

Define

$$\Psi_H = \frac{1}{\lambda_2} - \frac{\phi-2}{\phi(1-\lambda_1)} \quad (3.35)$$

and

$$1 + H_3(\xi) = \frac{\xi}{\Psi_H} \left[ -\frac{\nu_\beta g(\xi)}{f(\xi)} + \frac{1}{\lambda_2 \nu_{\beta H}} \right]$$

$$1 + H_4(\xi) = \frac{\xi}{\Psi_H} \left[ \frac{\nu_\beta g(\xi)}{f(\xi)} + \frac{1}{\lambda_2 \nu_{\beta H}} \right]$$

then equations (3.34) become

$$\int_0^{\infty} \frac{1}{\xi} (1+H_3(\xi)) E(\xi) J_0(\xi r) d\xi = \frac{4\Delta_H}{\Psi_H}$$

$$+ \int_0^{\infty} \frac{1}{\xi} (1+H_4(\xi)) F(\xi) J_0(\xi r) d\xi \quad , \quad r < r_0 \quad (3.36a)$$

$$\int_0^{\infty} \frac{1}{\xi} (1+H_3(\xi)) F(\xi) J_2(\xi r) d\xi =$$

$$\int_0^{\infty} \frac{1}{\xi} (1+H_4(\xi)) E(\xi) J_2(\xi r) d\xi \quad , \quad r < r_0 \quad (3.36b)$$

$$\int_0^{\infty} F(\xi) J_2(\xi r) d\xi = 0 \quad , \quad r > r_0 \quad (3.36c)$$

$$\int_0^{\infty} E(\xi) J_0(\xi r) d\xi = 0 \quad , \quad r > r_0 \quad (3.36d)$$

Equations (3.36) constitute two coupled sets of dual integral equations. They are identical in form to the isotropic results. These equations can be reduced to two coupled Fredholm integral equations following Gladwell (28). The coupled Fredholm equations were solved numerically by Wei (14) and by Luco and Westmann (12) for the isotropic problem. Alternatively, the shear stress component  $\sigma_{yz}$  may be assumed zero since it has been found to have a small effect (14), (16), (17). This is

accomplished by taking  $\sigma_{rz}^* + \sigma_{\theta z}^*$  equal to zero, since this quantity is proportional to  $\sigma_{yz}$ . From (3.34c) then,  $F(\xi) = 0$ . Thus, (3.36) reduce to

$$\int_0^{\infty} \frac{1}{\xi} (1+H_3(\xi))E(\xi)J_0(\xi r)d\xi = 4\Delta_H, \quad r < r_0 \quad (3.37a)$$

$$\int_0^{\infty} E(\xi)J_0(\xi r)d\xi = 0, \quad r > r_0 \quad (3.37b)$$

Equations (3.37) are similar to the vertical problem eqns.(3.13). Let

$$E(\xi) = \frac{8\xi\Sigma\Delta_H}{\pi\Psi_H} \int_0^{r_0} h_3(x)\cos(\xi x)dx \quad (3.38)$$

Equation (3.37b) is automatically satisfied and (3.37a) becomes

$$h_3(x) + \frac{1}{\pi} \int_0^{r_0} L_3(x,u)h_3(u)du = 1 \quad (3.39)$$

where

$$L_3(x,u) = 2 \int_0^{\infty} H_3(\xi)\cos(\xi x)\cos(\xi u)d\xi \quad (3.40)$$

The total force under the disc is

$$P_H = \int_0^{2\pi} \int_0^{r_0} \sigma_{xz} r dr d\theta$$

$$P_H = \int_0^{2\pi} \int_0^{r_0} \left[ \frac{\cos(2\theta)}{2} (\sigma_{rz} + \sigma_{\theta z}^*) + \frac{1}{2}(\sigma_{rz}^* - \sigma_{\theta z}^*) \right] r dr d\theta$$

$$P_H = \pi \int_0^{r_0} (\sigma_{rz}^* - \sigma_{\theta z}^*) r dr$$

Recall  $\sigma_{rz}^* - \sigma_{\theta z}^* = \int_0^\infty E(\xi) J_0(\xi r) d\xi$

and  $E(\xi)$  is given in (3.38), therefore

$$P_H = \frac{8G\Delta_H}{\Psi_H} \int_0^{r_0} \int_0^\infty \int_0^{r_0} r \xi \cos(\xi x) h_3(x) J_0(xr) dx d\xi dr$$

which leads to

$$P_H = \frac{8G\Delta_H}{\Psi_H} \int_0^{r_0} h_3(x) dx$$

The impedance is therefore

$$\bar{K}_H = \frac{P_H}{\Delta_H} = \frac{8G}{\Psi_H} \int_0^{r_0} h_3(x) dx \tag{3.41}$$

In the static case  $H_3(\xi)=0$ , and therefore  $h_3(x) = 1$  and so

$$K_H = \frac{8G}{\Psi_H} \int_0^{r_0} dx = \frac{8Gr_0}{\Psi_H} \tag{3.42}$$

### 3.3.c.1 Verification of Static Stiffness

Using equation (3.22) Gerrard's static horizontal solution, ref. (40), is easily shown to be

$$K_H = 8Gr_0 \left\{ \frac{1}{\frac{(C_{rz}+G)(1+\lambda_1)C_{zz}}{F(C_{rz}+C_{rr})(C_{rz}+C_{zz})} + \frac{1}{\lambda_2}} \right\} \tag{3.43}$$

By comparing the first term in the denominator with (3.23), equation (3.43) can be rewritten

$$K_H = 8Gr_0 \left[ \frac{1}{\frac{\psi_v}{\lambda_1} + \frac{1}{\lambda_2}} \right]$$

Thus the static solution obtained here agrees with Gerrard's if

$$\psi_H = \frac{\psi_v}{\lambda_1} + \frac{1}{\lambda_2} \quad (3.44)$$

Equation (3.44) is verified by comparing (3.35) with (3.11).

### 3.4 Reduction to dimensionless form

All the equations in the previous section can be reduced to dimensionless form by defining the following parameters

$$k = \epsilon/\beta$$

$$\gamma^2 = \alpha^2/\beta^2 = G/C_{rr}$$

$$a_0 = \omega r_0/c_2 = \beta r_0$$

$$V_\alpha^2 = k^2 - \gamma^2$$

$$V_\beta^2 = k^2 - 1$$

$$V_{\beta H}^2 = k^2 - 1/\lambda_2^2$$

$$F(k) = (\phi k^2 - 1)^2 - k^2 \phi^2 \lambda_1^2 V_\alpha V_\beta$$

$$\bar{X} = r/r_0$$

The pertinent results can be recapped as follows:

### 3.4.1 Vertical Vibrations

The Fredholm equation becomes

$$h_1(\bar{X}) + \frac{1}{\pi} \int_0^1 L_1(\bar{X}, U) h_1(U) dU = 1, \quad 0 < \bar{X} < 1 \quad (3.45)$$

where

$$L_1(\bar{X}, u) = 2 \int_0^\infty a_0 H_1(k) \cos(a_0 k \bar{X}) \cos(a_0 k u) dk \quad (3.46)$$

$$H_1(k) = - \frac{k \lambda_1 V_k [\phi k^2 (\phi - 2) + 1]}{\Psi_V F(k)} - 1 \quad (3.47)$$

and the impedance becomes

$$\bar{K}_V = K_V \int_0^1 h_1(\bar{X}) d\bar{X} \quad (3.48)$$

where 
$$K_V = \frac{4Gr_0}{\Psi_V}$$

For a given specified harmonic vertical displacement, the total force under the disc would be out of phase with the displacement because of the radiation of energy to infinity. The impedance would therefore be a complex quantity. For later use define

$$\operatorname{Re} \left( \int_0^1 h_1(\bar{X}) d\bar{X} \right) = k_V$$

$$\operatorname{Im} \left( \int_0^1 h_1(\bar{X}) d\bar{X} \right) = a_0 c_V$$

(3.48) becomes

$$\bar{K}_V = K_V (k_V + ia_0 c_V) \quad (3.49)$$

Again, for later use define the flexibility or compliance

$$\text{as } \bar{F}_V = \frac{1}{\bar{K}_V} = \frac{1}{K_V} \frac{1}{k + ia_0 c_V} = \frac{1}{K_V} (f_V + ig_V) \quad (3.50)$$

where

$$f_V = \frac{k_V}{k_V^2 + (a_0 c_V)^2} \quad (3.51)$$

$$g_V = \frac{-a_0 c_V}{k_V^2 + (a_0 c_V)^2} \quad (3.52)$$

### 3.4.2 Rocking Vibrations

The Fredholm integral equation becomes

$$h_2(\bar{X}) + \frac{1}{\pi} \int_0^1 L_2(\bar{X}, U) h_2(U) dU = \bar{X} \quad (3.53)$$

where

$$L_2(\bar{X}, ) = 2 \int_0^\infty a_0 H_1(k) \sin(a_0 k \bar{X}) \sin(a_0 k U) dk \quad (3.54)$$

and  $H_1(k)$  is given in (3.47)

The impedance becomes

$$\bar{K}_R = K_R \int_0^1 \bar{X} h_2(\bar{X}) d\bar{X} = K_R (K_R + ia_0 c_R) \quad (3.55)$$

where

$$K_R = \frac{8Gr_0^3}{3\Psi_V}$$

Write the flexibility or compliance as

$$\bar{F}_R = \frac{1}{K_R} \cdot \frac{1}{K_R + ia_0 c_R} = \frac{1}{K_R} (f_R + ig_R) \quad (3.56)$$

$$f_R = \frac{K_R}{k_R^2 + (a_0 c_R)^2} \quad (3.57)$$

$$g_R = \frac{-a_0 c_R}{k_R^2 + (a_0 c_R)^2} \quad (3.58)$$

### 3.4.3 Horizontal Vibrations

The Fredholm integral equation becomes

$$h_3(\bar{X}) + \frac{1}{\pi} \int_0^1 L_3(\bar{X}, U) h_3(U) dU = 1 \quad (3.59)$$

where

$$L_3(\bar{X}, U) = 2 \int_0^\infty a_0 H_3(k) \cos(a_0 k \bar{X}) \cos(a_0 k U) dk \quad (3.60)$$

$$H_3(k) = - \frac{k V_B [\phi k^2 (\phi - 2) + 1]}{\Psi_H F(k)} + \frac{1}{\lambda_2 V_{B_H} \Psi_H} - 1 \quad (3.61)$$

and the impedance becomes

$$\bar{K}_H = K_H \int_0^1 h_3(\bar{X}) d\bar{X} = K_H (K_H + ia_0 c_H) \quad (3.62)$$

where

$$K_H = \frac{8Gr_0}{\Psi_H}$$

The flexibility or compliance is written again as



$$\bar{F}_H = \frac{1}{K_H} \frac{1}{k_H + ia_0 c_H} = \frac{1}{K_H} (f_H + ig_H) \quad (3.63)$$

$$f_H = \frac{k_H}{(k_H^2 + (a_0 c_H)^2)} \quad (3.64)$$

$$g_H = \frac{-a_0 c_H}{(k_H^2 + (a_0 c_H)^2)} \quad (3.65)$$

### 3.5 Numerical Solution

Any numerical scheme used to solve the Fredholm integral equations previously derived will involve evaluation of the kernel functions a number of times. To reduce the computation time, the kernel functions defined by equation 3.46, 3.54, 3.60 may be reduced to finite integrals by contour integration. A discussion of this integration and the resulting finite integrals is given in the Appendix A.

The numerical procedure used to solve the integral equations is similar to the method used by Kashio in ref. (15) and Wei in ref. (14). A summary of the procedure follows.

Assume the interval  $[0, 1]$  is divided by  $N + 1$  equally spaced points. Replace the integral in the integral equations with a summation yielding

$$h(\bar{X}) + \sum_{j=1}^{N+1} L(\bar{X}, U_j) h(U_j) W_j = 1 \text{ or } \bar{X}$$

where the  $W_j$  are weights (Simpson's Rule was used here).

Now evaluate the equation at each  $\bar{X}_i$ , i.e.

$$h(\bar{X}_i) + \sum_{j=1}^{N+1} L(\bar{X}_i, U_j) h(U_j) W_j = 1 \text{ or } \bar{X}_i, \quad i = 1, N+1$$

Defining  $Y_j = h(U_j) W_j$  this can be rewritten

$$\frac{Y_i}{W_i} + \sum_{j=1}^{N+1} L(\bar{X}_i, U_j) Y_j = 1 \text{ or } \bar{X}_i$$

$$\text{or } \sum_{j=1}^{N+1} \left( \frac{\delta_{ij}}{W_i} + L(\bar{X}_i, U_j) \right) Y_j = 1 \text{ or } \bar{X}_i$$

where  $\delta_{ij}$  is the Kronecker delta.

In matrix form this is

$$[L] \{Y\} = \{1\} \text{ or } \{\bar{X}\}$$

Realizing that the kernel function and the unknown are complex, make the following definitions

$$[L] = [L_R] + i [L_I]$$

$$\{Y\} = \{Y_R\} + i \{Y_I\}$$

Equation (3.66) becomes

$$[L_R]\{Y_R\} + i[L_R]\{Y_I\} + i[L_I]\{Y_R\} - [L_I]\{Y_I\} = \{1\} \text{ or } \{\bar{X}\}$$

Equating real and imaginary parts leads to the following  
 $2(N+1)$  equations

$$\begin{bmatrix} -[L_R] & [L_I] \\ [L_I] & [L_R] \end{bmatrix} \begin{Bmatrix} \{Y_R\} \\ \{Y_I\} \end{Bmatrix} = \begin{Bmatrix} -\{1\} \quad \text{or} \quad -\{\bar{X}\} \\ \{0\} \end{Bmatrix} \quad (3.67)$$

$$\text{thus } \begin{Bmatrix} \{Y_R\} \\ \{Y_I\} \end{Bmatrix} = \begin{bmatrix} -[L_R] & [L_I] \\ [L_I] & [L_R] \end{bmatrix}^{-1} \begin{Bmatrix} -\{1\} \quad \text{or} \quad \{\bar{X}\} \\ \{0\} \end{Bmatrix}$$

To compute the impedance, an integration of the function  $h(\bar{X})$  must be performed.

Recall

$$K_{V,H} + i a_0 c_{V,H} = \int_0^1 h_{1,3}(\bar{X}) d\bar{X}$$

$$K_R + i a_0 c_R = \int_0^1 \bar{X} h_2(\bar{X}) d\bar{X}$$

Replacing these integrals with the same scheme as used above yields

$$K_{V,H} + i a_0 c_{V,H} = \sum_{j=1}^{N+1} h_{1,3}(\bar{X}_j) W_j = \sum_{j=1}^{N+1} (Y_{Rj} + i Y_{Ij})_{V,H} \quad (3.68a)$$

$$K_R + i a_0 c_R = \sum_{j=1}^{N+1} \bar{X}_j h_2(\bar{X}_j) W_j = \sum_{j=1}^{N+1} \bar{X}_j (Y_{Rj} + i Y_{Ij})_R \quad (3.69a)$$

or in matrix form

$$K_{V,H} = \{1\}^T \{Y_R\}_{V,H} \quad (3.69b)$$

$$a_0 c_{V,H} = \{1\}^T \{Y_I\}_{V,H} \quad (3.68c)$$

$$k_R = \{\bar{X}\}^T \{Y_R\}_R \quad (3.69b)$$

$$a_0 c_R = \{\bar{X}\}^T \{Y_I\}_R \quad (3.69c)$$

It should be noted that the kernel functions  $L(\bar{X}_i, U_j)$  are actually only functions of  $|\bar{X}_i - U_j|$  and  $(\bar{X}_i + U_j)$  which can be expressed as

$$|\bar{X}_i - U_j| = |i-j| / N$$

$$(\bar{X}_i + U_j) = (i+j-2)/N$$

As  $i$  and  $j$  range from one to  $N + 1$  there are actually only  $2N + 1$  different values of  $|\bar{X}_i - U_j|$  and  $(\bar{X}_i + U_j)$ . Therefore, with the proper bookkeeping the kernels only need be evaluated  $(2N + 1)$  times instead of  $N(N + 1)/2$  times. Since the kernel functions themselves involve a numerical integration, this savings is considerable.

Examining the kernel functions as given in the Appendix, it can be seen that they behave as  $\sqrt{\gamma^2 - k^2}$  or  $\sqrt{1 - k^2}$  as  $k$  approaches  $\gamma$  from below or one from below. Thus there is a slope discontinuity at the endpoints of the integrals. The special Gauss quadratures of ref. (42) were employed to evaluate them.

Also, the terms in the kernels involving

$\sin(a_0 k |\bar{X}-u|)$  exhibit a slope discontinuity at  $\bar{X} = U$  , and a special integration scheme must be used to avoid having to use a large N. The technique used is the same as Kashio (15) and Wei (14).

Let

$$I = \int_{U_{n-1}}^{U_{n+1}} h(U) dU \int_0^1 G(k) \sin(a_0 k |U - \bar{X}_n|) dk$$

where  $G(k)$  represents the non-oscillatory part of any of the kernels. Interchanging the order of integration.

$$I = \int_0^1 G(k) dk \left\{ \int_{U_{n-1}}^{U_n} h(U) \sin(a_0 k (\bar{X}_n - U)) dU + \int_{U_n}^{U_{n+1}} h(U) \sin(a_0 k (U - \bar{X}_n)) dU \right\}$$

If a parabola is fit through the three points  $h(U_{n-1})$ ,  $h(U_n)$  and  $h(U_{n+1})$  and the integrations on  $U$  performed the following expression results

$$I = \frac{1}{2N} \{h(U_{n-1}) + h(U_{n+1})\} \int_0^1 G(k) \sin(a_0 k/N) dk \quad (3.70)$$

Thus, certain terms in the L matrix of equation (3.66) need to be modified according to (3.70).

In summary, replacing the integral in the Fredholm equations by a numerical quadrature, leads to a set of simultaneous algebraic equations of the form of equation (3.67). Solution of (3.67) followed by the inner products given in equations (3.68) and (3.69) yields the impedance

coefficients.

### 3.6 Results

For each set of dimensionless constants in Table 2.2 equations (3.67) were formulated and solved for the vertical, rocking and horizontal problems over a wide range of the dimensionless frequency parameter,  $a_0$ . It should be noted that the vertical and rocking problems are independent of  $\lambda_2$ . Thus the vertical and rocking results can be referred to simply as Case 1, 2, etc. as shown in Table 2.2. However, the horizontal problem is dependent on  $\lambda_2$  and results must refer to Case 1a, b or c to indicate whether  $\lambda_2 = 0.5, 1.0$  or  $2.5$ .

The numerical results obtained are presented in Appendix B as Tables 3.1, 3.2, 3.3 for the vertical, rocking and horizontal problems respectively.

For comparison purposes, the results are also presented in graphical form. Each curve is labeled as follows. On the impedance plots, the curves are labeled k, case no. or c, case no., the k or c indicating the real or imaginary part of the impedance. (see eqn. 3.49 for instance), and the case no. referring to the dimensionless constants from Table 2.2. Note these curves are dimensionless and must be multiplied by the static stiffness to obtain the total impedance. On the compliance plots, the real part is labeled f, case no. and the imaginary part

-g, case no. indicating that the negative of the imaginary part is plotted. Again, these are dimensionless and must be multiplied by the static flexibility.

It should be noted from Table 2.2 that case no's. one through four correspond to isotropic properties with Poisson's ratios of 1/2, 1/3, 1/4, 0 respectively. The effect of the anisotropy can be measured, for the vertical and rocking problems, by holding  $\gamma^2$  constant and varying  $\lambda_1$ . The properties in Table 2.2 are thus broken into four groups, i.e.,  $\gamma^2=0$  cases 1, 5, 9, 12, 14;

$\gamma^2 = 1/4$ , cases 2, 6, 10, 13;  $\gamma^2 = 1/3$ , cases 3, 7, 11;  $\gamma^2 = 1/2$ , cases 4, 8.

The vertical impedance curves are presented in Figures 3.2, through 3.5. The compliances in Figures 3.6 and 3.9. In general, the real part of the impedance tends to increase with increasing  $\lambda_1$ , while the imaginary part shows much less variability. The compliance plots are more uniform, the real and imaginary parts increasing with increasing  $\lambda_1$ , the real part in the higher frequencies and the imaginary part in the lower frequencies.

Similar sets of curves for the rocking impedances and compliances are presented in Figures 3.10 through 3.17. As with the vertical, the group with  $\gamma^2=0$  has the most variability.

As might be expected, the horizontal results show little variation with  $\lambda_1$ . A similar set of plots

that were presented for the vertical and rocking problem are shown in Figure 3.18 through 3.25 for  $\lambda_2=2.5$ . The data for  $\lambda_2 = 0.5$  and  $1.0$  are similar. To indicate the variability with  $\lambda_2$ , cases 1, 2, 3, and 4 were each plotted for all three values of  $\lambda_2$  in Figures 3.26 through 3.33. Because of the results above, these curves can be taken as approximately correct for all values of  $\lambda_1$ . For all values of  $\gamma^2$  the curves behave similarly. The real part of the impedance increases with increasing frequency for  $\lambda_2 = 1/2$ , stays fairly constant for  $\lambda_2 = 1.0$  and decreased for  $\lambda_2=2.5$ . The imaginary part stays fairly constant, with the curves for  $\lambda_2 = 1/2$  and  $2.5$  being close together while for  $\lambda_2 = 1.0$  it is slightly greater. The real part of the compliance decreases with increasing  $\lambda_2$  as does the imaginary part.

It is sometimes helpful when viewing these complex impedance plots to draw the analogy between the force-displacement relationship of the massless disc-halfspace system and the force-displacement relationship for a simple Kelvin-Voigt model, that is a spring and dashpot in parallel. The static stiffness times the real part of the impedance is the equivalent spring and the static stiffness times the imaginary part of the impedance is the equivalent dashpot coefficient. However, for certain cases, for instance, see Figure 3.2, the stiffness can



become negative. There are ways to avoid this unappealing situation, however, they are introduced more readily when considering massive footings and so will be relegated to Chapter five.

To summarize this chapter, the solutions have been presented for the vertical, rocking and horizontal impedance and compliance coefficients of a rigid, massless disc vibrating harmonically on a transversely isotropic elastic halfspace. For vertical and rocking vibrations, the effect of the anisotropy can be measured by the magnitude of the dimensionless parameter,  $\lambda_1$ . For horizontal vibrations, the results are practically independent of  $\lambda_1$ , the effect of the anisotropy being almost totally measured by  $\lambda_2$ .

CHAPTER IV  
APPROXIMATE SOLUTION OF THE  
VISCOELASTIC PROBLEM

4.1 General

In the solutions obtained to this point, the material was assumed to be an elastic solid. It is well known, however, that real soils exhibit an energy loss under cyclic loading due to plastic deformation or hysteresis. To avoid a difficult non-linear boundary value problem, investigators have modeled this energy loss by assuming the material to be linearly viscoelastic. Solutions to the linear viscoelastic problem can be obtained by application of the correspondence principle.<sup>(44)</sup> In general, however, for problems of this type, the elastic solution is not known in closed form. In ref. (17), Luco obtained the viscoelastic solution to the isotropic problem by replacing the elastic constants in the Fredholm integral equations with complex moduli. The computational effort was greatly increased because the kernel functions can no longer be reduced to finite integrals via contour integration. Wei (14) fit polynomials to the elastic solutions obtained at discrete points. He then took the polynomial to be the exact elastic solution and applied the correspondence principle to obtain the viscoelastic solution. This technique was simplified somewhat for practical use by Veletsos and Verbic (45). Luco (17) compared his results obtained by the more theoretically

correct method with those of Veletsos and Verbic and found good agreement. The simpler approach will be adopted herein.

#### 4.2 Viscoelastic Models

Biot (46) has shown that for a general anisotropic viscoelastic medium, the stress strain relations may be expressed

$$\sigma_{ij} = C_{ijkl}^* \epsilon_{kl}$$

where  $C_{ijkl}^*$  is a general operational tensor involving material constants and time derivatives. Assuming a Voigt type material, let

$$C_{ijkl}^* = C_{ijkl} + C'_{ijkl} \frac{d}{dt}$$

For a transversely isotropic material undergoing harmonic motions, the stress strain relation becomes

$$\sigma_{rr} = C_{rr}^* \epsilon_{rr} + C_{r\theta}^* \epsilon_{\theta\theta} + C_{rz}^* \epsilon_{zz}$$

$$\sigma_{\theta\theta} = C_{r\theta}^* \epsilon_{rr} + C_{rr}^* \epsilon_{\theta\theta} + C_{rz}^* \epsilon_{zz}$$

$$\sigma_{zz} = C_{rz}^* \epsilon_{rr} + C_{rz}^* \epsilon_{\theta\theta} + C_{zz}^* \epsilon_{zz}$$

$$\sigma_{r\theta} = G_H^* \gamma_{r\theta}$$

$$\sigma_{rz} = G^* \gamma_{rz}$$

$$\sigma_{\theta z} = G^* \gamma_{\theta z}$$

where

$$\begin{aligned}
 C_{rr}^* &= C_{rr} + i\omega C_{rr}' = C_{rr} \left(1 + i\omega \frac{C_{rr}'}{C_{rr}}\right) \\
 C_{r\theta}^* &= C_{r\theta} + i\omega C_{r\theta}' = C_{r\theta} \left(1 + i\omega \frac{C_{r\theta}'}{C_{r\theta}}\right) \\
 C_{rz}^* &= C_{rz} + i\omega C_{rz}' = C_{rz} \left(1 + i\omega \frac{C_{rz}'}{C_{rz}}\right) \\
 C_{zz}^* &= C_{zz} + i\omega C_{zz}' = C_{zz} \left(1 + i\omega \frac{C_{zz}'}{C_{zz}}\right) \\
 G_H^* &= G_H + i\omega G_H' = G_H \left(1 + i\omega \frac{G_H'}{G_H}\right) \\
 G^* &= G + i\omega G' = G \left(1 + i\omega \frac{G'}{G}\right)
 \end{aligned}$$

The dimensionless constants appearing in the elastic solution are now in general complex constants, i.e.,

$$(\lambda_1^*)^2 = \frac{C_{rr}^*}{C_{zz}^*} = \lambda_1^2 \frac{\left(1 + i\omega \frac{C_{rr}'}{C_{rr}}\right)}{\left(1 + i\omega \frac{C_{zz}'}{C_{zz}}\right)}$$

$$(\gamma^*)^2 = \frac{G^*}{C_{rr}^*} = \gamma^2 \frac{\left(1 + i\omega \frac{G'}{G}\right)}{\left(1 + i\omega \frac{C_{rr}'}{C_{rr}}\right)}$$

$$(\lambda_2^*)^2 = \frac{G_H^*}{G} = \lambda_2^2 \frac{\left(1 + i\omega \frac{G_H'}{G_H}\right)}{\left(1 + i\omega \frac{G'}{G}\right)}$$

$$\phi^* = \frac{C_{rz} \left(1 + i\omega \frac{C_{rz}'}{C_{rz}}\right) + C_{zz} \left(1 + i\omega \frac{C_{zz}'}{C_{zz}}\right)}{C_{zz} \left(1 + i\omega \frac{C_{zz}'}{C_{zz}}\right) - G \left(1 + i\omega \frac{G'}{G}\right)}$$

If we assume all the complex numbers in the above expressions are equal we see that the complex dimensionless constants become equal to the real dimensionless constants from the elastic problem.

This means we assume each component of the strain tensor lags the stress by the same amount. Further insight into the meaning of this assumption can be obtained by examining the stress strain relationships in terms of the Poisson ratios and the moduli of elasticity. From the relationships of Chapter 2 it is easily shown that

$$E_H = \frac{2G_H(C_{rr}C_{zz} + C_{r\theta}C_{zz} - 2C_{rz}^2)}{C_{rr}C_{zz} - C_{rz}^2}$$

$$E_V = \frac{2G_H(C_{rr}C_{zz} + C_{r\theta}C_{zz} - 2C_{rz}^2)}{(C_{rr}^2 - C_{r\theta}^2)}$$

$$n = \frac{E_H}{E_V} = \frac{C_{rr}^2 - C_{r\theta}^2}{C_{rr}C_{zz} - C_{rz}^2} = \frac{2G_H(C_{rr} + C_{r\theta})}{C_{rr}C_{zz} - C_{rz}^2} = \frac{\nu_{HV}}{\nu_{VH}}$$

$$\nu_{HV} = \frac{2G_H C_{rz}}{C_{rr}C_{zz} - C_{rz}^2}$$

$$\nu_H = 1 - \frac{2G_H C_{zz}}{C_{rr}C_{zz} - C_{rz}^2}$$

Substituting the complex constants yields

$$E_H^* = E_H \left( 1 + i\omega \frac{G_H'}{G_H} \right)$$

$$E_V^* = E_V \left( 1 + i\omega \frac{G_H'}{G_H} \right)$$

$$n^* = n$$

$$\nu_{HV}^* = \nu_{HV} ; \nu_H^* = \nu_H$$

Thus, the assumption stated above is equivalent to assuming the Poisson ratios to be real numbers and the moduli of elasticity to have the same phase lag, i.e.

$$E_H' / E_H = E_V' / E_V = G_H' / G_H$$

To show a disadvantage of this assumption, examine a sinusoidally oscillating hydrostatic stress state, i.e.

$$\sigma_{xx} = \sigma_{yy} = \sigma_{zz} = \sigma e^{i\omega t}$$

$$\sigma_{xy} = \sigma_{xz} = \sigma_{yz} = 0$$

The volumetric strain is then

$$\epsilon_V = \frac{2(1 - \nu_H) - 4n\nu_{HV} + n}{E_H(1 + i\omega G_H' / G_H)} \quad (3\sigma)$$

Thus, unless the material is incompressible there are energy losses caused by hydrostatic stresses.

Since this assumption is required for the simplified treatment to be employed and since we will be examining

materials with small damping we will accept its approximate nature.

A dimensionless measure of the energy loss is the damping capacity defined as (47)

$$\frac{\Delta W}{W} = \frac{\text{energy lost per cycle}}{\text{max. strain energy}}$$

For shear deformations we get from 4.1e or f

$$\frac{\Delta W}{W} = 2\pi\omega \frac{G'}{G}$$

Thus for the Voigt type material assumed, the energy lost is proportional to the exciting frequency. Actual tests on soils indicate, however, that the energy loss is independent of the frequency, (25, 27) and due primarily to hysteresis. This led to the development of the hysteretic damping model, where  $G'$  is taken inversely proportional to frequency.

Define  $\tan\delta = \frac{\omega G'}{G}$

$\tan\delta$  is known as the loss coefficient. The complex moduli now becomes, for eg.

$$G^* = G(1 + i \tan\delta)$$

In the following sections, both types of models will be investigated, that is, the frequency dependent Voigt model and the frequency independent hysteretic model.

### 4.3 Viscoelastic Impedance Functions

Recall the force-displacement relationship derived in Chapter 3 for harmonic vertical vibrations

$$P_V = K_V (k_V(a_0) + ia_0 c_V(a_0)) \Delta_V \quad (4.1)$$

The equation has been written in this form to indicate explicitly that  $k_V$  and  $c_V$  are functions of the dimensionless frequency parameter,  $a_0$ . Now following Wei (14) use least squares curve fitting to obtain an approximate continuous solution to the problem obtained previously at discrete frequencies only.

$$\text{Let} \quad k_V(a_0) = \sum_{n=0}^N A_n a_0^n \quad (4.2a)$$

$$c_V(a_0) = \sum_{n=0}^N B_n a_0^n \quad (4.2b)$$

The force displacement relationship for a viscoelastic medium is, by the correspondence principal

$$P_V = K_V^* (k_V^*(a_0^*) + ia_0^* c_V^*(a_0^*)) \Delta_V \quad (4.3)$$

where for the hysteretic model

$$K_V^* = \frac{4G^* r_0}{\psi_V} = \frac{4Gr_0}{\psi_V} (1 + i \tan \delta)$$

and

$$a_0^* = \frac{r_0 \sqrt{\rho}}{\sqrt{G^*}} = a_0 (1 + i \tan \delta)^{-1/2}$$

$$k_V^* = \sum A_n (a_0^*)^n = \sum A_n a_0^n (1 + i \tan \delta)^{-n/2}$$

$$c_V^* = \sum B_n (a_0^*)^n = \sum B_n a_0^n (1 + i \tan \delta)^{-n/2}$$

After some algebraic manipulation (4.3) can be rewritten



$$P_V = K_V (k_V^V(a_0) + i a_0 c_V^V(a_0)) \Delta_V \quad (4.4)$$

The superscript v refers to the viscoelastic case.

Similar expressions hold for the rocking and horizontal problems. For a Voigt model replace  $\tan\delta$  in the above with  $a_0 \zeta$ , where

$$\zeta = \frac{c_2}{r_0} \frac{G'}{G} \quad (4.5)$$

For values of  $a_0$  close to zero  $k_V^V$  and  $c_V^V$  are approximately given by

$$k_V^V = \begin{cases} 1 - \frac{c_V(a_0)}{2} a_0^2; \text{Voigt} & (4.6a) \\ 1 - \frac{c_V(a_0)}{2} (\tan\delta) a_0; \text{hysteretic} & (4.6b) \end{cases}$$

$$c_V^V = \begin{cases} c_V(a_0) + \zeta; \text{Voigt} & (4.6c) \\ c_V(a_0) + \frac{\tan\delta}{a_0}; \text{hysteretic} & (4.6d) \end{cases}$$

Observe that the force displacement relationship, equation (4.4), is analogous to a spring and dashpot in parallel;

$K_V k_V^V$  is the spring and  $K_V c_V^V$  is the equivalent dashpot. We see from (4.6b) that for a Voigt model,  $\zeta$  adds to the equivalent dashpot coefficient, while for the hysteretic model, the dashpot coefficient grows as

$$\frac{1}{a_0} \text{ as } a_0 \rightarrow 0$$

#### 4.4 Results

The viscoelastic impedance functions, equations (4.4), have been evaluated for the vertical, rocking and horizontal problems. Only representative results will be shown. The conclusions drawn also apply to the cases not shown.

Figure 4.1 shows the vertical impedance for a Voigt model with several values of  $\zeta$  considered. The elastic properties are case 2 of the Table 2.2 i.e. isotropic with Poisson's ratio equal to  $1/3$  and  $\lambda_1^2=1$ ,  $\gamma^2=1/4$ . Figure 4.3 and 4.5 show the same plots for cases 10 and 13 that is  $\gamma^2=1/4$  and  $\lambda_1^2= 2$  and 3 respectively. The same three plots are repeated in Figures 4.2, 4.4 and 4.6 for a constant hysteretic material for several values of  $\tan\delta$  .

The predominant effects of the material damping are a decrease in the spring stiffness,  $k_V$  and an increase in the damping coefficient,  $c_V$  . The lower frequency approximations, equations (4.6) are seen to hold up to a dimensionless frequency of about one.

The same six plots are presented in Figures 4.7 through 4.12 for the rocking problem. The same trends are seen to hold in general. However, the effect on the spring stiffness is not as great in the lower frequencies. It should be noted that the effect of the material damping on

$c_R$  is more important because of the lower values of the radiation damping.

Figure 4.13 shows the horizontal impedance plots for a Voigt material, case 2b, that is  $\lambda_1^2=1, \lambda_2^2=1, \gamma^2=1/4$ . The same plots for case 2c,  $\lambda_1^2=1, \lambda_2^2=2.5, \gamma^2=1/4$  are shown in Figure 4.15. These two plots are repeated for a constant hysteretic material in Figures 4.14 and 4.16. The effects of material damping are approximately the same.

The fact that the effect of the material damping is similar for varying degrees of anisotropy is not surprising. By virtue of the assumption made at the beginning of this chapter, the damping enters the solution only through the shear modulus,  $G$  just as it does in the isotropic problem, thus we expect a similar effect.

In summary, by making the assumption that all the complex moduli have the same loss coefficient, we have been able to obtain approximate solutions to the viscoelastic problem by application of the correspondence principle.

## CHAPTER 5

### MASSIVE FOUNDATIONS

#### 5.1 General

The previous two chapters considered the harmonic force-displacement relationship of a rigid massless disc vibrating on the surface of a transversely isotropic elastic or viscoelastic half space. Given this relationship, the equations of motion for any given structure or machine, mounted on a circular foundation, can be written to include the effect of the soil mass. This chapter will study the response of a massive circular foundation vibrating harmonically on the surface of a transversely isotropic half space.

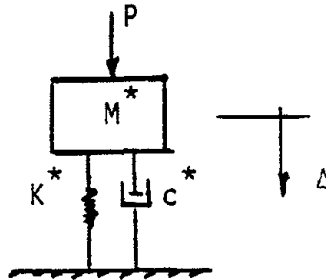
#### 5.2 Equivalent Single Degree of Freedom Representation

As pointed out in Chapter 3, the harmonic force displacement relationship for the massless disc on a half space is analogous to the force displacement relationship of a simple Kelvin-Voigt model. The analogy is not always helpful because for certain values of the elastic constants the real part of the impedance or the equivalent spring stiffness can become negative. For use later in the chapter, a somewhat more consistent approach due to Veletsos and Verbic (45) will be presented below.

The force displacement relationship for a single degree of freedom (SDOF) oscillator undergoing steady state harmonic motion is (see figure below)

$$P = (K^* - \omega^2 M^* + i \omega c^*) \Delta \quad (5.1)$$

(the factor  $e^{i\omega t}$  is omitted)



Recall the force displacement relationship for the massless disc-half space system (this expression is the general form for vertical, rocking or horizontal vibration)

$$P = K (k + i a_0 c) \Delta \quad (5.2)$$

From (5.1) and (5.2) we get

$$K^* - \omega^2 M^* + i \omega c^* = Kk + i a_0 Kc$$

Equating imaginary terms yields

$$c^* = c \frac{K r_0}{c_2} \quad (5.3)$$

Since  $a_0 = \omega r_0 / c_2$ , where  $c_2$  is the shear wave velocity,  $\sqrt{G/\rho}$ .

We are left with one equation to determine  $K^*$  and  $M^*$ . To avoid the problem of the negative spring stiffness define

$$K^* = K \quad (5.4)$$

then the effective or virtual mass becomes

$$M^* = (1-k) \left( \frac{K}{\omega^2} \right) \quad (5.5)$$

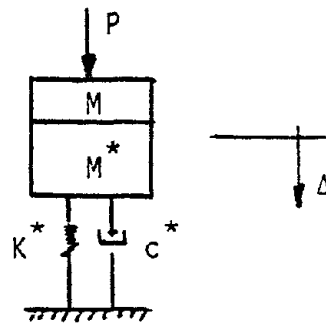
Eliminate  $\omega^2$  from this equation by defining the dimensionless virtual mass ratio

$$B^* = \frac{1 - k}{a_0^2} \quad (5.6)$$

then

$$M^* = B^* \left[ \frac{K r_0^2}{c_2^2} \right] \quad (5.7)$$

The effect of foundation mass can be accounted for by simply adding the actual mass to the virtual mass (see figure below)



The "natural frequency" of this equivalent SDOF is then

$$\omega_n = \sqrt{\frac{K}{(M+M^*)}} \quad (5.8)$$

and the percentage of critical damping is

$$\beta = \frac{c^*}{2 \sqrt{K (M+M^*)}} \quad (5.9)$$

Equations (5.8) and (5.9) can be rewritten using the dimensionless mass ratio,

$$B = \frac{M c_2^2}{K r_0^2} \quad (5.10)$$

then

$$\beta = \frac{c}{2 \sqrt{B+B^*}} \quad (5.11)$$

and

$$\omega_n = \sqrt{\frac{B}{B+B^*}} (\omega_0) \quad (5.12)$$

where

$$\omega_0 = \sqrt{\frac{K}{M}} \quad (5.13)$$

The ratio of the amplitude of the dynamic displacement to the static displacement, or the dynamic magnification factor (DMF) is given by the familiar formula

$$DMF = \left| \frac{\Delta}{P/K} \right| = \frac{1}{\sqrt{\{1 - (\omega/\omega_n)^2\}^2 - 4\beta^2 (\omega/\omega_n)^2}} \quad (5.14)$$

In all the equations above,  $M$  and  $M^*$  should be replaced by  $I$  and  $I^*$ , the mass moments of inertia for the rocking problem.

Recalling the expressions for the static stiffnesses, the dimensionless mass ratio may be written for each mode of vibration as

$$B_V = \frac{\psi_V}{4} \frac{M}{\rho r_0^3} \text{ (vertical)} \quad (5.15a)$$

$$B_R = \frac{3\psi_V}{8} \frac{I}{\rho r_0^5} \text{ (rocking)} \quad (5.15b)$$

$$B_H = \frac{\psi_H}{8} \frac{M}{\rho r_0^3} \text{ (horizontal)} \quad (5.15c)$$

Although the SDOF oscillator representation is sometimes helpful, the DMF can certainly be expressed directly in terms of the impedance functions as

$$\text{DMF} = \frac{1}{\sqrt{(k-a_0^2 B)^2 + (a_0 c)^2}} \quad (5.16)$$

Both expressions will prove useful.

In what follows we wish to choose a foundation with set dimensions and weight and compare the DMF for soils possessing different degrees of anisotropy. In Chapters 3 and 4 we found it convenient to measure the effect of the anisotropy by fixing  $\gamma^2$  and varying  $\lambda_1^2$  or  $\lambda_2^2$ . It should be pointed out that it was implicitly assumed that the shear modulus,  $G$ , was also held constant as  $\lambda_1^2$  (or  $\lambda_2^2$ ) varied. This was to make the dimensionless frequency,  $a_0$  always have the same meaning. For  $\gamma^2$  and  $G$  held constant, the static stiffness will always be different for different  $\lambda_1^2$  and/or  $\lambda_2^2$ . Note also, from eqn.(5.15), that the dimensionless mass ratios will also vary with  $\lambda_1^2$  and/or  $\lambda_2^2$ .

### 5.3 RESULTS

Using equation (5.14) or (5.16) and the results of Chapters 3 and 4, the DMF can be evaluated for varying degrees of soil anisotropy and mass ratio. To provide a baseline from which to measure, we first present results for a massless footing, that is  $B=0$ . As expected, equation(5.16)



yields the inverse of the amplitude of the impedance function for the DMF.

Figure 5.1 shows DMF plots for vertical vibration on an elastic soil for material cases 2, 6, 10, and 13, i.e.  $\gamma^2 = 1/4$  and  $\lambda_1^2 = 1, 1.5, 2.0$  and  $3.0$ . Figure 5.2 repeats these plots for a constant hysteretic material with  $\tan \delta = 0.3$ , while Figure 5.3 is for a viscous material with  $\zeta = 0.3$ .

Note the small effect that the soil anisotropy has, especially when the soil is considered viscoelastic. This can be explained by recalling the results of Chapter 3. For vertical vibrations, the real part of the impedance showed considerable variation with varying degrees of anisotropy only for the higher frequencies, while the imaginary part showed little variability and was fairly constant over the frequency range investigated. We see from equation (5.16) (for  $B = 0$ ) that as  $a_0$  increases the term involving  $c$  predominates and thus the variability of  $k$  is not so important. Recall from Chapter 4 that as material damping is added,  $k$  decreases and  $c$  increases and thus the soil anisotropy has even less effect.

Figures 5.4 through 5.6 show a similar set of plots for the rocking problem, only for material cases 3, 7, 11, i.e.  $\gamma^2 = 1/3$ ,  $\lambda_1^2 = 1.0, 1.5, 2.0$ .

These results are similar to the vertical and an analogous explanation applies. The principal difference

between the vertical and the rocking is a region of amplification due to the small amount of radiation damping for this mode of vibration.

Figures 5.7 through 5.9 show a similar set of plots for the horizontal problem, material cases 1a, 1b, 1c, i.e.  $\gamma^2 = 0, \lambda_2^2 0.5, 1.0, 2.5$ . Here the anisotropy has more of an effect; the effect again decreasing with the addition of material damping. The reason the anisotropy has more of an effect in this case is that not only does the real part of the impedance vary for different degrees of anisotropy but so does the imaginary part.

The results presented above were typical for all values of  $\gamma^2$ . The balance of the results will be presented for  $\gamma^2 = 1/4$  only.

We will now examine the vertical and rocking modes of vibration for material cases 2 and 13, i.e.  $\gamma^2 = 1/4$ ,  $\lambda_1^2 = 1.0$  and  $3.0$ . Let the mass ratio for material case 2 be  $0.2$ , then due to the difference in the values of  $\Psi_v$  the mass ratio for material case 13 is  $0.355$ . This corresponds to a foundation mass of  $1.2 \rho r_0^3$  (see eqn. (5.15a) ) for vertical vibrations and a mass moment of inertia of  $0.8 \rho r_0^5$  for rocking vibrations. Figure 5.10 is a plot of the DMF for the vertical mode for an elastic material.

The anisotropy again has little effect and no

amplification occurs. The effects of this foundation mass on the results for the damped soil were similar.

Figure 5.11 shows the DMF plots for the same two material cases for the rocking mode and an elastic soil. Here the anisotropic result is significantly different. The result for a hysteretic material with  $\tan \delta = .3$  is shown in Figure 5.12 and for a viscous material with  $\zeta = 0.3$  is shown in Figure 5.13. From eqn. (5.16) we see that this value of the foundation mass is large enough to cause  $(k - a_0^2 B)$  to be small over a frequency range when  $a_0 c$  is also small, resulting in a fairly large amplification. From the previous results for the massless foundation, we infer that the difference between the two curves is due principally to the difference in the values of  $\Psi_v$  rather than differences between the impedance coefficients. To verify this, the DMF plots are repeated for the same two material cases and with  $B = 0.355$  for both cases in Figure 5.14. Similar curves for damped soils show even less difference.

The DMF plots for horizontal vibrations for material cases 2B and 2C and elastic soil are shown in Figure 5.15. For horizontal vibrations a mass ratio of .2 for an isotropic material case 2B, means a foundation mass of  $0.06 \rho_0^3$ . For material case 2c a foundation mass of  $0.96 \rho_0^3$  is equivalent to a mass ratio of 1.56. Similar to the vertical problem almost no amplification occurs. With soil damping included the two

curves are even closer together.

The DMF plots will now be examined for the same material cases with a mass ratio of 2.0 for the isotropic material, case 2. This implies a mass ratio of 3.55 for the vertical and rocking problems, case 13, and a mass ratio of 1.56 for the horizontal problem case 2c. The vertical and rocking results are presented in figures 5.16 through 5.21 for elastic and viscoelastic soils. Here the vertical problem shows a significant amount of amplification. The important result is that with this increased mass ratio, the difference between the isotropic and anisotropic results is due even more to the different values of  $\Psi_V$ , than it was for the lower mass ratio. This is exemplified by replotting Figure 5.16 using a mass ratio of 3.55 for both material cases. This is shown in Figure 5.22.

The DMF plots for the horizontal problem, material cases 2b and 2c, elastic and viscoelastic, are presented in Figures 5.23 through 5.25. Again the difference between the two curves is due almost entirely to the difference in the values of  $\Psi_H$ .

To recap the above results; we have shown that the difference in the DMF between an isotropic material and an anisotropic material, having the same  $\gamma^2$  and  $G$ , is due primarily to the different values of  $\Psi_V$  (or  $\Psi_H$ ) rather than to differences in the impedance coefficients.

This might have been intuitively expected, but the results herein have served to quantify this. This result is very useful particularly in the design of machine foundations, where the forcing function is indeed harmonic. Recall that we have only discussed the amplitude of the response, not the phase angle. When the forcing function is an arbitrary function of time, such as an earthquake, the phase angles are also required for Fourier synthesis. Since the ratio  $a_0 c/k$  does differ significantly from the isotropic particularly for higher frequencies, the phasing can be quite different.

It is standard to present the results from a study such as this in nondimensional form. However, this sometimes makes certain things obscure. Therefore, several simple examples are presented in Appendix C to better define some of the quantities involved.

CHAPTER VI  
SUMMARY & CONCLUSION

The response of a circular foundation resting on a transversely isotropic half space was studied. The results should be useful in the design of machine foundations and in the design of structures to resist dynamic loads. The basis of the study was the solution of the problem of the rigid, massless, circular disc vibrating harmonically on the surface of a transversely isotropic elastic half space. The solution was obtained by restricting the materials considered to those which satisfy a certain constraint equation (see eqn. (2.8)). The principal results from the solution were dimensionless compliance and impedance coefficients, presented in tabular and graphical form. It was found that the vertical and rocking problems could be studied by holding  $\gamma^2$  constant and varying  $\lambda_1^2$ , while the horizontal problem could be studied by holding  $\gamma^2$  constant and varying  $\lambda_2^2$ . In general, the real part of the impedance showed significant variation from the isotropic only in the higher values of the dimensionless frequency. The imaginary part of the impedance showed much less variability throughout the frequency range investigated.

An approximate solution was also obtained for the viscoelastic problem. Two principal assumptions were involved in this solution. First, it was assumed

that each component of the strain tensor lags the stress by the same amount. In other words the loss coefficient or phase angle for all complex constants was assumed equal. From the elastic solution, least squares curve fitting was employed to obtain an approximate analytical solution in polynomial form. This approximate analytical solution was taken to be the exact solution in order to use the viscoelastic correspondence principle. Compliance and impedance plots were presented for representative sets of material constants. Principally because of the first assumption above, the results of material damping were found to be similar to the isotropic problem.

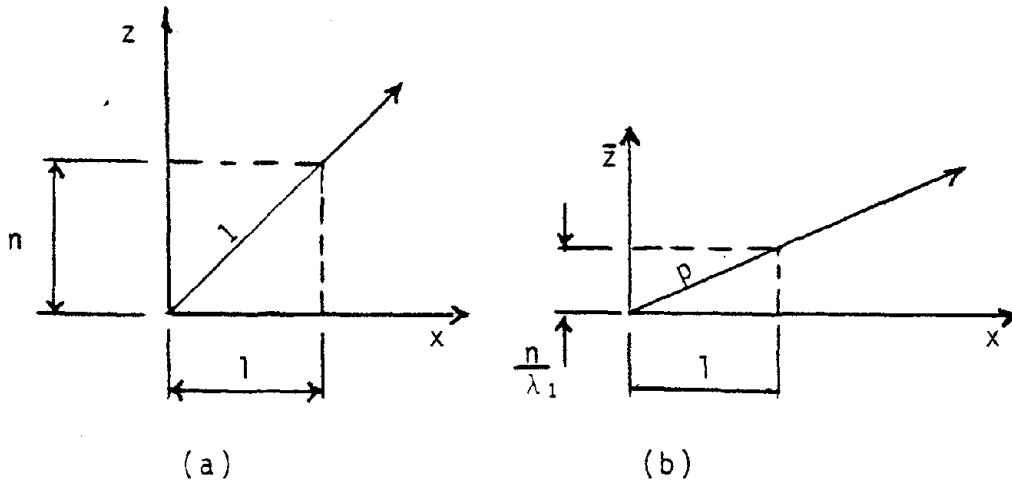
The effect of foundation mass was studied by plotting the ratio of the maximum dynamic displacement to static displacement, for various values of a dimensionless mass. It was found that the principal difference between the response of a massive foundation resting on an anisotropic soil and one resting on an isotropic soil, with an equivalent  $\gamma^2$ , was due to the difference in the expressions for the static stiffnesses and not due to the differences in the impedance coefficients. This result is important for the design of machine foundations, since it allows for an approximate analysis by using the available isotropic impedance coefficients, along with the proper anisotropic static stiffness expression. For very massive foundations this approximate

technique yields very accurate results.

For transient analysis in the frequency domain the phase angle also becomes important. Especially for the higher values of the dimensionless frequency the phase angle for an anisotropic soil may be significantly different than the phase angle for an isotropic soil with an equivalent  $\gamma^2$ . Using the results obtained herein a future study might undertake to determine the effect of soil anisotropy under transient loadings.

It should also be mentioned that for the special material considered herein, most of the techniques developed to analyze foundations on isotropic soils could easily be extended to anisotropic soils.





DIRECTION OF PROPOGATION IN ORIGINAL (a)  
AND DISTORTED (b) COORDINATE SYSTEMS

FIGURE 2.1

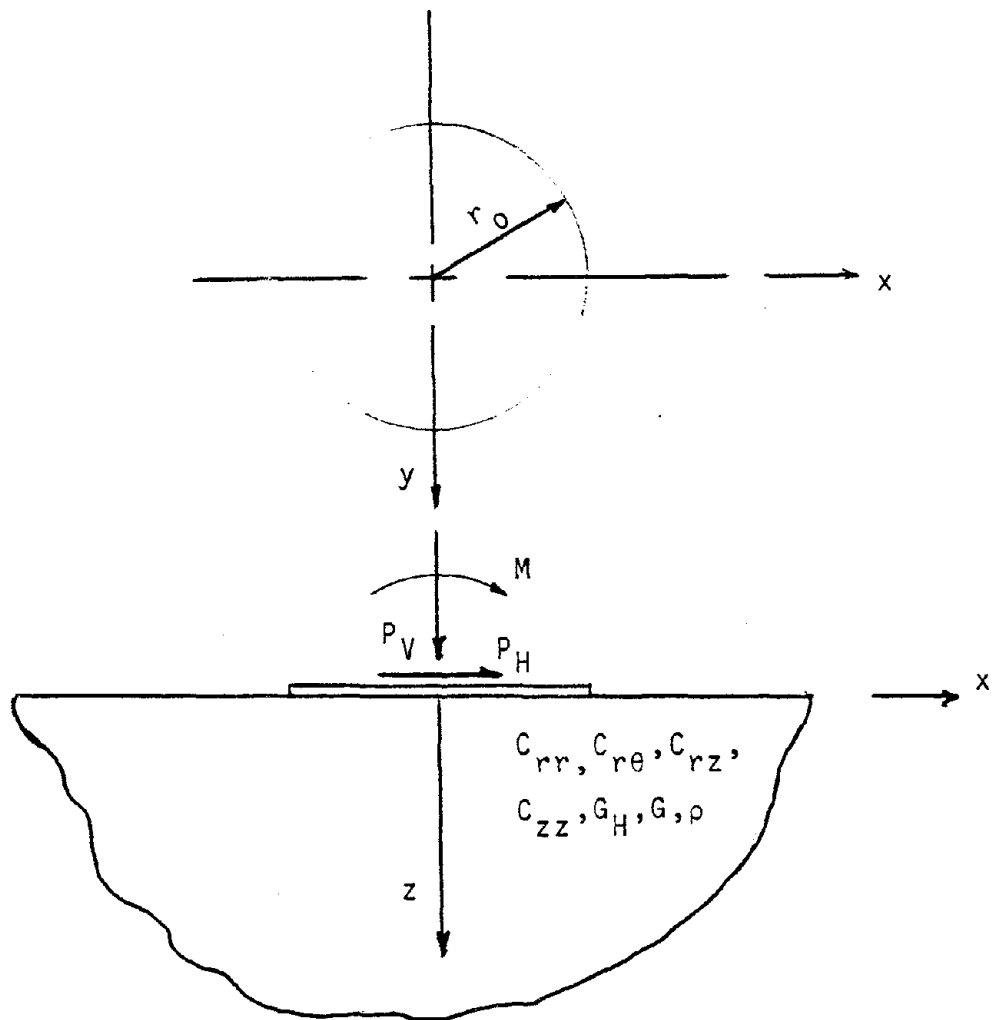


FIGURE 3.1

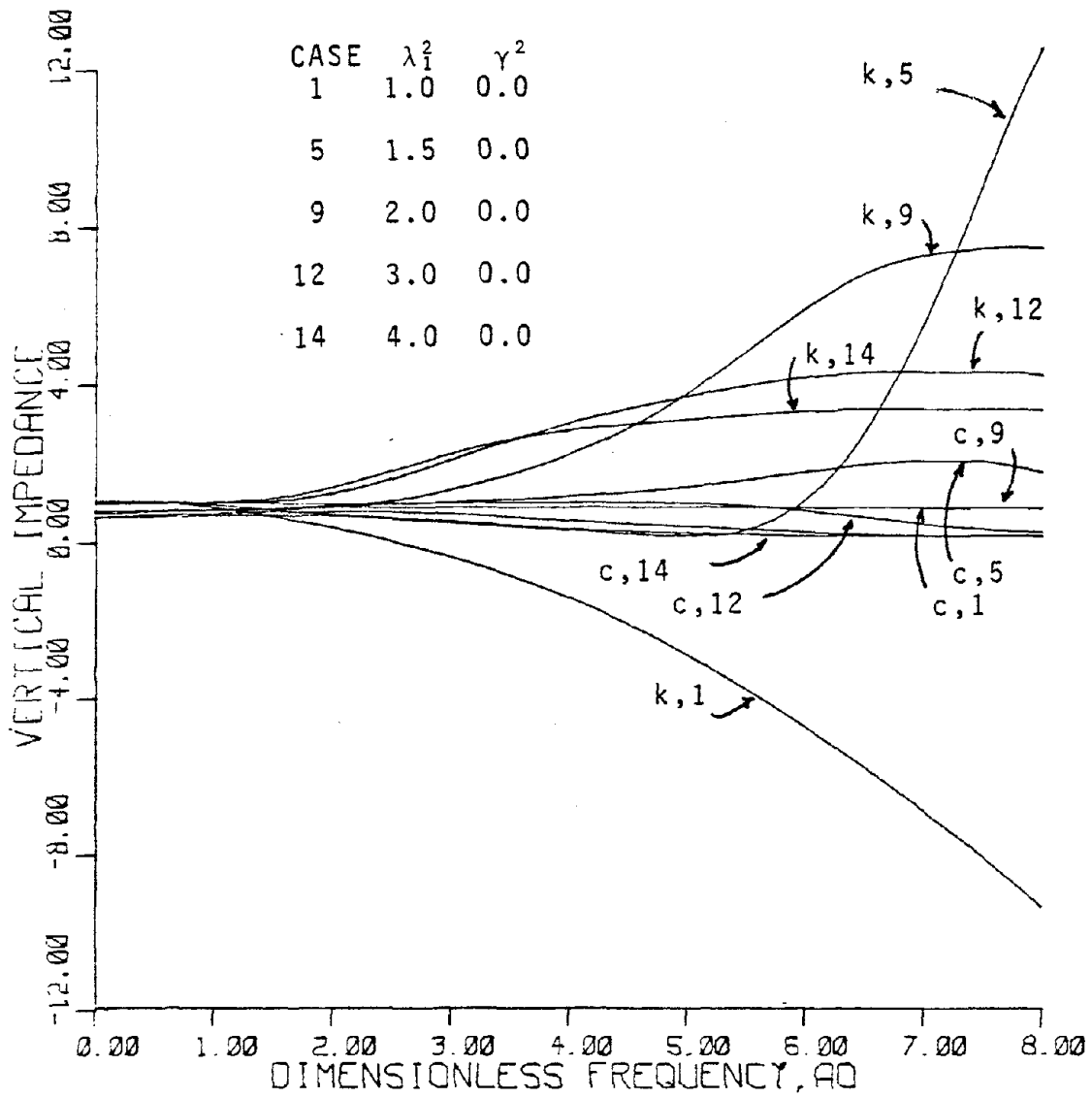


FIGURE 3.2

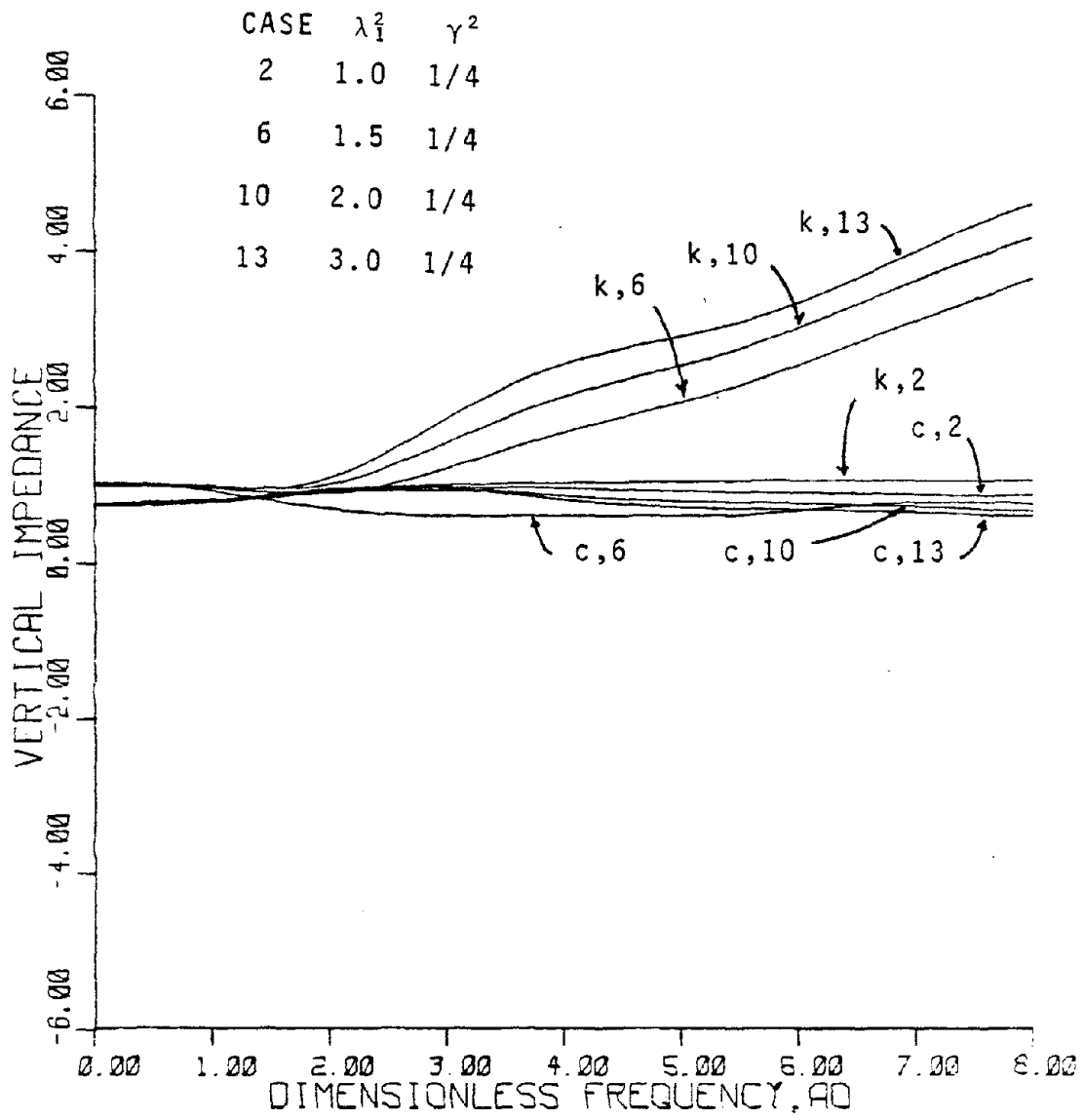


FIGURE 3.3

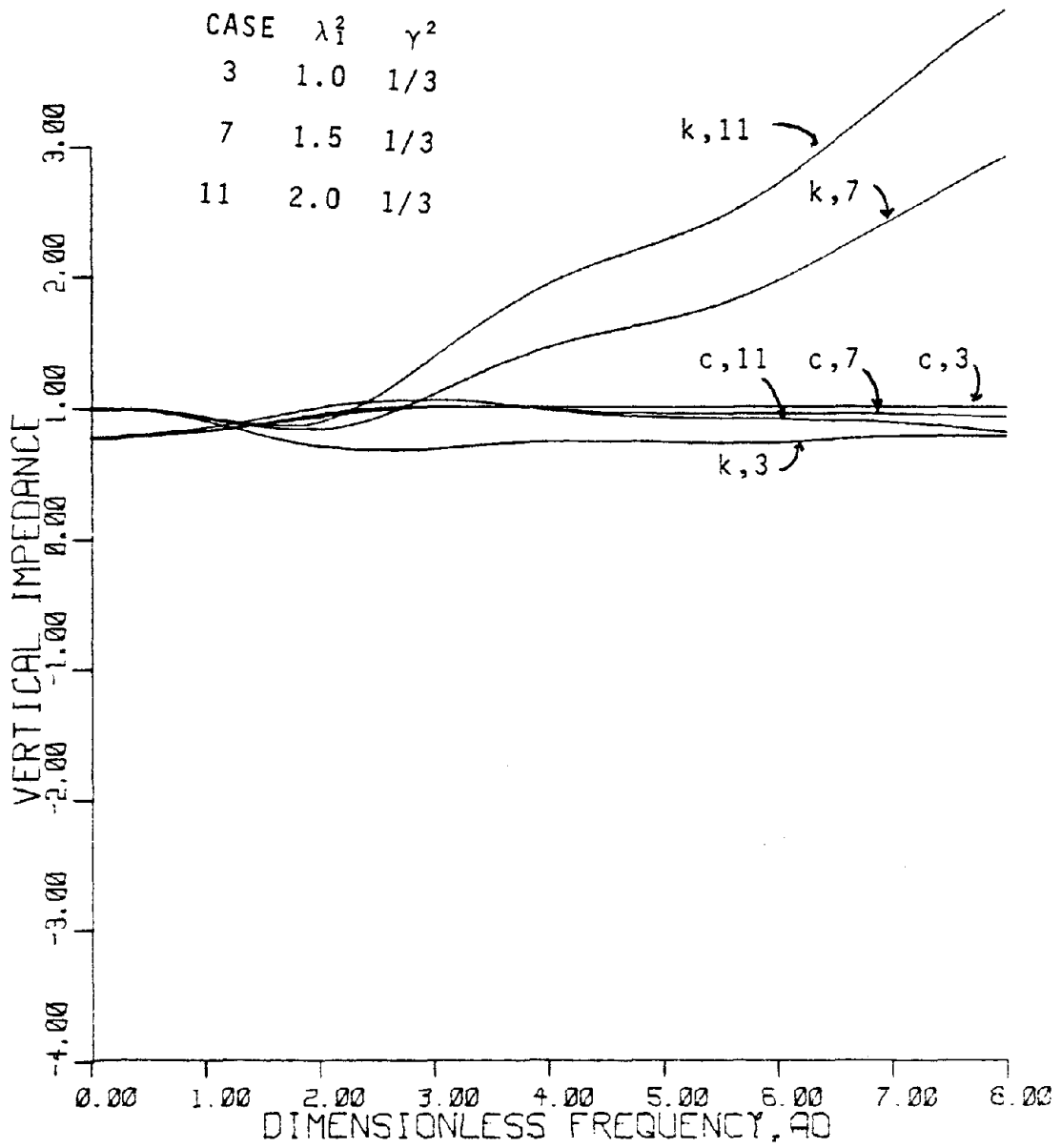


FIGURE 3.4

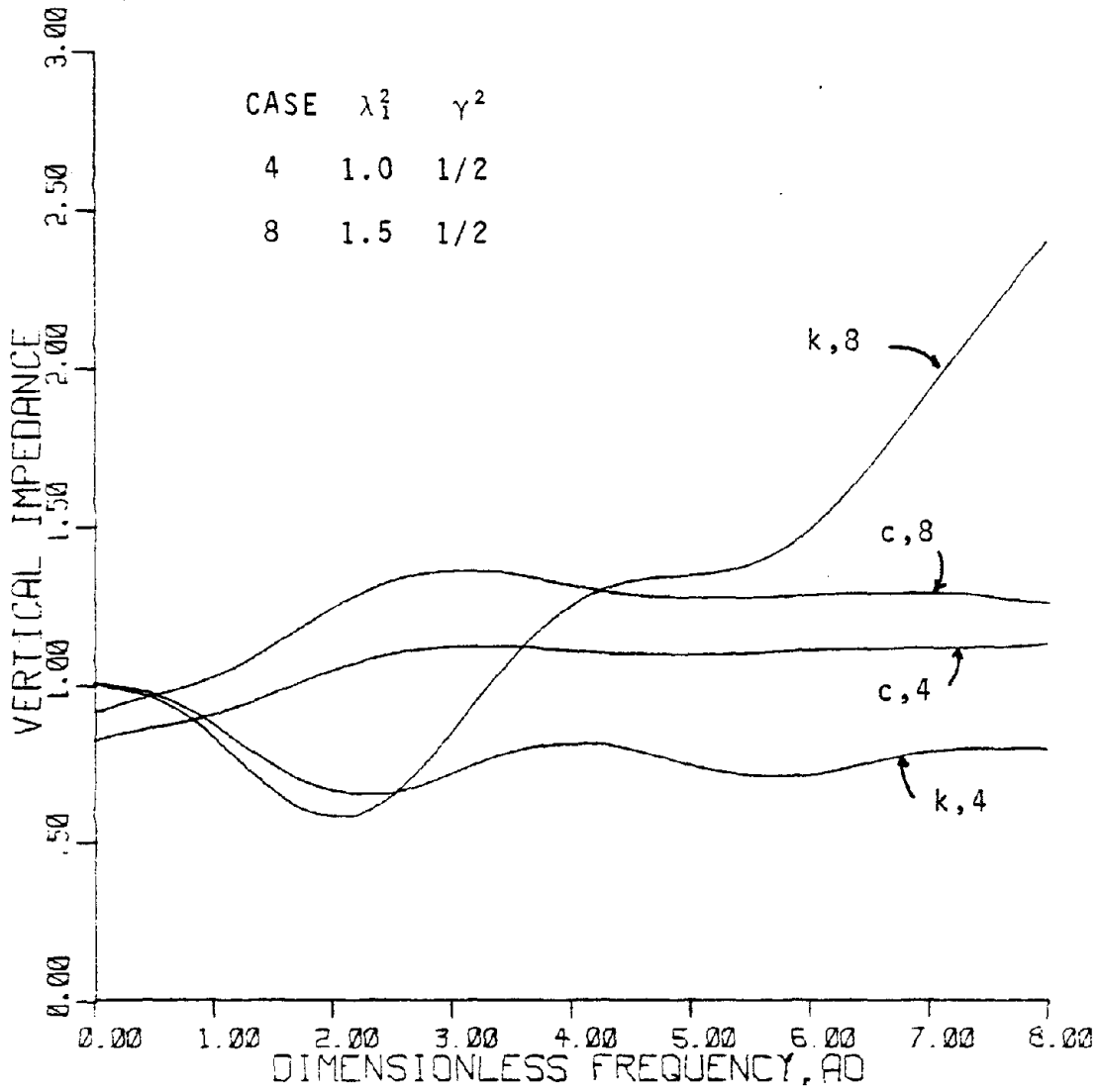


FIGURE 3.5

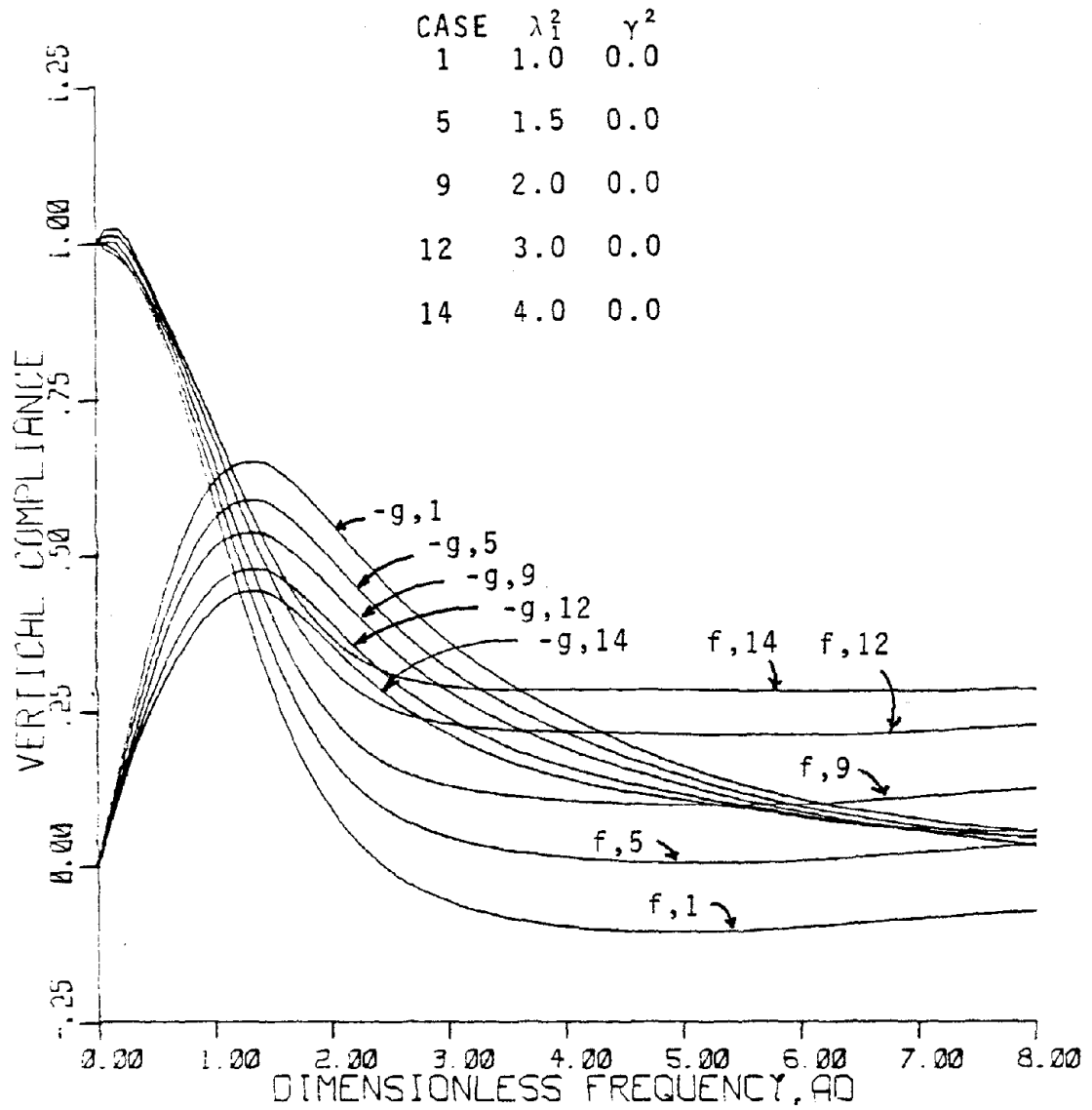


FIGURE 3.6

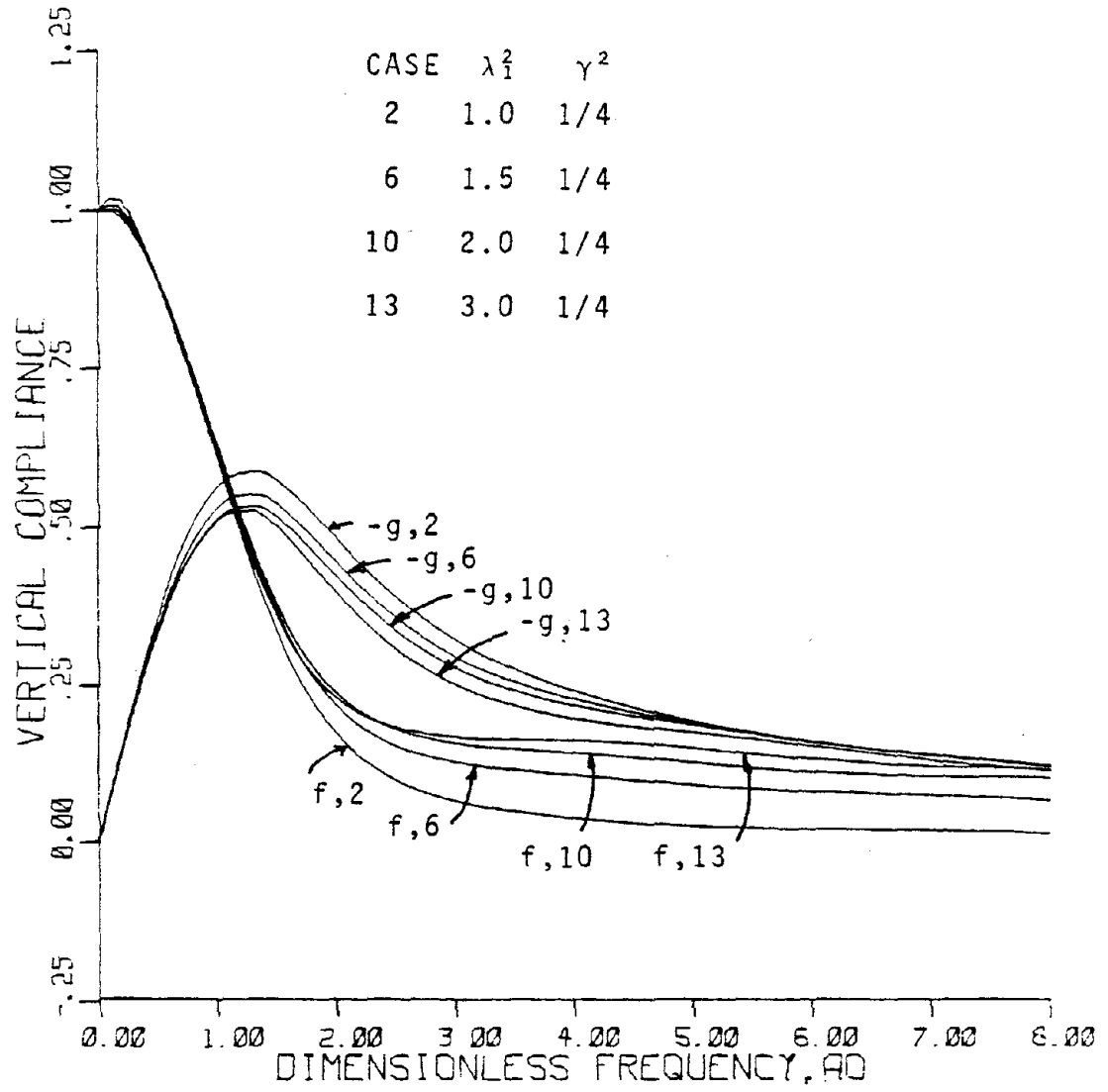


FIGURE 3.7



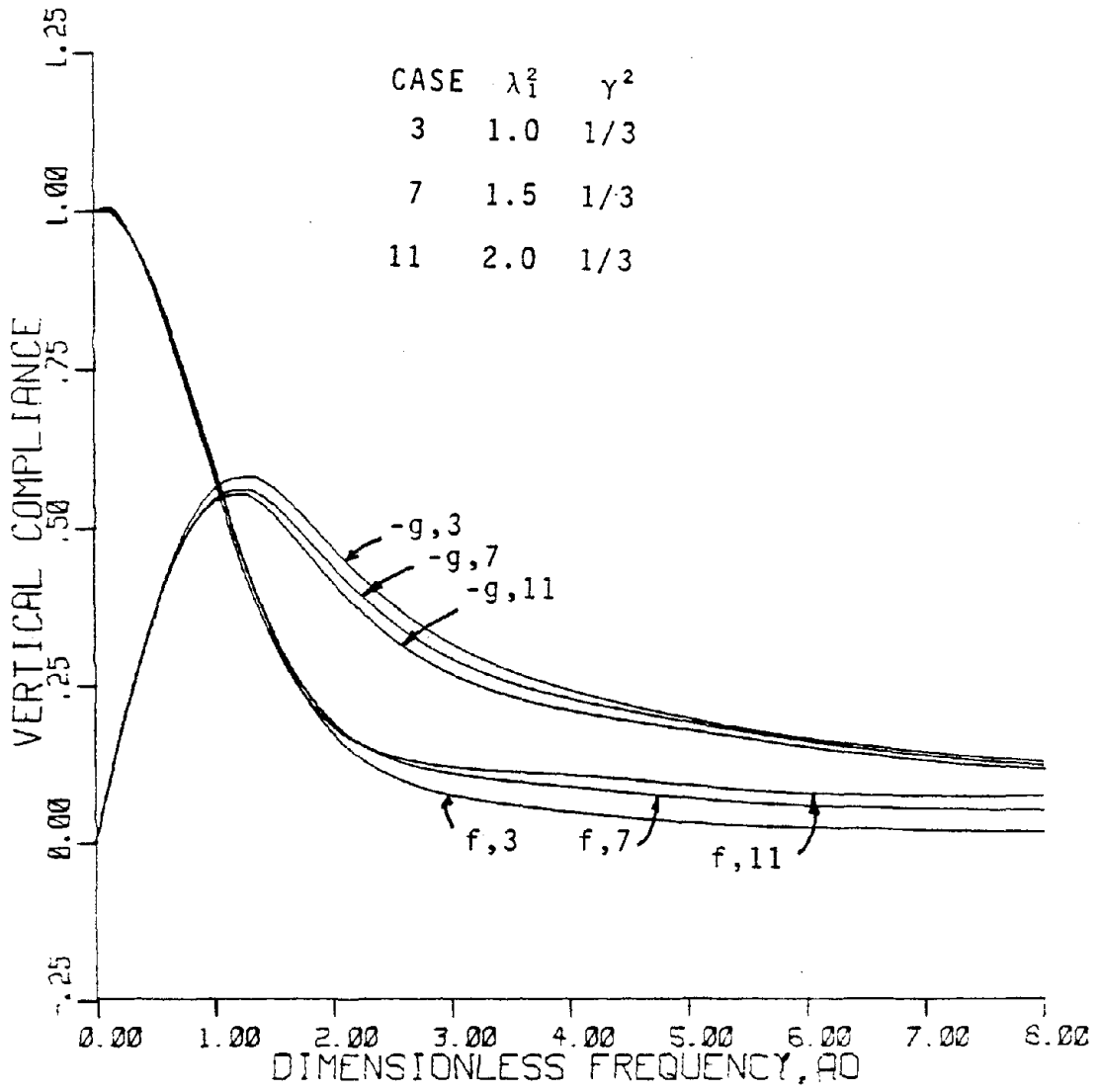


FIGURE 3.8

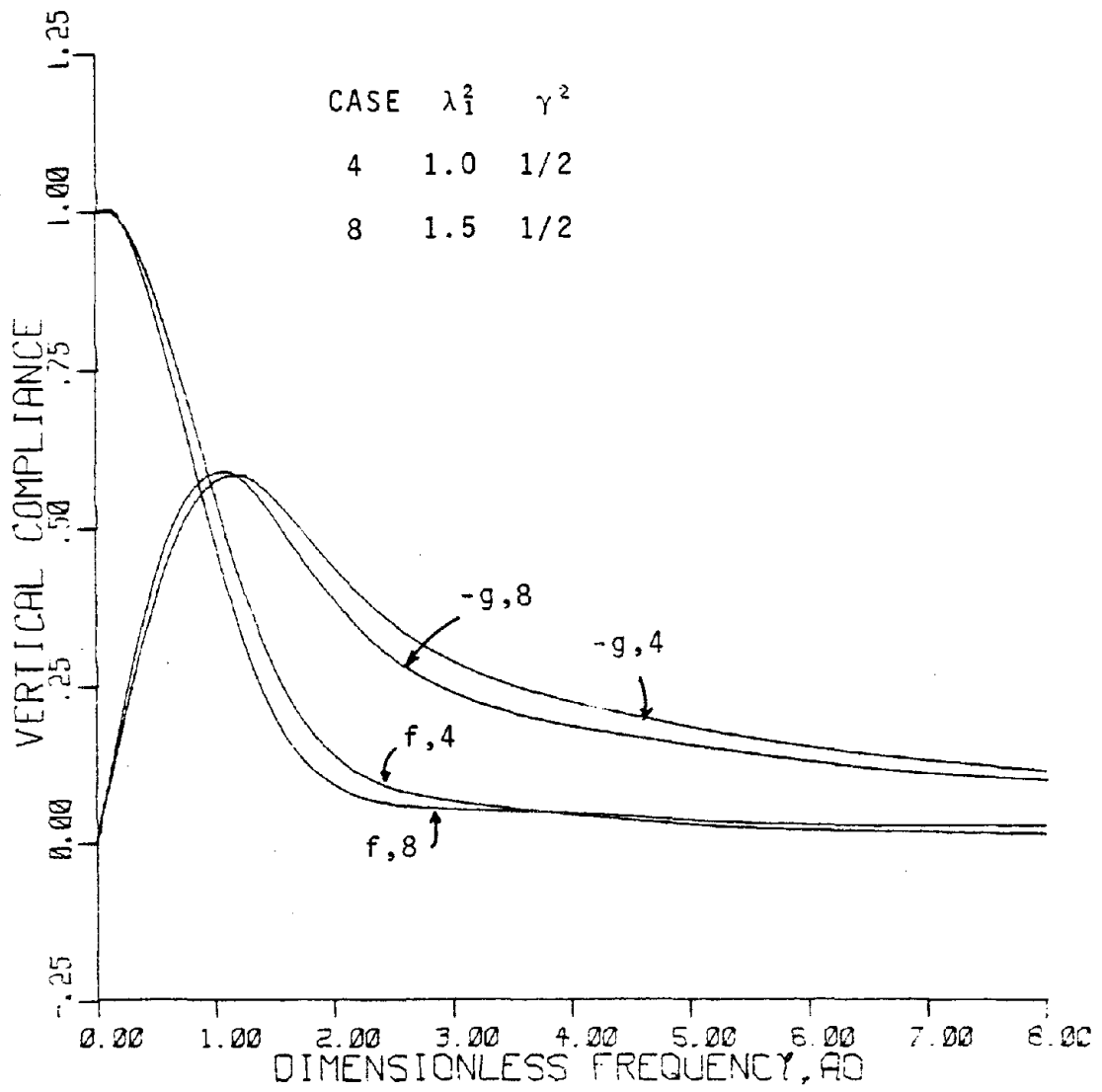


FIGURE 3.9

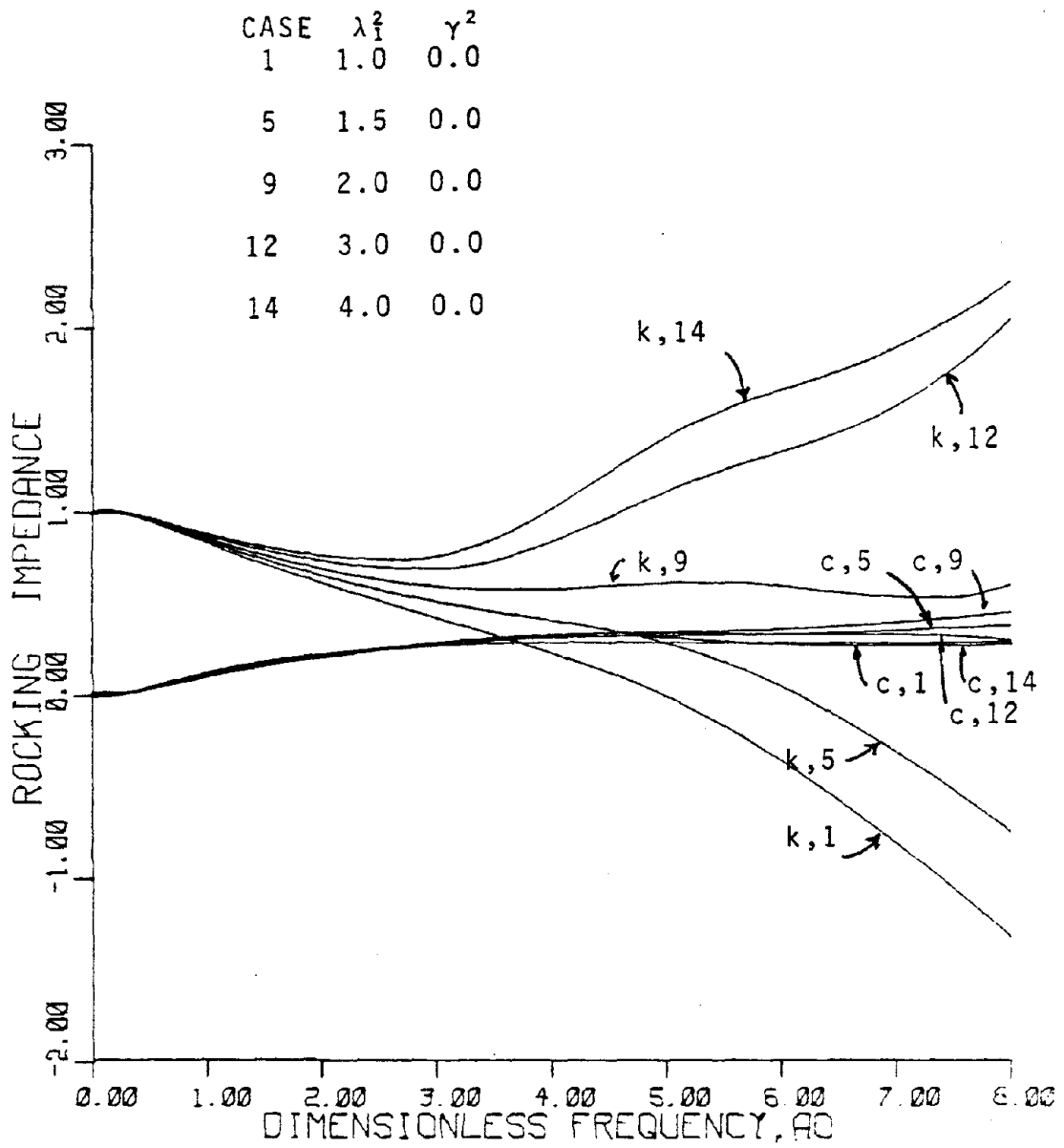


FIGURE 3.10

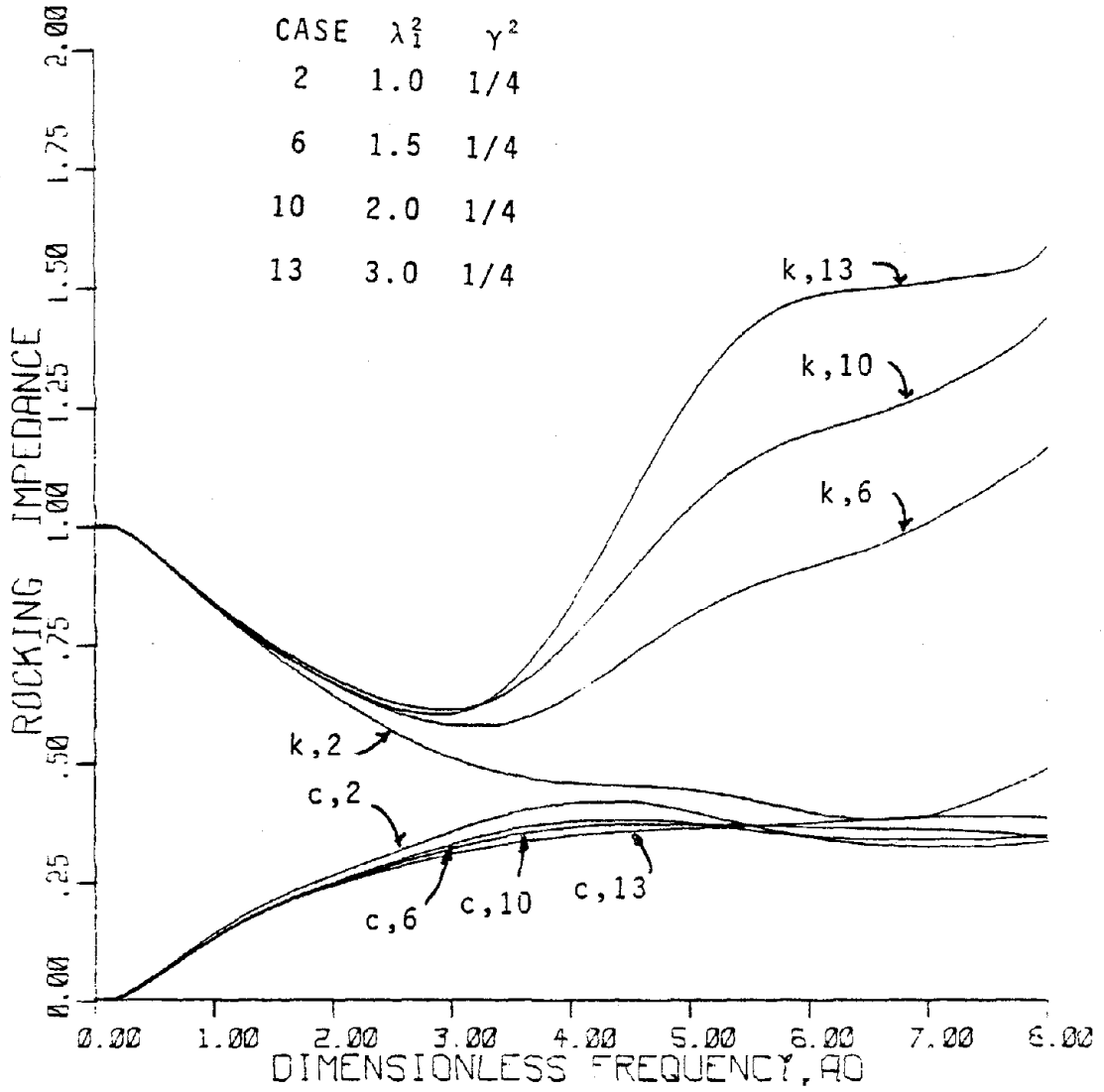


FIGURE 3.11

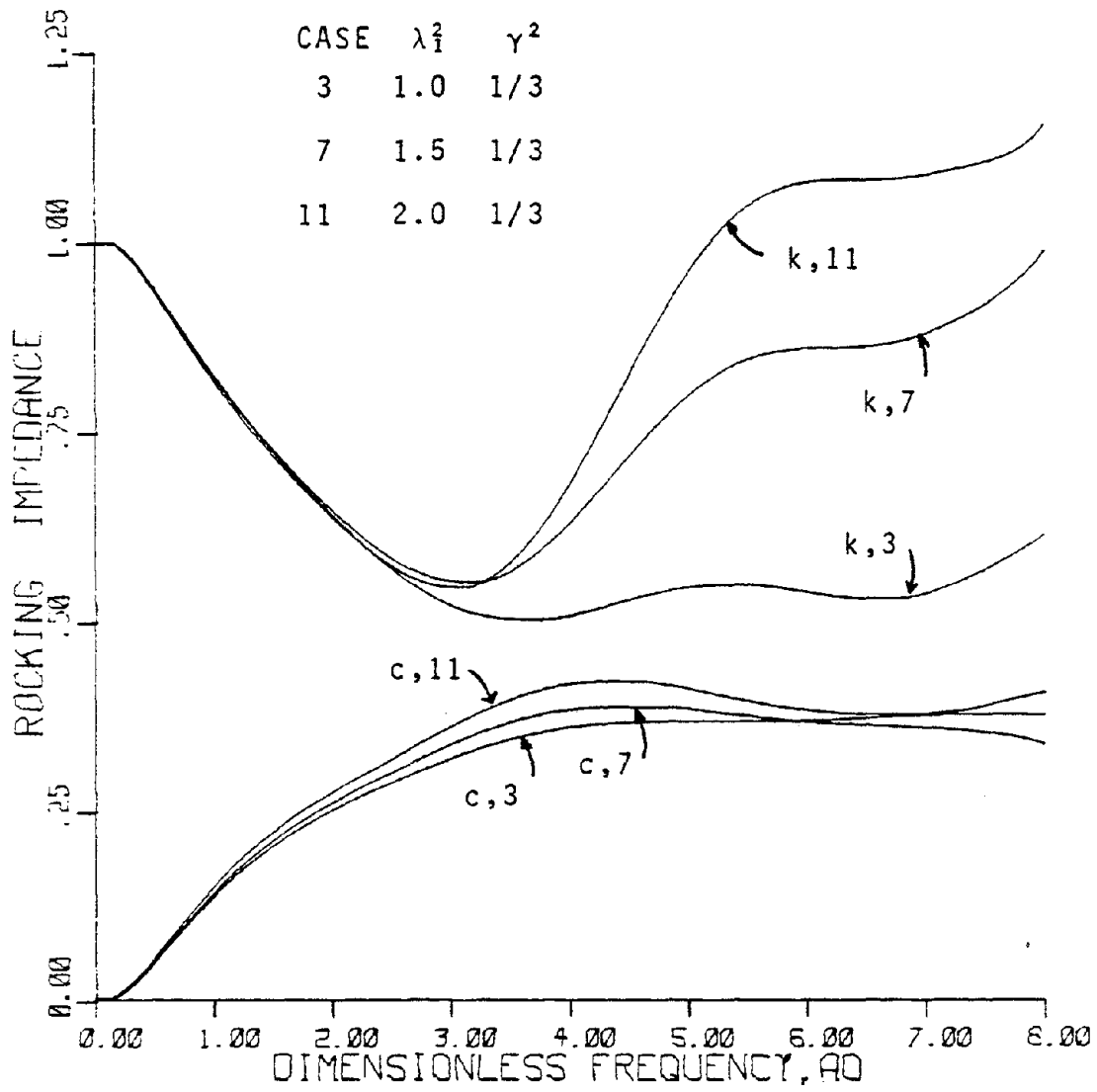


FIGURE 3.12

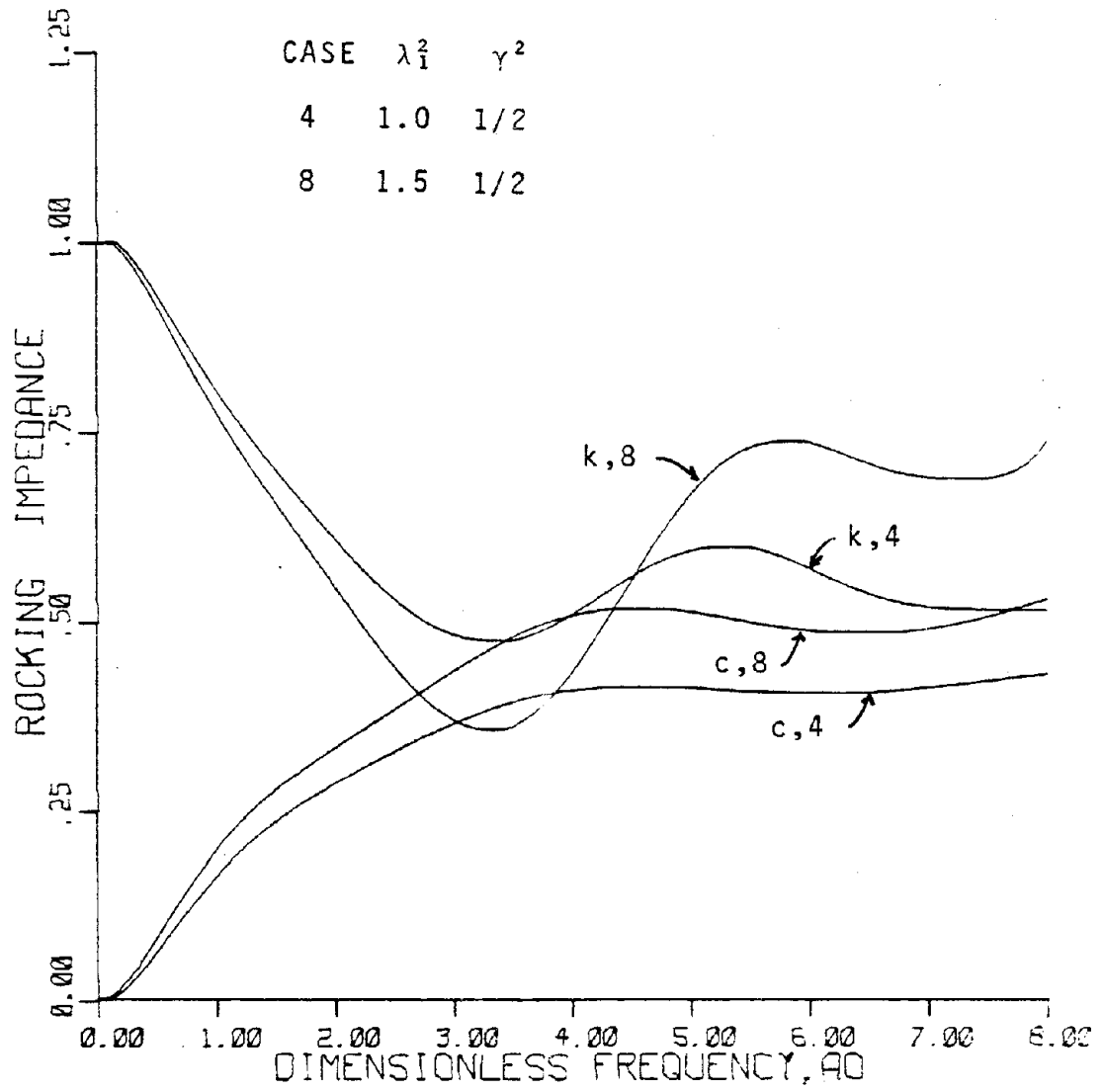


FIGURE 3.13

CASE	$\lambda_1^2$	$\gamma^2$
1	1.0	0.0
5	1.5	0.0
9	2.0	0.0
12	3.0	0.0
14	4.0	0.0

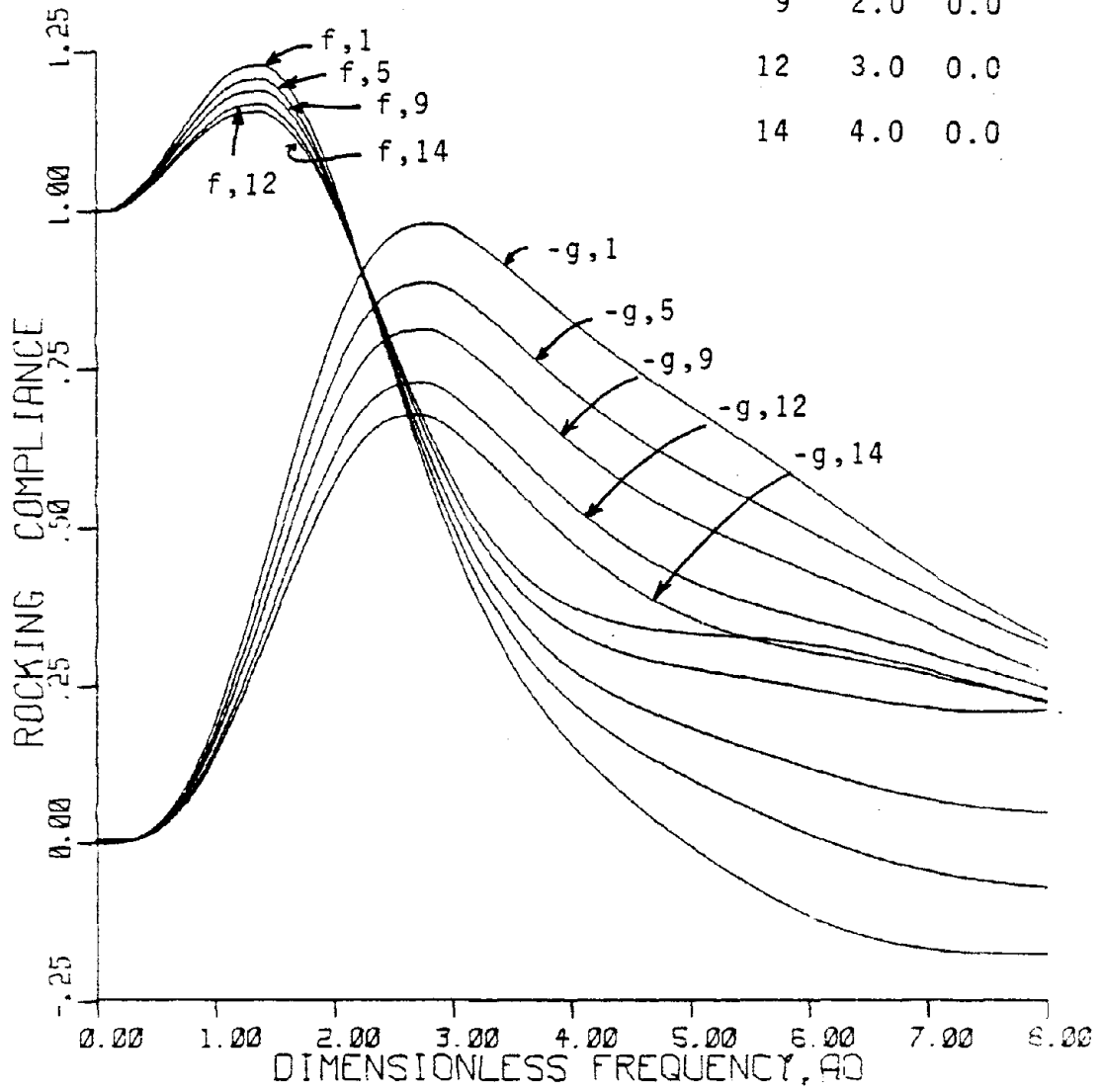


FIGURE 3.14

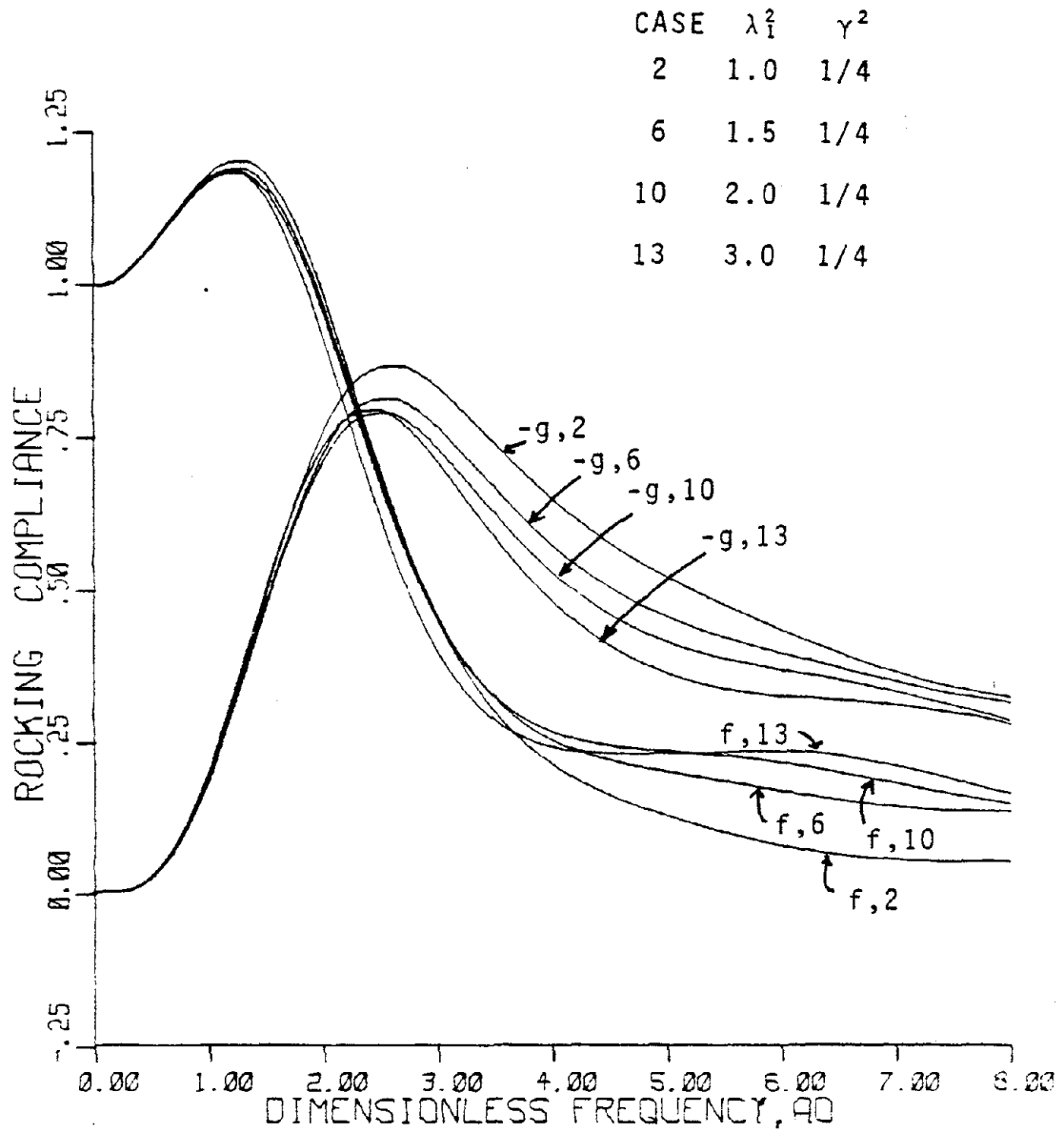


FIGURE 3.15



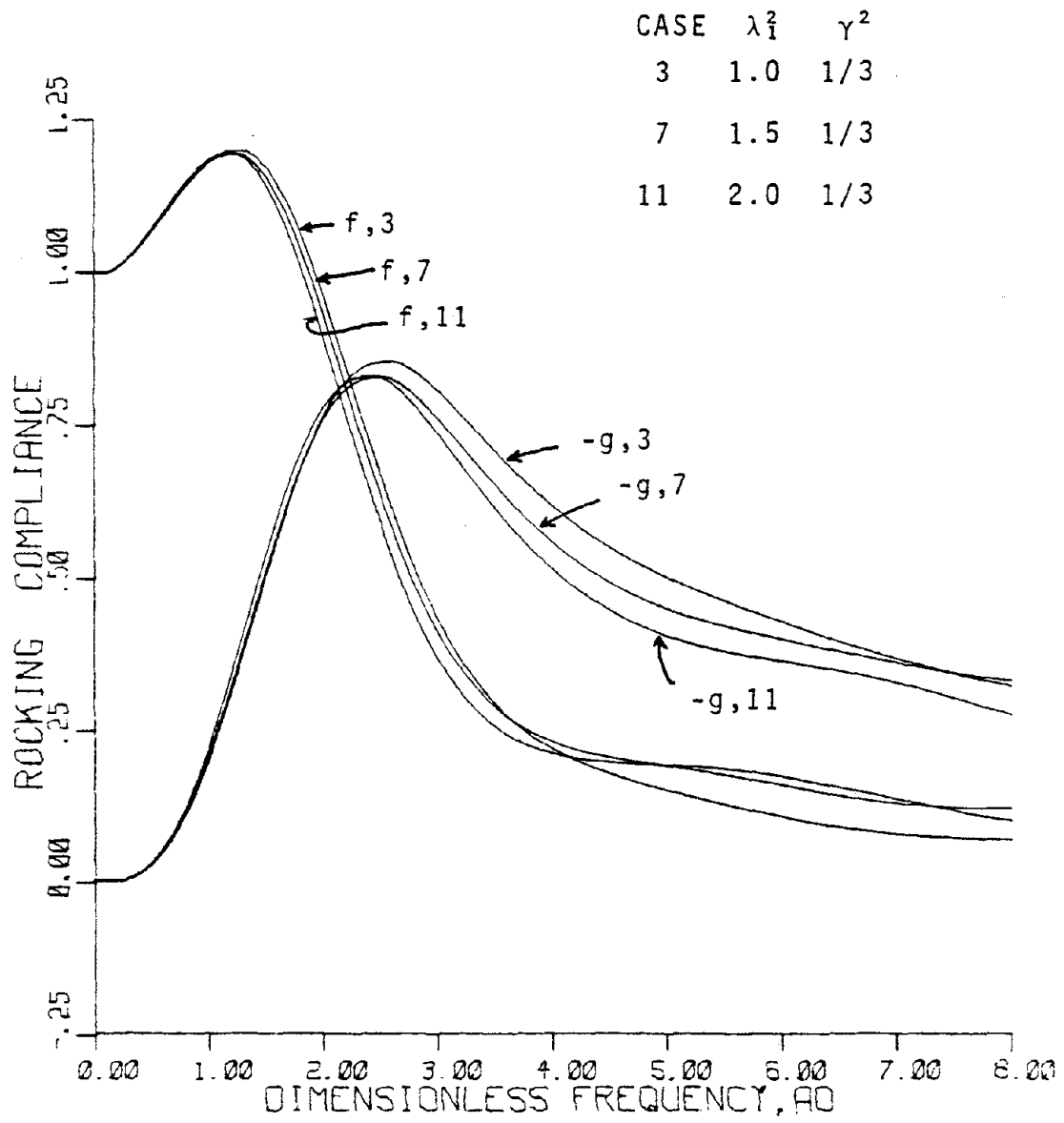


FIGURE 3.16

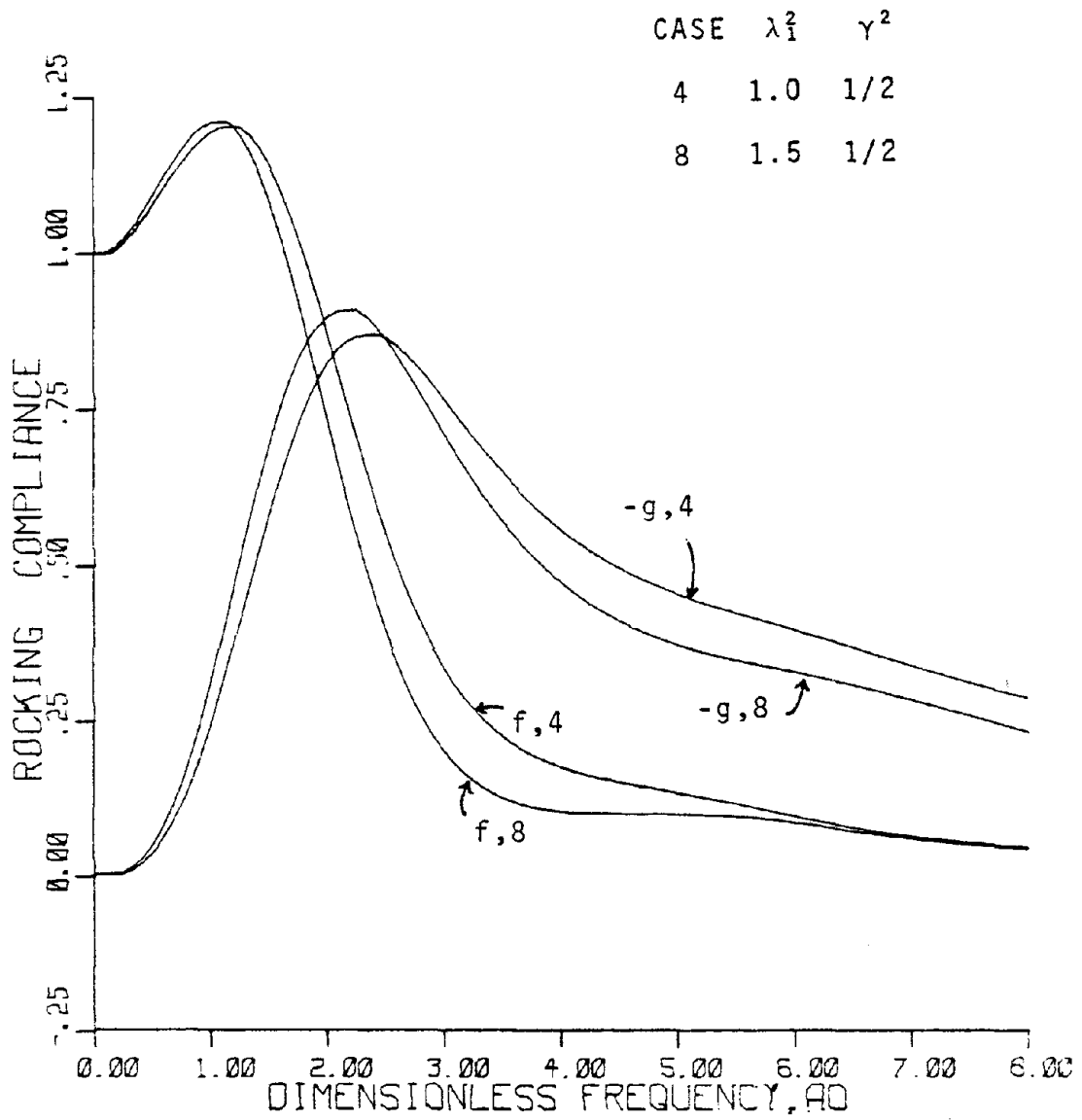


FIGURE 3.17

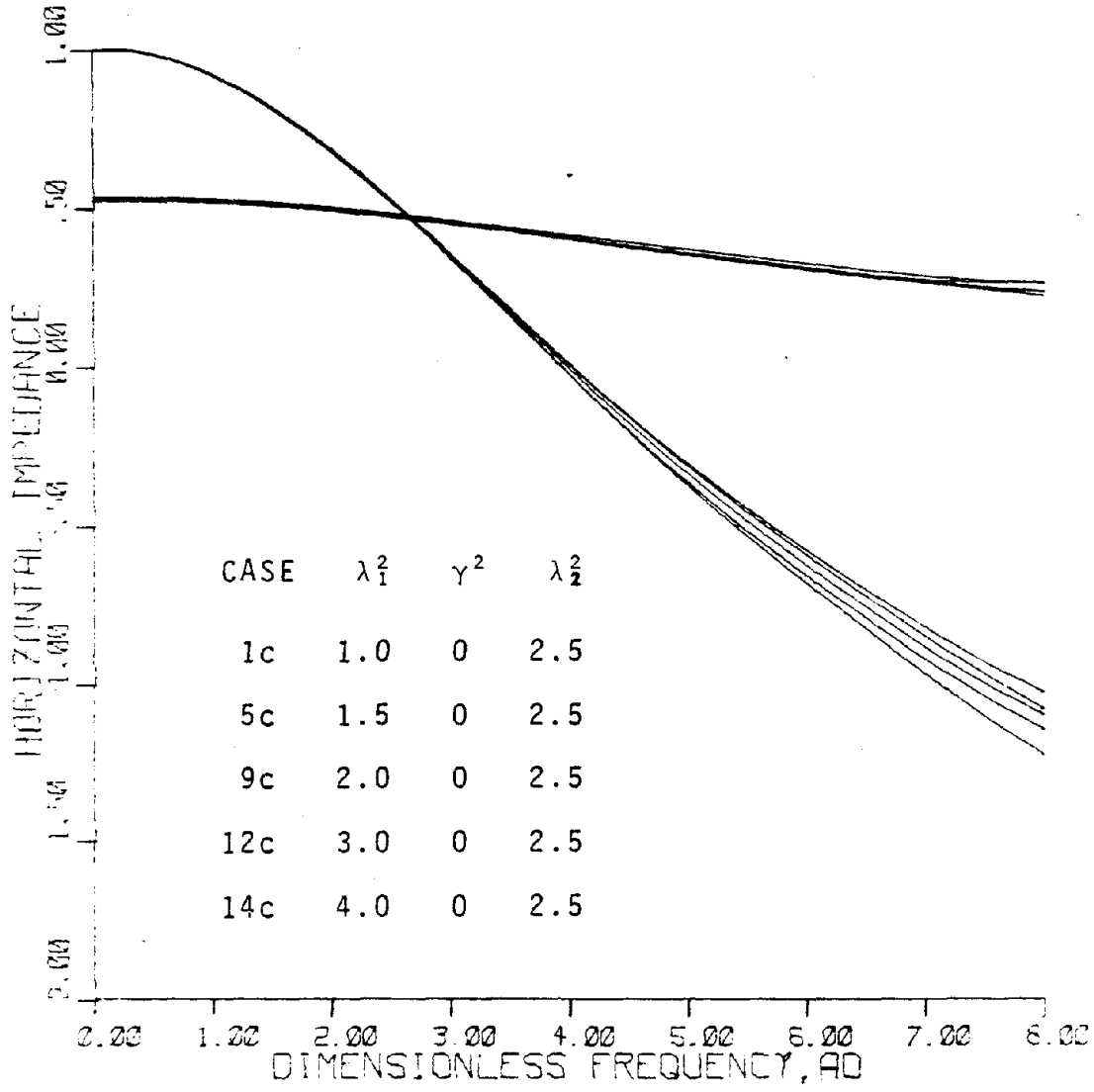


FIGURE 3.18

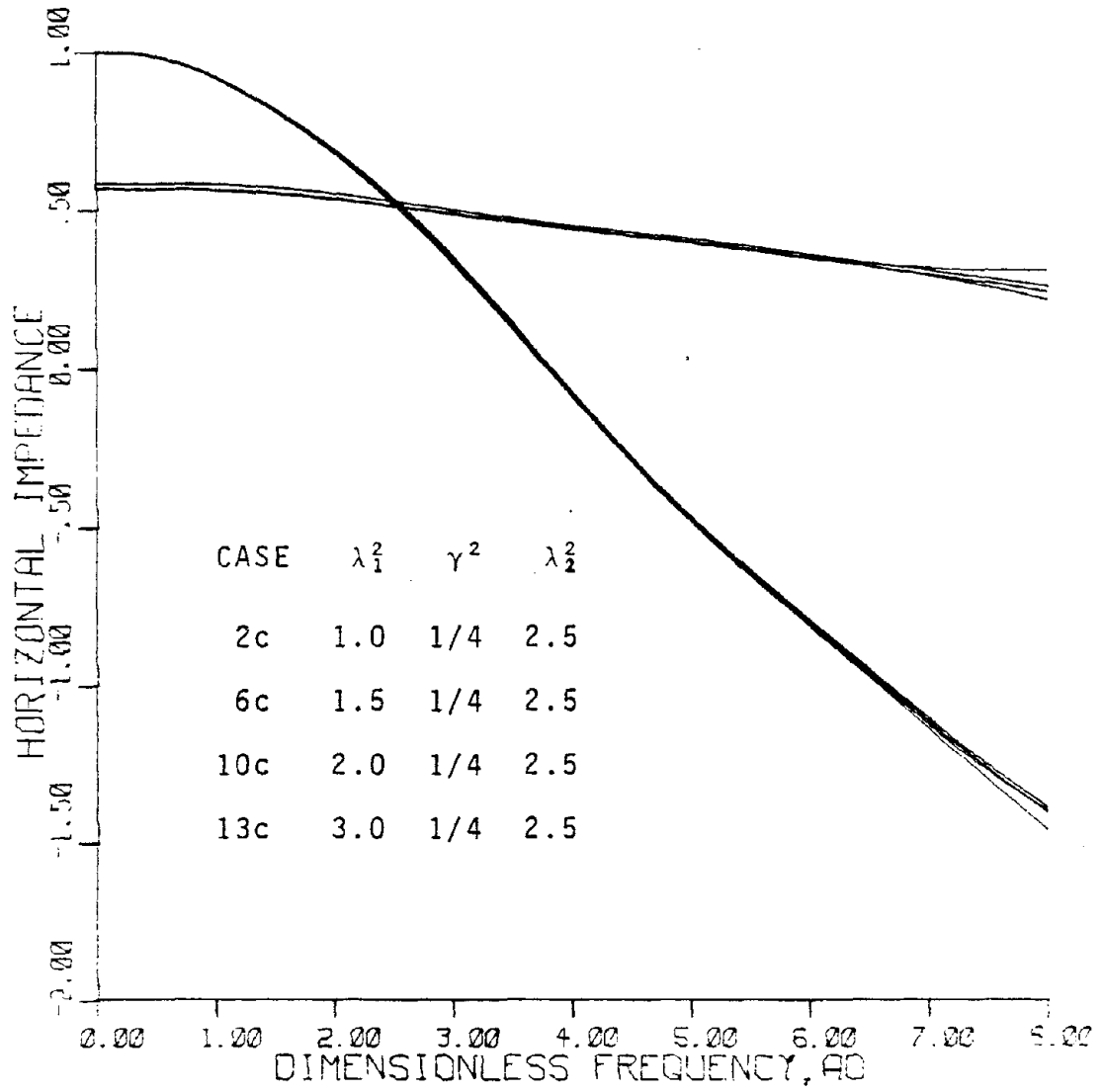


FIGURE 3.19

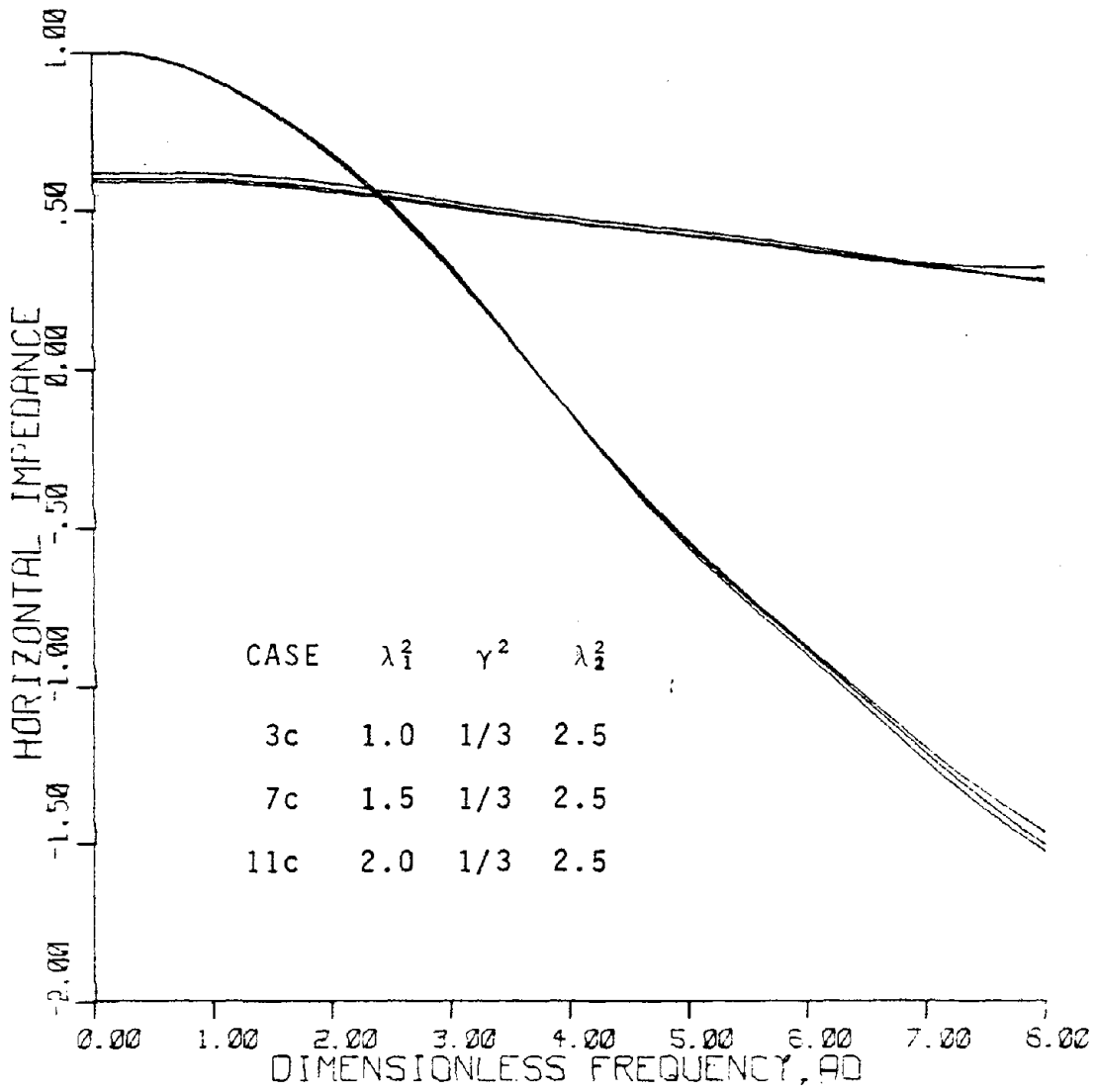


FIGURE 3.20

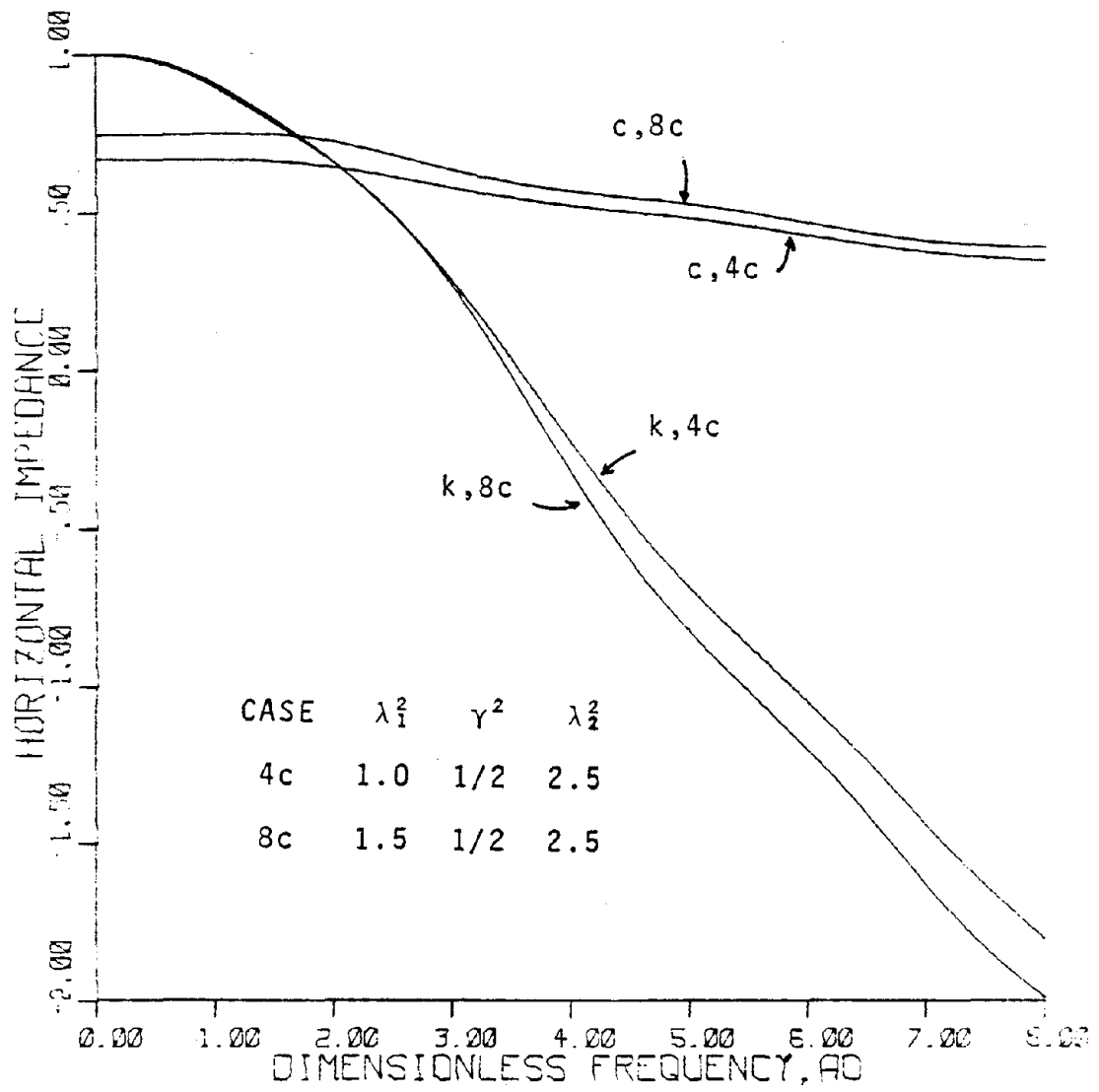


FIGURE 3.21

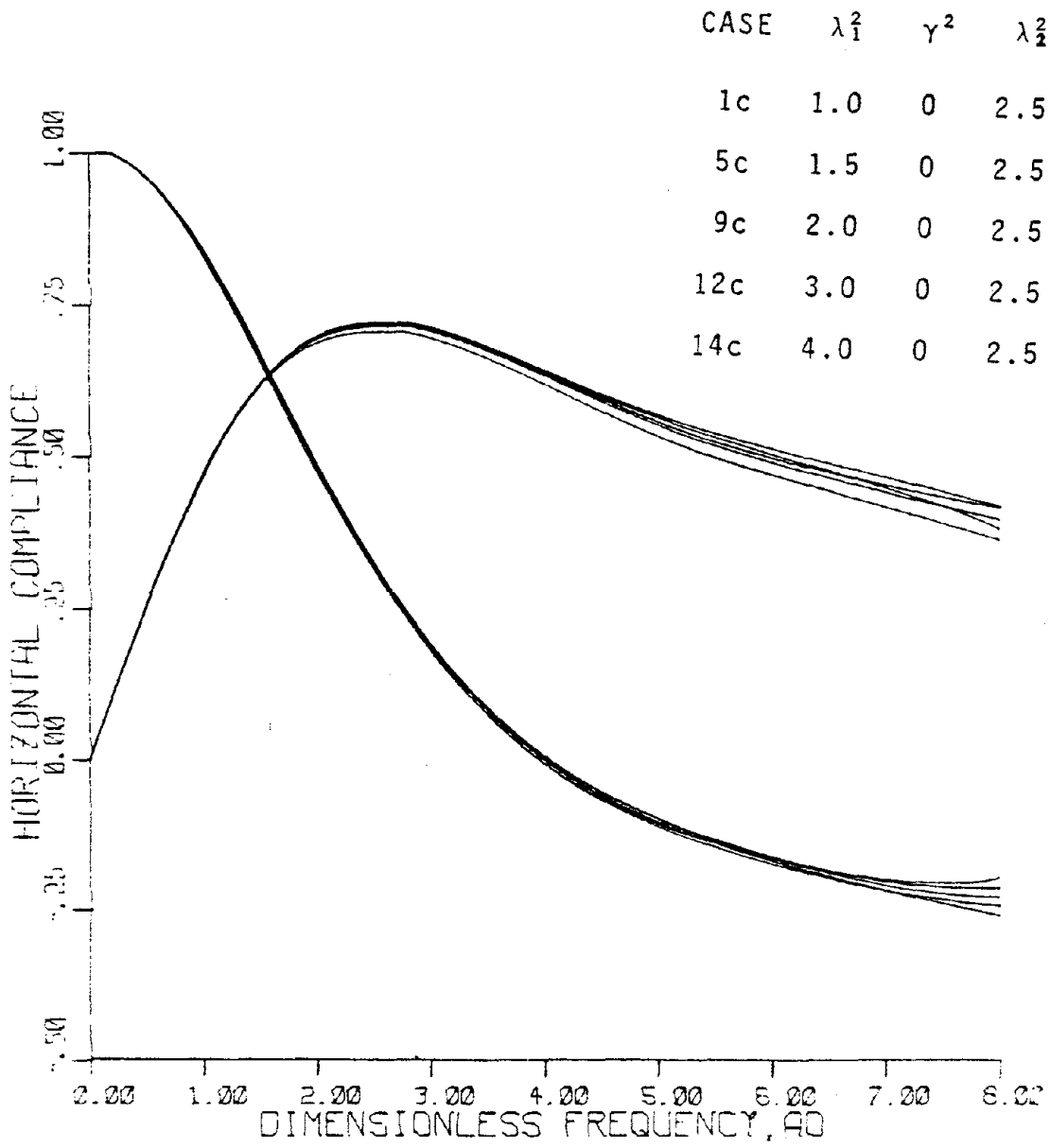


FIGURE 3.22

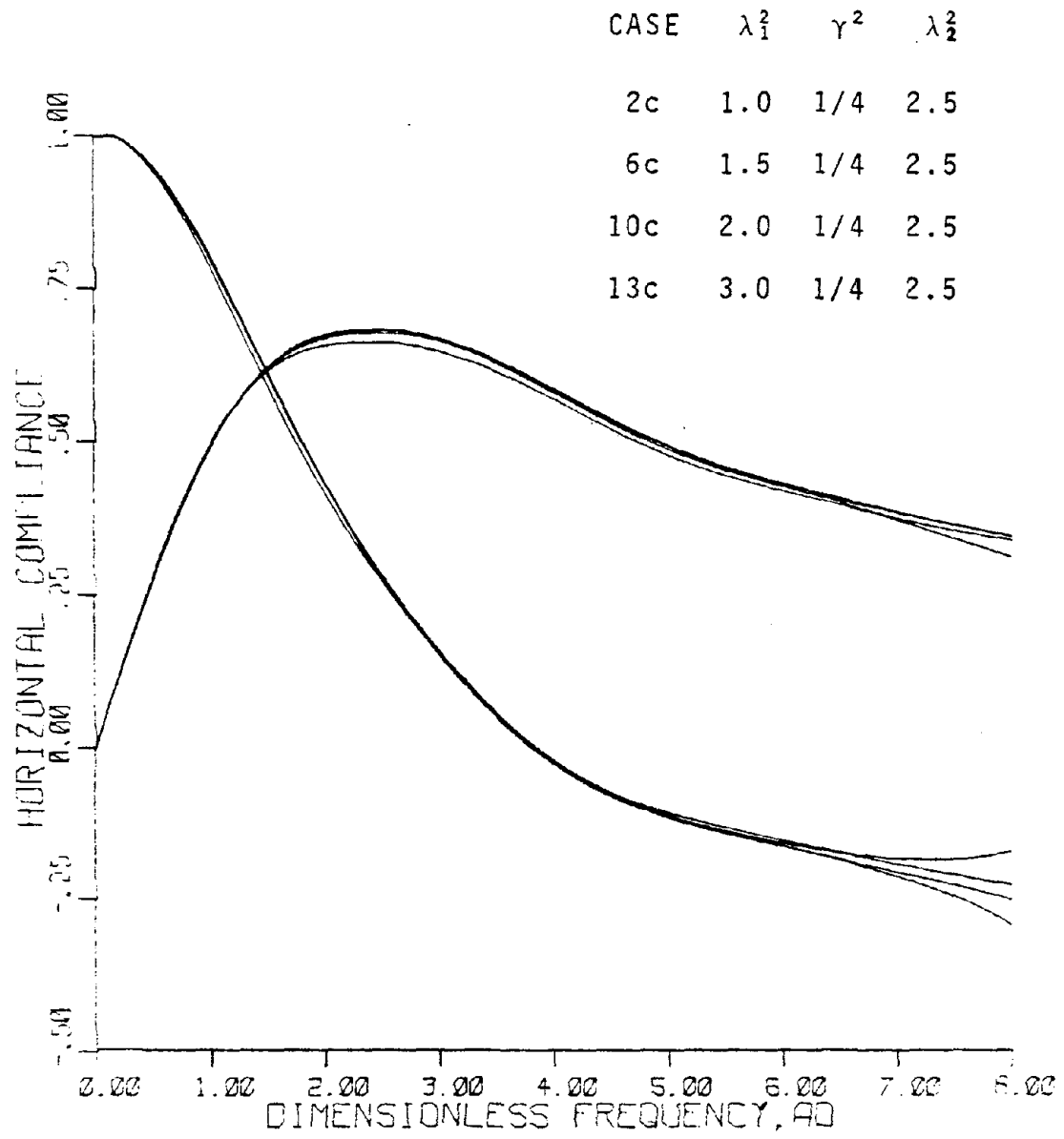


FIGURE 3.23



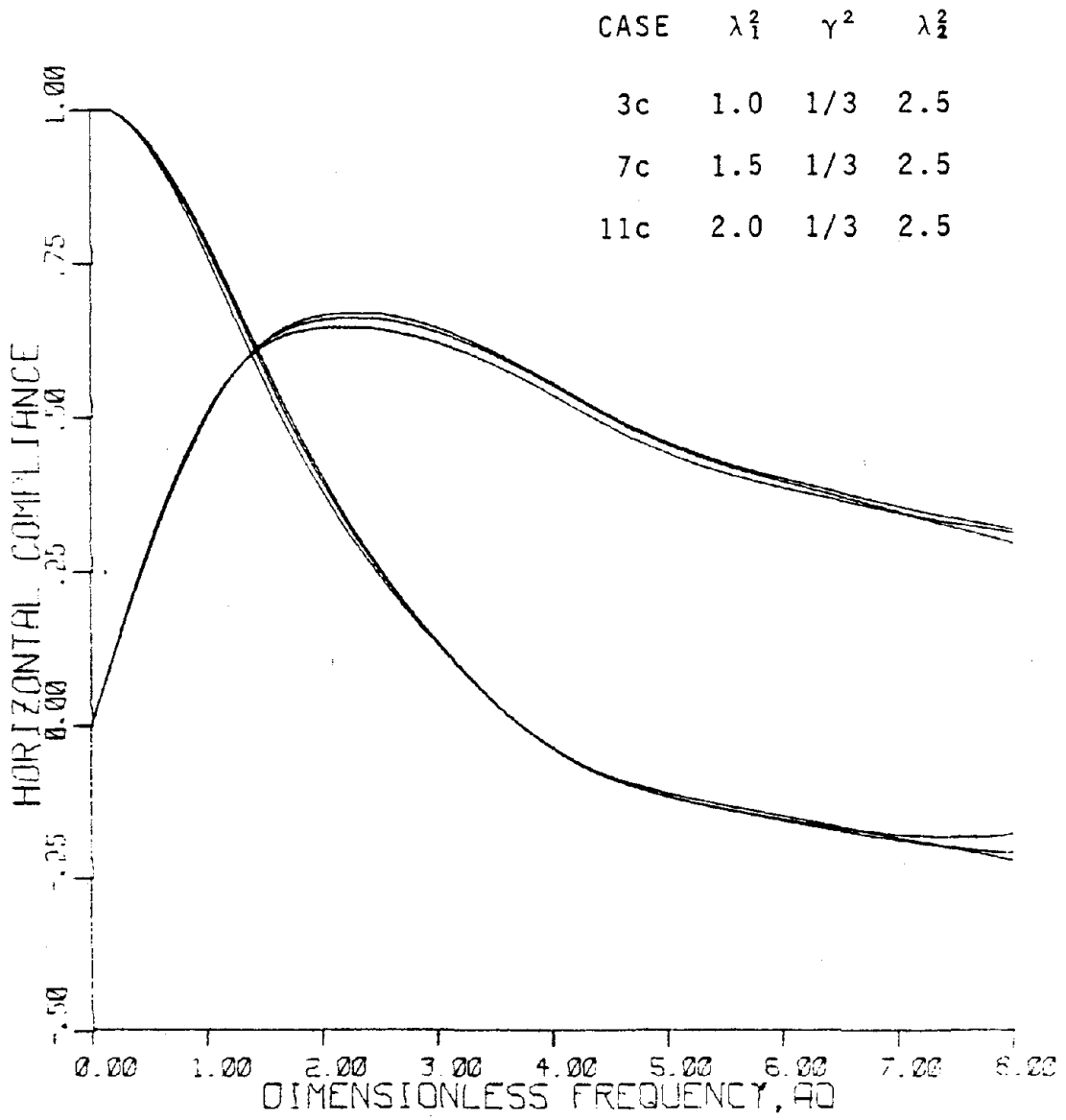


FIGURE 3.24

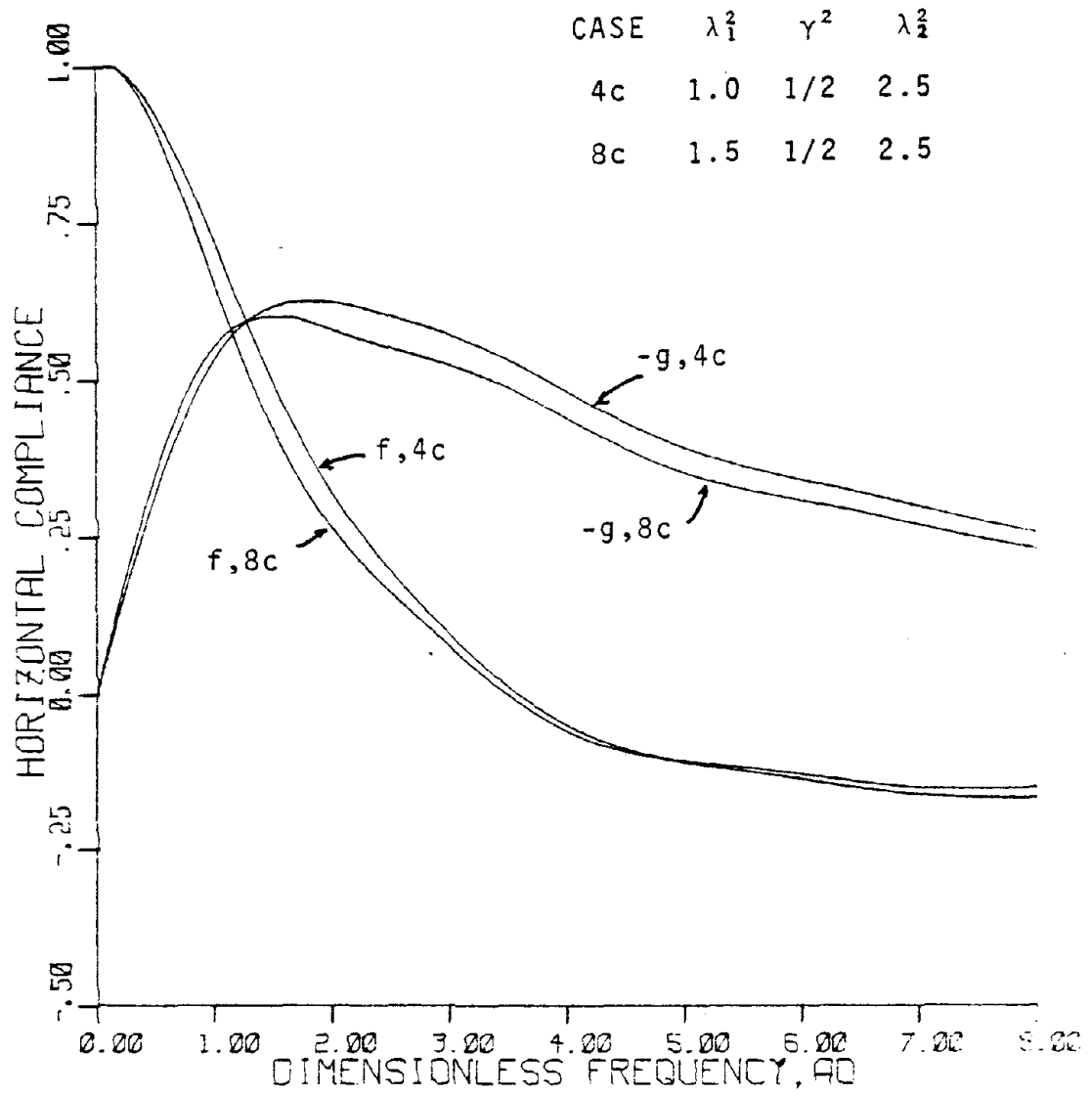


FIGURE 3.25

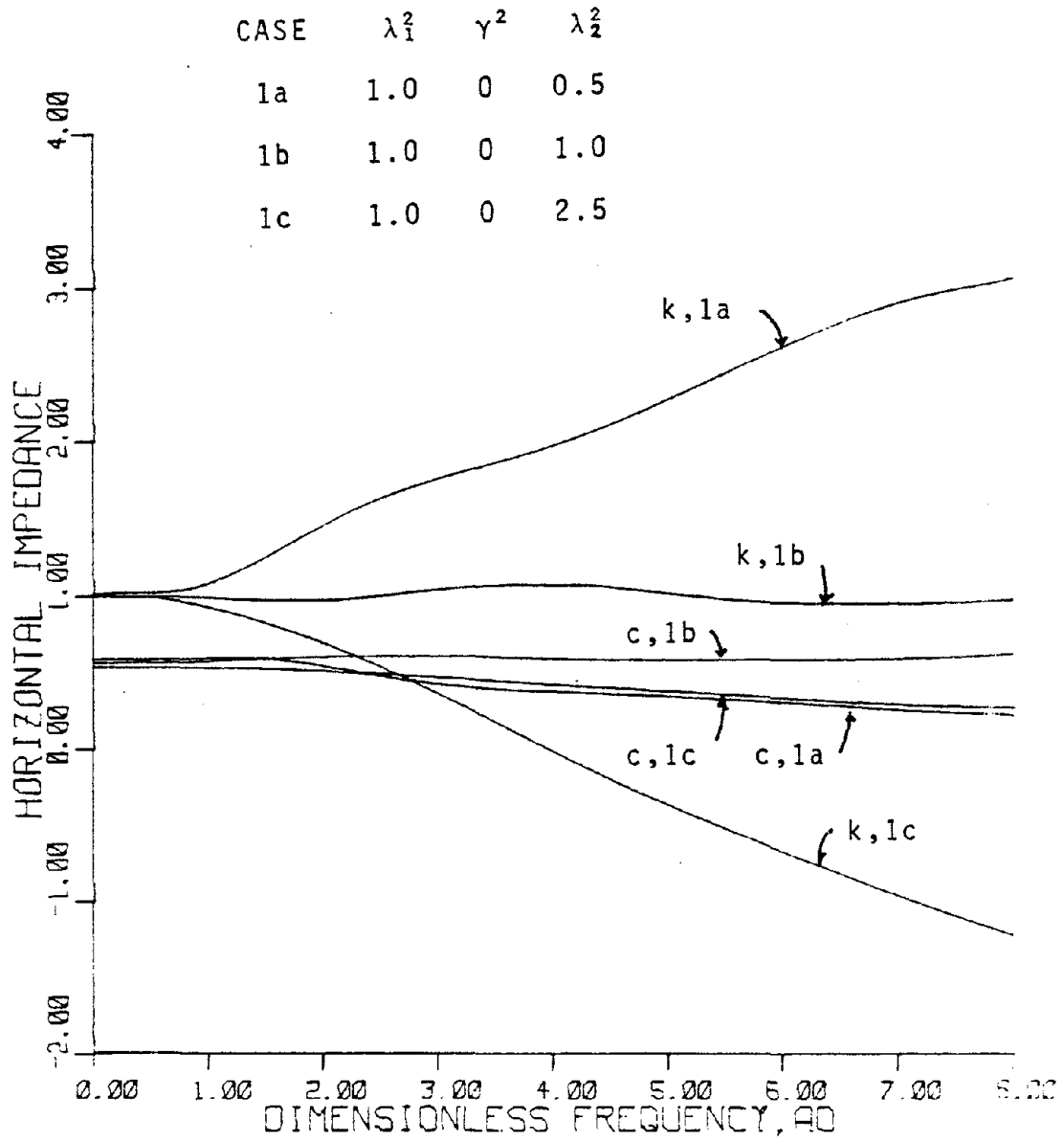


FIGURE 3.26

CASE	$\lambda_1^2$	$\gamma^2$	$\lambda_2^2$
2a	1.0	1/4	0.5
2b	1.0	1/4	1.0
2c	1.0	1/4	2.5

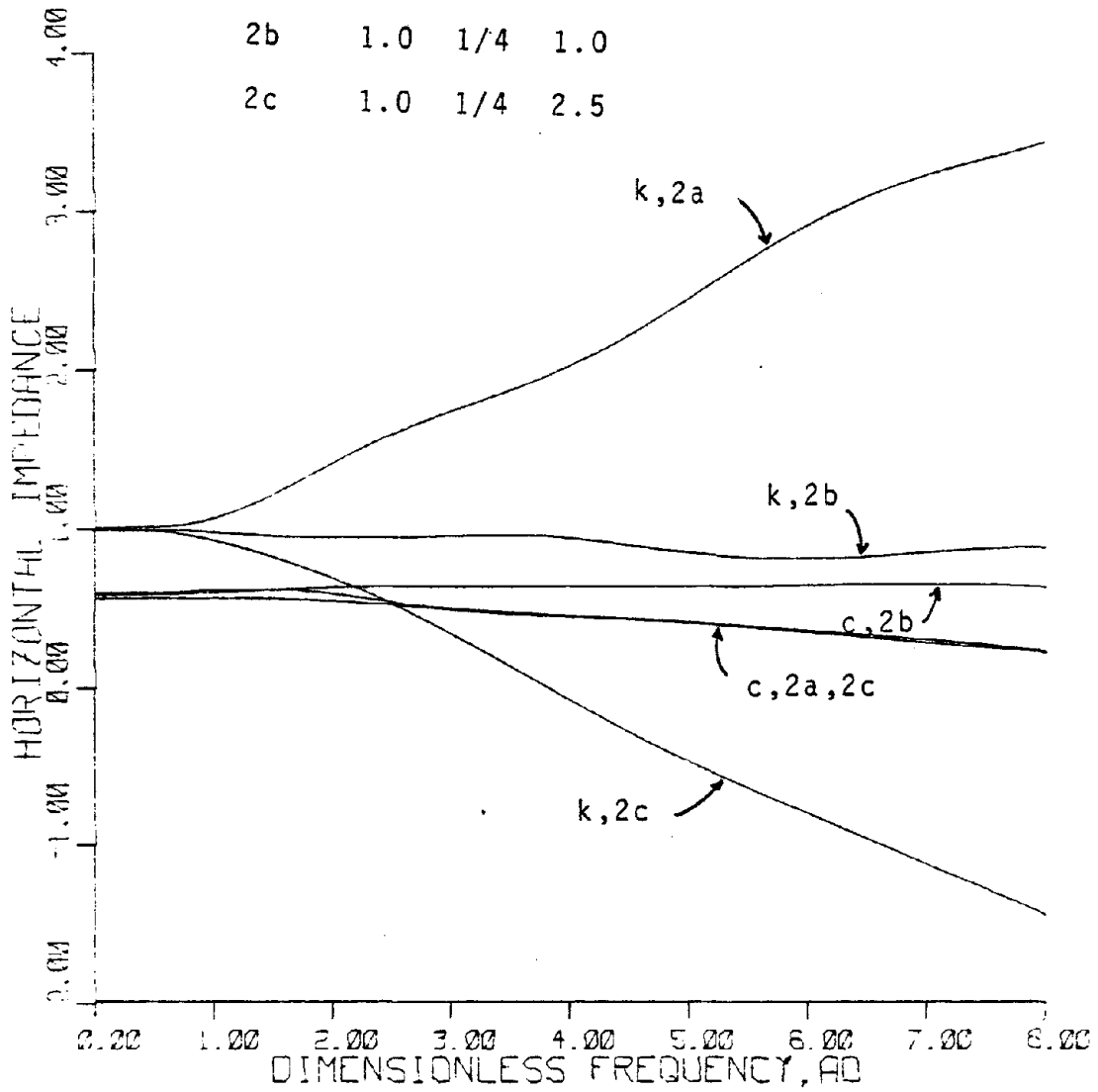


FIGURE 3.27

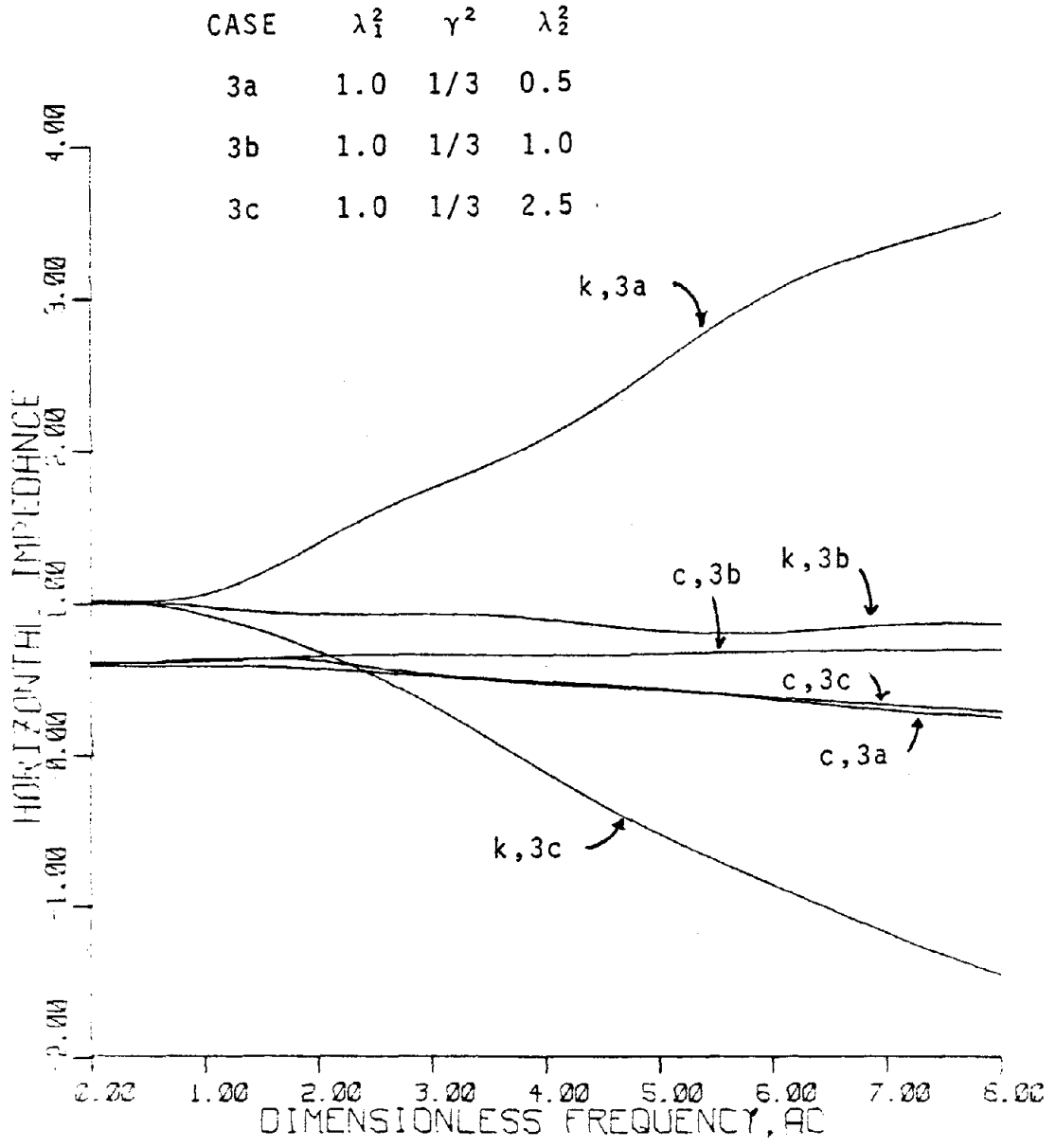


FIGURE 3.28

CASE	$\lambda_1^2$	$\gamma^2$	$\lambda_2^2$
4a	1.0	1/2	0.5
4b	1.0	1/2	1.0
4c	1.0	1/2	2.5

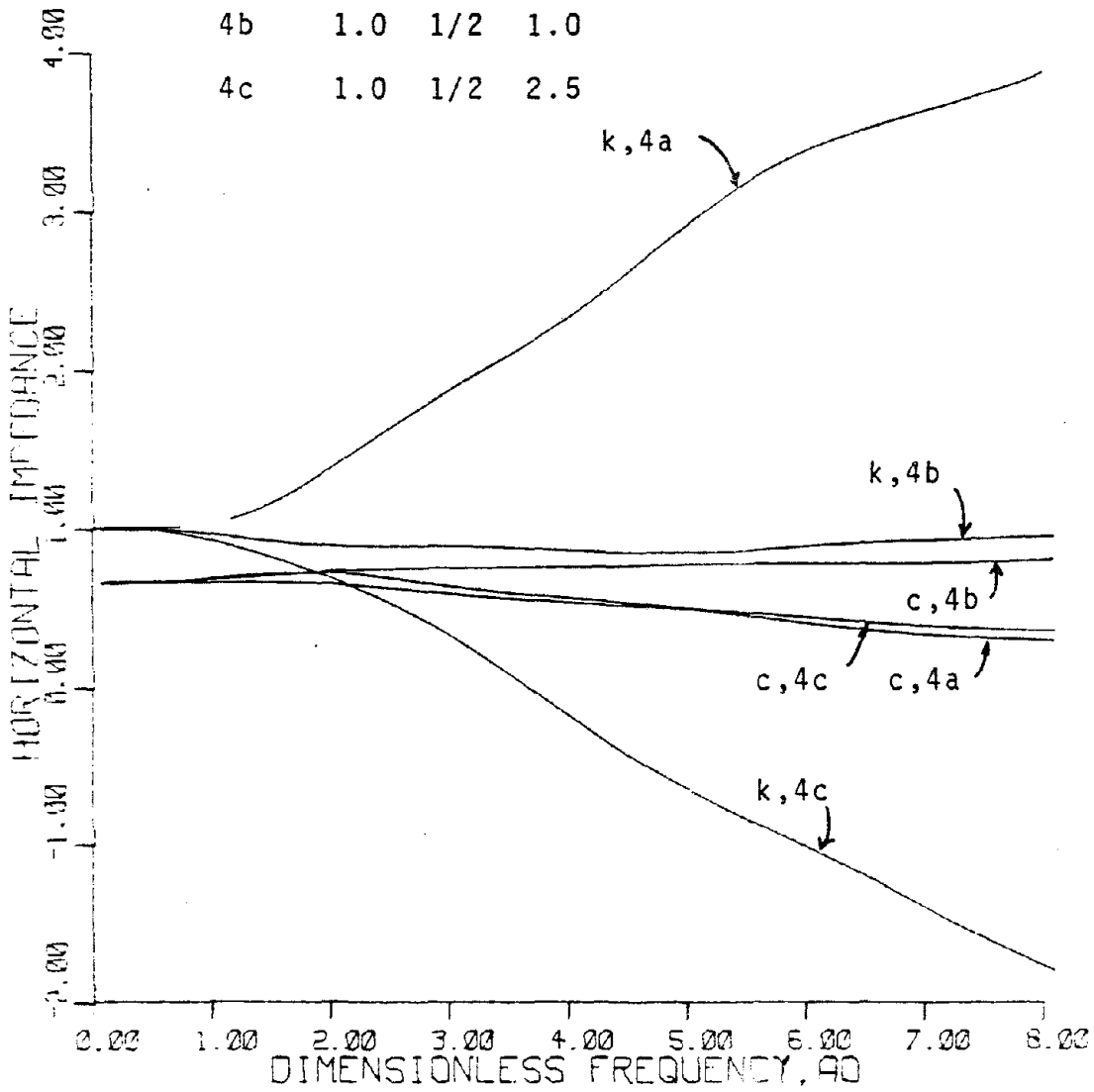


FIGURE 3.29

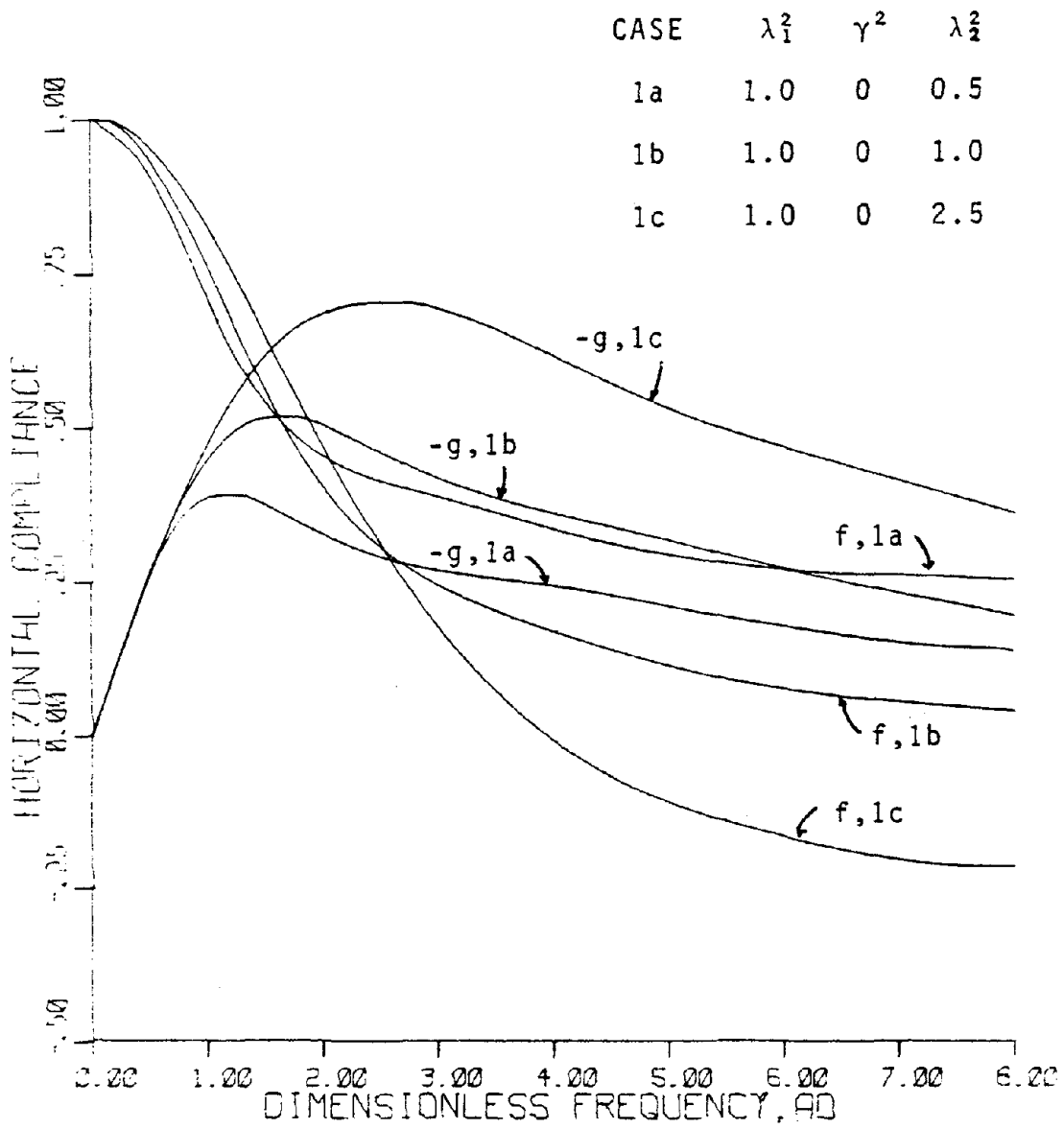


FIGURE 3.30

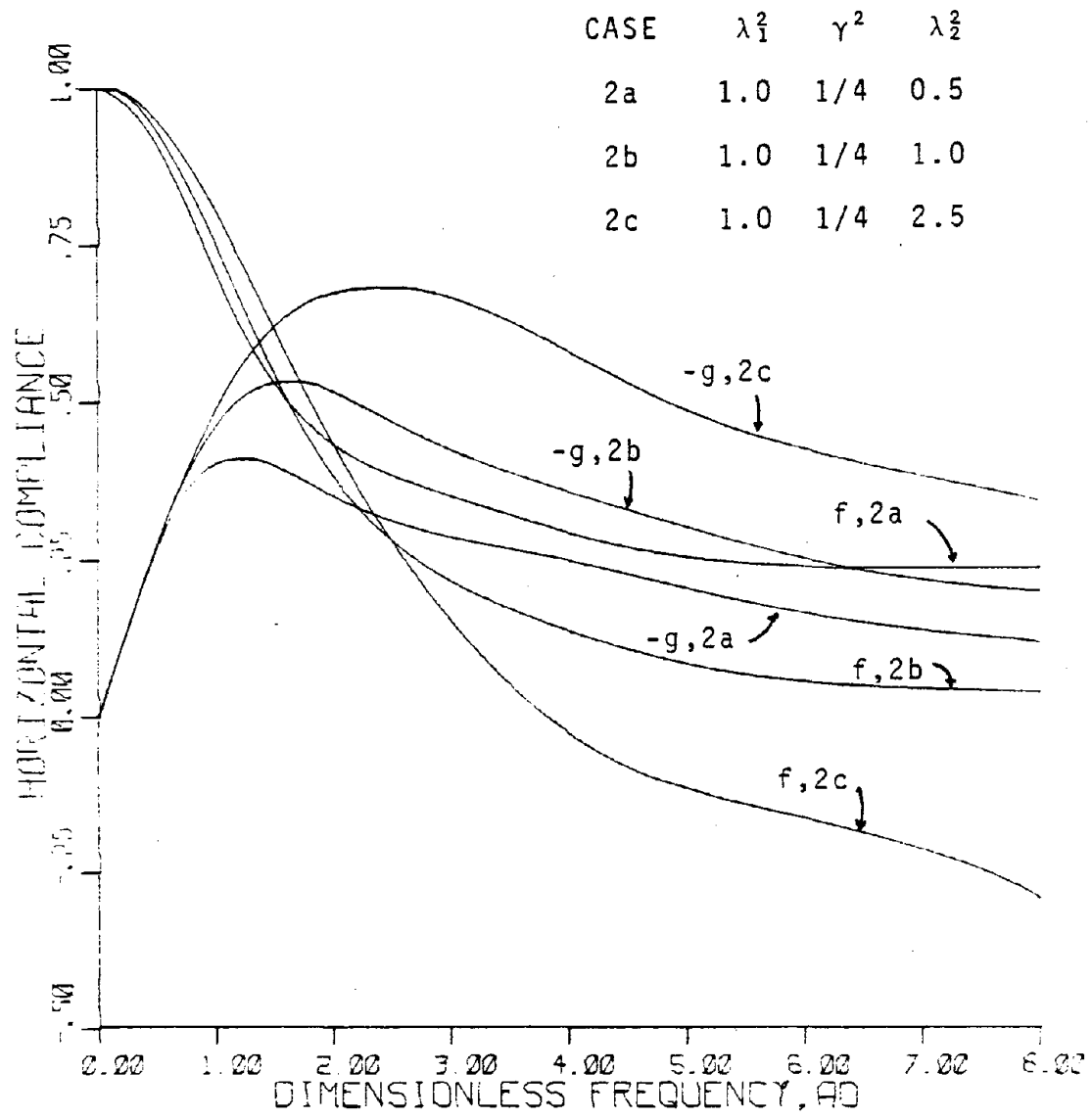


FIGURE 3.31



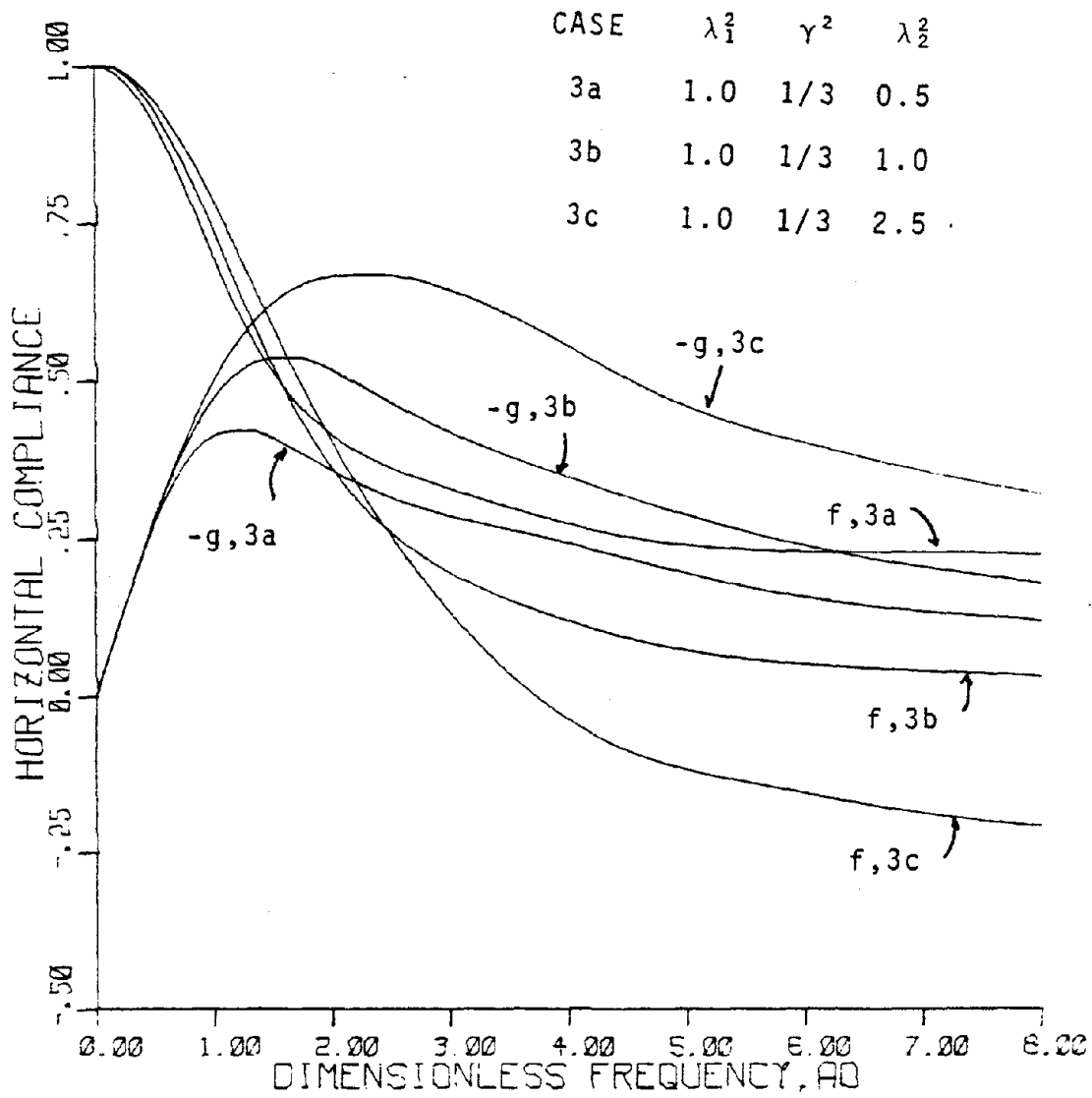


FIGURE 3.32

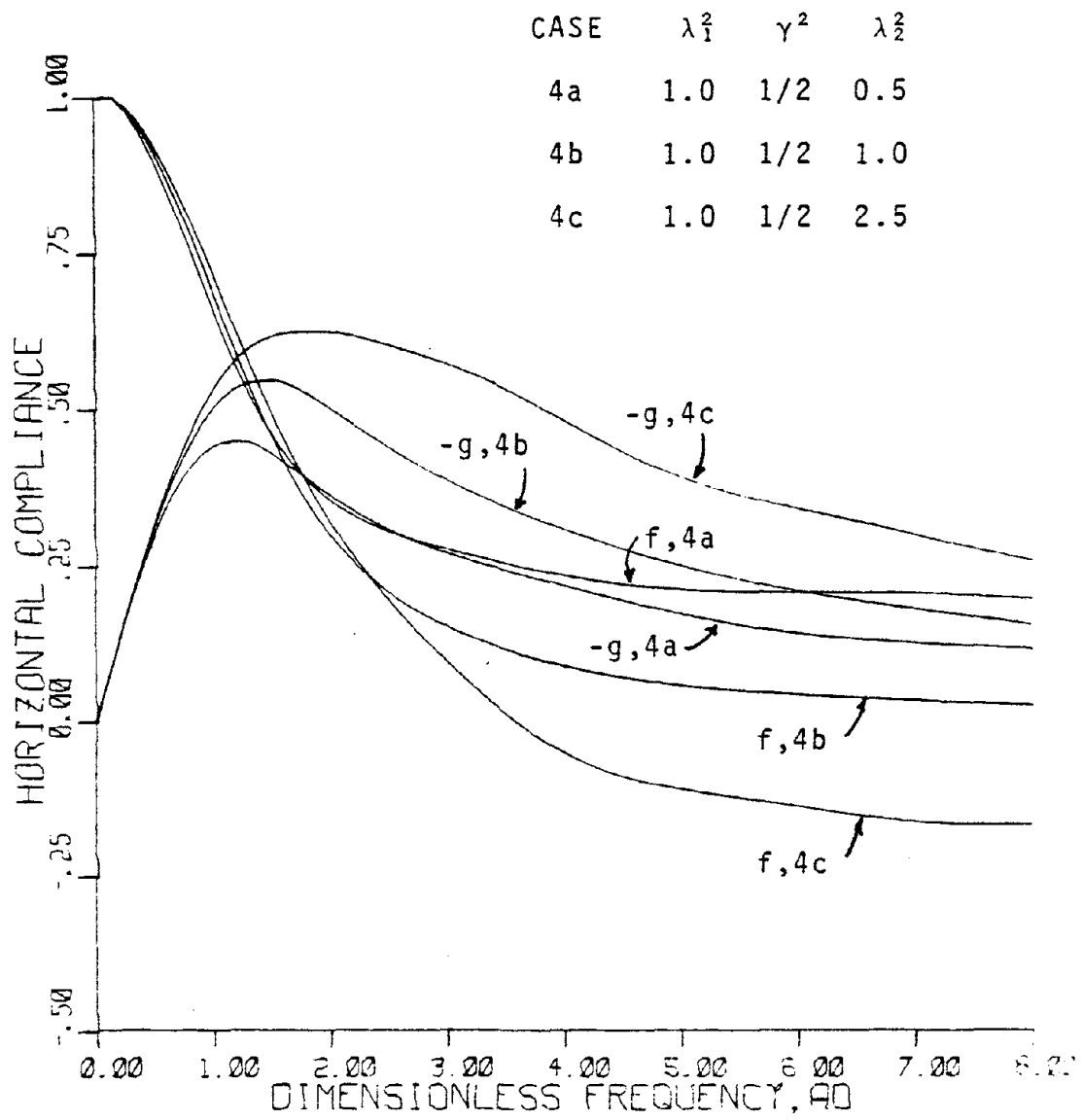
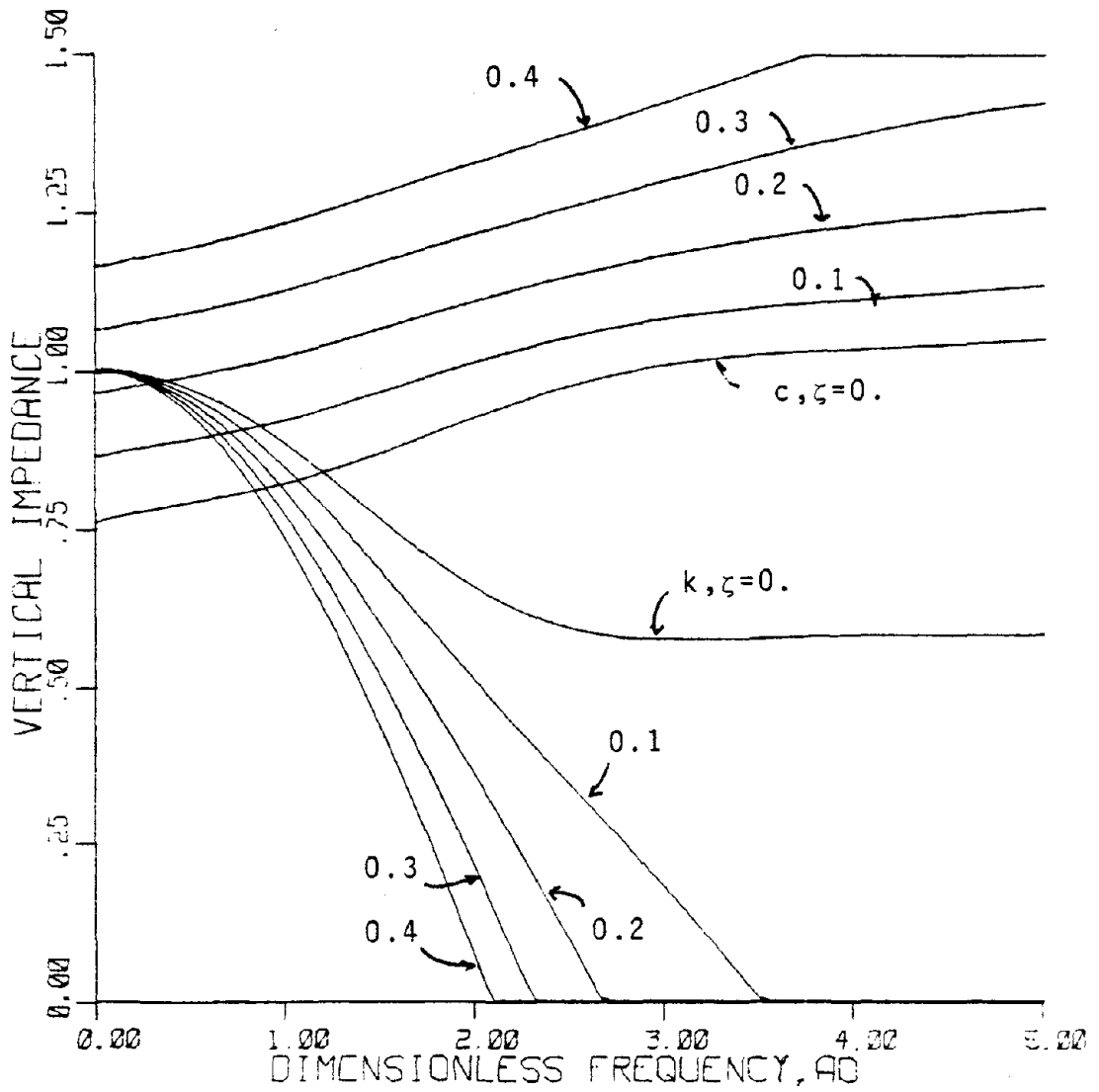


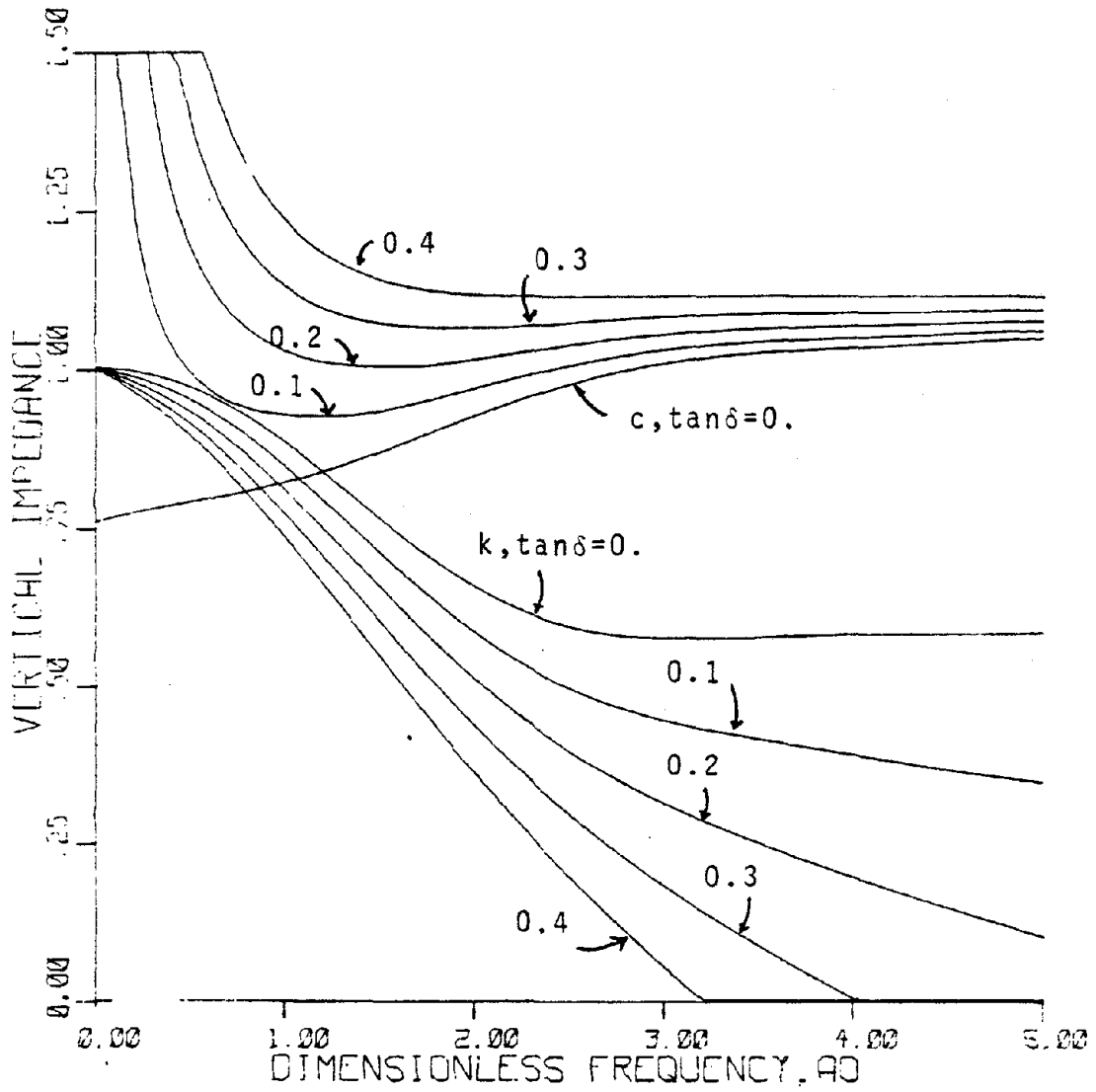
FIGURE 3.33



EFFECT OF  $\zeta$  ON VERTICAL IMPEDANCE

ISOTROPIC  $\lambda_1^2=1, \gamma^2=1/4$

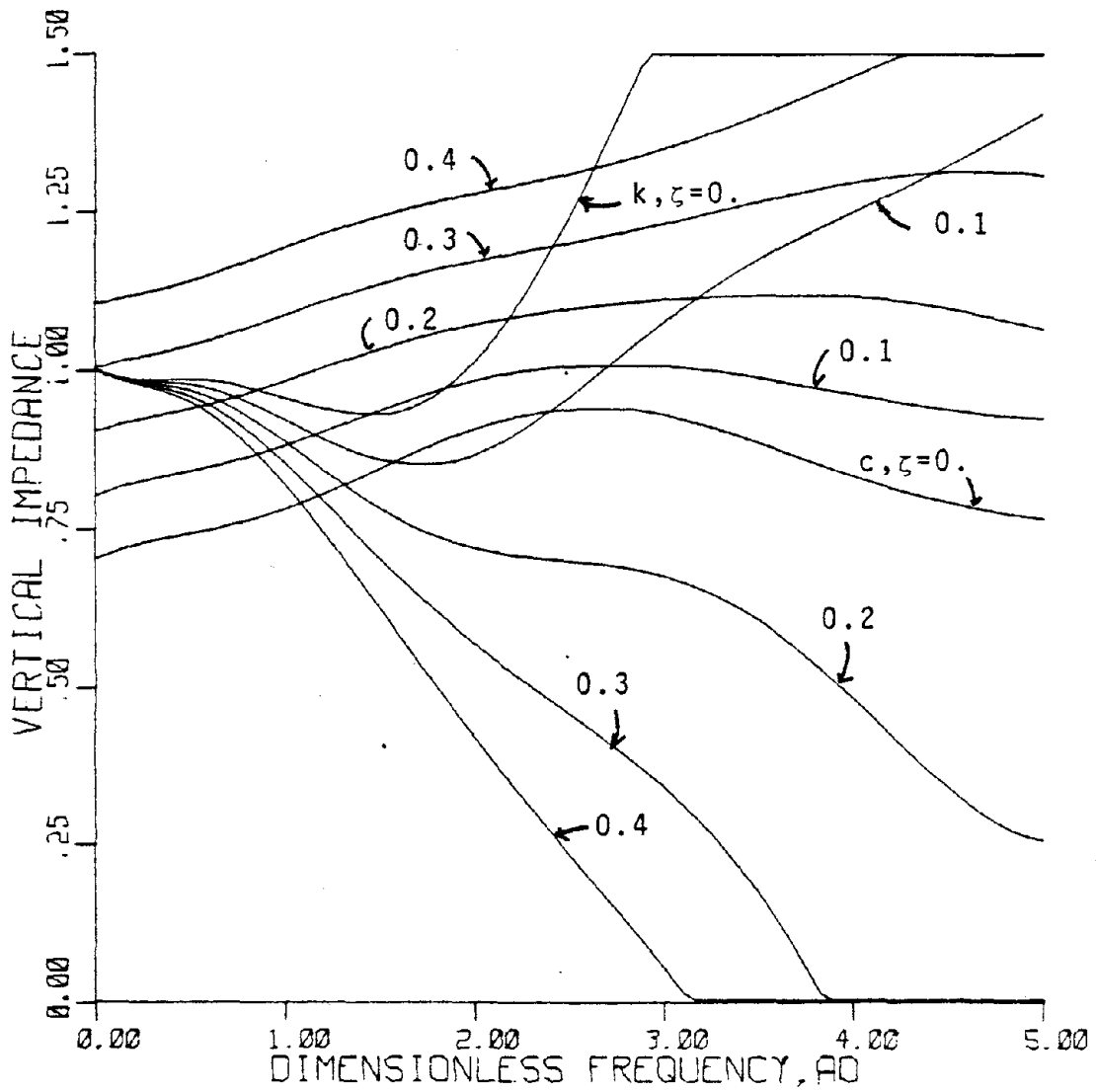
FIGURE 4.1



EFFECT OF TAN  $\delta$  ON VERTICAL IMPEDANCE

ISOTROPIC  $\lambda_1^2=1, \gamma^2=1/4$

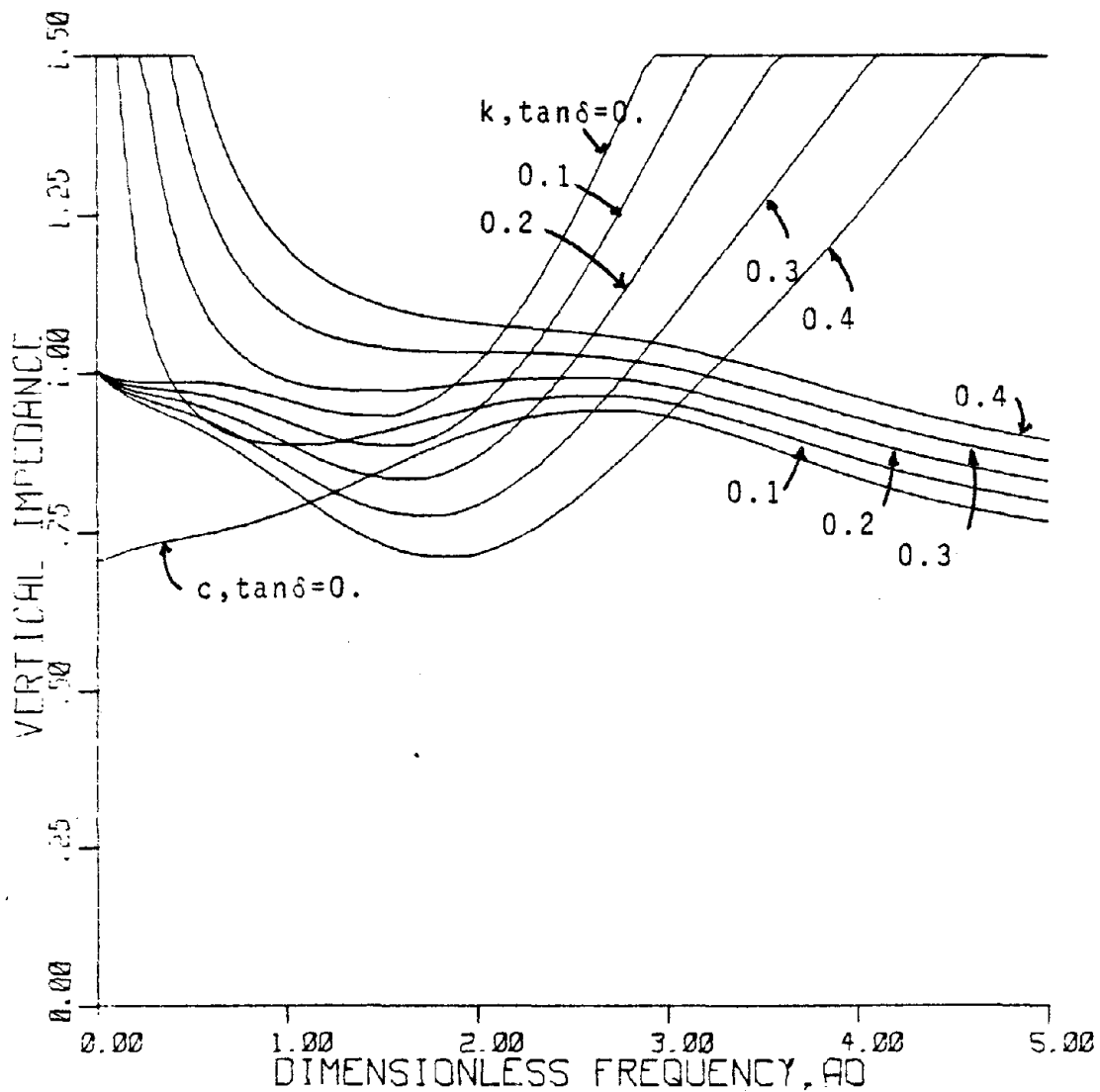
FIGURE 4.2



EFFECT OF  $\zeta$  ON VERTICAL IMPEDANCE

CASE 10:  $\lambda_1^2=2, \gamma^2=1/4$

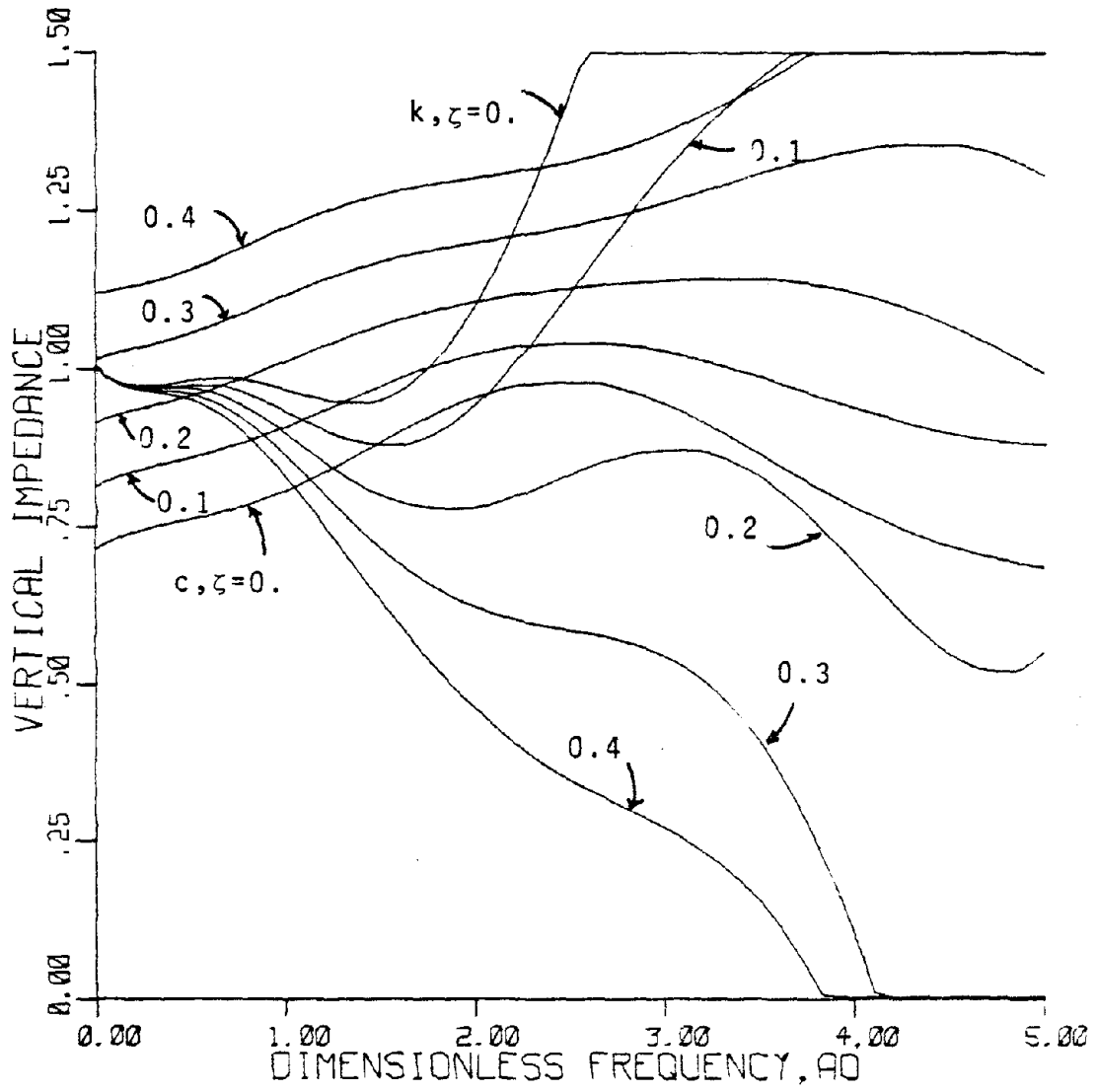
FIGURE 4.3



EFFECT OF  $\tan \delta$  ON VERTICAL IMPEDANCE

CASE 10:  $\lambda_1^2 = 2, \gamma^2 = 1/4$

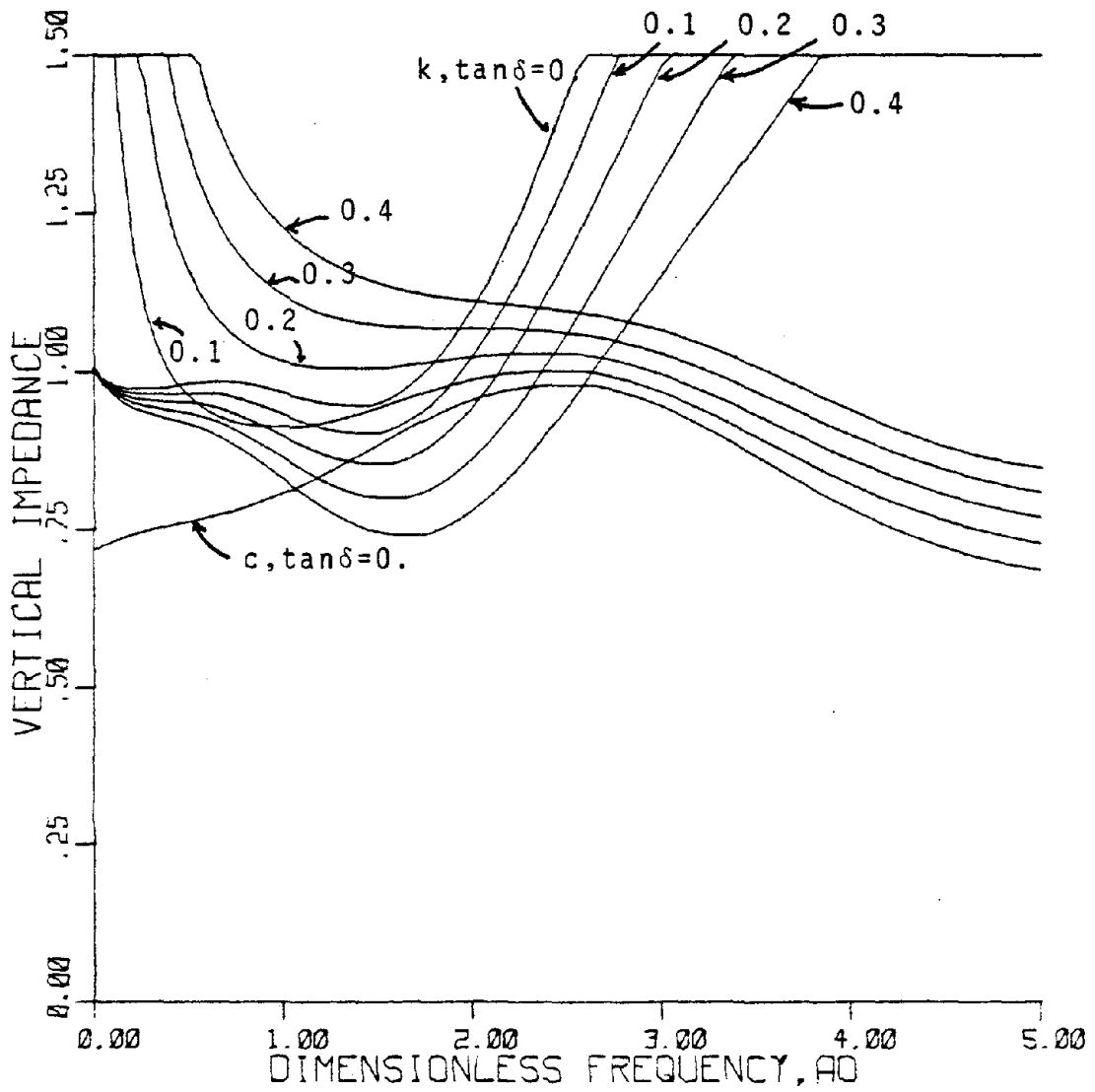
FIGURE 4.4



EFFECT OF  $\zeta$  ON VERTICAL IMPEDANCE

CASE 13:  $\lambda_1^2=3.0, \gamma^2=1/4$

FIGURE 4.5

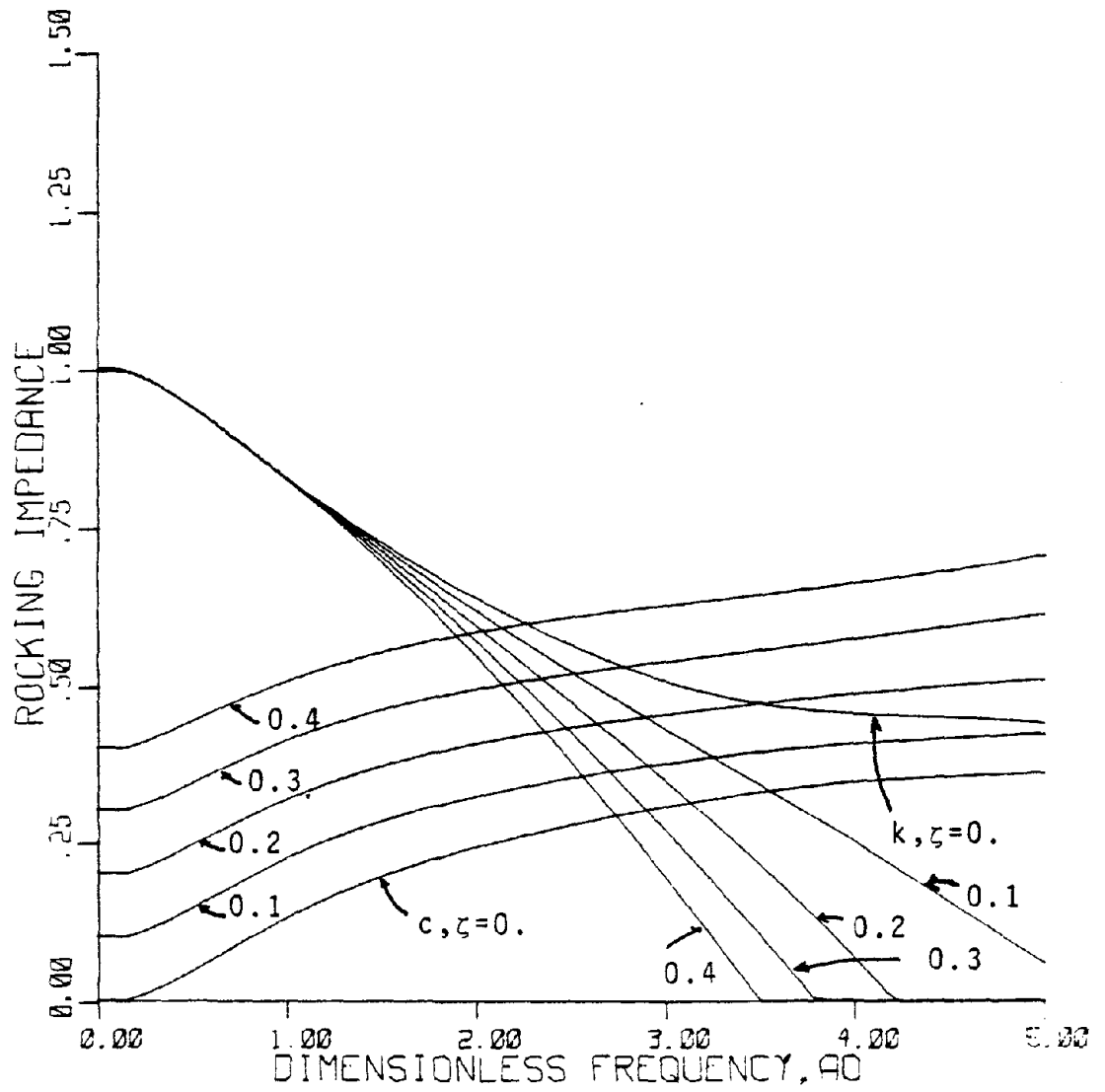


EFFECT OF  $\tan \delta$  ON VERTICAL IMPEDANCE

CASE 13:  $\lambda_1^2 = 3.0, \gamma^2 = 1/4$

FIGURE 4.6

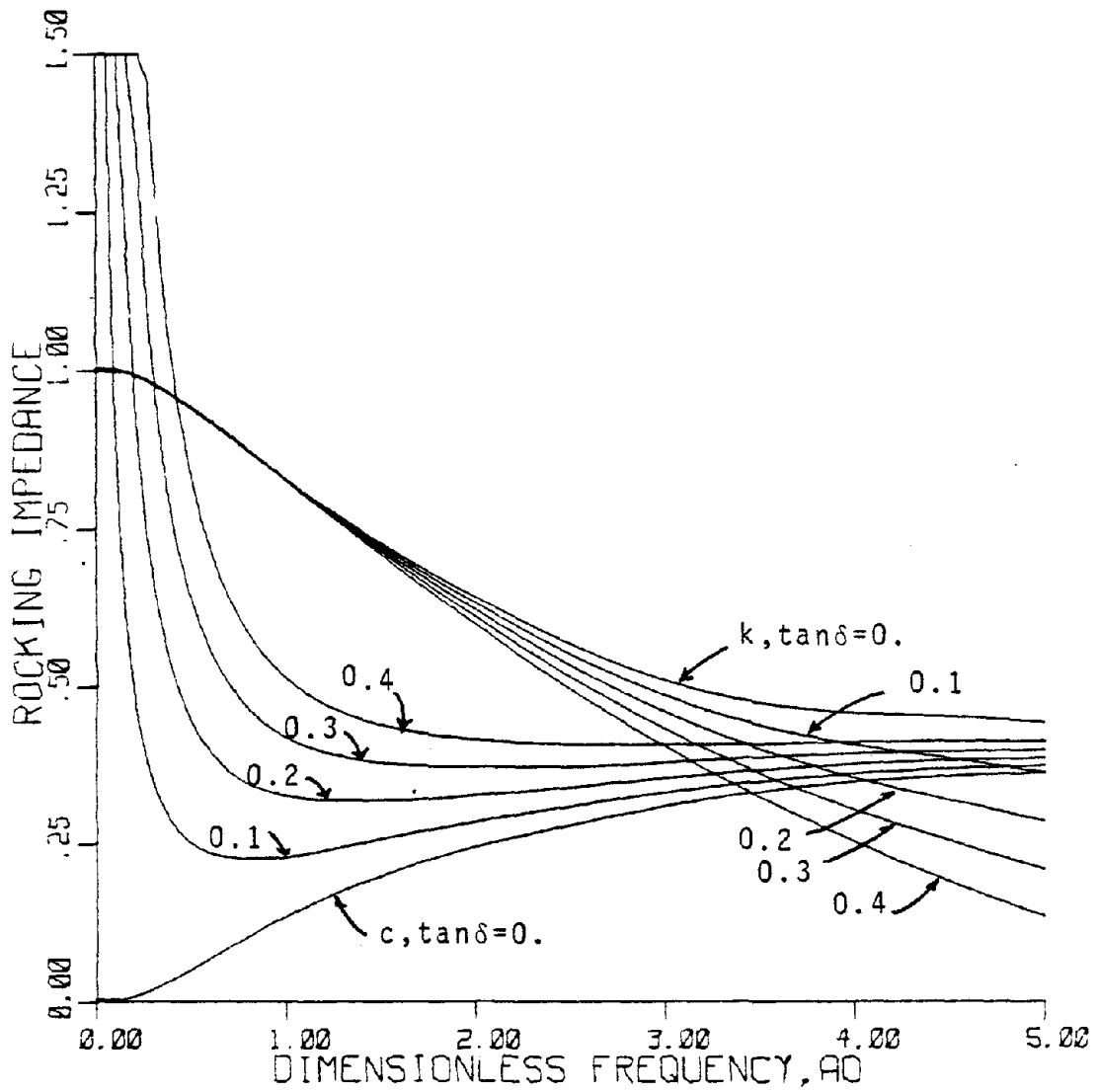




EFFECT OF  $\zeta$  ON ROCKING IMPEDANCE

ISOTROPIC :  $\lambda_1^2 = 1, \gamma^2 = 1/4$

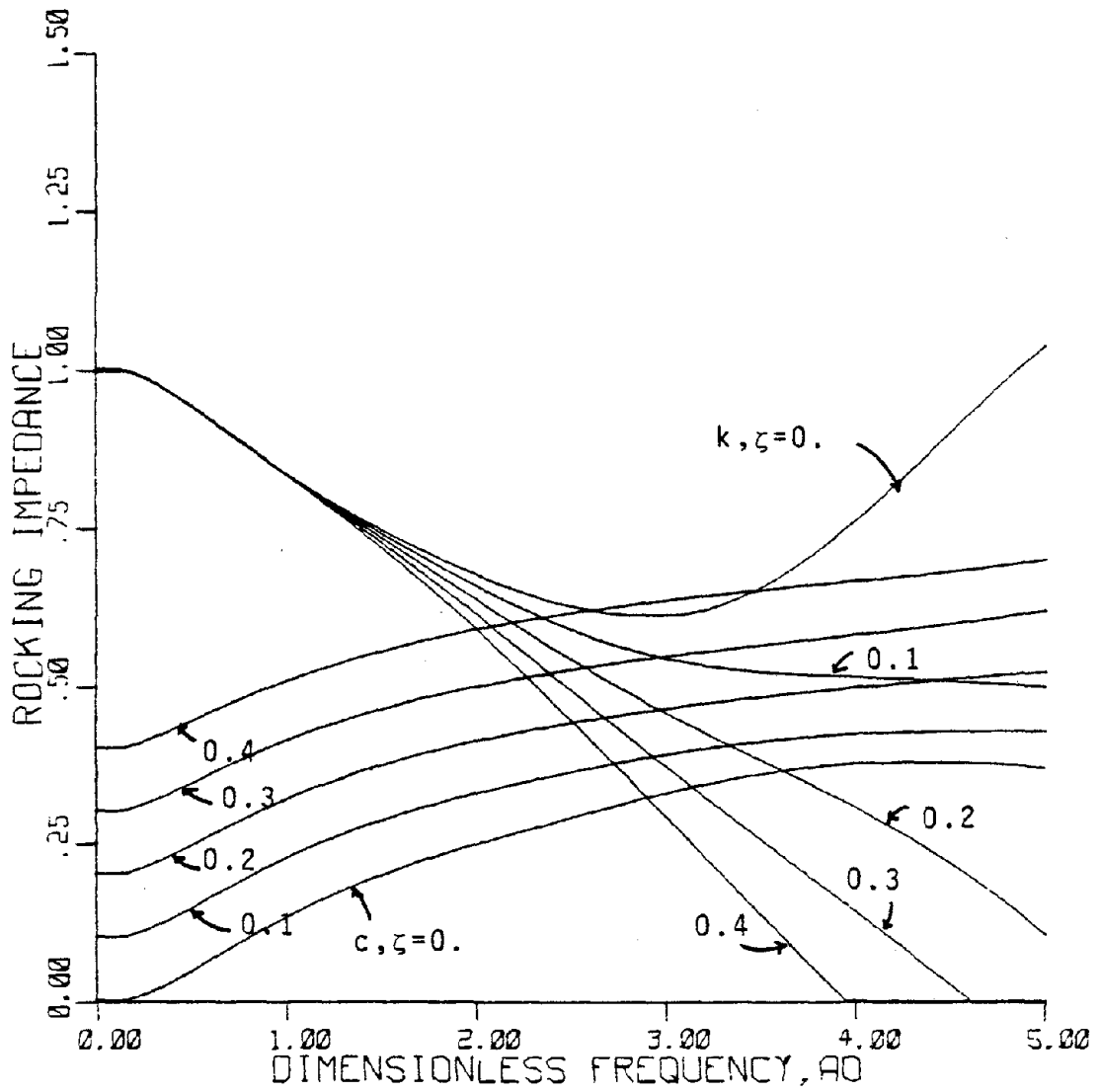
FIGURE 4.7



EFFECT OF  $\tan \delta$  ON ROCKING IMPEDANCE

ISOTROPIC :  $\lambda_1^2 = 1, \gamma^2 = 1/4$

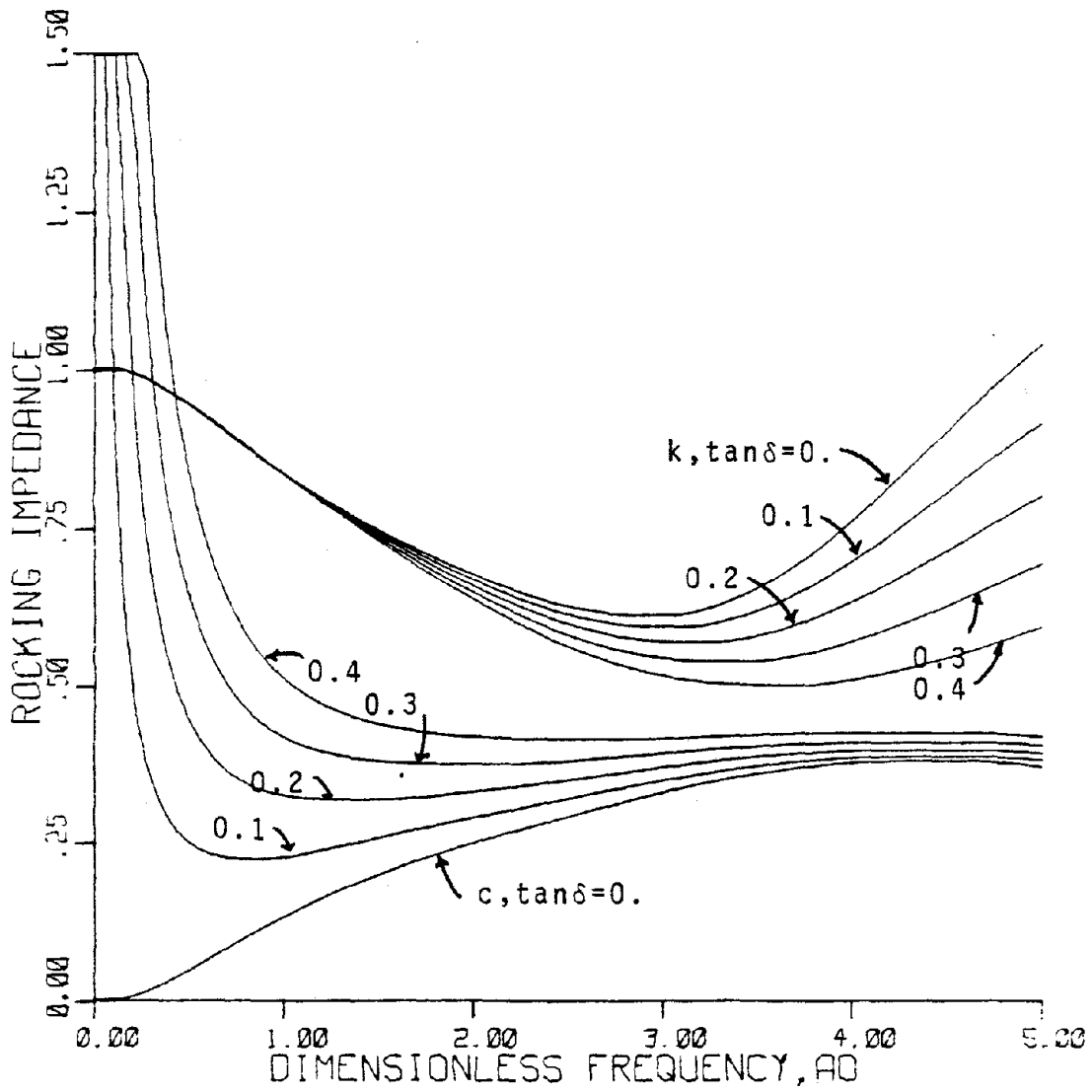
FIGURE 4.8



EFFECT OF  $\zeta$  ON ROCKING IMPEDANCE

CASE 10:  $\lambda_1^2 = 2, \gamma^2 = 1/4$

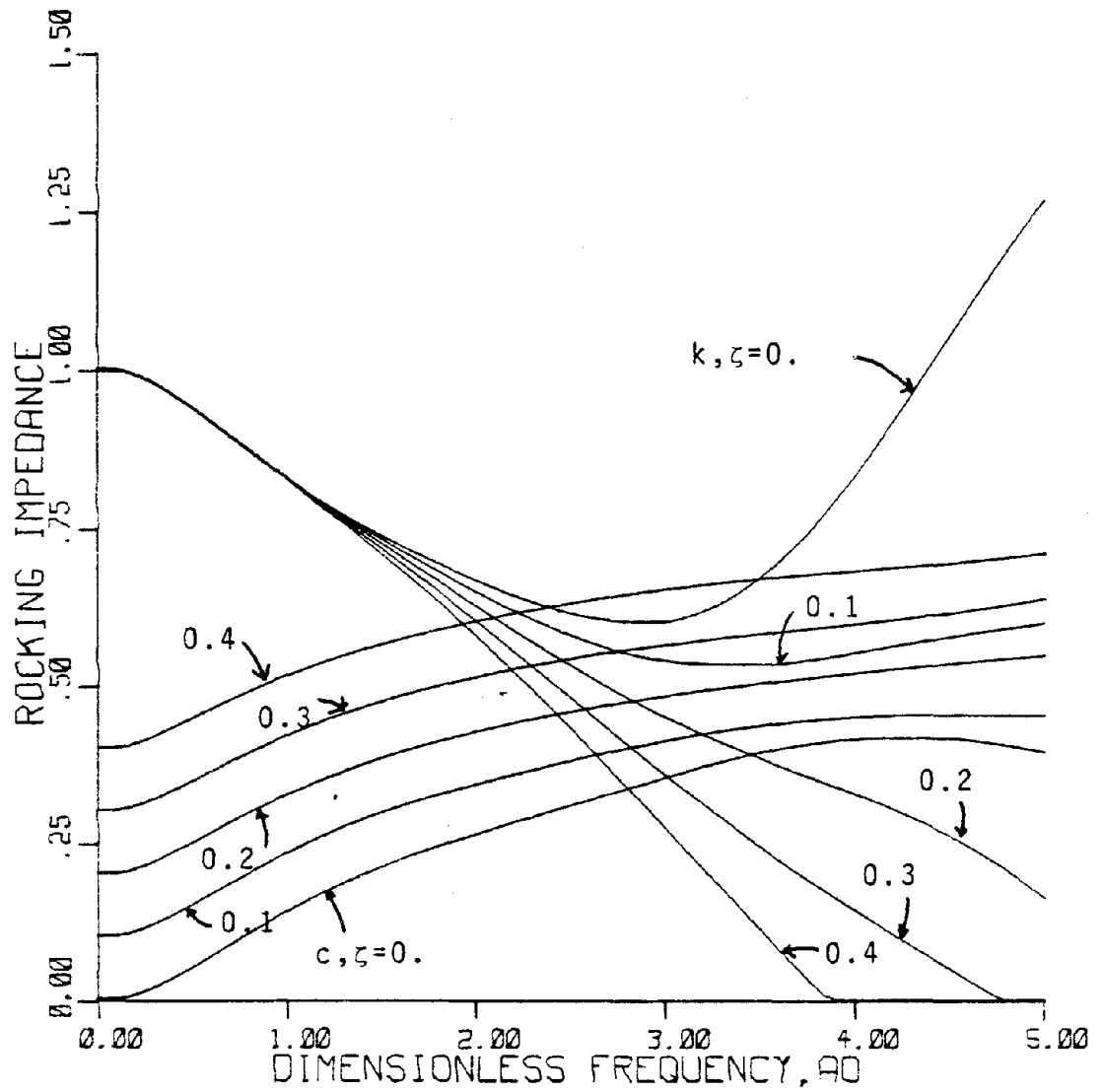
FIGURE 4.9



EFFECT OF  $\tan \delta$  ON ROCKING IMPEDANCE

CASE 10:  $\lambda_1^2 = 2, \gamma^2 = 1/4$

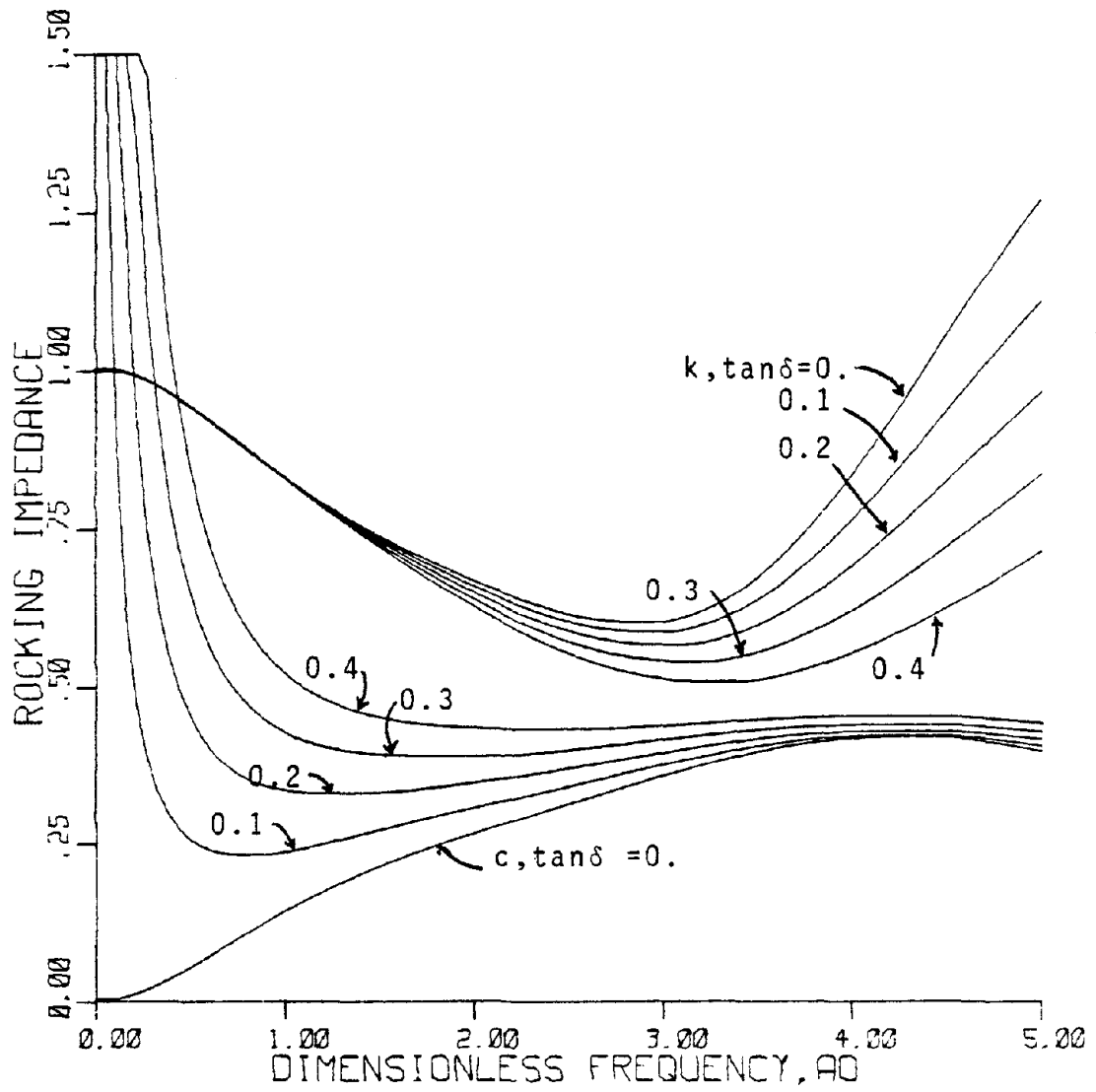
FIGURE 4.10



EFFECT OF  $\zeta$  ON ROCKING IMPEDANCE

CASE 13:  $\lambda_1^2=3, \gamma^2=1/4$

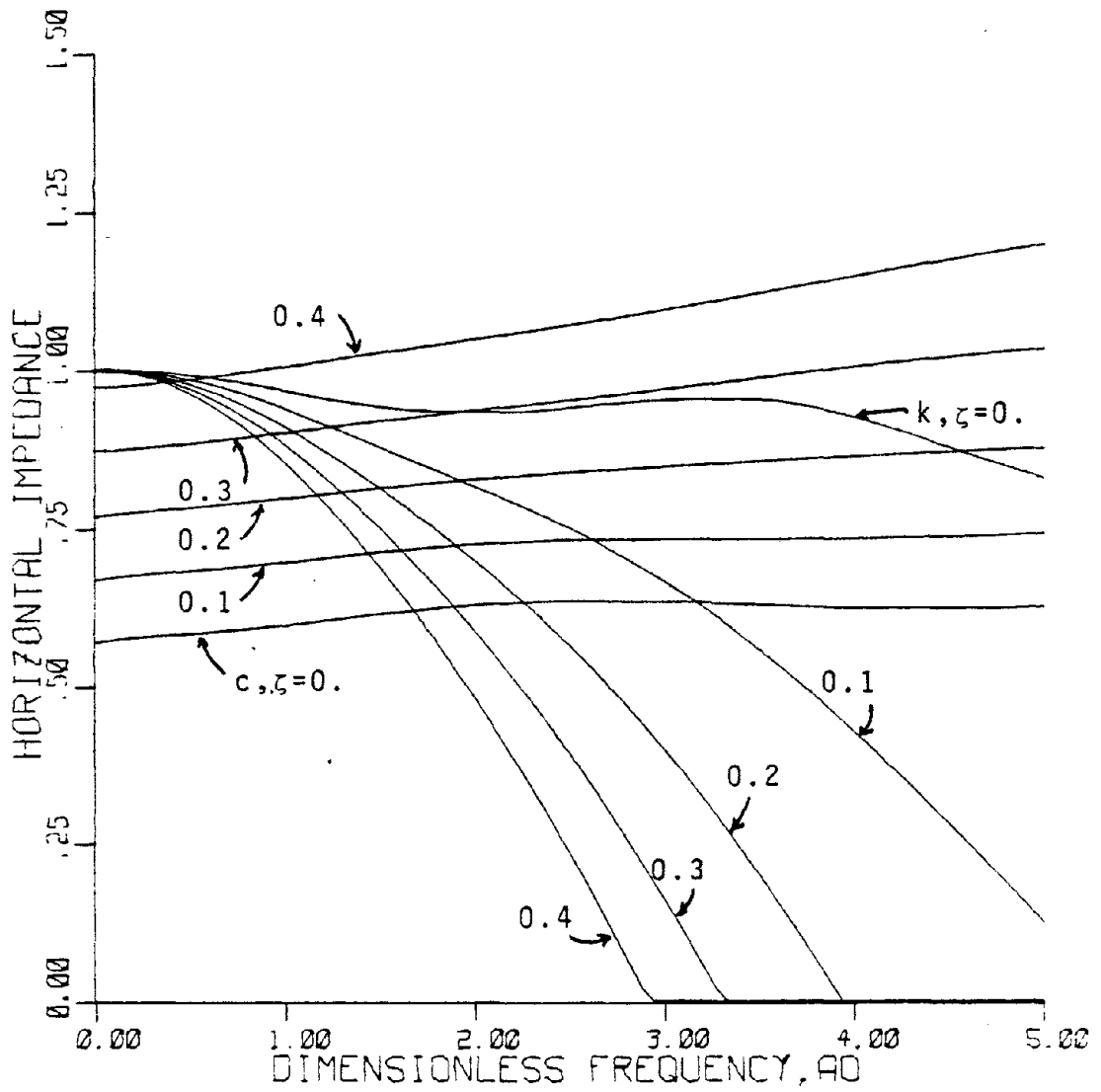
FIGURE 4.11



EFFECT OF TAN  $\delta$  ON ROCKING IMPEDANCE

CASE 13:  $\lambda_1^2 = 3, \gamma^2 = 1/4$

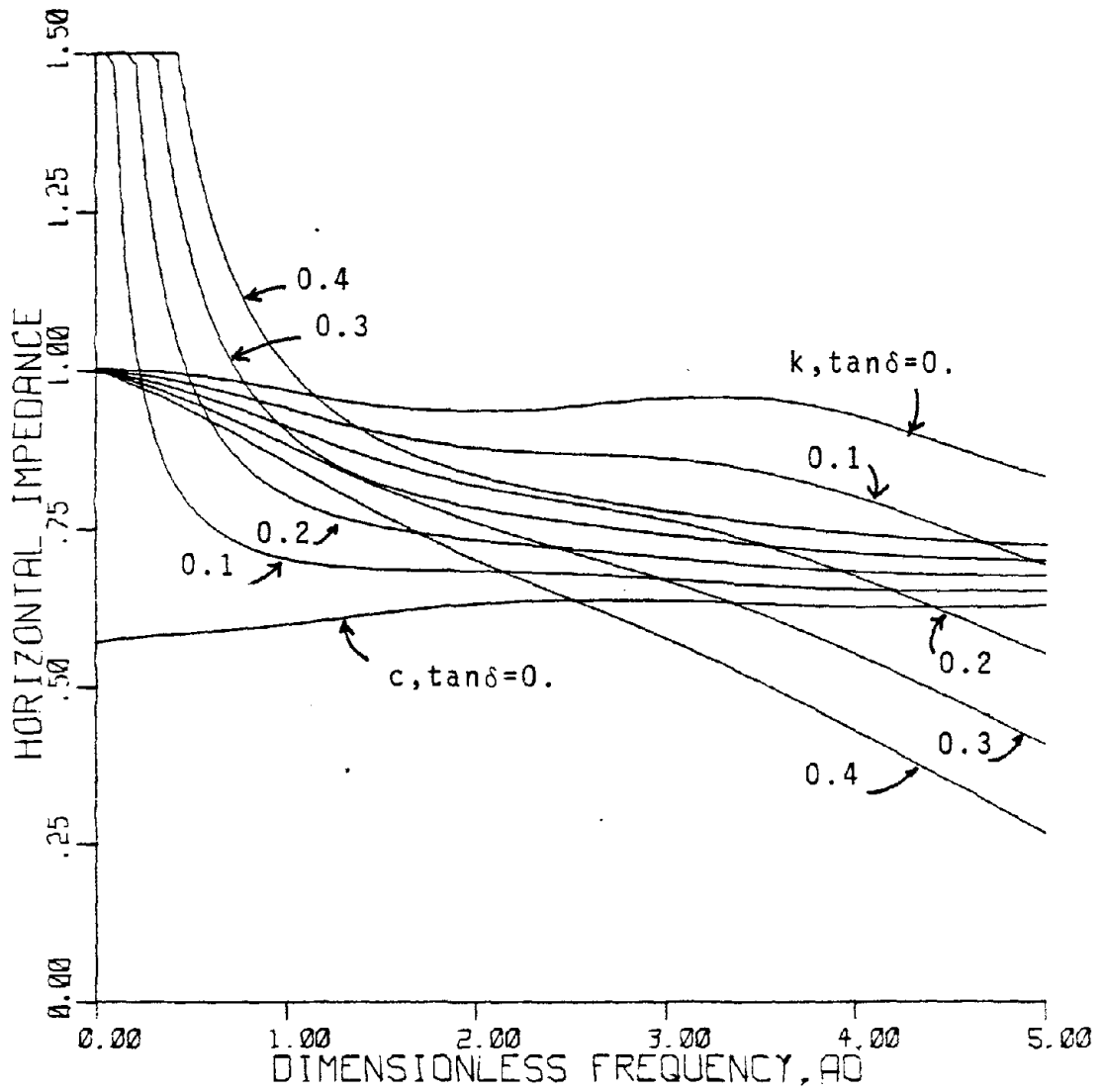
FIGURE 4.12



EFFECT OF  $\zeta$  ON HORIZONTAL IMPEDANCE

ISOTROPIC:  $\lambda_1^2=1, \lambda_2^2=1, \gamma^2=1/4$

FIGURE 4.13

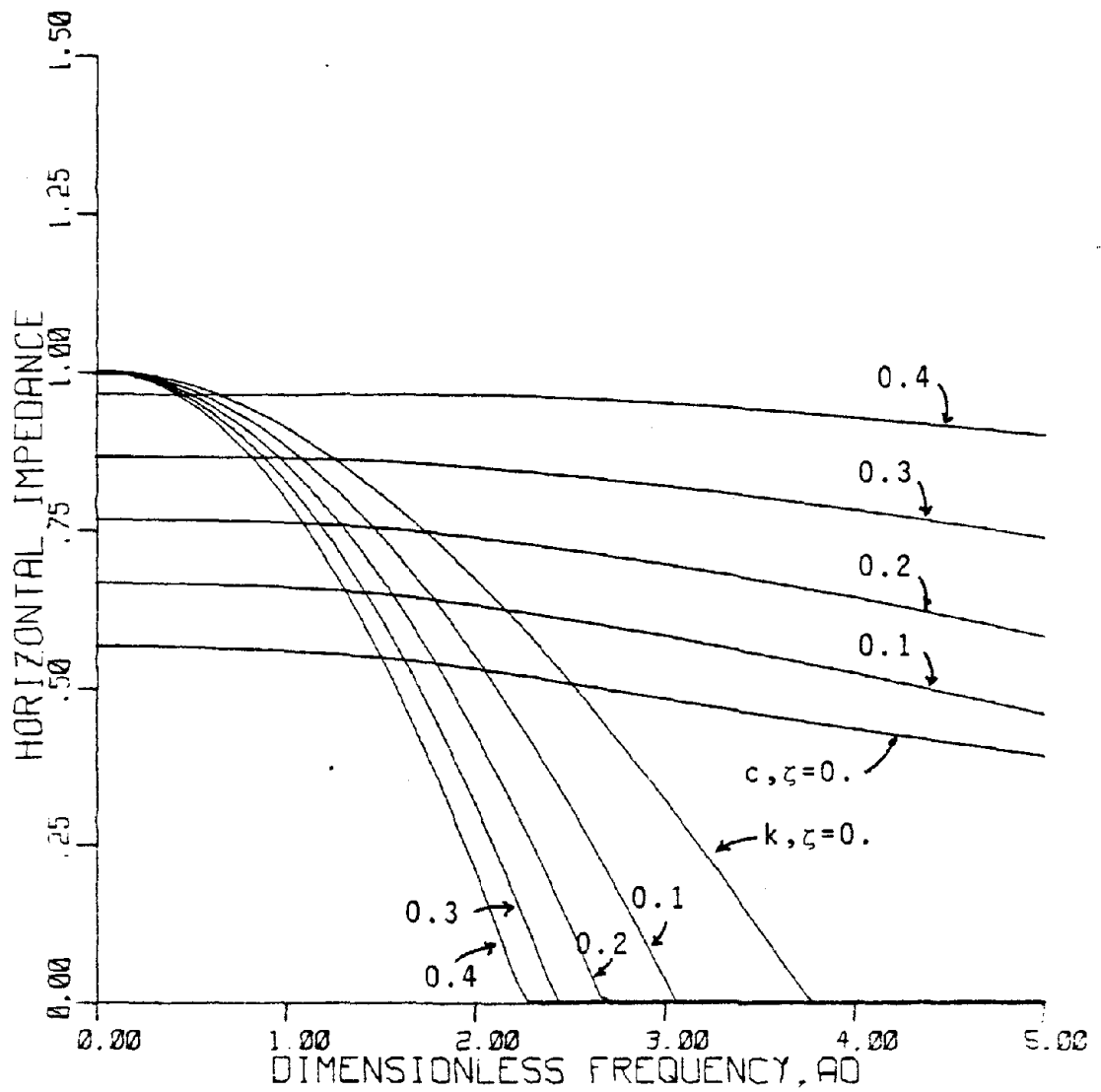


EFFECT OF TAN δ ON HORIZONTAL IMPEDANCE

ISOTROPIC:  $\lambda_1^2=1, \lambda_2^2=1, \gamma^2=1/4$

FIGURE 4.14

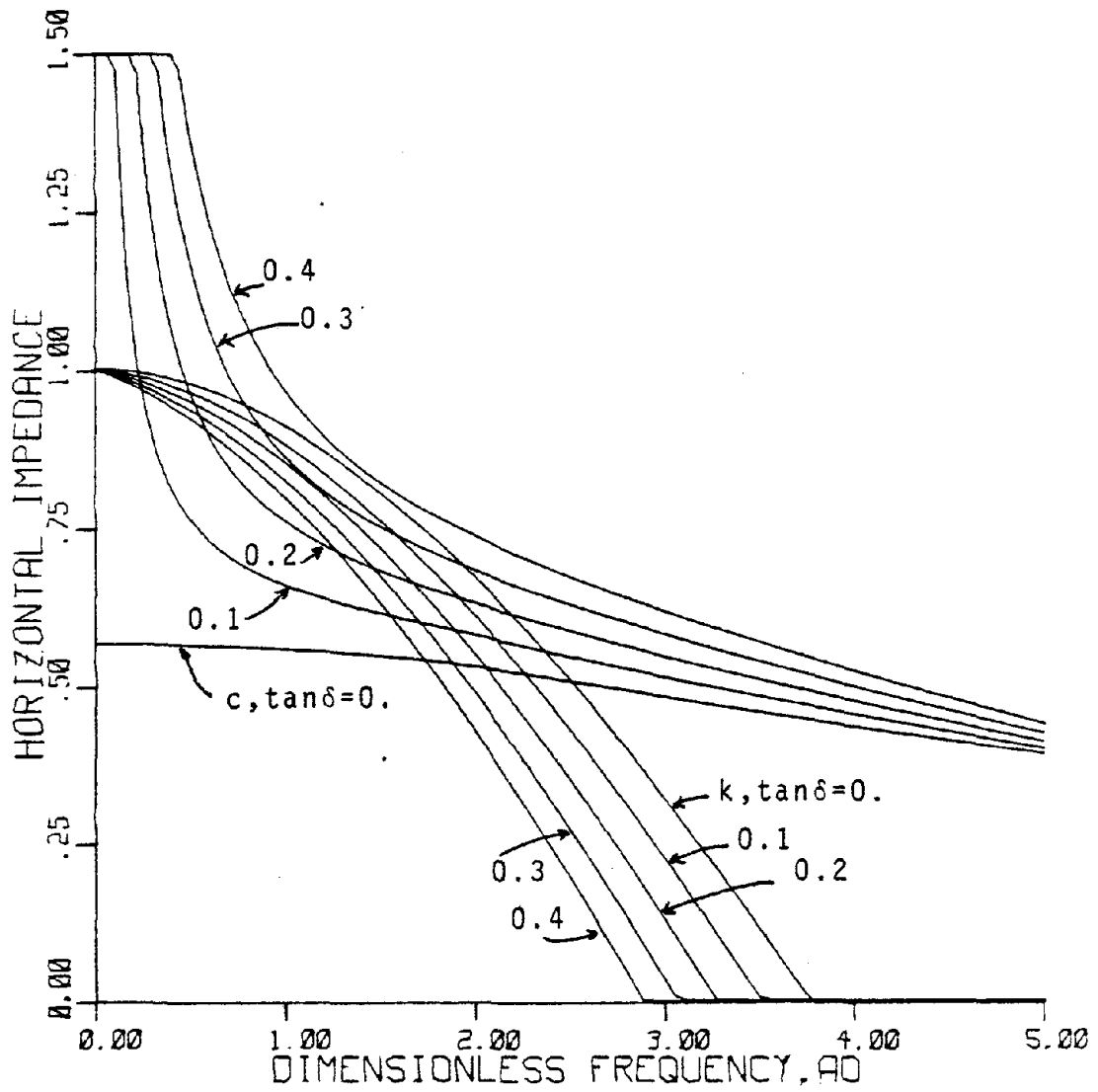




EFFECT OF  $\zeta$  ON HORIZONTAL IMPEDANCE

CASE 2c:  $\lambda_1^2=1, \lambda_2^2=2.5, \gamma^2=1/4$

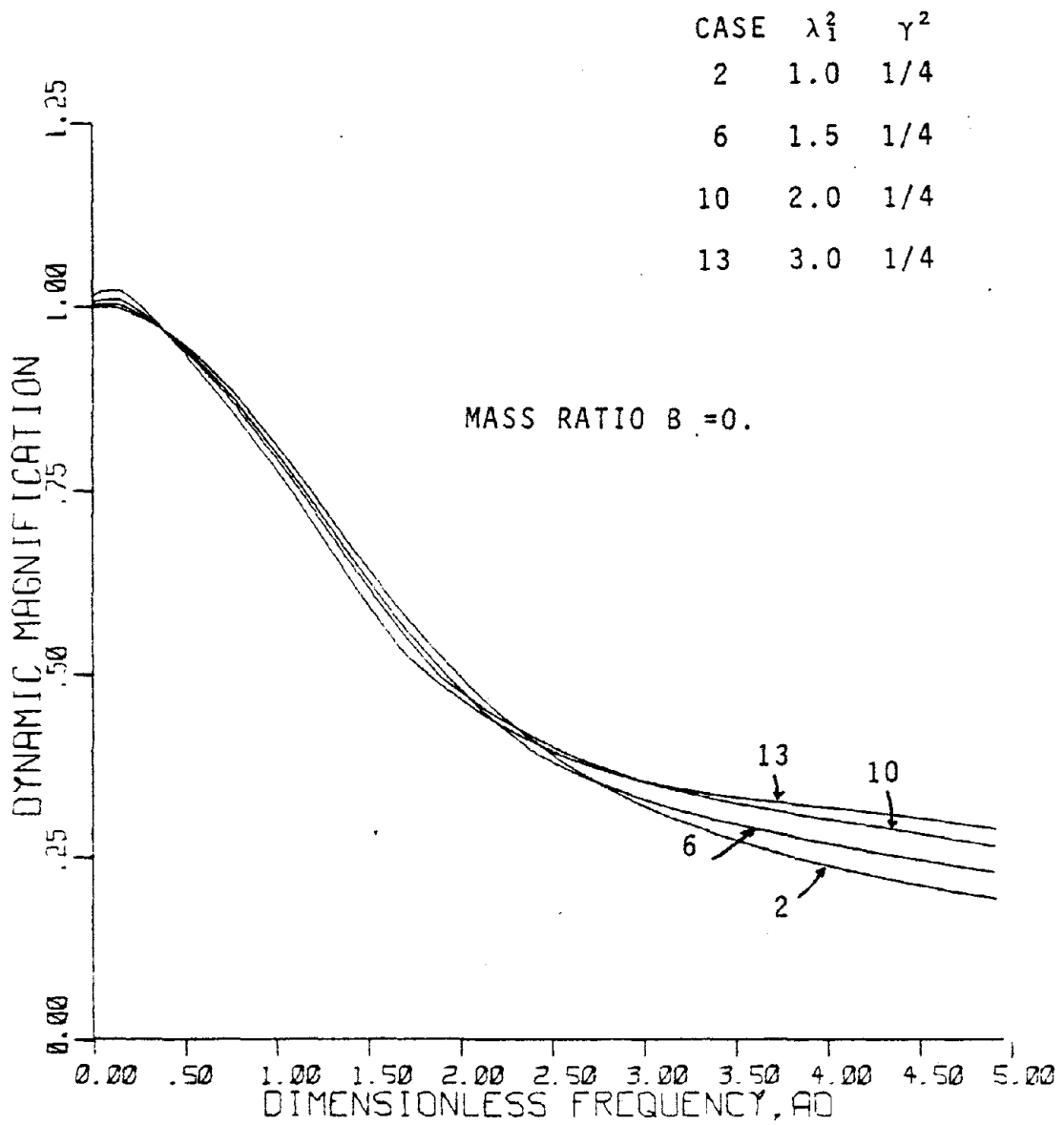
FIGURE 4.15



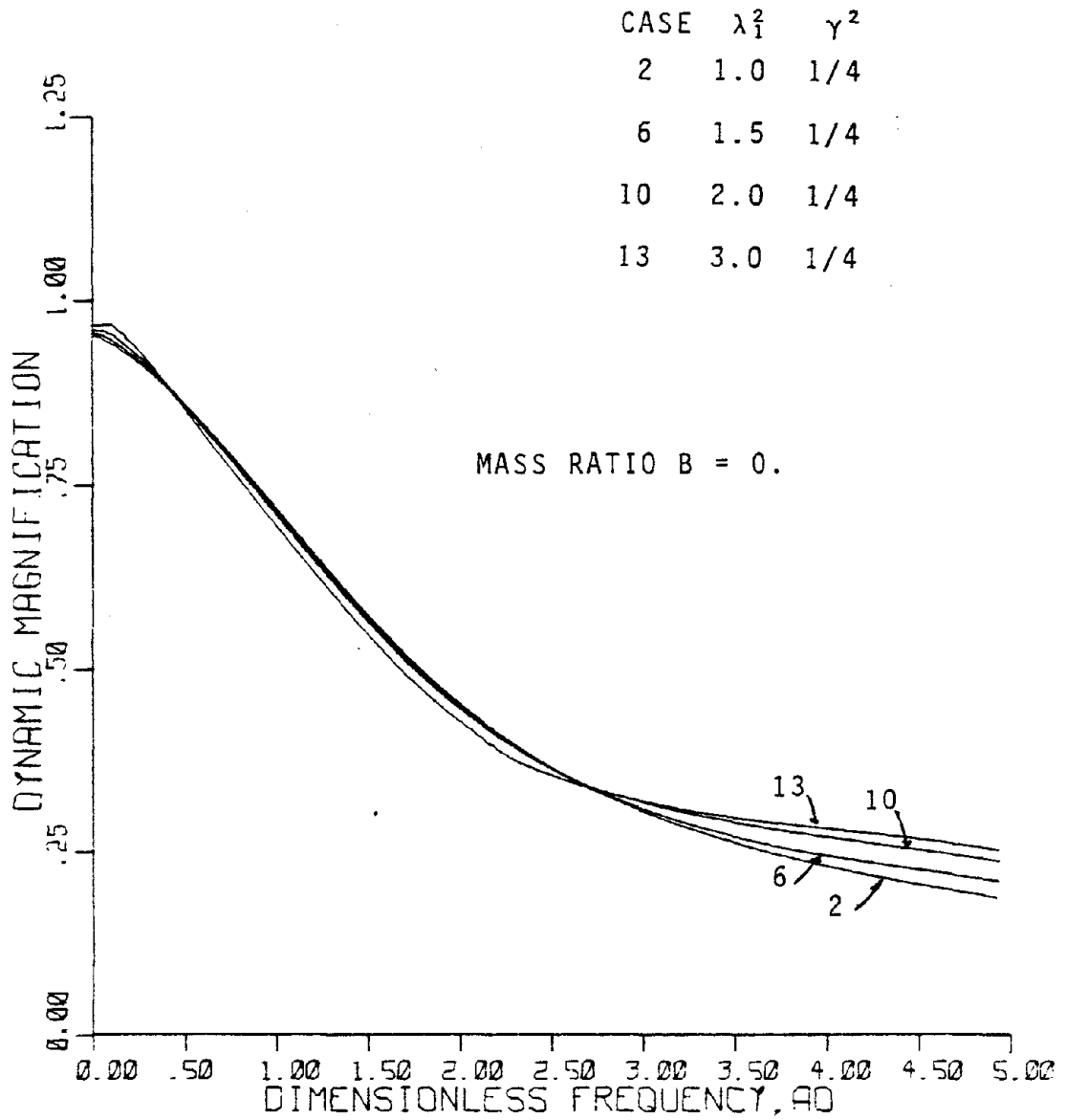
EFFECT OF  $\tan \delta$  ON HORIZONTAL IMPEDANCE

CASE 2c:  $\lambda_1^2=1, \lambda_2^2=2.5, \gamma^2=1/4$

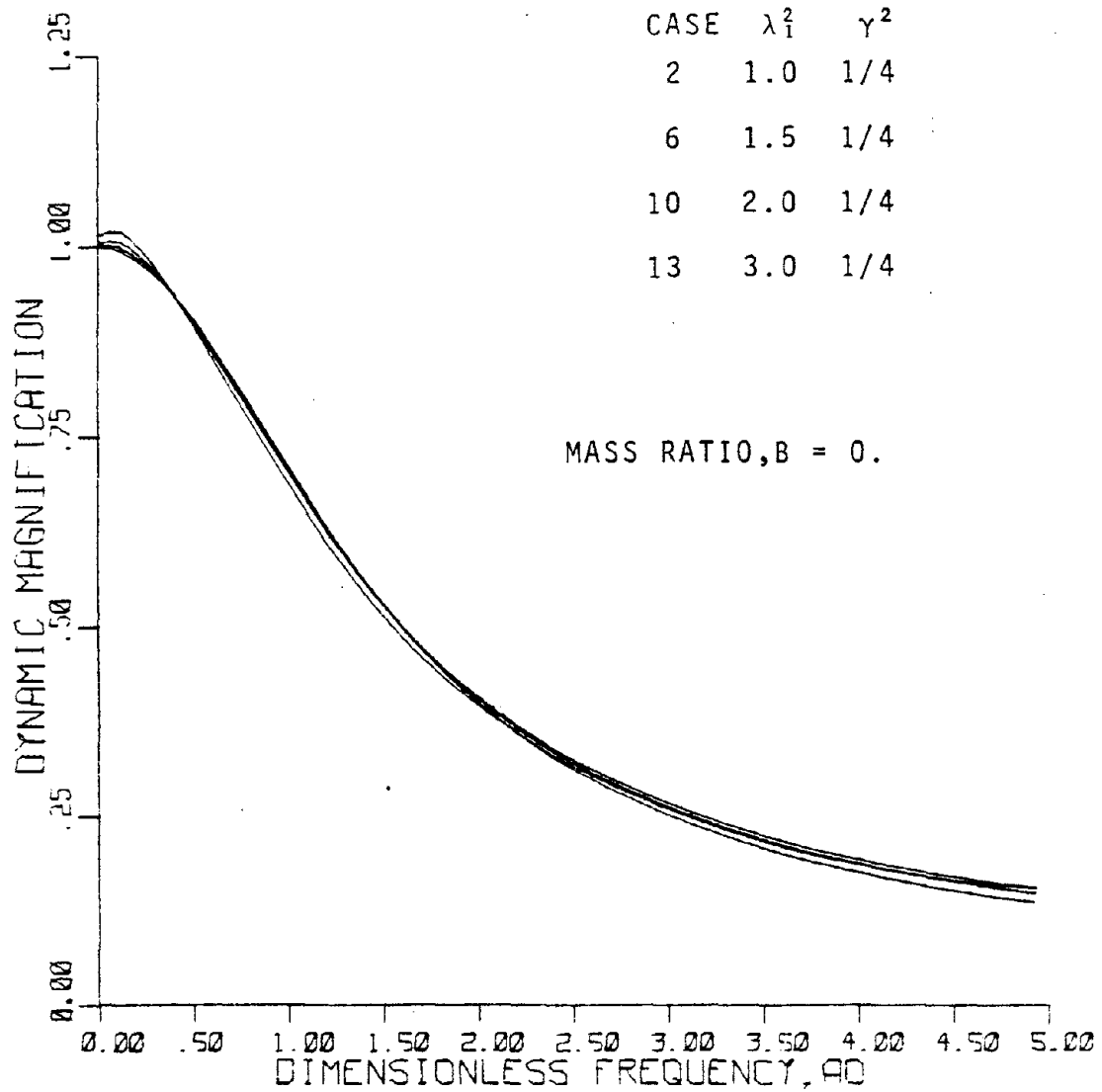
FIGURE 4.16



VERTICAL VIBRATION  
 FIGURE 5.1



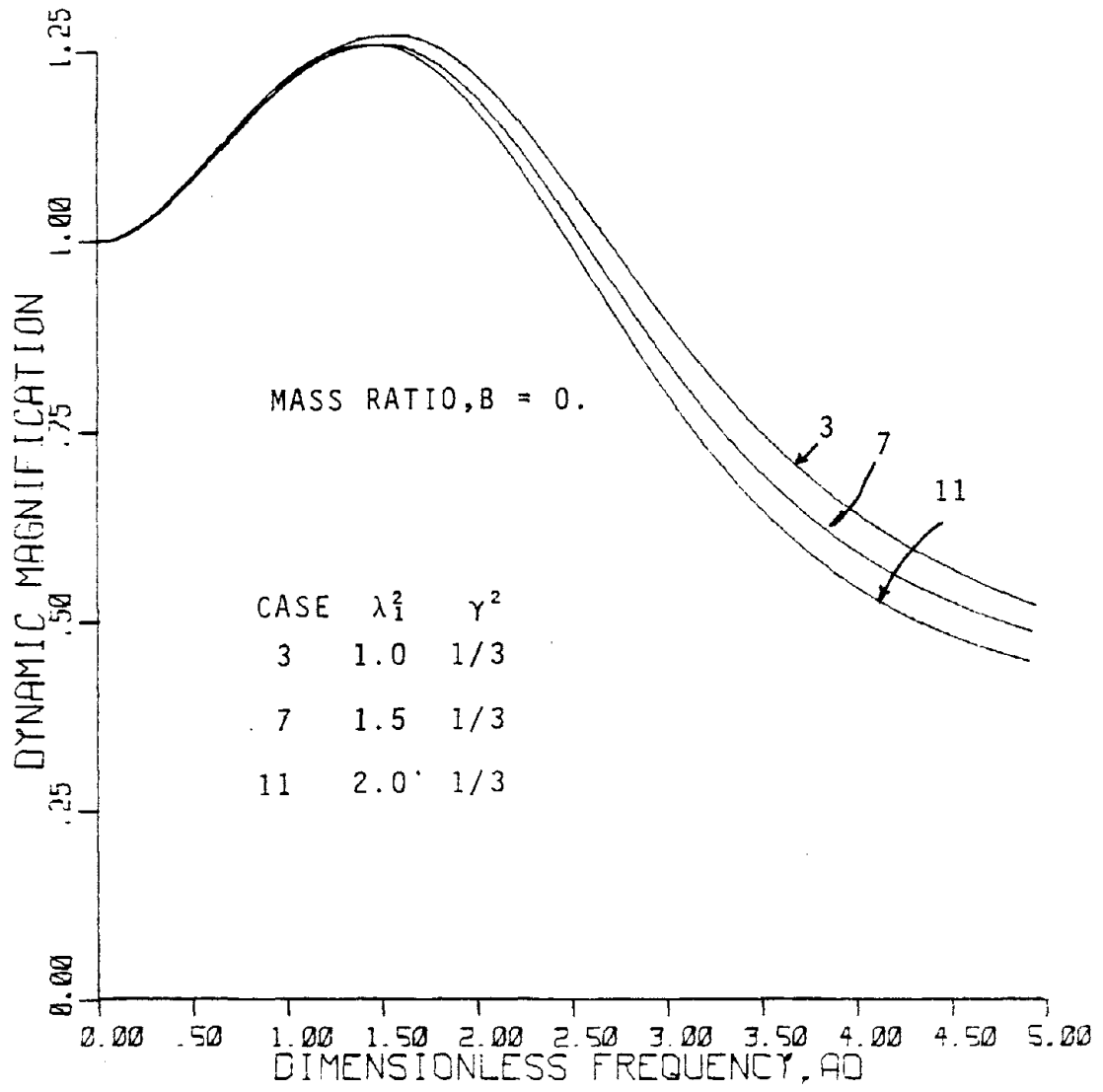
VERTICAL VIBRATION  
 CONSTANT HYSTERETIC,  $\tan\delta=0.3$   
 FIGURE 5.2



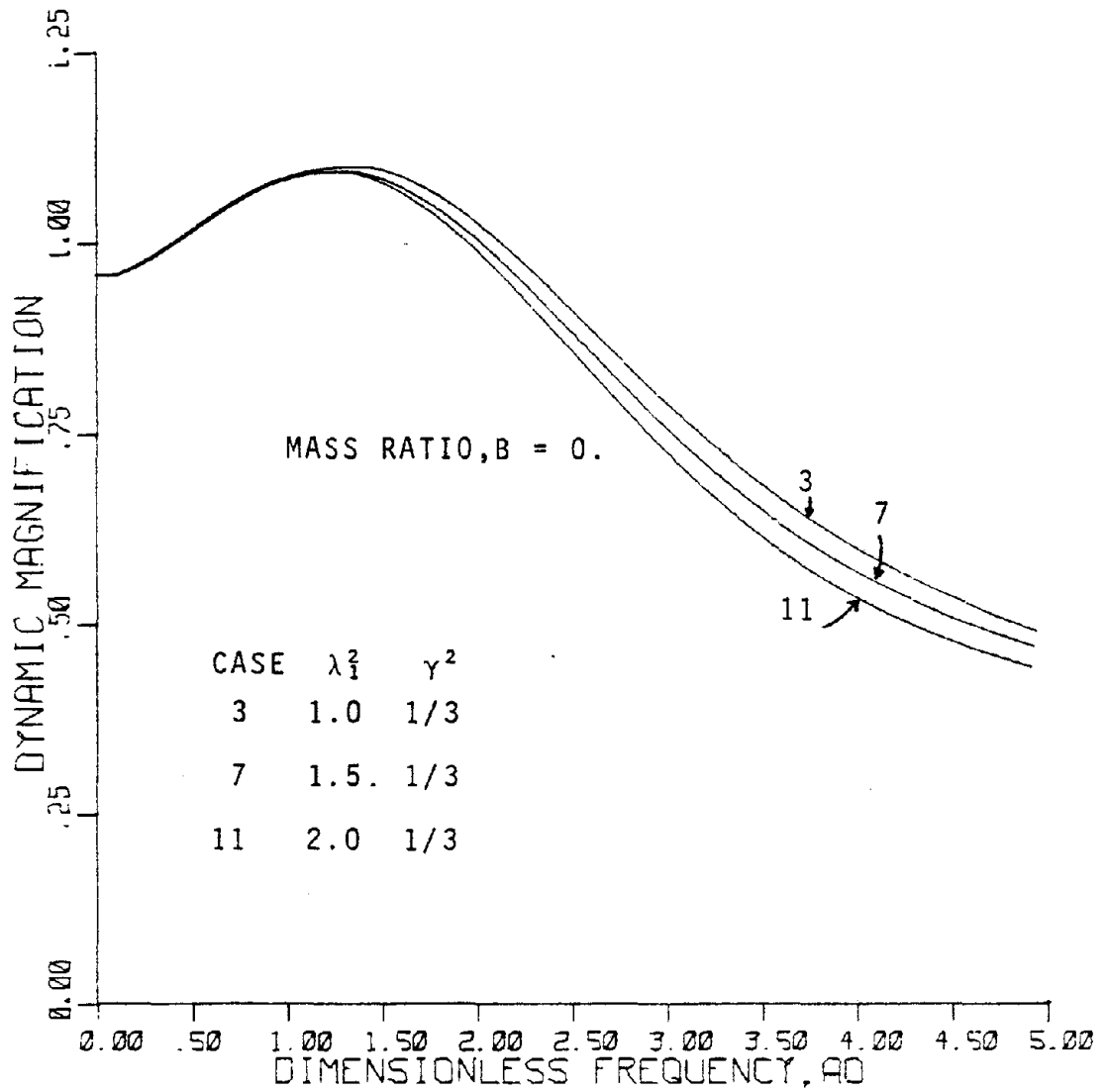
VERTICAL VIBRATION

VISCOUS,  $\zeta=0.3$

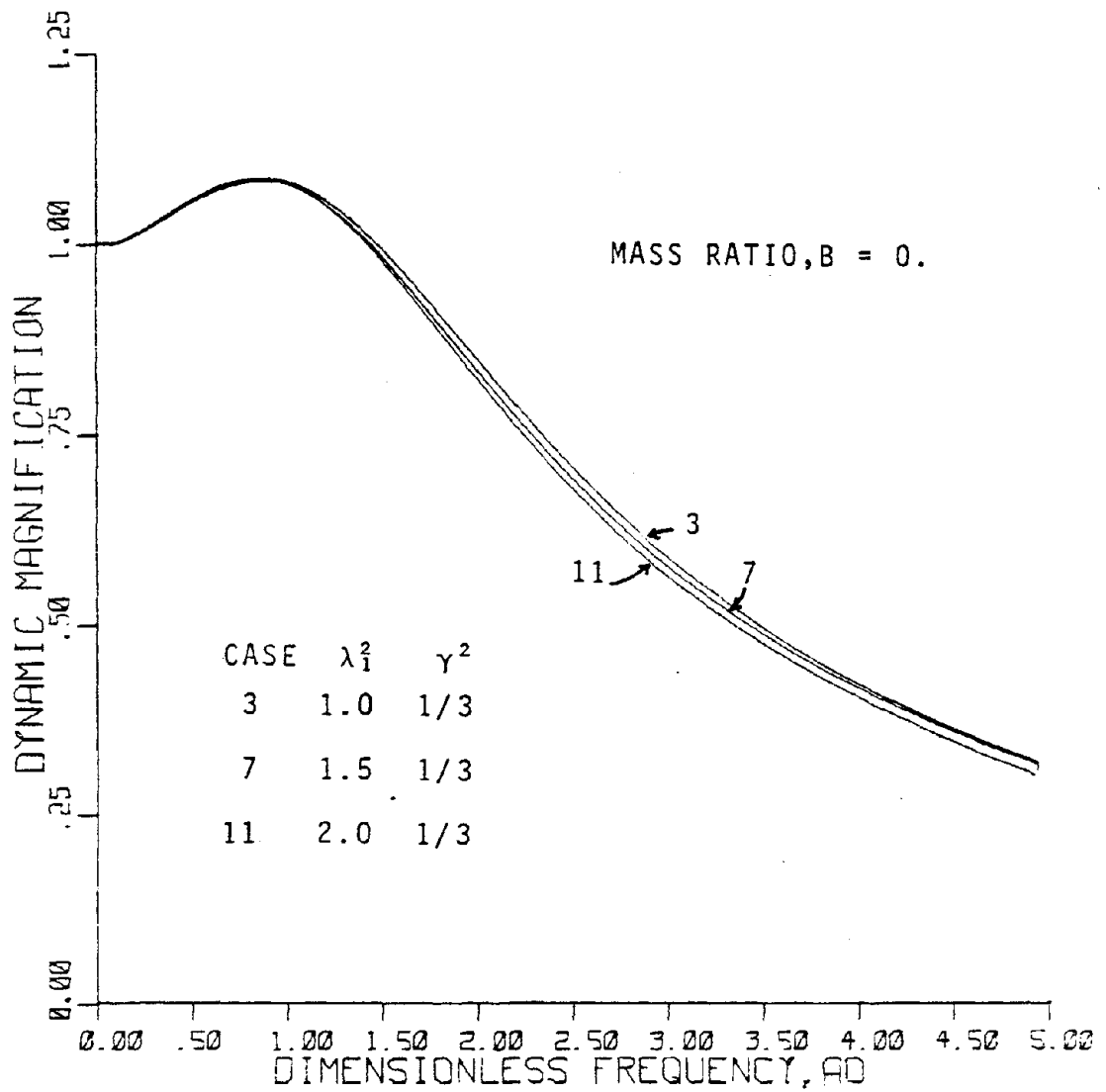
FIGURE 5.3



ROCKING VIBRATION  
FIGURE 5.4



ROCKING VIBRATION  
 CONSTANT HYSTERETIC,  $\tan\delta=0.3$   
 FIGURE 5.5

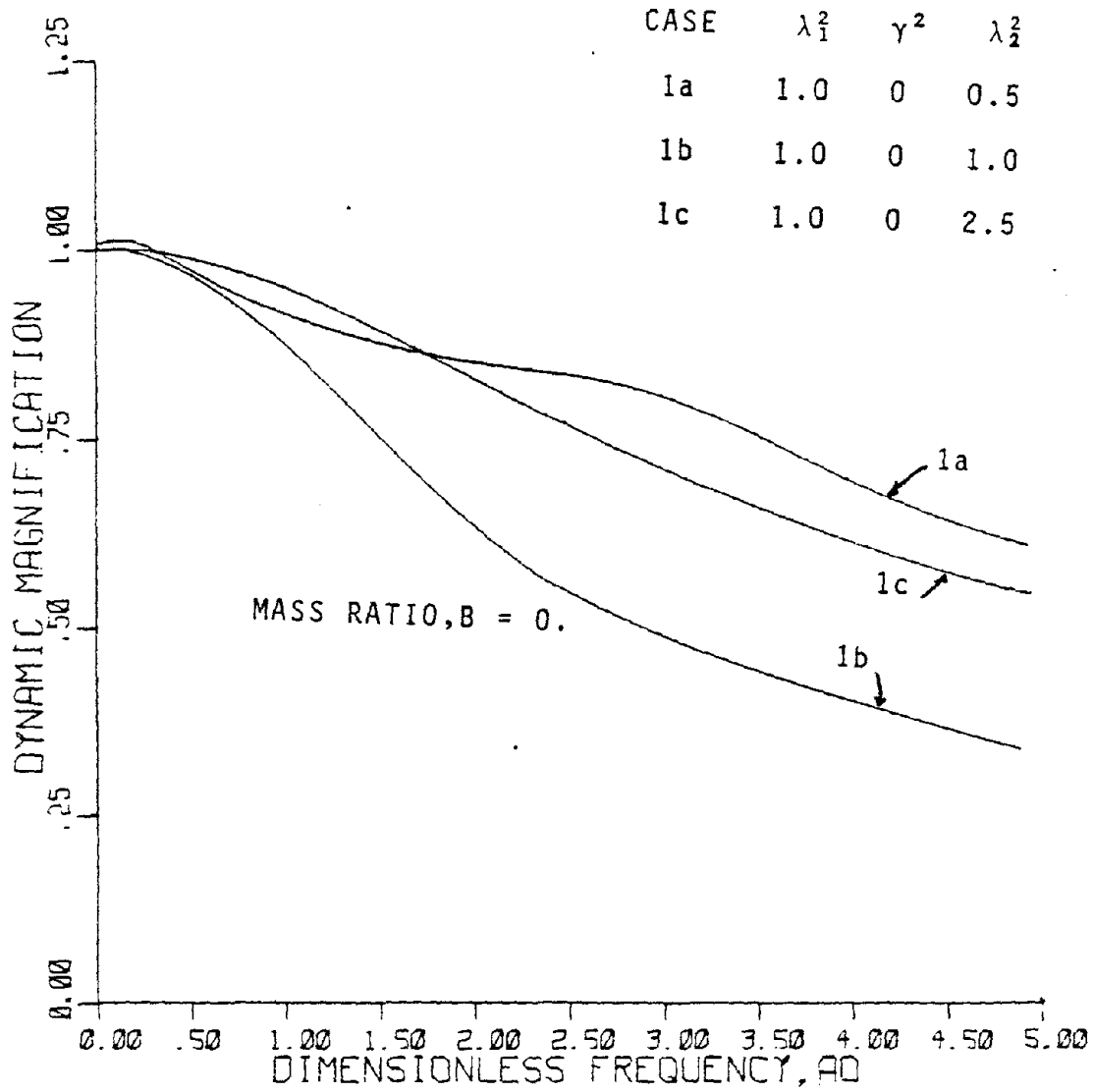


ROCKING VIBRATION

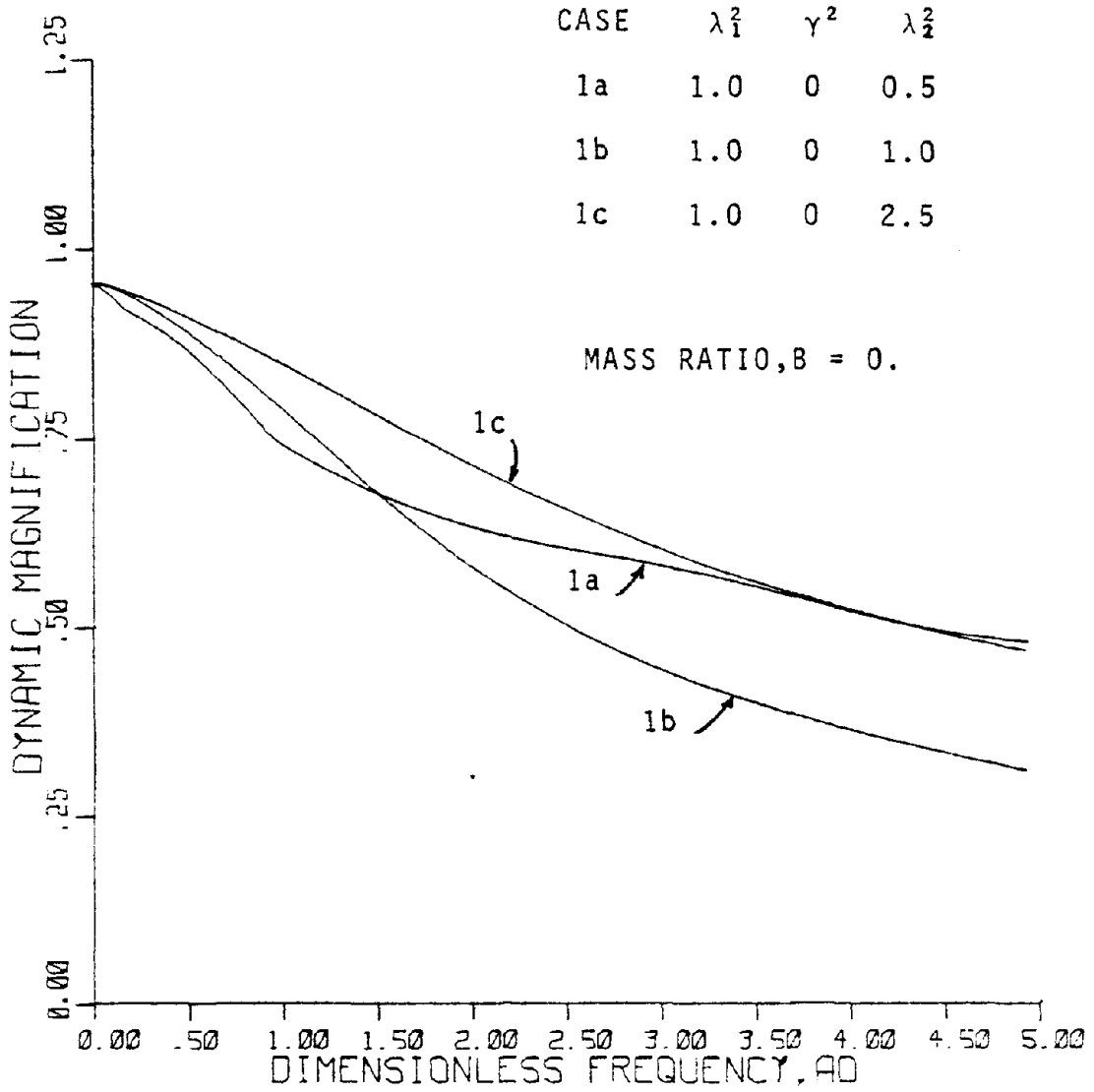
VISCOUS,  $\zeta=0.3$

FIGURE 5.6

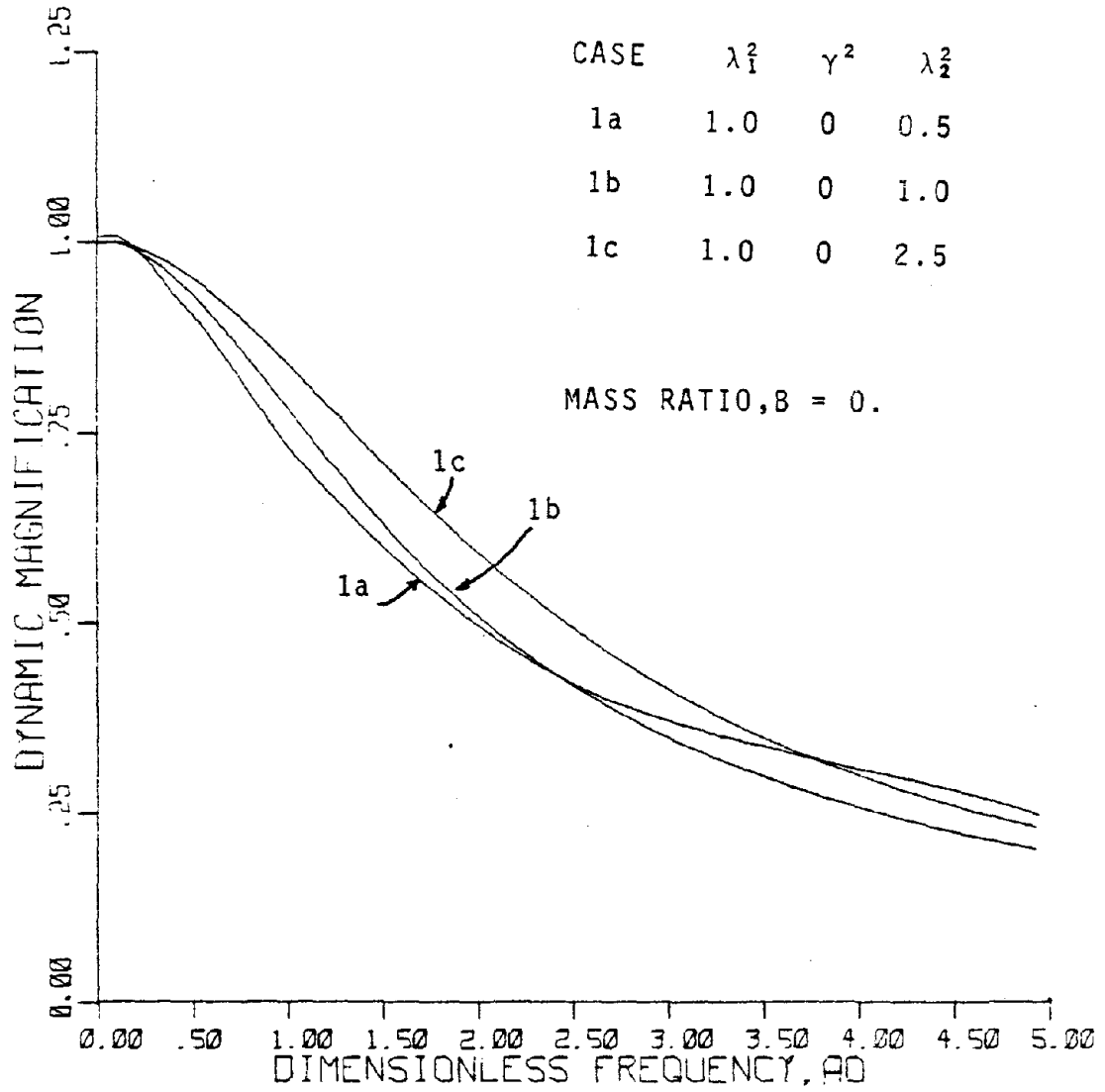




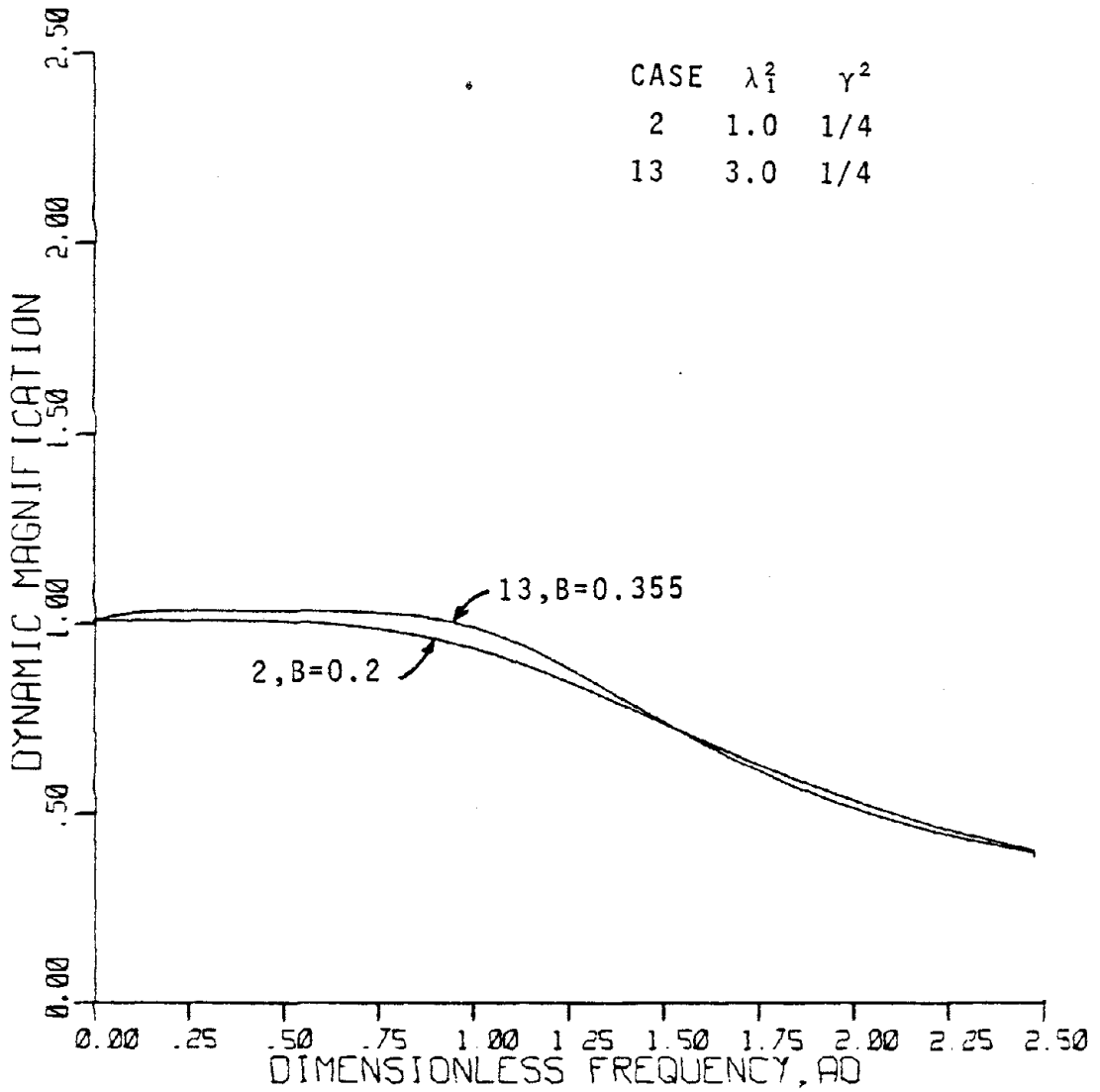
HORIZONTAL VIBRATION  
 FIGURE 5.7



HORIZONTAL VIBRATION  
 CONSTANT HYSTERETIC,  $\tan\delta=0.3$   
 FIGURE 5.8

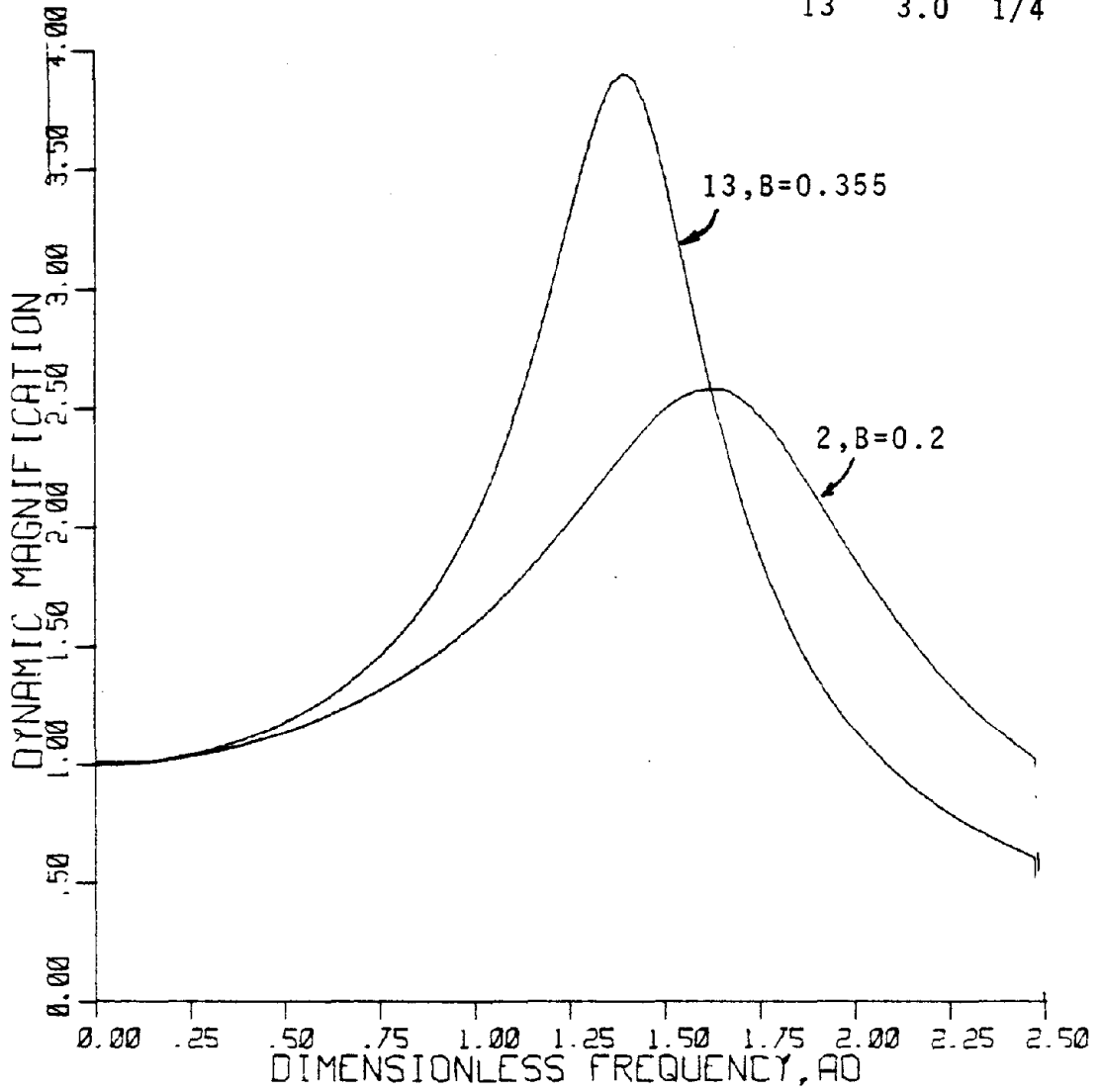


HORIZONTAL VIBRATION  
 VISCOUS,  $\zeta=0.3$   
 FIGURE 5.9

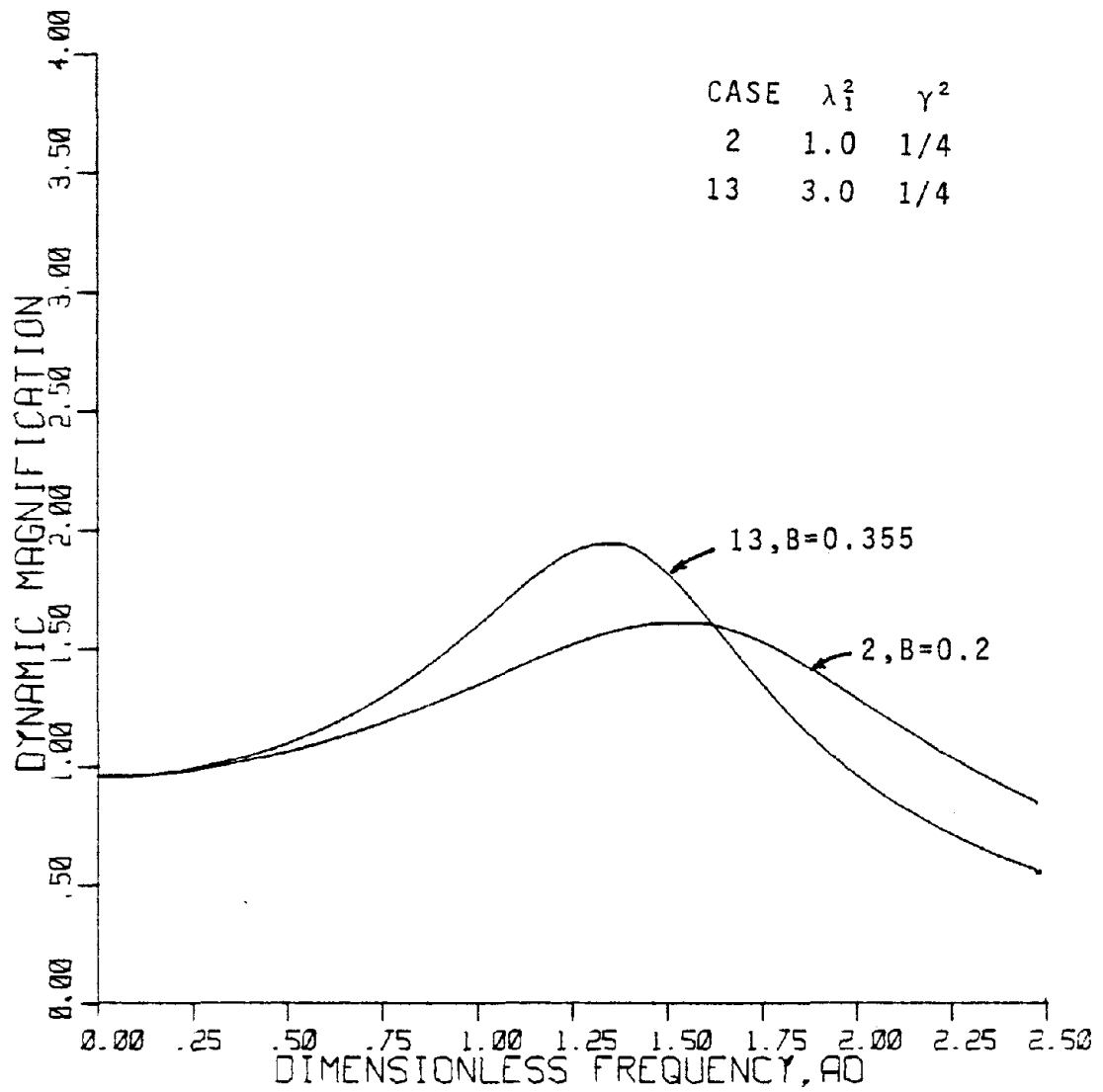


VERTICAL VIBRATION  
FIGURE 5.10

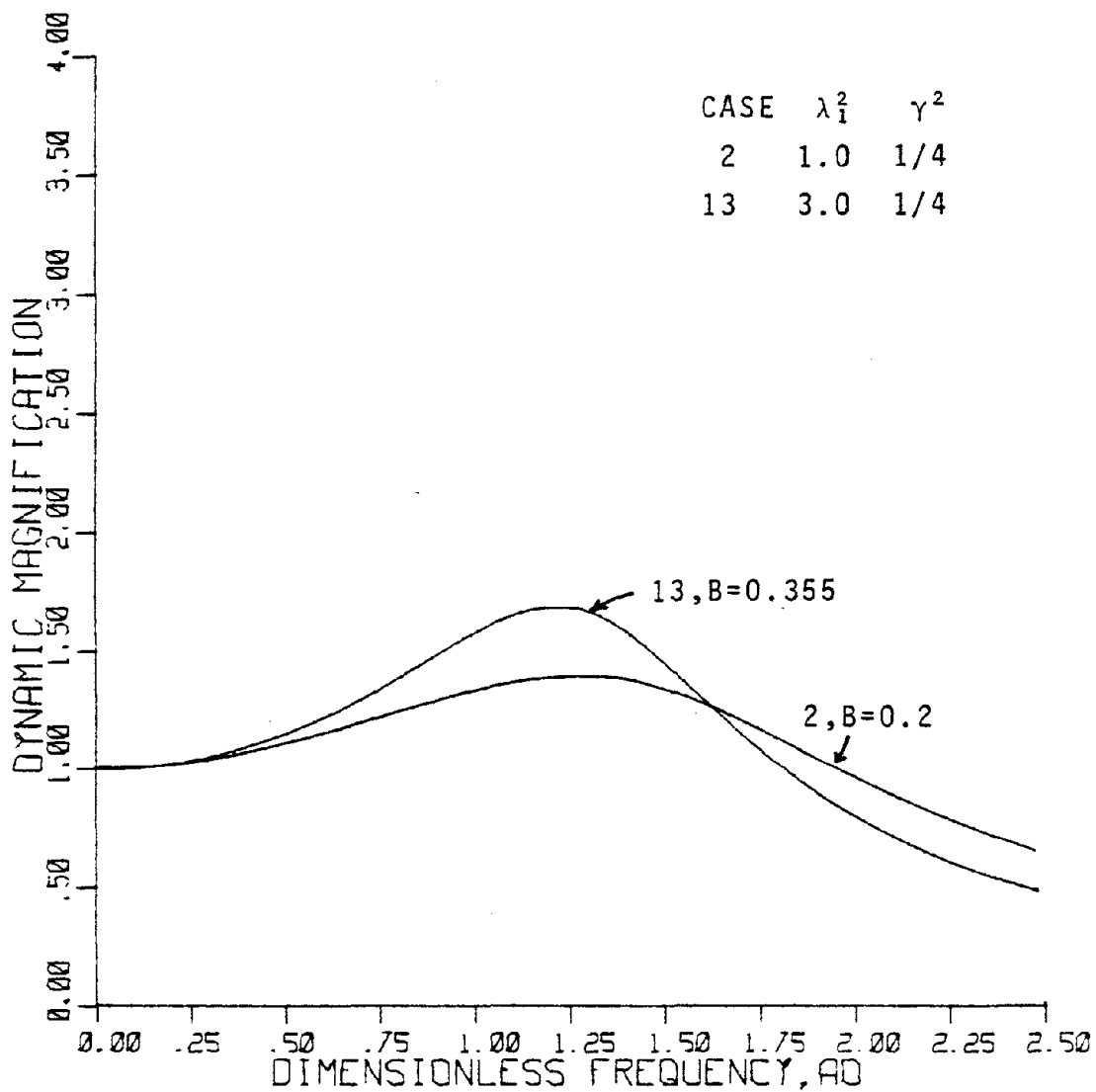
CASE	$\lambda_1^2$	$\gamma^2$
2	1.0	1/4
13	3.0	1/4



ROCKING VIBRATION  
FIGURE 5.11

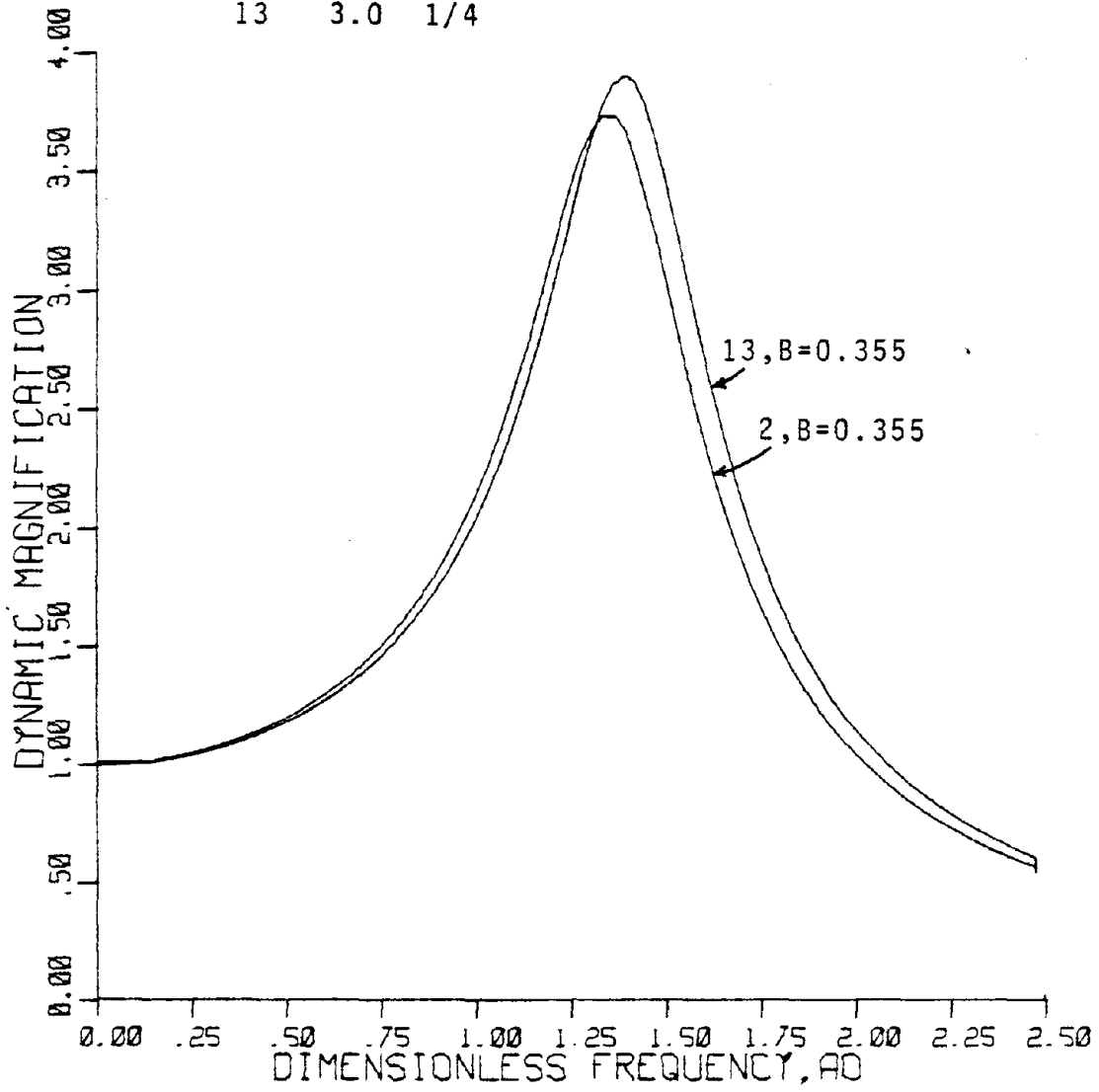


ROCKING VIBRATION  
 CONSTANT HYSTERETIC,  $\tan\delta=0.3$   
 FIGURE 5.12



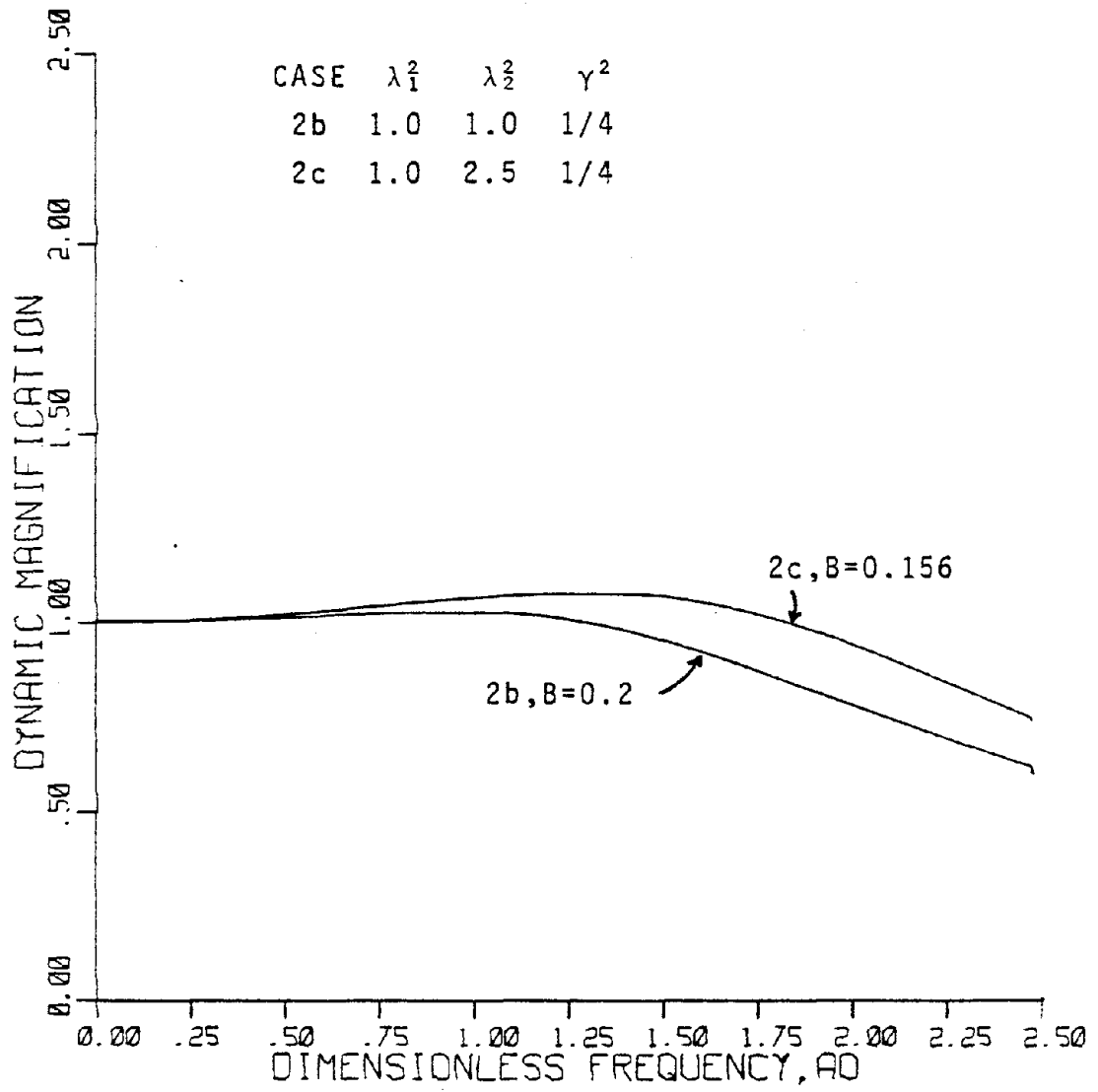
ROCKING VIBRATION  
VISCOUS,  $\zeta=0.3$   
FIGURE 5.13

CASE	$\lambda_1^2$	$\gamma^2$
2	1.0	1/4
13	3.0	1/4



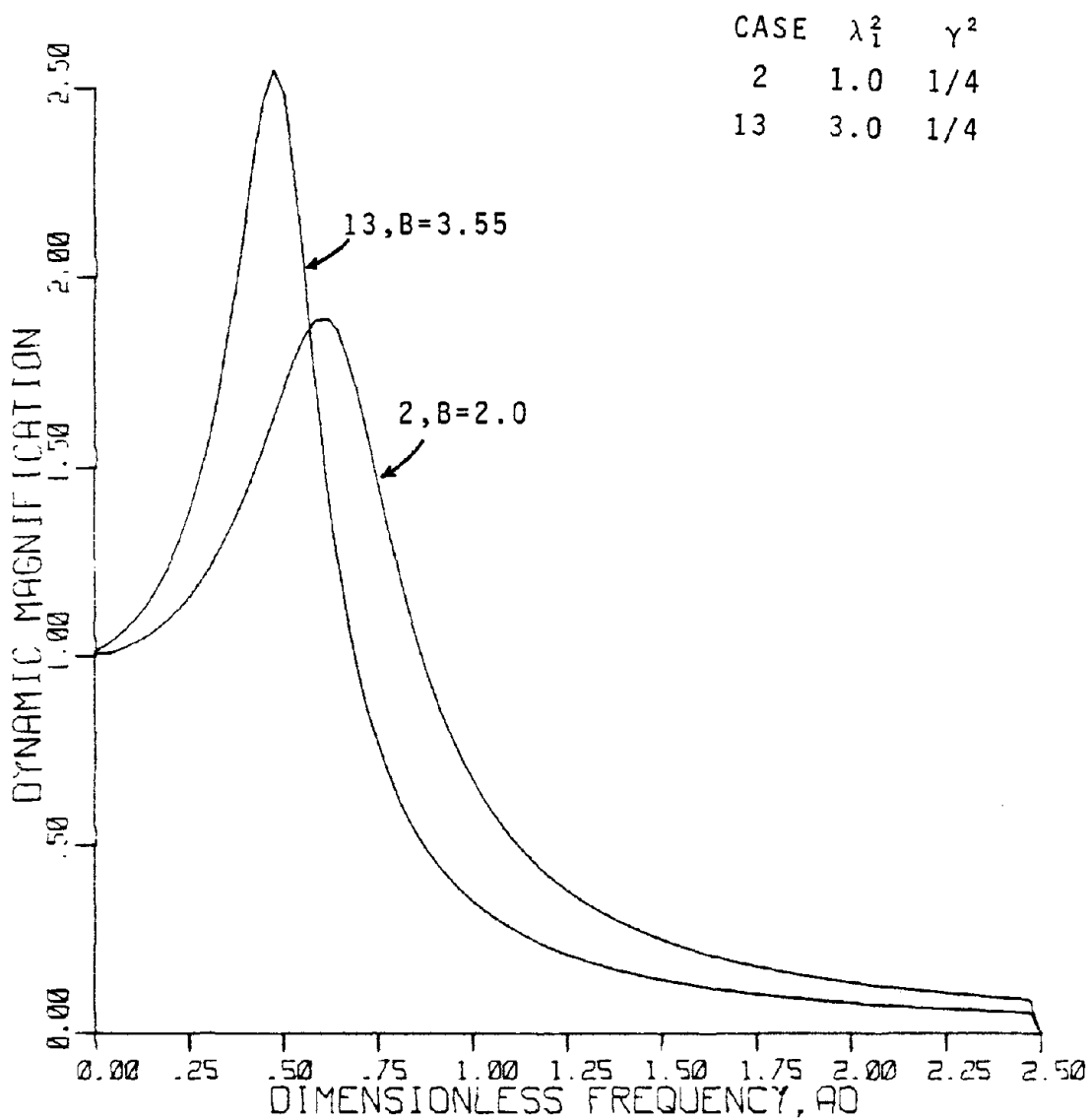
ROCKING VIBRATION  
FIGURE 5.14



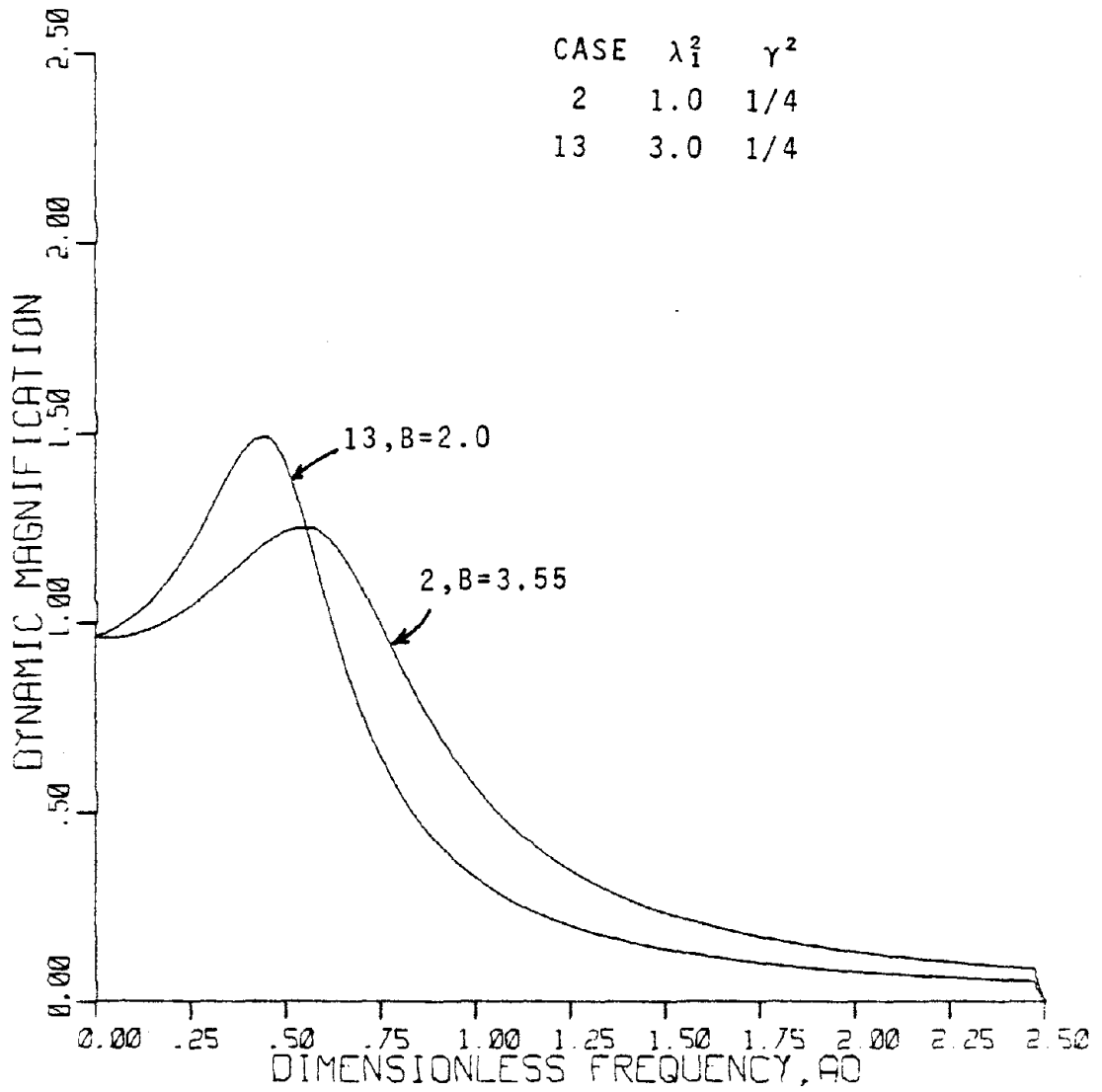


HORIZONTAL VIBRATION

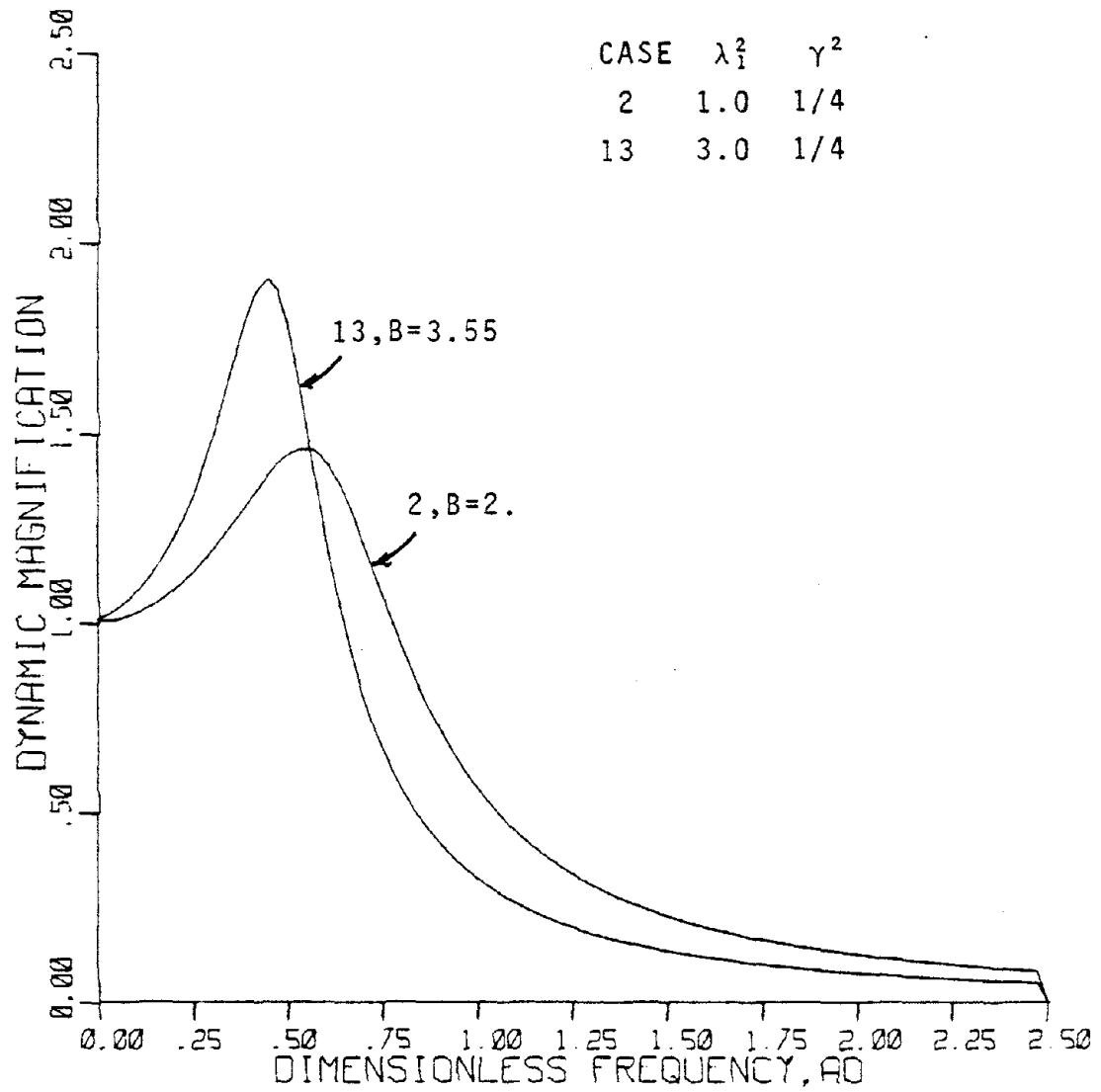
FIGURE 5.15



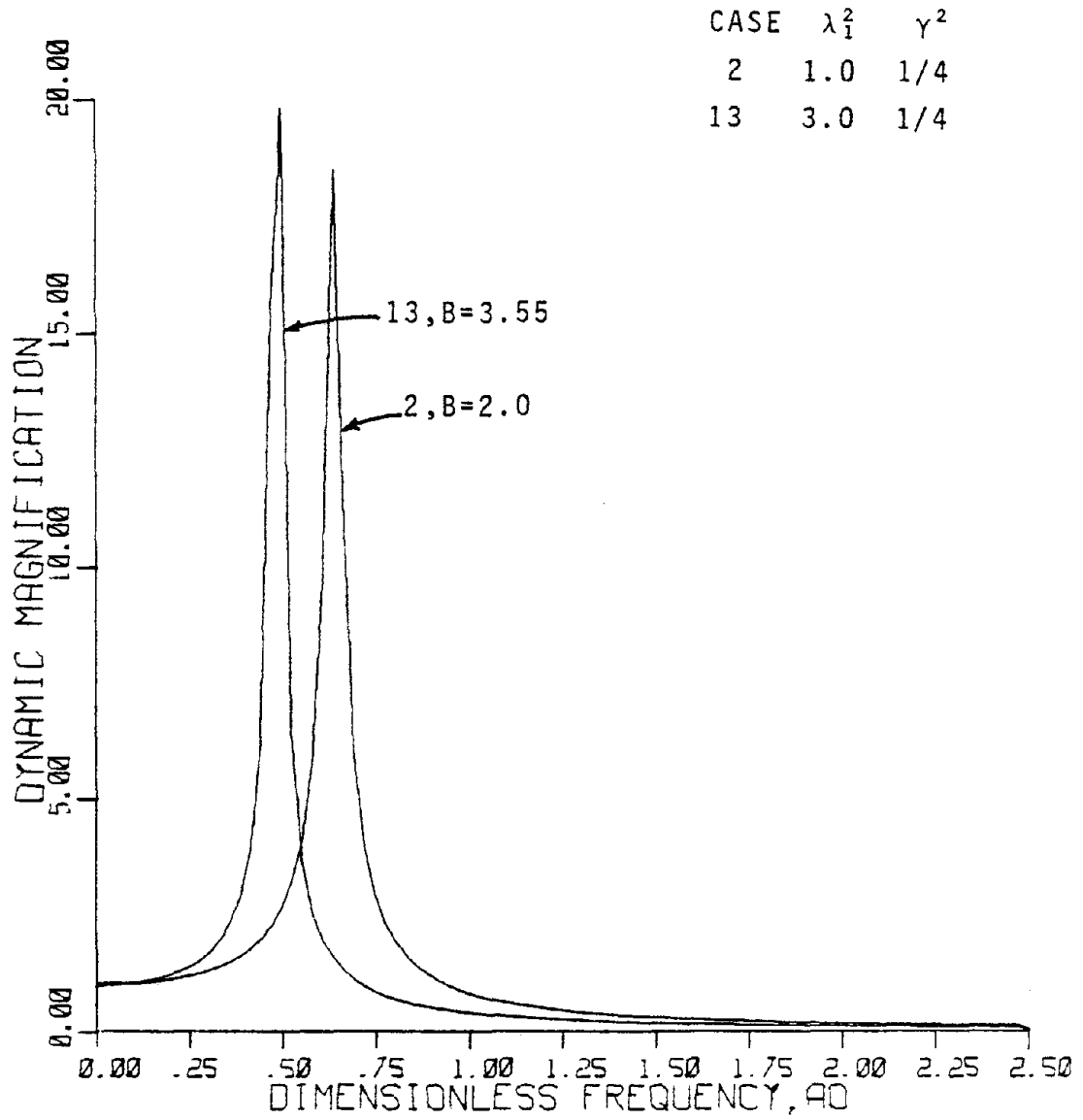
VERTICAL VIBRATION  
FIGURE 5.16



VERTICAL VIBRATION  
 CONSTANT HYSTERETIC,  $\tan\delta=0.3$   
 FIGURE 5.17



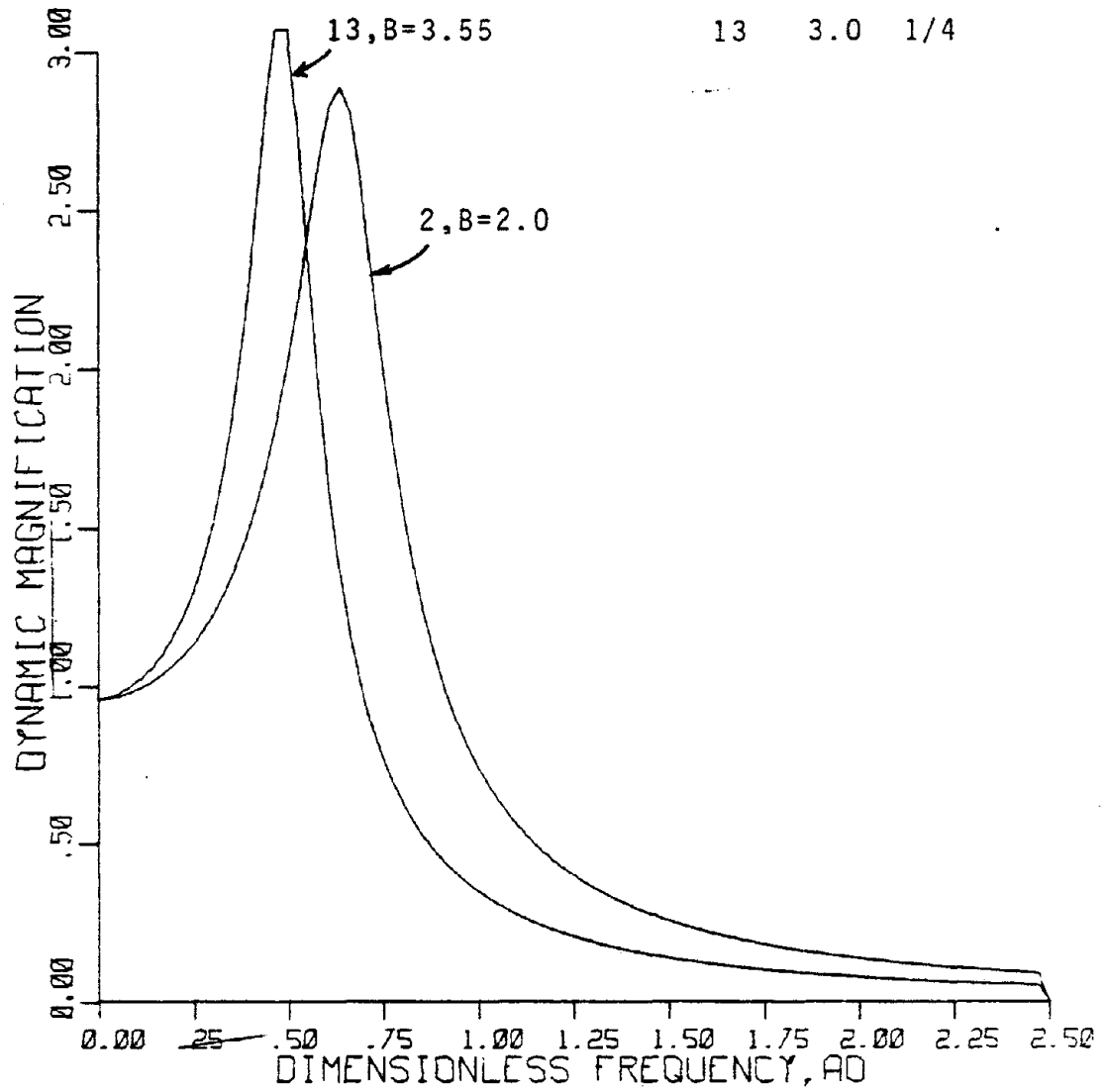
VERTICAL VIBRATION  
 VISCOUS,  $\zeta=0.3$   
 FIGURE 5.18



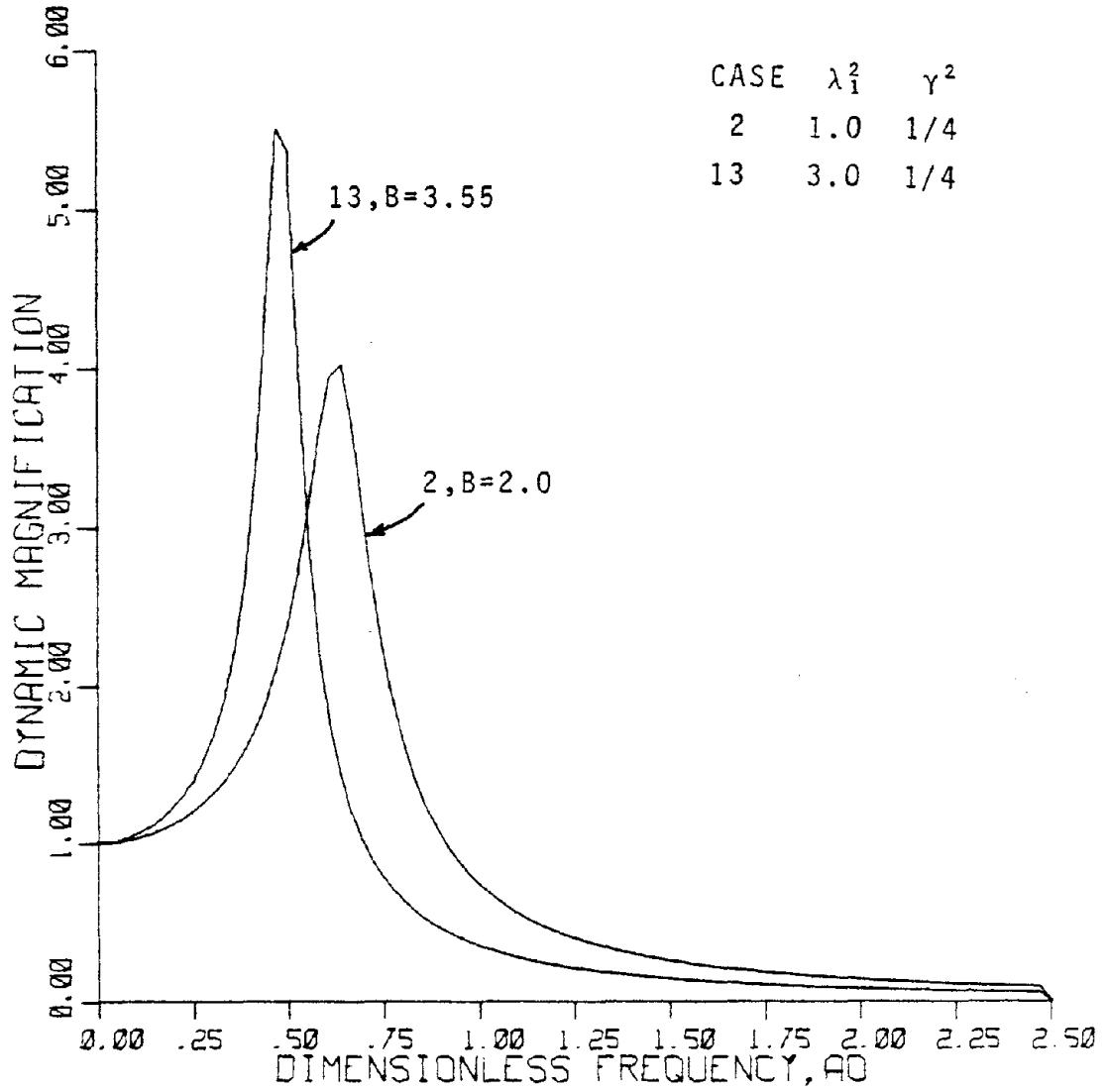
ROCKING VIBRATION

FIGURE 5.19

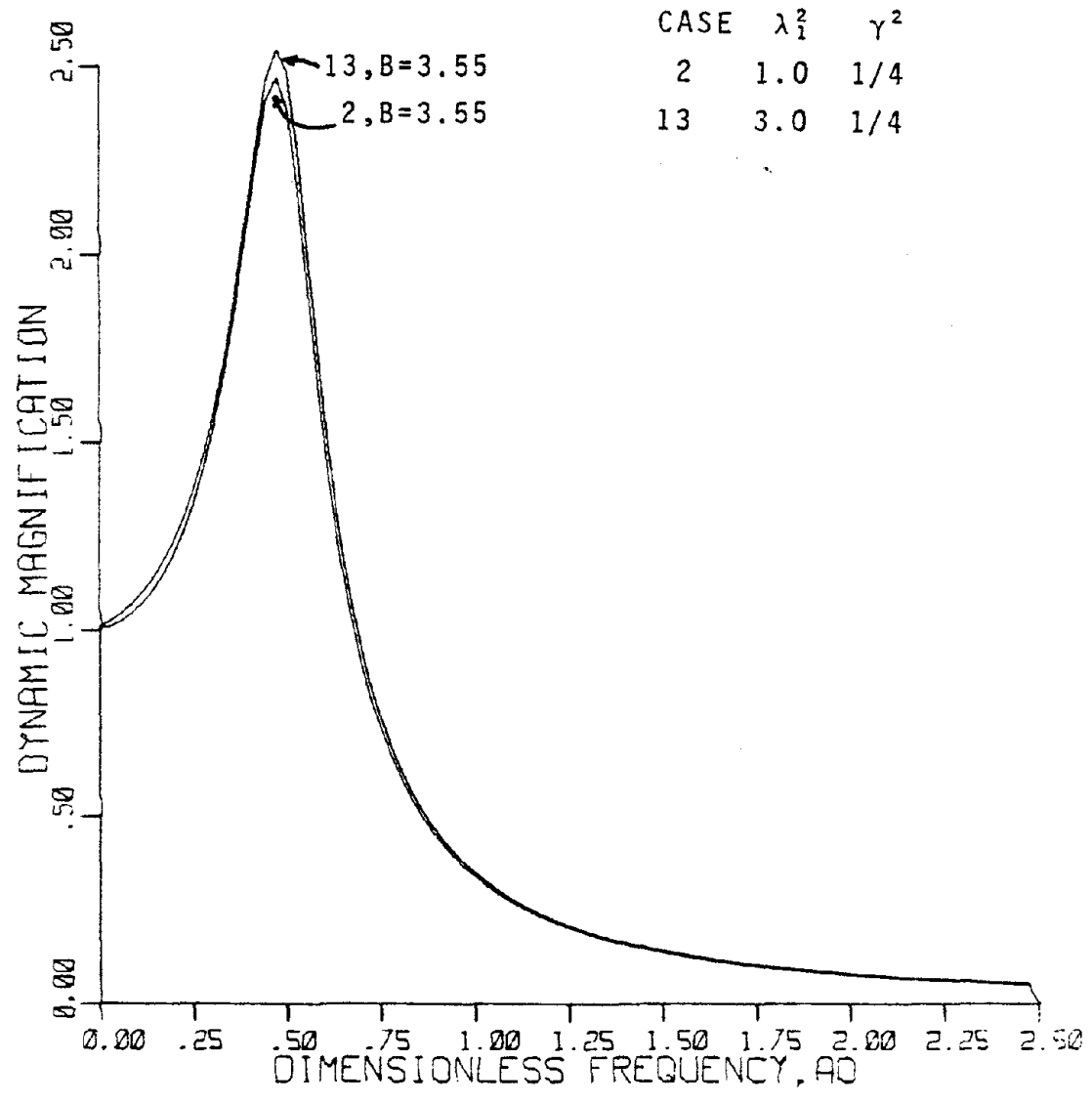
CASE	$\lambda_1^2$	$\gamma^2$
2	1.0	1/4
13	3.0	1/4



ROCKING VIBRATION  
CONSTANT HYSTERETIC,  $\tan\delta=0.3$   
FIGURE 5.20

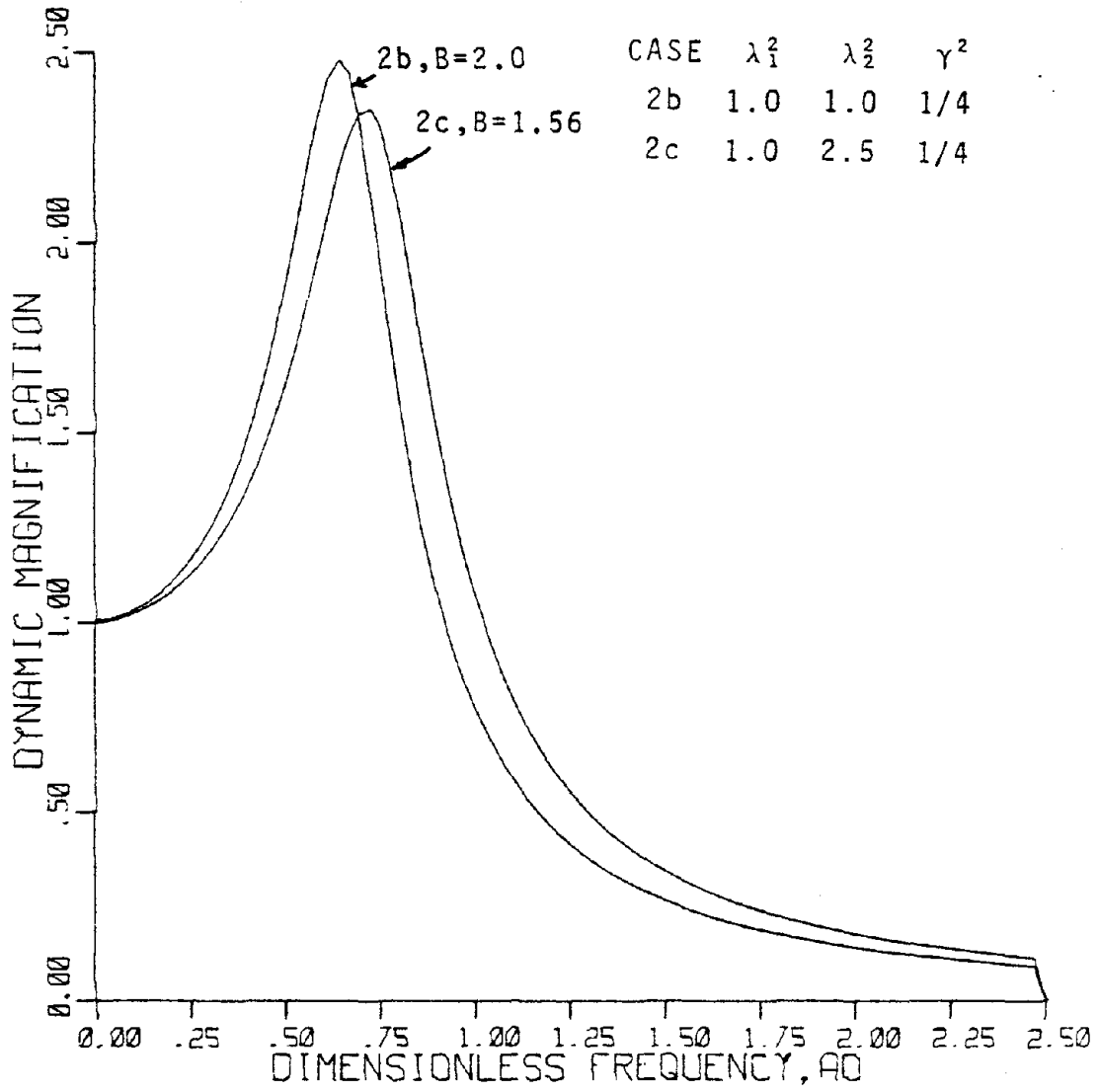


ROCKING VIBRATION  
 VISCOUS,  $\zeta=0.3$   
 FIGURE 5.21



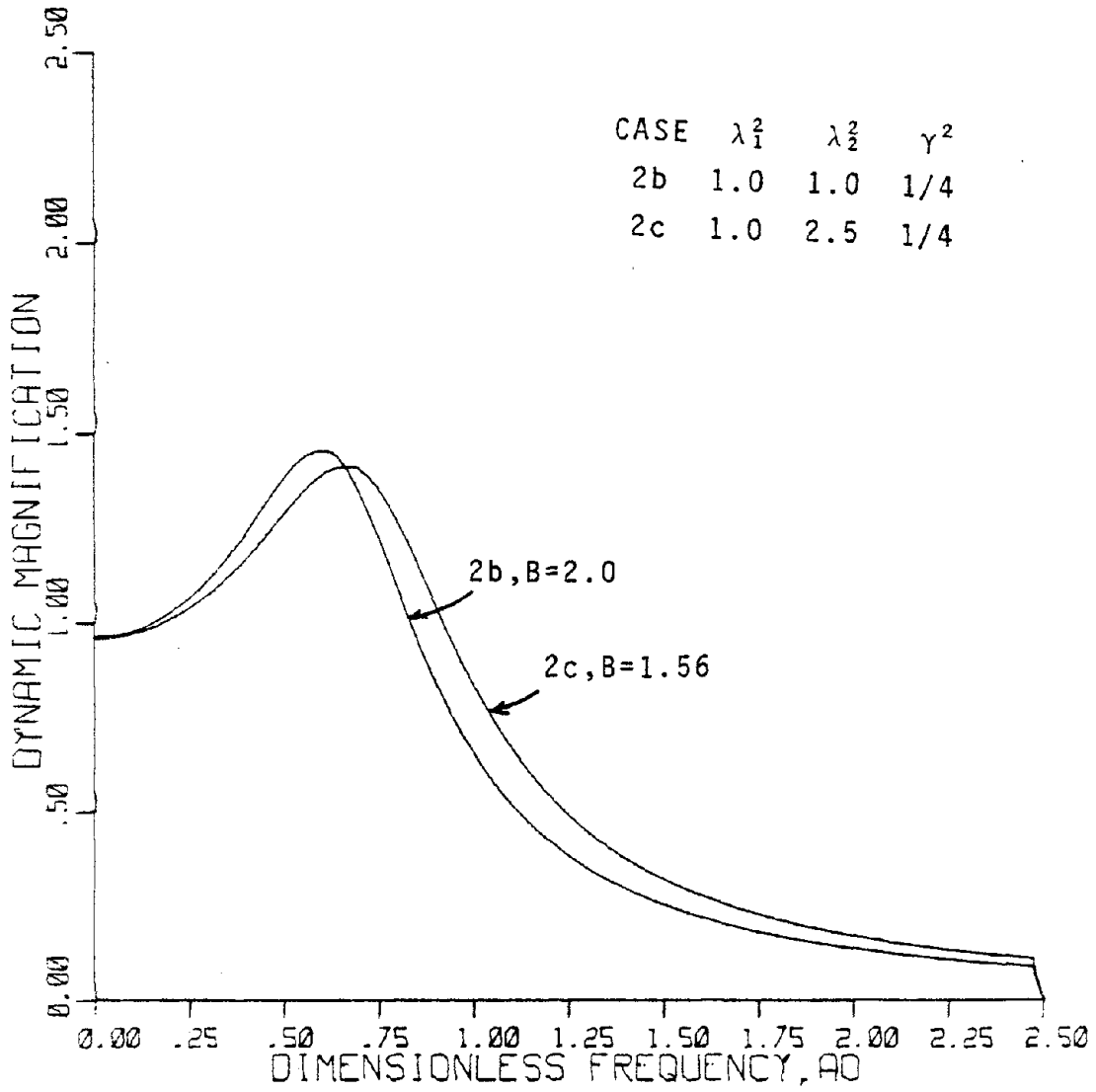
VERTICAL VIBRATION  
 FIGURE 5.22



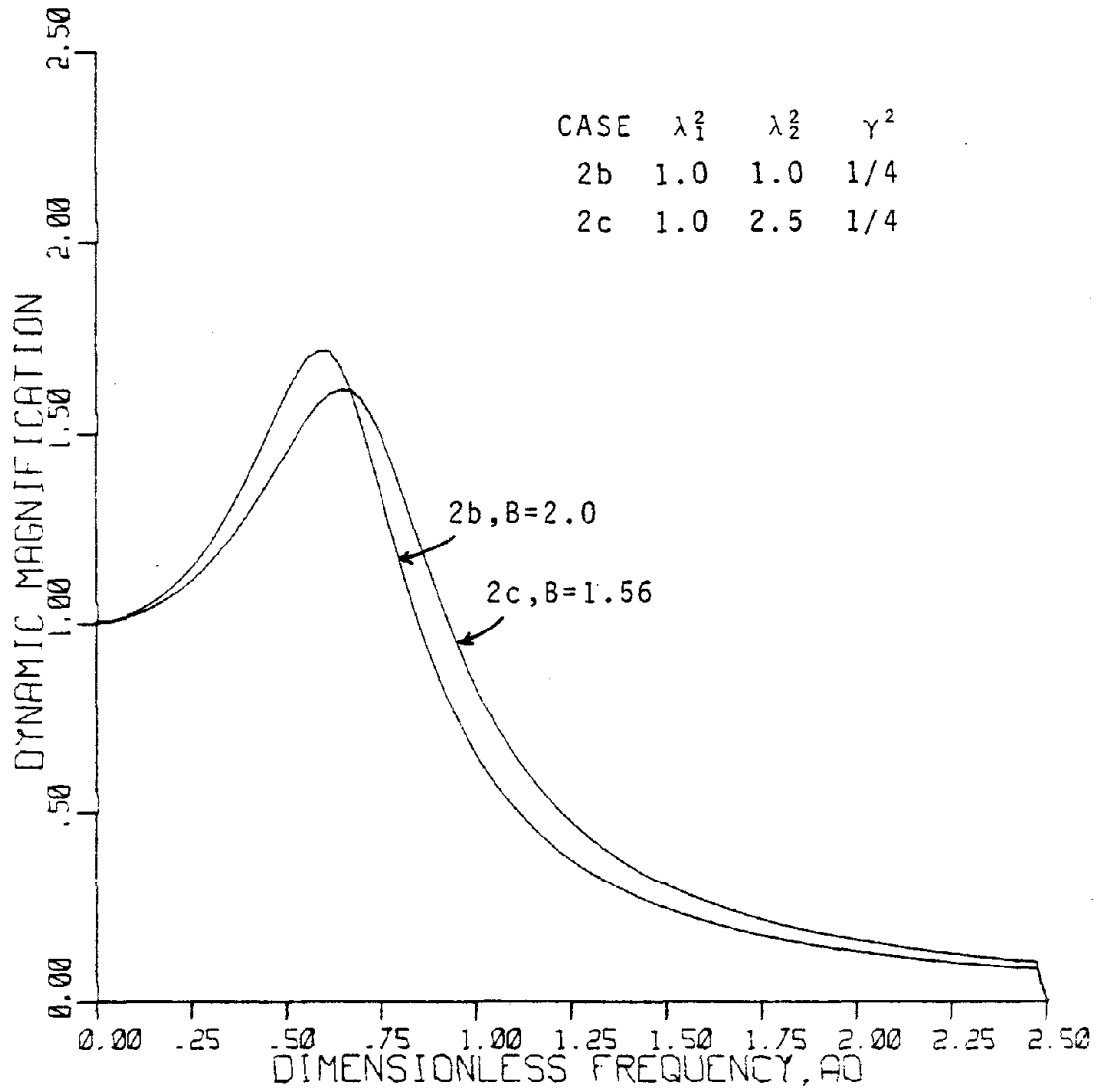


HORIZONTAL VIBRATION

FIGURE 5.23



HORIZONTAL VIBRATION  
 CONSTANT HYSTERETIC,  $\tan\delta=0.3$   
 FIGURE 5.24



HORIZONTAL VIBRATION

VISCOUS,  $\zeta=0.3$

FIGURE 5.25

TABLE 2.1

No.	$n = \frac{E_H}{E_V}$	$\nu_{VH}$	$\nu_H$	$\frac{G}{E_H}$	$\lambda_1^2$	$\lambda_2^2$	$\gamma^2$	$\frac{G}{E_H}(\text{calc})$
1	2	.375	.125	.223	1.46	2.00	.109	.236
2	4	.188	.125	.16	3.49	2.78	.124	.164
3	4	.188	.125	.04	3.49	11.11	.031	.164
4	0.5	.167	.75	.60	1.13	.476	.236	.818
5	2	.167	.333	.225	2.125	1.667	.177	.273
6	4	.083	.333	.15	1.094	2.5	.126	.50
7	1.5	.20	.25	.30	1.5	1.33	.25	.323
8	3.0	0.3	.10	.167	2.212	2.73	.09	.193
9	1.235	0.5	.383	.287	1.0	1.235	0	.293
10	1.33	0.5	.335	.272	1.0	1.33	0	.282

TABLE 2.2

DIMENSIONLESS CONSTANTS

Case No. *	$\lambda_1^2$	$\gamma^2$	$\phi$	$\lambda_2^2$	s **
1 a,b,c	1.0	0.	2.0	0.5, 1.0, 2.5	1.04678
2 a,b,c	1.0	0.25	2.0		1.07236
3 a,b,c	1.0	0.33	2.0		1.08767
4 a,b,c	1.0	0.50	2.0		1.14414
5 a,b,c	1.5	0.	2.22		1.04173
6 a,b,c	1.5	0.25	2.34		1.07476
7 a,b,c	1.5	0.33	2.41		1.09855
8 a,b,c	1.5	0.50	2.73		1.21480
9 a,b,c	2.0	0.	2.41		1.03794
10 a,b,c	2.0	0.25	2.73		1.07868
11 a,b,c	2.0	0.33	3.00		1.11535
12 a,b,c	3.0	0.	2.73		1.0325
13 a,b,c	3.0	0.25	4.00		1.09445
14 a,b,c	4.0	0.	3.00	0.5, 1.0, 2.5	1.02872

\* Case No. 1 indicates  $\lambda_1^2 = 1.$ ,  $\gamma^2 = 0.$ ,  $\phi = 2$ ,  $s = 1.04678$ , the a,b, or c indicated whether  $\lambda_2^2 = 0.5, 1.0$  or  $2.5$  respectively.

\*\* s is the ratio of the surface wave velocity to the shear wave velocity,  $\sqrt{G/\rho}$

## APPENDIX A

### A.1 WEBER SCHAFFHEITLIN TYPE INTEGRAL

From reference (43)

$$W(\lambda, \mu, \nu, a, b) = \int_0^{\infty} t^{\lambda} J_{\mu}(at) J_{\nu}(bt) dt$$

$$W(\lambda, \mu, \nu, a, b) = \frac{\left(\frac{b}{a}\right)^{\nu} \left(\frac{a}{2}\right)^{\lambda-1} \Gamma\left(\frac{\mu+\nu-\lambda+1}{2}\right)}{2\Gamma(\nu+1)\Gamma\left(\frac{\mu-\nu+\lambda+1}{2}\right)} {}_2F_1(c, d, e, f)$$

If  $\lambda = \mu - \nu - 1$

$$W(\lambda, \mu, \nu, a, b) = \begin{cases} 0 & , 0 < a < b \\ \frac{b^{\nu} (a^2 - b^2)^{\lambda}}{2^{\lambda} a^{\mu} \Gamma(\lambda + 1)} & , 0 < b < a \end{cases}$$

where  $\Gamma(\ )$  is the gamma function and  ${}_2F_1$  is the hypergeometric series and

$$c = \frac{\mu + \nu - \lambda + 1}{2}$$

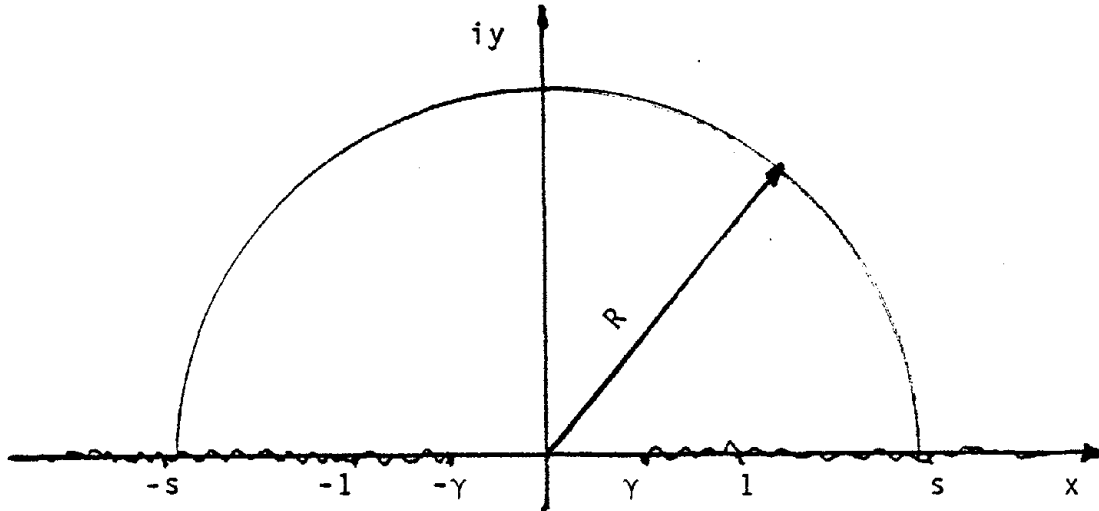
$$d = \frac{\nu - \mu - \lambda + 1}{2}$$

$$e = \nu + 1$$

$$f = (b/a)^2$$

A.2 CONTOUR INTEGRATION

The semi infinite integrals appearing in the kernels of the integral equations of Chapter 3 can be reduced to finite integrals by a contour integration around the closed contour shown below.



Replace  $k$  in the semi infinite integrals with the complex variable  $z=x+iy$ . According to the branch cuts indicated interpret  $V_\alpha, V_\beta$  and  $V_{\beta H}$

$$V_\alpha = \begin{cases} (z^2 - \gamma^2)^{\frac{1}{2}} & , z > \gamma \\ -(z^2 - \gamma^2)^{\frac{1}{2}} & , z < -\gamma \end{cases}$$

$$V_\beta = \begin{cases} (z^2 - 1)^{\frac{1}{2}} & , z > 1 \\ -(z^2 - 1)^{\frac{1}{2}} & , z < -1 \end{cases}$$

$$V_{\beta H} = \begin{cases} (z^2 - 1/\lambda_2^2)^{1/2} & , z > 1/\lambda_2 \\ -(z^2 - 1/\lambda_2^2)^{1/2} & , z < -1/\lambda_2 \end{cases}$$

This interpretation is consistent with the radiation condition at infinity. The kernel functions after contour integration are

$$L(\bar{X}, U) = \bar{L}_1(\bar{X}+U) + \bar{L}_1(|\bar{X}-U|)$$

where

$$\begin{aligned} \bar{L}_1(t) = & -\frac{a_0 i}{\Psi_V} \{ \pi R_V(s) e^{-ia_0 s t} \\ & + \int_0^\gamma \frac{k(\gamma^2 - k^2)^{1/2} \lambda_1 (\phi k^2 (\phi - 2) + 1) e^{-ia_0 k t} dk}{(\phi k^2 - 1)^2 + \phi^2 k^2 \lambda_1 (1 - k^2)^{1/2} (\gamma^2 - k^2)^{1/2}} \\ & + \int_\gamma^1 \frac{k(\phi k^2 - 1)^2 (\gamma^2 - k^2)^{1/2} \lambda_1 (\phi k^2 (\phi - 2) + 1) e^{-ia_0 k t} dk}{(\phi k^2 - 1)^4 + \phi^4 k^4 \lambda_1^2 (k^2 - \gamma^2) (1 - k^2)} \} \end{aligned} \quad (A.1)$$

where the residue term is

$$R_V(s) = \frac{s \lambda_1 (s^2 - \gamma^2)^{1/2} (\phi s^2 (\phi - 2) + 1)}{\left. \frac{dF(k)}{dk} \right|_{k=s}} \quad (A.2)$$

$$F(k) = (\phi k^2 - 1)^4 + \phi^4 k^4 \lambda_1^2 (k^2 - \gamma^2) (1 - k^2)$$

and s is the real root of f(k)=0.

where  $f(k) = (\phi k^2 - 1)^2 - \phi^2 k^2 \lambda_1 (1 - k^2)^{1/2} (\gamma^2 - k^2)^{1/2}$

surface wave equation (see Chapter 2)



$$L_2(\underline{X}, U) = -(\bar{L}_1(\underline{X}+U) - \bar{L}_1(|\underline{X}-U|))$$

$$L_3(\underline{X}, U) = \bar{L}_3(\underline{X}+U) + \bar{L}_3(|\underline{X}-U|)$$

where

$$\begin{aligned} \bar{L}(t) = & -\frac{a_0 i}{\Psi_H} \left\{ \pi R_H(s) e^{-ia_0 s t} \right. \\ & + \int_0^\gamma \frac{k(1-k^2)^{\frac{1}{2}}(\phi k^2(\phi-2)+1)e^{-ia_0 k t} dk}{(\phi k^2-1)^2 + \phi^2 k^2 \lambda_1 (1-k^2)^{\frac{1}{2}}(\gamma^2-k^2)^{\frac{1}{2}}} \\ & + \int_\gamma^1 \frac{k(\phi k^2-1)^2(1-k^2)^{\frac{1}{2}}(\phi k^2(\phi-2)+1)e^{-ia_0 k t} dk}{(\phi k^2-1)^4 + \phi^4 k^4 \lambda_1^2 (k^2-\gamma^2)(1-k^2)} \\ & \left. + \int_0^{1/\lambda_2} \frac{k e^{-ia_0 k t} dk}{\lambda_2 (1/\lambda_2^2 - k^2)^{\frac{1}{2}}} \right\} \quad (A.3) \end{aligned}$$

where

$$R_H(s) = \frac{s(s^2-1)^{\frac{1}{2}}(\phi s^2(\phi-2)+1)}{\left. \frac{dF(k)}{dk} \right|_{k=s}} \quad (A.4)$$

APPENDIX B

TABLE 3-1  
VERTICAL VIBRATION  
COMPLIANCE & IMPEDANCE COEFFICIENTS

CASE 1  
 $\gamma^2 = 0.00$   
 $\lambda_1^2 = 1.00$   
 $\Psi_V = 0.50$

FREQUENCY	F	G	K	C
.50	.8602-00	-.3886-00	.9508-00	.8395-00
1.00	.5884-00	-.6187-00	.8070-00	.8515-00
1.50	.2850-00	-.6402-00	.5803-00	.8690-00
2.00	.8911-01	-.5490-00	.2880-00	.6873-00
2.50	-.1120-01	-.4441-00	-.5670-01	.9000-00
3.00	-.8104-01	-.3590-00	-.4804-00	.9025-00
3.50	-.8732-01	-.2931-00	-.9336-00	.8954-00
4.00	-.1019+00	-.2400-00	-.1500+01	.8826-00
4.50	-.1086+00	-.1954-00	-.2173+01	.8689-00
5.00	-.1088+00	-.1579-00	-.2958+01	.8586-00
5.50	-.1046+00	-.1270-00	-.3844+01	.8522-00
6.00	-.9773-01	-.1038+00	-.4808+01	.8511-00
6.50	-.9020-01	-.8547-01	-.5841+01	.8516-00
7.00	-.8296-01	-.7115-01	-.6945+01	.8509-00
7.50	-.7627-01	-.5967-01	-.8134+01	.8484-00
8.00	-.7005-01	-.5028-01	-.9421+01	.8453-00

CASE 2  
 $\gamma^2 = 0.25$   
 $\lambda_1^2 = 1.00$   
 $\Psi_V = 0.667$

FREQUENCY	F	G	K	C
.50	.8841-00	-.3618-00	.9689-00	.7930-00
1.00	.6056-00	-.5653-00	.8825-00	.8236-00
1.50	.3331-00	-.5700-00	.7643-00	.8718-00
2.00	.1688-00	-.4790-00	.6545-00	.9285-00
2.50	.9323-01	-.3861-00	.5910-00	.9790-00
3.00	.5995-01	-.3178-00	.5731-00	.1013+01
3.50	.4359-01	-.2705-00	.5805-00	.1029+01
4.00	.3327-01	-.2363-00	.5844-00	.1038+01
4.50	.2591-01	-.2095-00	.5815-00	.1045+01
5.00	.2096-01	-.1875-00	.5886-00	.1054+01
5.50	.1769-01	-.1694-00	.6166-00	.1061+01
6.00	.1649-01	-.1549-00	.6792-00	.1064+01
6.50	.1557-01	-.1435-00	.7470-00	.1059+01
7.00	.1446-01	-.1344-00	.7909-00	.1050+01
7.50	.1291-01	-.1268-00	.7951-00	.1041+01
8.00	.1104-01	-.1198+00	.7625-00	.1035+01

TABLE 3.1 CONTINUED

CASE 3  
 $\gamma^2 = 0.333$   
 $\lambda_1^2 = 1.00$   
 $\Psi_V = 0.75$

FREQUENCY	F	G	K	C
.50	.8810-00	-.3640-00	.9696-00	.8012-00
1.00	.5982-00	-.5631-00	.8863-00	.8343-00
1.50	.3282-00	-.5605-00	.7779-00	.8858-00
2.00	.1709-00	-.4670-00	.6910-00	.9442-00
2.50	.1011+00	-.3764-00	.6654-00	.9913-00
3.00	.7075-01	-.3121-00	.6907-00	.1016+01
3.50	.5520-01	-.2689-00	.7326-00	.1020+01
4.00	.4417-01	-.2381-00	.7535-00	.1015+01
4.50	.3509-01	-.2138-00	.7473-00	.1012+01
5.00	.2791-01	-.1933-00	.7318-00	.1014+01
5.50	.2204-01	-.1756-00	.7222-00	.1018+01
6.00	.1945-01	-.1608-00	.7411-00	.1021+01
6.50	.1725-01	-.1487-00	.7695-00	.1021+01
7.00	.1532-01	-.1388-00	.7854-00	.1017+01
7.50	.1352-01	-.1302-00	.7771-00	.1013+01
8.00	.1155-01	-.1225+00	.7504-00	.1012+01

CASE 4  
 $\gamma^2 = 0.50$   
 $\lambda_1^2 = 1.00$   
 $\Psi_V = 1.00$

FREQUENCY	F	G	K	C
.50	.8822-00	-.3892-00	.9835-00	.8698-00
1.00	.5476-00	-.5776-00	.8645-00	.9119-00
1.50	.2742-00	-.5435-00	.7394-00	.9777-00
2.00	.1350-00	-.4338-00	.6538-00	.1051+01
2.50	.8138-01	-.3428-00	.6571-00	.1104+01
3.00	.6088-01	-.2836-00	.7216-00	.1124+01
3.50	.4972-01	-.2457-00	.7909-00	.1117+01
4.00	.4049-01	-.2193-00	.8139-00	.1102+01
4.50	.3173-01	-.1982-00	.7873-00	.1093+01
5.00	.2431-01	-.1795-00	.7407-00	.1094+01
5.50	.1885-01	-.1627-00	.7030-00	.1103+01
6.00	.1591-01	-.1483-00	.7149-00	.1111+01
6.50	.1425-01	-.1367-00	.7547-00	.1114+01
7.00	.1274-01	-.1273-00	.7905-00	.1111+01
7.50	.1132-01	-.1193+00	.8016-00	.1107+01
8.00	.1004-01	-.1122+00	.7905-00	.1105+01

TABLE 3.1 CONTINUED

CASE 5

$\gamma^2 = 0.00$

$\lambda_1^2 = 1.5$

$\Psi_V = 0.54$

FREQUENCY	F	G	K	C
.50	.8906-00	-.3527-00	.9706-00	.7689-00
1.00	.6220-00	-.5605-00	.8471-00	.7987-00
1.50	.3480-00	-.5770-00	.7653-00	.8468-00
2.00	.1709-00	-.4911-00	.6323-00	.9082-00
2.50	.8312-01	-.3930-00	.5151-00	.9742-00
3.00	.4202-01	-.3152-00	.4155-00	.1039+01
3.50	.2155-01	-.2571-00	.3237-00	.1103+01
4.00	.9917-02	-.2117-00	.2207-00	.1178+01
4.50	.3501-02	-.1740-00	.1182+00	.1277+01
5.00	.1034-02	-.1410-00	.9149-01	.1412+01
5.50	.3927-02	-.1141+00	.3014-00	.1592+01
6.00	.9094-02	-.9163-01	.1073+01	.1801+01
6.50	.1505-01	-.7380-01	.2745+01	.1993+01
7.00	.2247-01	-.5990-01	.5491+01	.2091+01
7.50	.2905-01	-.4876-01	.9018+01	.2018+01
8.00	.3525-01	-.3970-01	.1250+02	.1760+01

CASE 6

$\gamma^2 = 0.25$

$\lambda_1^2 = 1.5$

$\Psi_V = 0.792$

FREQUENCY	F	G	K	C
.50	.8804-00	-.3433-00	.9794-00	.7569-00
1.00	.6221-00	-.5328-00	.9273-00	.7942-00
1.50	.3651-00	-.5318-00	.8774-00	.8521-00
2.00	.2143-00	-.4419-00	.8885-00	.9162-00
2.50	.1405-00	-.3535-00	.1010+01	.9618-00
3.00	.1220+00	-.2912-00	.1224+01	.9738-00
3.50	.1090+00	-.2505-00	.1466+01	.9570-00
4.00	.1012+00	-.2228-00	.1690+01	.9302-00
4.50	.9334-01	-.2020-00	.1885+01	.9060-00
5.00	.8607-01	-.1845-00	.2076+01	.8902-00
5.50	.7908-01	-.1689-00	.2288+01	.8797-00
6.00	.7571-01	-.1551-00	.2541+01	.8677-00
6.50	.7297-01	-.1435-00	.2816+01	.8519-00
7.00	.7094-01	-.1339-00	.3090+01	.8331-00
7.50	.6945-01	-.1259-00	.3350+01	.8143-00
8.00	.6708-01	-.1188+00	.3603+01	.7977-00

TABLE 3.1 CONTINUED

CASE 7

$\gamma^2 = 0.333$

$\lambda_1^2 = 1.5$

$\Psi_V = 0.927$

FREQUENCY	F	G	K	C
.50	.8795-00	-.3586-00	.9749-00	.7950-00
1.00	.5907-00	-.5475-00	.9099-00	.8348-00
1.50	.3543-00	-.5343-00	.8415-00	.8967-00
2.00	.1807-00	-.4370-00	.8326-00	.9644-00
2.50	.1200-00	-.3482-00	.9337-00	.1011+01
3.00	.1050+00	-.2881-00	.1117+01	.1021+01
3.50	.9559-01	-.2499-00	.1314+01	.1003+01
4.00	.8446-01	-.2242-00	.1471+01	.9764-00
4.50	.7528-01	-.2040-00	.1584+01	.9565-00
5.00	.6847-01	-.1874-00	.1681+01	.9479-00
5.50	.5900-01	-.1713-00	.1798+01	.9490-00
6.00	.5412-01	-.1565-00	.1973+01	.9510-00
6.50	.5125-01	-.1439-00	.2196+01	.9486-00
7.00	.4946-01	-.1336-00	.2436+01	.9406-00
7.50	.4800-01	-.1250-00	.2677+01	.9295-00
8.00	.4654-01	-.1177+00	.2905+01	.9184-00

CASE 8

$\gamma^2 = 0.50$

$\lambda_1^2 = 1.5$

$\Psi_V = 1.457$

FREQUENCY	F	G	K	C
.50	.8552-00	-.4244-00	.9529-00	.9709-00
1.00	.4732-00	-.5918-00	.8242-00	.1031+01
1.50	.2006-00	-.5120-00	.8634-00	.1129+01
2.00	.8702-01	-.3815-00	.5718-00	.1245+01
2.50	.5018-01	-.2890-00	.8480-00	.1334+01
3.00	.4091-01	-.2343-00	.8540-00	.1363+01
3.50	.4070-01	-.2019-00	.1088+01	.1343+01
4.00	.4526-01	-.1809-00	.1250+01	.1307+01
4.50	.3804-01	-.1650-00	.1327+01	.1279+01
5.00	.3225-01	-.1509-00	.1355+01	.1268+01
5.50	.2701-01	-.1373-00	.1379+01	.1275+01
6.00	.2407-01	-.1249+00	.1489+01	.1287+01
6.50	.2201-01	-.1143+00	.1679+01	.1295+01
7.00	.2254-01	-.1058+00	.1911+01	.1293+01
7.50	.2197-01	-.9895-01	.2138+01	.1284+01
8.00	.2140-01	-.9321-01	.2340+01	.1274+01

TABLE 3:1 CONTINUED

## CASE 9

$\gamma^2 = 0.00$

$\lambda_1^2 = 2.0$

$\Psi_V = 0.581$

FREQUENCY	F	G	K	C
.50	.8993-00	-.3231-01	.9848-01	.7077-00
1.00	.8529-00	-.5128-00	.9475-00	.7440-00
1.50	.4001-00	-.5288-00	.9148-00	.8028-00
2.00	.2380-00	-.4440-00	.9378-00	.8747-00
2.50	.1800-00	-.3512-00	.1074+01	.9433-00
3.00	.1260-00	-.2787-00	.1347+01	.9931-00
3.50	.1108+00	-.2282-00	.1746+01	.1019+01
4.00	.1028+00	-.1867-00	.2260+01	.1029+01
4.50	.9788-01	-.1547-00	.2917+01	.1027+01
5.00	.9585-01	-.1271-00	.3780+01	.1005+01
5.50	.9847-01	-.1030+00	.4848+01	.9403-00
6.00	.1003+00	-.8245-01	.5950+01	.8154-00
6.50	.1039+00	-.6573-01	.6817+01	.6509-00
7.00	.1123+00	-.5245-01	.7310+01	.4878-00
7.50	.1188+00	-.4193-01	.7485+01	.3521-00
8.00	.1251-00	-.3350-01	.7458+01	.2498-00

## CASE 10

$\gamma^2 = 0.25$

$\lambda_1^2 = 2.0$

$\Psi_V = 0.913$

FREQUENCY	F	G	K	C
.50	.8892-00	-.3357-01	.9842-01	.7430-00
1.00	.8287-00	-.5175-00	.9488-00	.7834-00
1.50	.3787-00	-.5110-00	.9347-00	.8452-00
2.00	.2339-00	-.4197-00	.1013+01	.9090-00
2.50	.1747-00	-.3329-00	.1238+01	.9421-00
3.00	.1529-00	-.2735-00	.1557+01	.9284-00
3.50	.1440-00	-.2384-00	.1880+01	.8817-00
4.00	.1373-00	-.2128-00	.2143+01	.8299-00
4.50	.1297-00	-.1958-00	.2352+01	.7887-00
5.00	.1213+00	-.1817-00	.2542+01	.7613-00
5.50	.1130+00	-.1681-00	.2754+01	.7449-00
6.00	.1088+00	-.1549-00	.3018+01	.7300-00
6.50	.1024+00	-.1427-00	.3319+01	.7118-00
7.00	.9978-01	-.1323-00	.3634+01	.6883-00
7.50	.9797-01	-.1238+00	.3937+01	.6625-00
8.00	.9841-01	-.1183+00	.4224+01	.6370-00

TABLE 3.1 CONTINUED

CASE 11  
 $\gamma^2 = 0.333$   
 $\lambda_1^2 = 2.0$   
 $\Psi_V = 1.138$

FREQUENCY	F	G	K	C
.50	.8735-00	-.3035-00	.9758-00	.8123-00
1.00	.5809-00	-.5451-00	.9154-00	.8589-00
1.50	.3190-00	-.5179-00	.8631-00	.9322-00
2.00	.1834-00	-.4125-00	.8998-00	.1012+01
2.50	.1028-00	-.3222-00	.1092+01	.1062+01
3.00	.1157+00	-.2638-00	.1395+01	.1060+01
3.50	.1090+00	-.2282-00	.1705+01	.1020+01
4.00	.1031+00	-.2056-00	.1950+01	.9717-00
4.50	.9582-01	-.1892-00	.2130+01	.9347-00
5.00	.8750-01	-.1750-00	.2285+01	.9142-00
5.50	.7941-01	-.1610-00	.2464+01	.9083-00
6.00	.7508-01	-.1472-00	.2716+01	.9053-00
6.50	.7034-01	-.1347-00	.3046+01	.8970-00
7.00	.6881-01	-.1243+00	.3416+01	.8798-00
7.50	.6795-01	-.1158+00	.3767+01	.8563-00
8.00	.6719-01	-.1090+00	.4099+01	.8311-00

CASE 12  
 $\gamma^2 = 0.00$   
 $\lambda_1^2 = 3.0$   
 $\Psi_V = 0.633$

FREQUENCY	F	G	K	C
.50	.9090-00	-.2884-00	.9490-00	.6335-00
1.00	.6882-00	-.4569-00	.1008+01	.6643-00
1.50	.4612-00	-.4669-00	.1071+01	.7227-00
2.00	.3188-00	-.3889-00	.1259+01	.7733-00
2.50	.2500-00	-.3018-00	.1627+01	.7861-00
3.00	.2247-00	-.2352-00	.2123+01	.7411-00
3.50	.2183-00	-.1891-00	.2621+01	.6540-00
4.00	.2131-00	-.1567-00	.3046+01	.5600-00
4.50	.2109-00	-.1321-00	.3405+01	.4740-00
5.00	.2092-00	-.1115+00	.3722+01	.3967-00
5.50	.2085-00	-.9287-01	.4002+01	.3240-00
6.00	.2100-00	-.7594-01	.4210+01	.2537-00
6.50	.2137-00	-.6128-01	.4324+01	.1908-00
7.00	.2188-00	-.4930-01	.4350+01	.1400-00
7.50	.2246-00	-.3990-01	.4317+01	.1023+00
8.00	.2304-00	-.3267-01	.4255+01	.7542-01

TABLE 3.1 CONTINUED

## CASE 13

$\gamma^2 = 0.25$

$\lambda_1^2 = 3.00$

$\Psi_V = 1.183$

FREQUENCY	F	G	K	C
.50	.8029-00	-.3414-00	.9853-01	.7619-00
1.00	.8095-00	-.5163-00	.9553-00	.8091-00
1.50	.3095-00	-.4948-00	.9611-00	.6818-00
2.00	.2201-00	-.3939-00	.1090+01	.9548-00
2.50	.1770-00	-.3047-00	.1426+01	.9815-00
3.00	.1031-00	-.2465-00	.1867+01	.9406-00
3.50	.1099-00	-.2120-00	.2267+01	.8580-00
4.00	.1575-00	-.1919-00	.2556+01	.7784-00
4.50	.1027-00	-.1792-00	.2755+01	.7184-00
5.00	.1452-00	-.1695-00	.2915+01	.6600-00
5.50	.1358-00	-.1590-00	.3093+01	.6609-00
6.00	.1272-00	-.1482-00	.3335+01	.6474-00
6.50	.1211+00	-.1361-00	.3650+01	.6300-00
7.00	.1170+00	-.1248+00	.4001+01	.6055-00
7.50	.1103+00	-.1153+00	.4338+01	.5733-00
8.00	.1157+00	-.1070+00	.4633+01	.5389-00

## CASE 14

$\gamma^2 = 0.00$

$\lambda_1^2 = 4.00$

$\Psi_V = 0.667$

FREQUENCY	F	G	K	C
.50	.9100-00	-.2666-00	.1006+01	.5859-00
1.00	.7107-00	-.4220-00	.1040+01	.6177-00
1.50	.4995-00	-.4298-00	.1150+01	.6599-00
2.00	.3606-00	-.3547-00	.1409+01	.6835-00
2.50	.3000-00	-.2713-00	.1830+01	.6488-00
3.00	.2001-00	-.2082-00	.2285+01	.5543-00
3.50	.2622-00	-.1657-00	.2635+01	.4422-00
4.00	.2625-00	-.1377-00	.2861+01	.3486-00
4.50	.2626-00	-.1180+00	.3013+01	.2797-00
5.00	.2615-00	-.1025+00	.3137+01	.2284-00
5.50	.2798-00	-.8814-01	.3252+01	.1863-00
6.00	.2793-00	-.7418-01	.3344+01	.1480-00
6.50	.2610-00	-.6117-01	.3398+01	.1138+00
7.00	.2646-00	-.5009-01	.3408+01	.8568-01
7.50	.2694-00	-.4138-01	.3387+01	.6458-01
8.00	.2944-00	-.3490-01	.3350+01	.4964-01



TABLE 3.2  
ROCKING VIBRATION  
COMPLIANCE & IMPEDANCE COEFFICIENTS

## CASE 1

$\gamma^2 = 0.00$

$\lambda_1^2 = 1.00$

$\Psi_v = 0.50$

FREQUENCY	F	G	K	C
.50	.1000+01	-.2805-01	.4359-00	.4917-01
1.00	.1194+01	-.1932-00	.8160-00	.1320-00
1.50	.1215+01	-.5008-00	.7034-00	.1933-00
2.00	.1040+01	-.8057-00	.6010-00	.2329-00
2.50	.7406-00	-.9627-00	.5030-00	.2595-00
3.00	.4735-00	-.9676-00	.4080-00	.2779-00
3.50	.2603-00	-.9003-00	.3153-00	.2693-00
4.00	.1551-00	-.8209-00	.2195-00	.2943-00
4.50	.0292-01	-.7501-00	.1111+00	.2942-00
5.00	-.9412-02	-.6869-00	-.1994-01	.2911-00
5.50	-.7104-01	-.6250-00	-.1795-00	.2872-00
6.00	-.1200+00	-.5609-00	-.3671-00	.2840-00
6.50	-.1503-00	-.4958-00	-.5783-00	.2822-00
7.00	-.1775-00	-.4342-00	-.8066-00	.2819-00
7.50	-.1870-00	-.3797-00	-.1046+01	.2822-00
8.00	-.1913-00	-.3330-00	-.1297+01	.2622-00

## CASE 2

$\gamma^2 = 0.25$

$\lambda_1^2 = 1.00$

$\Psi_v = 0.667$

FREQUENCY	F	G	K	C
.50	.1065+01	-.2847-01	.9381-00	.5014-01
1.00	.1180+01	-.1934-00	.8251-00	.1352-00
1.50	.1178+01	-.4892-00	.7239-00	.2004-00
2.00	.9825-00	-.7585-00	.6377-00	.2462-00
2.50	.6934-00	-.8656-00	.5637-00	.2815-00
3.00	.4487-00	-.8285-00	.5055-00	.3111-00
3.50	.2948-00	-.7356-00	.4694-00	.3346-00
4.00	.2086-00	-.6445-00	.4545-00	.3511-00
4.50	.1583-00	-.5720-00	.4493-00	.3608-00
5.00	.1238+00	-.5162-00	.4393-00	.3664-00
5.50	.9606-01	-.4699-00	.4176-00	.3714-00
6.00	.7397-01	-.4281-00	.3920-00	.3781-00
6.50	.5853-01	-.3892-00	.3779-00	.3866-00
7.00	.5013-01	-.3546-00	.3910-00	.3950-00
7.50	.4703-01	-.3261-00	.4333-00	.4005-00
8.00	.4639-01	-.3041-00	.4901-00	.4016-00

TABLE 3.2 CONTINUED

## CASE 3

$\gamma^2 = 0.333$

$\lambda_1^2 = 1.00$

$\psi_v = 0.75$

FREQUENCY	F	G	K	C
.50	.1007+01	-.2983-01	.9366-00	.5238-01
1.00	.1101+01	-.2013-00	.8227-00	.1402-00
1.50	.1109+01	-.5020-00	.7220-00	.2069-00
2.00	.9508-00	-.7046-00	.6375-00	.2542-00
2.50	.0057-00	-.8543-00	.5675-00	.2913-00
3.00	.4290-00	-.8020-00	.5184-00	.3228-00
3.50	.2008-00	-.7037-00	.4992-00	.3475-00
4.00	.2148-00	-.6130-00	.5091-00	.3033-00
4.50	.1742-00	-.5449-00	.5323-00	.3700-00
5.00	.1405-00	-.4957-00	.5485-00	.3710-00
5.50	.1226+00	-.4574-00	.5468-00	.3709-00
6.00	.1012+00	-.4250-00	.5337-00	.3722-00
6.50	.8504-01	-.3910-00	.5227-00	.3750-00
7.00	.7182-01	-.3621-00	.5270-00	.3790-00
7.50	.6443-01	-.3300-00	.5478-00	.3819-00
8.00	.5944-01	-.3165-00	.5732-00	.3815-00

## CASE 4

$\gamma^2 = 0.50$

$\lambda_1^2 = 1.00$

$\psi_v = 1.00$

FREQUENCY	F	G	K	C
.50	.1077+01	-.3701-01	.9277-00	.6378-01
1.00	.1194+01	-.2430-00	.8039-00	.1640-00
1.50	.1140+01	-.5800-00	.6964-00	.2364-00
2.00	.8077-00	-.8261-00	.6045-00	.2878-00
2.50	.5510-00	-.8602-00	.5280-00	.3297-00
3.00	.5524-00	-.7638-00	.4790-00	.3669-00
3.50	.2210-00	-.6463-00	.4737-00	.3958-00
4.00	.1715-00	-.5530-00	.5105-00	.4121-00
4.50	.1477-00	-.4909-00	.5620-00	.4151-00
5.00	.1304-00	-.4496-00	.5951-00	.4103-00
5.50	.1119+00	-.4192-00	.5944-00	.4049-00
6.00	.9228-01	-.3920-00	.5089-00	.4028-00
6.50	.7408-01	-.3645-00	.5387-00	.4051-00
7.00	.6174-01	-.3373-00	.5251-00	.4098-00
7.50	.5597-01	-.3129-00	.5352-00	.4138-00
8.00	.4925-01	-.2929-00	.5581-00	.4150-00

TABLE 3.2 CONTINUED

## CASE 5

$\gamma^2 = 0.00$

$\lambda_1^2 = 1.5$

$\Psi_V = 0.54$

FREQUENCY	F	G	K	C
.50	.1002+01	-.2580-01	.9411-00	.4573-01
1.00	.1177+01	-.1775-00	.8309-00	.1253-00
1.50	.1193+01	-.4595-00	.7299-00	.1874-00
2.00	.1027+01	-.7373-00	.6424-00	.2306-00
2.50	.7530-00	-.8755-00	.5646-00	.2626-00
3.00	.4999-00	-.8693-00	.4971-00	.2882-00
3.50	.3204-00	-.7952-00	.4417-00	.3075-00
4.00	.2194-00	-.7127-00	.3945-00	.3204-00
4.50	.1497-00	-.6434-00	.3431-00	.3276-00
5.00	.9048-01	-.5875-00	.2722-00	.3315-00
5.50	.4909-01	-.5378-00	.1710-00	.3352-00
6.00	.8900-02	-.4886-00	.0729-01	.3410-00
6.50	-.2407-01	-.4376-00	-.1254-00	.3505-00
7.00	-.4000-01	-.3865-00	-.3088-00	.3643-00
7.50	-.5977-01	-.3387-00	-.5051-00	.3817-00
8.00	-.8500-01	-.2964-00	-.7117-00	.4020-00

## CASE 6

$\gamma^2 = 0.25$

$\lambda_1^2 = 1.5$

$\Psi_V = 0.792$

FREQUENCY	F	G	K	C
.50	.1003+01	-.2781-01	.9403-00	.4921-01
1.00	.1171+01	-.1882-00	.8323-00	.1338-00
1.50	.1103+01	-.4726-00	.7382-00	.2001-00
2.00	.9656-00	-.7244-00	.6627-00	.2486-00
2.50	.0841-00	-.8135-00	.6055-00	.2880-00
3.00	.4537-00	-.7627-00	.5760-00	.3228-00
3.50	.3170-00	-.6622-00	.5481-00	.3510-00
4.00	.2407-00	-.5688-00	.5454-00	.3690-00
4.50	.2139-00	-.4993-00	.7298-00	.3750-00
5.00	.1909-00	-.4513-00	.8120-00	.3723-00
5.50	.1807-00	-.4173-00	.8737-00	.3669-00
6.00	.1643-00	-.3901-00	.9171-00	.3629-00
6.50	.1484-00	-.3648-00	.9568-00	.3618-00
7.00	.1354-00	-.3402-00	.1010+01	.3625-00
7.50	.1203-00	-.3174-00	.1083+01	.3626-00
8.00	.1206+00	-.2979-00	.1168+01	.3605-00

TABLE 3.2 CONTINUED

CASE 7  
 $\gamma^2 = 0.333$   
 $\lambda^2 = 1.5$   
 $\psi = 0.927$

FREQUENCY	F	G	K	C
.50	.1007+01	-.3092-01	.9360-01	.5425-01
1.00	.1179+01	-.2072-00	.8227-00	.1440-00
1.50	.1155+01	-.5102-00	.7246-00	.2134-00
2.00	.9294-00	-.7602-00	.6446-00	.2635-00
2.50	.6538-00	-.8278-00	.5631-00	.3046-00
3.00	.4060-00	-.7571-00	.5514-00	.3412-00
3.50	.2822-00	-.6475-00	.5669-00	.3704-00
4.00	.2200-00	-.5535-00	.6321-00	.3875-00
4.50	.2005-00	-.4872-00	.7224-00	.3901-00
5.00	.1507-00	-.4444-00	.8007-00	.3832-00
5.50	.1709-00	-.4159-00	.8454-00	.3740-00
6.00	.1555-00	-.3937-00	.8597-00	.3675-00
6.50	.1347-00	-.3720-00	.8606-00	.3550-00
7.00	.1179+00	-.3490-00	.8680-00	.3674-00
7.50	.1053+00	-.3259-00	.8980-00	.3704-00
8.00	.9694-01	-.3049-00	.9471-00	.3725-00

CASE 8  
 $\gamma^2 = 0.50$   
 $\lambda^2 = 1.5$   
 $\psi = 1.457$

FREQUENCY	F	G	K	C
.50	.1092+01	-.4468-01	.9143-01	.4155-01
1.00	.1210+01	-.3100-00	.7750-00	.1988-00
1.50	.1007+01	-.6930-00	.6542-00	.2782-00
2.00	.7291-00	-.9013-00	.5425-00	.3353-00
2.50	.5917-00	-.8576-00	.4407-00	.3859-00
3.00	.1993-00	-.7083-00	.3682-00	.4361-00
3.50	.1215+00	-.5661-00	.3600-00	.4809-00
4.00	.9941-01	-.4688-00	.4332-00	.5105-00
4.50	.9684-01	-.4057-00	.5566-00	.5182-00
5.00	.9601-01	-.3676-00	.6686-00	.5089-00
5.50	.9162-01	-.3433-00	.7272-00	.4943-00
6.00	.8203-01	-.3245-00	.7321-00	.4827-00
6.50	.6904-01	-.3059-00	.7051-00	.4783-00
7.00	.5703-01	-.2856-00	.6789-00	.4807-00
7.50	.4946-01	-.2649-00	.6813-00	.4865-00
8.00	.4505-01	-.2460-00	.7201-00	.4919-00

TABLE 3.2 CONTINUED

## CASE 9

$\gamma^2 = 0.00$

$\lambda_1^2 = 2.0$

$\Psi_V = 0.581$

FREQUENCY	F	G	K	C
.50	.1057+01	-.2385-01	.9456-00	.4267-01
1.00	.1102+01	-.1640-00	.8436-00	.1191+00
1.50	.1176+01	-.4244-00	.7524-00	.1811-00
2.00	.1020+01	-.6805-00	.6785-00	.2264-00
2.50	.7615-00	-.8051-00	.6201-00	.2622-00
3.00	.5242-00	-.7920-00	.5812-00	.2927-00
3.50	.3649-00	-.7137-00	.5680-00	.3174-00
4.00	.2720-00	-.6287-00	.5796-00	.3349-00
4.50	.2171-00	-.5594-00	.6030-00	.3453-00
5.00	.1764-00	-.5068-00	.6179-00	.3511-00
5.50	.1446-00	-.4645-00	.6111-00	.3569-00
6.00	.1129+00	-.4254-00	.5827-00	.3660-00
6.50	.8402-01	-.3852-00	.5440-00	.3810-00
7.00	.6200-01	-.3435-00	.5156-00	.4025-00
7.50	.4901-01	-.3025-00	.5216-00	.4295-00
8.00	.4203-01	-.2649-00	.5844-00	.4604-00

## CASE 10

$\gamma^2 = 0.25$

$\lambda_1^2 = 2.0$

$\Psi_V = 0.913$

FREQUENCY	F	G	K	C
.50	.1062+01	-.2794-01	.9408-00	.4949-01
1.00	.1168+01	-.1884-00	.8346-00	.1347-00
1.50	.1153+01	-.4701-00	.7435-00	.2020-00
2.00	.9511-00	-.7132-00	.6730-00	.2523-00
2.50	.6702-00	-.7898-00	.6246-00	.2944-00
3.00	.4406-00	-.7283-00	.6119-00	.3326-00
3.50	.3198-00	-.6210-00	.6553-00	.3636-00
4.00	.2623-00	-.5245-00	.7626-00	.3813-00
4.50	.2402-00	-.4551-00	.9072-00	.3819-00
5.00	.2313-00	-.4104-00	.1042+01	.3698-00
5.50	.2236-00	-.3827-00	.1138+01	.3542-00
6.00	.2126-00	-.3643-00	.1195+01	.3413-00
6.50	.1979-00	-.3486-00	.1232+01	.3337-00
7.00	.1821-00	-.3320-00	.1270+01	.3308-00
7.50	.1662-00	-.3138-00	.1327+01	.3301-00
8.00	.1576-00	-.2956-00	.1404+01	.3292-00

TABLE 3.2 CONTINUED

## CASE 11

$\gamma^2 = 0.333$

$\lambda_1^2 = 2.0$

$\Psi_V = 1.138$

FREQUENCY	F	G	K	C
.50	.1071+01	-.3338-01	.9332-00	.5820-01
1.00	.1163+01	-.2217-00	.8169-00	.1532-00
1.50	.1142+01	-.5368-00	.7171-00	.2247-00
2.00	.8928-00	-.7797-00	.6354-00	.2775-00
2.50	.5858-00	-.8243-00	.5728-00	.3224-00
3.00	.3651-00	-.7325-00	.5451-00	.3645-00
3.50	.2520-00	-.6105-00	.5778-00	.3999-00
4.00	.2068-00	-.5103-00	.6821-00	.4208-00
4.50	.1927-00	-.4421-00	.8284-00	.4224-00
5.00	.1800-00	-.4002-00	.9619-00	.4094-00
5.50	.1820-00	-.3752-00	.1047+01	.3923-00
6.00	.1709-00	-.3587-00	.1082+01	.3786-00
6.50	.1551-00	-.3439-00	.1090+01	.3717-00
7.00	.1378-00	-.3267-00	.1096+01	.3712-00
7.50	.1229+00	-.3068-00	.1125+01	.3745-00
8.00	.1125+00	-.2864-00	.1189+01	.3781-00

## CASE 12

$\gamma^2 = 0.00$

$\lambda_1^2 = 3.0$

$\Psi_V = 0.633$

FREQUENCY	F	G	K	C
.50	.1051+01	-.2153-01	.9509-00	.3895-01
1.00	.1145+01	-.1480-00	.8588-00	.1110+00
1.50	.1156+01	-.3831-00	.7795-00	.1722-00
2.00	.1012+01	-.6140-00	.7224-00	.2192-00
2.50	.7728-00	-.7234-00	.6896-00	.2582-00
3.00	.5535-00	-.7032-00	.6912-00	.2927-00
3.50	.4097-00	-.6203-00	.7413-00	.3207-00
4.00	.3323-00	-.5319-00	.8449-00	.3381-00
4.50	.2939-00	-.4612-00	.9825-00	.3427-00
5.00	.2725-00	-.4109-00	.1121+01	.3381-00
5.50	.2552-00	-.3755-00	.1238+01	.3312-00
6.00	.2309-00	-.3476-00	.1339+01	.3274-00
6.50	.2170-00	-.3211-00	.1445+01	.3289-00
7.00	.1982-00	-.2926-00	.1587+01	.3346-00
7.50	.1839-00	-.2621-00	.1793+01	.3409-00
8.00	.1753-00	-.2320-00	.2073+01	.3430-00

TABLE 3.2 CONTINUED

CASE 13  
 $\gamma^2 = 0.25$   
 $\lambda_1^2 = 3.00$   
 $\Psi_V = 1.183$

FREQUENCY	F	G	K	C
.50	.1065+01	-.3043-01	.9378-00	.5357-01
1.00	.1172+01	-.2035-00	.8282-00	.1438-00
1.50	.1142+01	-.4990-00	.7353-00	.2142-00
2.00	.9134-00	-.7373-00	.6629-00	.2675-00
2.50	.6178-00	-.7909-00	.6134-00	.3141-00
3.00	.3968-00	-.7056-00	.6055-00	.3589-00
3.50	.2811-00	-.5826-00	.6718-00	.3978-00
4.00	.2367-00	-.4773-00	.8339-00	.4204-00
4.50	.2276-00	-.4037-00	.1060+01	.4177-00
5.00	.2312-00	-.3582-00	.1272+01	.3941-00
5.50	.2354-00	-.3332-00	.1414+01	.3640-00
6.00	.2345-00	-.3212-00	.1482+01	.3385-00
6.50	.2262-00	-.3151-00	.1504+01	.3222-00
7.00	.2114-00	-.3087-00	.1510+01	.3150-00
7.50	.1958-00	-.2984-00	.1531+01	.3143-00
8.00	.1777-00	-.2835-00	.1587+01	.3166-00

CASE 14  
 $\gamma^2 = 0.00$   
 $\lambda_1^2 = 4.00$   
 $\Psi_V = 0.667$

FREQUENCY	F	G	K	C
.50	.1048+01	-.2004-01	.9543-00	.3652-01
1.00	.1105+01	-.1378-00	.8684-00	.1055+00
1.50	.1144+01	-.3564-00	.7967-00	.1657-00
2.00	.1007+01	-.5722-00	.7505-00	.2131-00
2.50	.7812-00	-.6726-00	.7350-00	.2532-00
3.00	.5701-00	-.6490-00	.7645-00	.2886-00
3.50	.4385-00	-.5640-00	.8591-00	.3157-00
4.00	.3698-00	-.4737-00	.1024+01	.3279-00
4.50	.3408-00	-.4019-00	.1227+01	.3216-00
5.00	.3297-00	-.3523-00	.1416+01	.3026-00
5.50	.3229-00	-.3202-00	.1562+01	.2816-00
6.00	.3157-00	-.2967-00	.1672+01	.2653-00
6.50	.3081-00	-.2808-00	.1777+01	.2557-00
7.00	.2941-00	-.2614-00	.1906+01	.2500-00
7.50	.2895-00	-.2385-00	.2081+01	.2455-00
8.00	.2890-00	-.2137-00	.2290+01	.2363-00

TABLE 3.3  
HORIZONTAL VIBRATION  
COMPLIANCE & IMPEDANCE COEFFICIENTS

CASE 1a

$\gamma^2 = 0.00$

$\lambda_1^2 = 1.00$

$\lambda_2^2 = 0.50$

$\psi_H = 1.914$

FREQUENCY	F	G	K	C
.50	.9086-00	-.2599-00	.1017+01	.5821-00
1.00	.7071-00	-.3853-00	.1090+01	.5942-00
1.50	.5384-00	-.3742-00	.1252+01	.5802-00
2.00	.4511-00	-.3228-00	.1466+01	.5245-00
2.50	.4103-00	-.2850-00	.1644+01	.4568-00
3.00	.3828-00	-.2647-00	.1767+01	.4073-00
3.50	.3588-00	-.2520-00	.1870+01	.3774-00
4.00	.3309-00	-.2389-00	.1987+01	.3586-00
4.50	.3082-00	-.2234-00	.2127+01	.3426-00
5.00	.2901-00	-.2089-00	.2285+01	.3259-00
5.50	.2759-00	-.1903-00	.2456+01	.3080-00
6.00	.2600-00	-.1742-00	.2631+01	.2872-00
6.50	.2599-00	-.1597-00	.2793+01	.2641-00
7.00	.2583-00	-.1480-00	.2926+01	.2414-00
7.50	.2534-00	-.1389-00	.3034+01	.2218-00
8.00	.2503-00	-.1312-00	.3134+01	.2053-00

CASE 2a

$\gamma^2 = 0.25$

$\lambda_1^2 = 1.00$

$\lambda_2^2 = 0.50$

$\psi_H = 2.081$

FREQUENCY	F	G	K	C
.50	.9074-00	-.2685-00	.1013+01	.5998-00
1.00	.7011-00	-.4024-00	.1073+01	.6157-00
1.50	.5239-00	-.3964-00	.1214+01	.6123-00
2.00	.4274-00	-.3457-00	.1414+01	.5720-00
2.50	.3789-00	-.3056-00	.1599+01	.5159-00
3.00	.3455-00	-.2809-00	.1743+01	.4723-00
3.50	.3154-00	-.2625-00	.1873+01	.4454-00
4.00	.2875-00	-.2432-00	.2028+01	.4287-00
4.50	.2650-00	-.2214-00	.2223+01	.4126-00
5.00	.2490-00	-.1991-00	.2450+01	.3917-00
5.50	.2389-00	-.1781-00	.2690+01	.3647-00
6.00	.2339-00	-.1600-00	.2913+01	.3320-00
6.50	.2322-00	-.1457-00	.3090+01	.2983-00
7.00	.2316-00	-.1354-00	.3218+01	.2688-00
7.50	.2304-00	-.1277-00	.3320+01	.2453-00
8.00	.2284-00	-.1212+00	.3416+01	.2265-00



TABLE 3.3 CONTINUED

## CASE 3a

$\gamma^2 = 0.333$

$\lambda_1^2 = 1.00$

$\lambda_2^2 = 0.50$

$\Psi_H = 2.164$

FREQUENCY	F	G	K	C
.50	.9053-00	-.2751-00	.1011+01	.6145-00
1.00	.6937-00	-.4129-00	.1064+01	.6335-00
1.50	.5164-00	-.4071-00	.1197+01	.6368-00
2.00	.4094-00	-.3540-00	.1398+01	.6042-00
2.50	.3583-00	-.3102-00	.1595+01	.5525-00
3.00	.3239-00	-.2816-00	.1758+01	.5097-00
3.50	.2943-00	-.2596-00	.1911+01	.4817-00
4.00	.2661-00	-.2373-00	.2091+01	.4628-00
4.50	.2478-00	-.2135-00	.2316+01	.4434-00
5.00	.2346-00	-.1902-00	.2572+01	.4171-00
5.50	.2272-00	-.1693-00	.2830+01	.3835-00
6.00	.2244-00	-.1523-00	.3052+01	.3452-00
6.50	.2238-00	-.1396-00	.3216+01	.3086-00
7.00	.2235-00	-.1308-00	.3333+01	.2785-00
7.50	.2222-00	-.1243+00	.3429+01	.2557-00
8.00	.2197-00	-.1184+00	.3528+01	.2376-00

## CASE 4a

$\gamma^2 = 0.50$

$\lambda_1^2 = 1.00$

$\lambda_2^2 = 0.50$

$\Psi_H = 2.414$

FREQUENCY	F	G	K	C
.50	.8950-00	-.2984-00	.1006+01	.6705-00
1.00	.6603-00	-.4435-00	.1044+01	.7010-00
1.50	.4589-00	-.4280-00	.1165+01	.7245-00
2.00	.3515-00	-.3603-00	.1387+01	.7111-00
2.50	.3012-00	-.3040-00	.1644+01	.6640-00
3.00	.2716-00	-.2662-00	.1878+01	.6134-00
3.50	.2490-00	-.2384-00	.2095+01	.5732-00
4.00	.2300-00	-.2138-00	.2332+01	.5421-00
4.50	.2160-00	-.1900-00	.2610+01	.5102-00
5.00	.2080-00	-.1681-00	.2908+01	.4700-00
5.50	.2047-00	-.1501-00	.3177+01	.4236-00
6.00	.2041-00	-.1369-00	.3380+01	.3776-00
6.50	.2039-00	-.1277-00	.3523+01	.3394-00
7.00	.2025-00	-.1212+00	.3636+01	.3109-00
7.50	.1996-00	-.1154+00	.3754+01	.2896-00
8.00	.1962-00	-.1090+00	.3896+01	.2705-00

TABLE 3.3 CONTINUED

## CASE 5a

$\gamma^2 = 0.00$

$\lambda_1^2 = 1.5$

$\lambda_2^2 = 0.50$

$\Psi_H = 1.855$

FREQUENCY	F	G	K	C
.50	.9078-00	-.2596-00	.1018+01	.5825-00
1.00	.7054-00	-.3829-00	.1095+01	.5944-00
1.50	.5376-00	-.3687-00	.1265+01	.5784-00
2.00	.4528-00	-.3154-00	.1487+01	.5179-00
2.50	.4148-00	-.2771-00	.1667+01	.4454-00
3.00	.3902-00	-.2571-00	.1787+01	.3925-00
3.50	.3607-00	-.2458-00	.1882+01	.3604-00
4.00	.3425-00	-.2350-00	.1985+01	.3404-00
4.50	.3207-00	-.2221-00	.2107+01	.3244-00
5.00	.3023-00	-.2083-00	.2243+01	.3091-00
5.50	.2809-00	-.1939-00	.2393+01	.2941-00
6.00	.2751-00	-.1790-00	.2554+01	.2770-00
6.50	.2672-00	-.1649-00	.2710+01	.2573-00
7.00	.2623-00	-.1530-00	.2845+01	.2371-00
7.50	.2505-00	-.1434-00	.2958+01	.2188-00
8.00	.2548-00	-.1352-00	.3062+01	.2031-00

## CASE 6a

$\gamma^2 = 0.25$

$\lambda_1^2 = 1.5$

$\lambda_2^2 = 0.50$

$\Psi_H = 2.061$

FREQUENCY	F	G	K	C
.50	.9069-00	-.2685-00	.1014+01	.6004-00
1.00	.7001-00	-.4013-00	.1075+01	.6163-00
1.50	.5233-00	-.3938-00	.1220+01	.6121-00
2.00	.4283-00	-.3421-00	.1425+01	.5693-00
2.50	.3815-00	-.3018-00	.1612+01	.5101-00
3.00	.3498-00	-.2778-00	.1753+01	.4640-00
3.50	.3210-00	-.2609-00	.1876+01	.4357-00
4.00	.2934-00	-.2436-00	.2018+01	.4187-00
4.50	.2701-00	-.2235-00	.2198+01	.4041-00
5.00	.2527-00	-.2021-00	.2413+01	.3861-00
5.50	.2411-00	-.1813-00	.2650+01	.3622-00
6.00	.2351-00	-.1626-00	.2877+01	.3317-00
6.50	.2328-00	-.1477-00	.3063+01	.2986-00
7.00	.2321-00	-.1366-00	.3200+01	.2692-00
7.50	.2310-00	-.1285-00	.3306+01	.2451-00
8.00	.2293-00	-.1216+00	.3404+01	.2256-00

TABLE 3.3 CONTINUED

## CASE 7a

$\gamma^2 = 0.333$

$\lambda_1^2 = 1.5$

$\lambda_2^2 = 0.50$

$\psi_H = 2.171$

FREQUENCY	F	G	K	C
.50	.9038-00	-.2776-00	.1011+01	.6211-00
1.00	.6891-00	-.4153-00	.1065+01	.6415-00
1.50	.5043-00	-.4069-00	.1201+01	.6461-00
2.00	.4040-00	-.3512-00	.1410+01	.6128-00
2.50	.3547-00	-.3060-00	.1616+01	.5578-00
3.00	.3224-00	-.2772-00	.1783+01	.5112-00
3.50	.2946-00	-.2561-00	.1933+01	.4803-00
4.00	.2691-00	-.2355-00	.2105+01	.4604-00
4.50	.2464-00	-.2131-00	.2319+01	.4420-00
5.00	.2343-00	-.1903-00	.2572+01	.4177-00
5.50	.2262-00	-.1693-00	.2833+01	.3856-00
6.00	.2231-00	-.1520-00	.3061+01	.3476-00
6.50	.2225-00	-.1391-00	.3231+01	.3107-00
7.00	.2223-00	-.1301-00	.3351+01	.2802-00
7.50	.2210-00	-.1234+00	.3449+01	.2568-00
8.00	.2167-00	-.1174+00	.3549+01	.2381-00

## CASE 8a

$\gamma^2 = 0.50$

$\lambda_1^2 = 1.5$

$\lambda_2^2 = 0.50$

$\psi_H = 2.604$

FREQUENCY	F	G	K	C
.50	.8811-00	-.3218-00	.1001+01	.7314-00
1.00	.6206-00	-.4658-00	.1031+01	.7735-00
1.50	.4091-00	-.4318-00	.1156+01	.8136-00
2.00	.3065-00	-.3500-00	.1416+01	.8084-00
2.50	.2647-00	-.2879-00	.1731+01	.7529-00
3.00	.2422-00	-.2492-00	.2005+01	.6879-00
3.50	.2243-00	-.2231-00	.2241+01	.6369-00
4.00	.2077-00	-.2006-00	.2491+01	.6014-00
4.50	.1949-00	-.1780-00	.2797+01	.5678-00
5.00	.1862-00	-.1569-00	.3135+01	.5228-00
5.50	.1861-00	-.1400-00	.3432+01	.4695-00
6.00	.1861-00	-.1281-00	.3645+01	.4182-00
6.50	.1858-00	-.1201+00	.3796+01	.3776-00
7.00	.1840-00	-.1140+00	.3928+01	.3476-00
7.50	.1811-00	-.1080+00	.4074+01	.3239-00
8.00	.1764-00	-.1013+00	.4239+01	.3009-00

TABLE 3.3 CONTINUED

CASE 9a

$\gamma^2 = 0.00$

$\lambda_1^2 = 2.00$

$\lambda_2^2 = 0.50$

$\Psi_H = 1.825$

FREQUENCY	F	G	K	C
.50	.9076-00	-.2583-00	.1019+01	.5802-00
1.00	.7052-00	-.3794-00	.1100+01	.5916-00
1.50	.5308-00	-.3630-00	.1277+01	.5734-00
2.00	.4500-00	-.3083-00	.1505+01	.5088-00
2.50	.4202-00	-.2693-00	.1687+01	.4324-00
3.00	.3978-00	-.2494-00	.1805+01	.3771-00
3.50	.3704-00	-.2387-00	.1895+01	.3433-00
4.00	.3541-00	-.2292-00	.1990+01	.3221-00
4.50	.3334-00	-.2182-00	.2100+01	.3054-00
5.00	.3155-00	-.2063-00	.2220+01	.2904-00
5.50	.2997-00	-.1938-00	.2353+01	.2766-00
6.00	.2870-00	-.1804-00	.2497+01	.2616-00
6.50	.2780-00	-.1670-00	.2643+01	.2444-00
7.00	.2720-00	-.1553-00	.2772+01	.2262-00
7.50	.2674-00	-.1457-00	.2883+01	.2095-00
8.00	.2633-00	-.1374-00	.2985+01	.1948-00

CASE 10a

$\gamma^2 = 0.25$

$\lambda_1^2 = 2.00$

$\lambda_2^2 = 0.50$

$\Psi_H = 2.060$

FREQUENCY	F	G	K	C
.50	.9004-00	-.2689-00	.1014+01	.6017-00
1.00	.6907-00	-.4012-00	.1076+01	.6180-00
1.50	.5217-00	-.3924-00	.1224+01	.6139-00
2.00	.4274-00	-.3395-00	.1435+01	.5698-00
2.50	.3818-00	-.2985-00	.1626+01	.5084-00
3.00	.3514-00	-.2744-00	.1768+01	.4601-00
3.50	.3239-00	-.2581-00	.1888+01	.4299-00
4.00	.2971-00	-.2419-00	.2024+01	.4120-00
4.50	.2737-00	-.2232-00	.2195+01	.3977-00
5.00	.2557-00	-.2027-00	.2402+01	.3808-00
5.50	.2433-00	-.1821-00	.2634+01	.3584-00
6.00	.2307-00	-.1634-00	.2862+01	.3292-00
6.50	.2341-00	-.1482-00	.3050+01	.2970-00
7.00	.2331-00	-.1368-00	.3191+01	.2676-00
7.50	.2320-00	-.1283-00	.3300+01	.2434-00
8.00	.2304-00	-.1212+00	.3399+01	.2235-00

TABLE 3.3 CONTINUED

## CASE 11a

$\gamma^2 = 0.333$

$\lambda_1^2 = 2.00$

$\lambda_2^2 = 0.50$

$\Psi_H = 2.219$

FREQUENCY	F	G	K	C
.50	.9015-00	-.2821-00	.1010+01	.6323-00
1.00	.6810-00	-.4205-00	.1063+01	.6552-00
1.50	.4938-00	-.4091-00	.1201+01	.6633-00
2.00	.3932-00	-.3497-00	.1420+01	.6315-00
2.50	.3452-00	-.3019-00	.1641+01	.5741-00
3.00	.3151-00	-.2717-00	.1820+01	.5233-00
3.50	.2894-00	-.2505-00	.1975+01	.4885-00
4.00	.2654-00	-.2307-00	.2146+01	.4664-00
4.50	.2452-00	-.2092-00	.2360+01	.4474-00
5.00	.2312-00	-.1868-00	.2616+01	.4228-00
5.50	.2234-00	-.1661-00	.2883+01	.3898-00
6.00	.2205-00	-.1491-00	.3113+01	.3507-00
6.50	.2200-00	-.1365-00	.3282+01	.3133-00
7.00	.2197-00	-.1277-00	.3402+01	.2826-00
7.50	.2184-00	-.1210+00	.3503+01	.2589-00
8.00	.2102-00	-.1149+00	.3606+01	.2397-00

## CASE 12a

$\gamma^2 = 0.00$

$\lambda_1^2 = 3.0$

$\lambda_2^2 = 0.50$

$\Psi_H = 1.779$

FREQUENCY	F	G	K	C
.50	.9069-00	-.2574-00	.1020+01	.5793-00
1.00	.7038-00	-.3761-00	.1105+01	.5906-00
1.50	.5362-00	-.3565-00	.1291+01	.5702-00
2.00	.4577-00	-.2995-00	.1530+01	.5005-00
2.50	.4246-00	-.2591-00	.1716+01	.4189-00
3.00	.4050-00	-.2386-00	.1833+01	.3599-00
3.50	.3806-00	-.2282-00	.1918+01	.3236-00
4.00	.3609-00	-.2198-00	.2005+01	.3004-00
4.50	.3404-00	-.2107-00	.2101+01	.2824-00
5.00	.3319-00	-.2013-00	.2202+01	.2672-00
5.50	.3106-00	-.1916-00	.2312+01	.2543-00
6.00	.3033-00	-.1806-00	.2434+01	.2416-00
6.50	.2929-00	-.1689-00	.2562+01	.2273-00
7.00	.2855-00	-.1581-00	.2681+01	.2120-00
7.50	.2798-00	-.1489-00	.2785+01	.1976-00
8.00	.2747-00	-.1407-00	.2884+01	.1847-00

TABLE 3.3 CONTINUED

CASE 13a  
 $\gamma^2 = 0.25$   
 $\lambda_1^2 = 3.0$   
 $\lambda_2^2 = 0.50$   
 $\Psi_H = 2.097$

FREQUENCY	F	G	K	C
.50	.9044-00	-.2731-00	.1013+01	.6121-00
1.00	.6921-00	-.4064-00	.1074+01	.6308-00
1.50	.5117-00	-.3950-00	.1225+01	.6302-00
2.00	.4105-00	-.3386-00	.1446+01	.5875-00
2.50	.3719-00	-.2946-00	.1652+01	.5234-00
3.00	.3436-00	-.2686-00	.1806+01	.4706-00
3.50	.3186-00	-.2517-00	.1932+01	.4362-00
4.00	.2939-00	-.2363-00	.2067+01	.4154-00
4.50	.2715-00	-.2188-00	.2233+01	.3999-00
5.00	.2537-00	-.1993-00	.2437+01	.3829-00
5.50	.2414-00	-.1793-00	.2670+01	.3606-00
6.00	.2347-00	-.1610-00	.2897+01	.3313-00
6.50	.2319-00	-.1462-00	.3086+01	.2992-00
7.00	.2307-00	-.1350-00	.3229+01	.2700-00
7.50	.2294-00	-.1265-00	.3343+01	.2458-00
8.00	.2278-00	-.1191+00	.3448+01	.2254-00

CASE 14a  
 $\gamma^2 = 0.00$   
 $\lambda_1^2 = 4.00$   
 $\lambda_2^2 = 0.50$   
 $\Psi_H = 1.748$

FREQUENCY	F	G	K	C
.50	.9062-00	-.2573-00	.1021+01	.5799-00
1.00	.7021-00	-.3745-00	.1109+01	.5914-00
1.50	.5308-00	-.3527-00	.1301+01	.5700-00
2.00	.4575-00	-.2939-00	.1547+01	.4970-00
2.50	.4200-00	-.2523-00	.1738+01	.4117-00
3.00	.4002-00	-.2311-00	.1855+01	.3501-00
3.50	.3917-00	-.2204-00	.1939+01	.3118-00
4.00	.3740-00	-.2124-00	.2022+01	.2870-00
4.50	.3573-00	-.2042-00	.2110+01	.2679-00
5.00	.3422-00	-.1961-00	.2200+01	.2521-00
5.50	.3277-00	-.1881-00	.2295+01	.2395-00
6.00	.3145-00	-.1790-00	.2402+01	.2278-00
6.50	.3036-00	-.1688-00	.2516+01	.2151-00
7.00	.2955-00	-.1589-00	.2625+01	.2016-00
7.50	.2891-00	-.1503-00	.2723+01	.1888-00
8.00	.2833-00	-.1426-00	.2817+01	.1772-00

TABLE 3.3 CONTINUED

CASE 1b  
 $\gamma^2 = 0.00$   
 $\lambda_1^2 = 1.00$   
 $\lambda_2^2 = 1.00$   
 $\Psi_H = 1.5$

FREQUENCY	F	G	K	C
.00	.9330-00	-.2643-00	.9622-00	.5622-00
1.00	.7610-00	-.4494-00	.9743-00	.5754-00
1.50	.5000-00	-.5186-00	.9613-00	.5926-00
2.00	.4025-00	-.5027-00	.9700-00	.6061-00
2.50	.3021-00	-.4573-00	.1006+01	.6090-00
3.00	.2408-00	-.4146-00	.1048+01	.6012-00
3.50	.1993-00	-.3820-00	.1074+01	.5879-00
4.00	.1600-00	-.3570-00	.1071+01	.5758-00
4.50	.1304-00	-.3351-00	.1042+01	.5689-00
5.00	.1103+00	-.3133-00	.1000+01	.5680-00
5.50	.8897-01	-.2900-00	.9621-00	.5717-00
6.00	.7510-01	-.2690-00	.9410-00	.5771-00
6.50	.6101-01	-.2492-00	.9374-00	.5815-00
7.00	.5000-01	-.2322-00	.9437-00	.5840-00
7.50	.4719-01	-.2177-00	.9512-00	.5850-00
8.00	.4104-01	-.2050-00	.9556-00	.5853-00

CASE 2b  
 $\gamma^2 = 0.25$   
 $\lambda_1^2 = 1.00$   
 $\lambda_2^2 = 1.00$   
 $\Psi_H = 1.667$

FREQUENCY	F	G	K	C
.00	.9290-00	-.2746-00	.9899-00	.5852-00
1.00	.7480-00	-.4643-00	.9650-00	.5990-00
1.50	.5400-00	-.5317-00	.9403-00	.6172-00
2.00	.3777-00	-.5123-00	.9322-00	.6323-00
2.50	.2748-00	-.4644-00	.9436-00	.6379-00
3.00	.2106-00	-.4192-00	.9569-00	.6348-00
3.50	.1601-00	-.3830-00	.9531-00	.6278-00
4.00	.1307-00	-.3527-00	.9241-00	.6232-00
4.50	.1013+00	-.3244-00	.8770-00	.6242-00
5.00	.7603-01	-.2965-00	.8300-00	.6308-00
5.50	.6139-01	-.2699-00	.8011-00	.6404-00
6.00	.5072-01	-.2463-00	.8018-00	.6490-00
6.50	.4395-01	-.2267-00	.8245-00	.6542-00
7.00	.3921-01	-.2106-00	.8543-00	.6555-00
7.50	.3534-01	-.1974-00	.8786-00	.6544-00
8.00	.3179-01	-.1862-00	.8911-00	.6523-00

TABLE 3.3 CONTINUED

CASE 3b

$\gamma^2 = 0.333$

$\lambda_1^2 = 1.00$

$\lambda_2^2 = 1.00$

$\Psi_H = 1.750$

FREQUENCY	F	G	K	C
.50	.9255-00	-.2824-01	.9485-00	.6033-00
1.00	.7005-00	-.4745-00	.9595-00	.6181-00
1.50	.5223-00	-.5362-00	.9286-00	.6379-00
2.00	.3502-00	-.5138-00	.9131-00	.6549-00
2.50	.2555-00	-.4622-00	.9160-00	.6628-00
3.00	.1919-00	-.4145-00	.9206-00	.6624-00
3.50	.1402-00	-.3755-00	.9099-00	.6586-00
4.00	.1143+00	-.3422-00	.8780-00	.6575-00
4.50	.0741-01	-.3115-00	.8350-00	.6613-00
5.00	.0755-01	-.2825-00	.8003-00	.6696-00
5.50	.0410-01	-.2565-00	.7885-00	.6792-00
6.00	.4576-01	-.2340-00	.8047-00	.6659-00
6.50	.4050-01	-.2159-00	.8355-00	.6685-00
7.00	.3614-01	-.2015-00	.8644-00	.6877-00
7.50	.3245-01	-.1891-00	.8815-00	.6851-00
8.00	.2887-01	-.1765-00	.8827-00	.6823-00

CASE 4b

$\gamma^2 = 0.50$

$\lambda_1^2 = 1.00$

$\lambda_2^2 = 1.00$

$\Psi_H = 2.000$

FREQUENCY	F	G	K	C
.50	.9105-00	-.3096-00	.9845-00	.6696-00
1.00	.6904-00	-.5037-00	.9452-00	.6896-00
1.50	.4584-00	-.5455-00	.9028-00	.7163-00
2.00	.2969-00	-.4996-00	.8792-00	.7396-00
2.50	.2038-00	-.4368-00	.8772-00	.7521-00
3.00	.1483-00	-.3836-00	.8767-00	.7561-00
3.50	.1112+00	-.3409-00	.8651-00	.7575-00
4.00	.8447-01	-.3047-00	.8448-00	.7619-00
4.50	.6567-01	-.2730-00	.8328-00	.7694-00
5.00	.5337-01	-.2459-00	.8426-00	.7766-00
5.50	.4521-01	-.2238-00	.8673-00	.7806-00
6.00	.3942-01	-.2059-00	.8969-00	.7808-00
6.50	.3464-01	-.1911-00	.9181-00	.7794-00
7.00	.3049-01	-.1784-00	.9311-00	.7781-00
7.50	.2697-01	-.1672-00	.9406-00	.7774-00
8.00	.2399-01	-.1572-00	.9483-00	.7770-00



TABLE 3.3 CONTINUED

CASE 5b  
 $\gamma^2 = 0.00$   
 $\lambda_1^2 = 1.50$   
 $\lambda_2^2 = 1.00$   
 $\psi_H = 1.441$

FREQUENCY	F	G	K	C
.50	.9329-00	-.2041-00	.9924-00	.5019-00
1.00	.7009-00	-.4489-00	.9750-00	.5752-00
1.50	.5007-00	-.5173-00	.9634-00	.5925-00
2.00	.4000-00	-.5000-00	.9757-00	.6060-00
2.50	.3000-00	-.4547-00	.1010+01	.6082-00
3.00	.2442-00	-.4119-00	.1065+01	.5988-00
3.50	.2044-00	-.3802-00	.1097+01	.5830-00
4.00	.1725-00	-.3507-00	.1099+01	.5679-00
4.50	.1450-00	-.3370-00	.1071+01	.5578-00
5.00	.1170+00	-.3177-00	.1025+01	.5537-00
5.50	.9510-01	-.2974-00	.9755-00	.5540-00
6.00	.7740-01	-.2770-00	.9362-00	.5580-00
6.50	.6429-01	-.2579-00	.9100-00	.5610-00
7.00	.5444-01	-.2409-00	.8925-00	.5042-00
7.50	.4070-01	-.2200-00	.8770-00	.5050-00
8.00	.4040-01	-.2120-00	.8620-00	.5669-00

CASE 6b  
 $\gamma^2 = 0.25$   
 $\lambda_1^2 = 1.50$   
 $\lambda_2^2 = 1.00$   
 $\psi_H = 1.647$

FREQUENCY	F	G	K	C
.50	.9207-00	-.2747-00	.9901-00	.5857-00
1.00	.7472-00	-.4638-00	.9661-00	.5996-00
1.50	.5395-00	-.5300-00	.9433-00	.6178-00
2.00	.3704-00	-.5098-00	.9387-00	.6323-00
2.50	.2770-00	-.4621-00	.9545-00	.6368-00
3.00	.2141-00	-.4177-00	.9718-00	.6320-00
3.50	.1703-00	-.3828-00	.9703-00	.6231-00
4.00	.1350-00	-.3540-00	.9408-00	.6165-00
4.50	.1050+00	-.3271-00	.8898-00	.6158-00
5.00	.8006-01	-.3002-00	.8346-00	.6213-00
5.50	.6208-01	-.2740-00	.7936-00	.6306-00
6.00	.5008-01	-.2501-00	.7810-00	.6399-00
6.50	.4338-01	-.2298-00	.7932-00	.6464-00
7.00	.3835-01	-.2131-00	.8179-00	.6493-00
7.50	.3449-01	-.1994-00	.8424-00	.6493-00
8.00	.3112-01	-.1879-00	.8584-00	.6476-00

TABLE 3.3 CONTINUED

## CASE 7b

$\gamma^2 = 0.333$

$\lambda_1^2 = 1.50$

$\lambda_2^2 = 1.00$

$\Psi_H = 1.757$

FREQUENCY	F	G	K	C
.50	.9235-00	-.2855-00	.9884-00	.6111-00
1.00	.7306-00	-.4771-00	.9595-00	.6266-00
1.50	.5147-00	-.5371-00	.9301-00	.6470-00
2.00	.3522-00	-.5095-00	.9180-00	.6640-00
2.50	.2522-00	-.4570-00	.9257-00	.6710-00
3.00	.1906-00	-.4095-00	.9342-00	.6691-00
3.50	.1400-00	-.3715-00	.9256-00	.6637-00
4.00	.1147+00	-.3393-00	.8938-00	.6612-00
4.50	.8794-01	-.3096-00	.8491-00	.6642-00
5.00	.6707-01	-.2812-00	.8108-00	.6720-00
5.50	.5406-01	-.2554-00	.7933-00	.6814-00
6.00	.4534-01	-.2332-00	.8033-00	.6886-00
6.50	.3905-01	-.2149-00	.8300-00	.6922-00
7.00	.3550-01	-.2001-00	.8599-00	.6923-00
7.50	.3199-01	-.1877-00	.8820-00	.6902-00
8.00	.2869-01	-.1772-00	.8901-00	.6873-00

## CASE 8b

$\gamma^2 = 0.50$

$\lambda_1^2 = 1.50$

$\lambda_2^2 = 1.00$

$\Psi_H = 2.190$

FREQUENCY	F	G	K	C
.50	.8926-00	-.3360-00	.9808-00	.7396-00
1.00	.6403-00	-.5249-00	.9341-00	.7658-00
1.50	.3904-00	-.5384-00	.8887-00	.7987-00
2.00	.2511-00	-.4747-00	.8707-00	.8231-00
2.50	.1716-00	-.4089-00	.8728-00	.8317-00
3.00	.1237+00	-.3578-00	.8630-00	.8323-00
3.50	.9052-01	-.3167-00	.8342-00	.8340-00
4.00	.6700-01	-.2811-00	.8024-00	.8416-00
4.50	.5108-01	-.2503-00	.7939-00	.8512-00
5.00	.4272-01	-.2254-00	.8119-00	.8567-00
5.50	.3613-01	-.2058-00	.8274-00	.8569-00
6.00	.3009-01	-.1899-00	.8291-00	.8553-00
6.50	.2593-01	-.1760-00	.8193-00	.8555-00
7.00	.2230-01	-.1636-00	.8184-00	.8575-00
7.50	.1979-01	-.1528-00	.8335-00	.8582-00
8.00	.1775-01	-.1438-00	.8455-00	.8561-00

TABLE 3.3 CONTINUED

## CASE 9b

$\gamma^2 = 0.00$

$\lambda_1^2 = 2.00$

$\lambda_2^2 = 1.00$

$\Psi_H = 1.411$

FREQUENCY	F	G	K	C
.50	.9332-00	-.2624-00	.9930-00	.5585-00
1.00	.7619-00	-.4458-00	.9778-00	.5721-00
1.50	.5628-00	-.5131-00	.9703-00	.5898-00
2.00	.4003-00	-.4955-00	.9895-00	.6034-00
2.50	.3005-00	-.4489-00	.1040+01	.6052-00
3.00	.2506-00	-.4059-00	.1101+01	.5946-00
3.50	.2127-00	-.3744-00	.1147+01	.5770-00
4.00	.1825-00	-.3519-00	.1161+01	.5599-00
4.50	.1551-00	-.3337-00	.1146+01	.5476-00
5.00	.1297-00	-.3162-00	.1110+01	.5415-00
5.50	.1070+00	-.2979-00	.1068+01	.5406-00
6.00	.8806-01	-.2791-00	.1034+01	.5424-00
6.50	.7441-01	-.2610-00	.1010+01	.5451-00
7.00	.6343-01	-.2445-00	.9938-00	.5474-00
7.50	.5474-01	-.2298-00	.9811-00	.5491-00
8.00	.4708-01	-.2165-00	.9699-00	.5506-00

## CASE 10b

$\gamma^2 = 0.25$

$\lambda_1^2 = 2.00$

$\lambda_2^2 = 1.00$

$\Psi_H = 1.646$

FREQUENCY	F	G	K	C
.50	.9201-00	-.2752-00	.9904-00	.5873-00
1.00	.7455-00	-.4637-00	.9672-00	.6016-00
1.50	.5375-00	-.5282-00	.9465-00	.6200-00
2.00	.3775-00	-.5066-00	.9457-00	.6346-00
2.50	.2776-00	-.4583-00	.9668-00	.6385-00
3.00	.2100-00	-.4142-00	.9898-00	.6327-00
3.50	.1732-00	-.3799-00	.9935-00	.6227-00
4.00	.1305-00	-.3520-00	.9683-00	.6150-00
4.50	.1087+00	-.3261-00	.9203-00	.6134-00
5.00	.8412-01	-.3000-00	.8663-00	.6180-00
5.50	.6500-01	-.2743-00	.8246-00	.6269-00
6.00	.5318-01	-.2506-00	.8102-00	.6364-00
6.50	.4521-01	-.2302-00	.8217-00	.6436-00
7.00	.3994-01	-.2132-00	.8491-00	.6474-00
7.50	.3607-01	-.1992-00	.8804-00	.6482-00
8.00	.3203-01	-.1874-00	.9066-00	.6470-00

TABLE 3.3 CONTINUED

CASE 11b  
 $\gamma^2 = 0.333$   
 $\lambda_1^2 = 2.00$   
 $\lambda_2^2 = 1.00$   
 $\psi_H = 1.805$

FREQUENCY	F	G	K	C
.50	.9201-00	-.2908-00	.9881-00	.6246-00
1.00	.7205-00	-.4819-00	.9590-00	.6414-00
1.50	.5015-00	-.5360-00	.9308-00	.6633-00
2.00	.3410-00	-.5031-00	.9230-00	.6810-00
2.50	.2444-00	-.4485-00	.9368-00	.6876-00
3.00	.1804-00	-.4008-00	.9510-00	.6851-00
3.50	.1446-00	-.3630-00	.9473-00	.6793-00
4.00	.1127+00	-.3311-00	.9211-00	.6767-00
4.50	.8717-01	-.3017-00	.8840-00	.6798-00
5.00	.6816-01	-.2740-00	.8550-00	.6874-00
5.50	.5500-01	-.2490-00	.8461-00	.6963-00
6.00	.4651-01	-.2275-00	.8627-00	.7033-00
6.50	.4066-01	-.2096-00	.8960-00	.7071-00
7.00	.3601-01	-.1949-00	.9359-00	.7078-00
7.50	.3355-01	-.1826-00	.9729-00	.7062-00
8.00	.3059-01	-.1723-00	.9987-00	.7033-00

CASE 12b  
 $\gamma^2 = 0.00$   
 $\lambda_1^2 = 3.00$   
 $\lambda_2^2 = 1.00$   
 $\psi_H = 1.365$

FREQUENCY	F	G	K	C
.50	.9332-00	-.2615-00	.9936-00	.5568-00
1.00	.7619-00	-.4437-00	.9802-00	.5708-00
1.50	.5629-00	-.5095-00	.9764-00	.5892-00
2.00	.4072-00	-.4902-00	.1003+01	.6036-00
2.50	.3110-00	-.4420-00	.1065+01	.6053-00
3.00	.2551-00	-.3981-00	.1141+01	.5936-00
3.50	.2196-00	-.3663-00	.1204+01	.5738-00
4.00	.1919-00	-.3443-00	.1235+01	.5540-00
4.50	.1668-00	-.3275-00	.1235+01	.5388-00
5.00	.1431-00	-.3122-00	.1213+01	.5295-00
5.50	.1212+00	-.2964-00	.1182+01	.5255-00
6.00	.1026+00	-.2801-00	.1153+01	.5246-00
6.50	.8738-01	-.2641-00	.1129+01	.5251-00
7.00	.7506-01	-.2490-00	.1110+01	.5259-00
7.50	.6494-01	-.2350-00	.1092+01	.5271-00
8.00	.5654-01	-.2221-00	.1076+01	.5285-00

TABLE 3.3 CONTINUED

CASE 13b

 $\gamma^2 = 0.25$  $\lambda_1^2 = 3.00$  $\lambda_2^2 = 1.00$  $\Psi_H = 1.683$ 

FREQUENCY	F	G	K	C
.50	.9251-00	-.2803-00	.9901-00	.6000-00
1.00	.7302-00	-.4687-00	.9665-00	.6154-00
1.50	.5246-00	-.5281-00	.9468-00	.6354-00
2.00	.3658-00	-.5013-00	.9499-00	.6509-00
2.50	.2689-00	-.4504-00	.9773-00	.6548-00
3.00	.2100-00	-.4054-00	.1007+01	.6483-00
3.50	.1693-00	-.3710-00	.1018+01	.6374-00
4.00	.1303-00	-.3433-00	.9992-00	.6291-00
4.50	.1001+00	-.3179-00	.9586-00	.6267-00
5.00	.8471-01	-.2928-00	.9120-00	.6304-00
5.50	.6667-01	-.2682-00	.8754-00	.6383-00
6.00	.5454-01	-.2454-00	.8629-00	.6471-00
6.50	.4637-01	-.2255-00	.8746-00	.6545-00
7.00	.4093-01	-.2087-00	.9049-00	.6591-00
7.50	.3710-01	-.1947-00	.9446-00	.6609-00
8.00	.3409-01	-.1829-00	.9844-00	.6603-00

CASE 14b

 $\gamma^2 = 0.00$  $\lambda_1^2 = 4.00$  $\lambda_2^2 = 1.00$  $\Psi_H = 1.333$ 

FREQUENCY	F	G	K	C
.50	.9330-00	-.2614-00	.9938-00	.5570-00
1.00	.7611-00	-.4432-00	.9812-00	.5714-00
1.50	.5617-00	-.5081-00	.9791-00	.5905-00
2.00	.4000-00	-.4874-00	.1009+01	.6057-00
2.50	.3105-00	-.4378-00	.1078+01	.6079-00
3.00	.2559-00	-.3928-00	.1165+01	.5958-00
3.50	.2219-00	-.3604-00	.1239+01	.5749-00
4.00	.1960-00	-.3382-00	.1283+01	.5534-00
4.50	.1727-00	-.3218-00	.1295+01	.5361-00
5.00	.1505-00	-.3076-00	.1284+01	.5247-00
5.50	.1297-00	-.2933-00	.1261+01	.5184-00
6.00	.1116+00	-.2768-00	.1238+01	.5153-00
6.50	.9629-01	-.2643-00	.1217+01	.5138-00
7.00	.8344-01	-.2506-00	.1196+01	.5132-00
7.50	.7254-01	-.2376-00	.1175+01	.5132-00
8.00	.6325-01	-.2254-00	.1154+01	.5141-00

TABLE 3.3 CONTINUED

CASE 1c

$\gamma^2 = 0.00$

$\lambda_1^2 = 1.00$

$\lambda_2^2 = 2.50$

$\Psi_H = 1.132$

FREQUENCY	F	G	K	C
.50	.9532-00	-.2582-00	.9774-00	.5296-00
1.00	.8251-00	-.4735-00	.9117-00	.5232-00
1.50	.6501-00	-.6171-00	.8091-00	.5120-00
2.00	.4692-00	-.6880-00	.6766-00	.4961-00
2.50	.3065-00	-.7055-00	.5204-00	.4760-00
3.00	.1754-00	-.6906-00	.3455-00	.4534-00
3.50	.6947-01	-.6571-00	.1591-00	.4300-00
4.00	-.1144-01	-.6142-00	-.3033-01	.4069-00
4.50	-.7025-01	-.5695-00	-.2133-00	.3843-00
5.00	-.1123+00	-.5292-00	-.3837-00	.3617-00
5.50	-.1441-00	-.4953-00	-.5414-00	.3385-00
6.00	-.1704-00	-.4669-00	-.6900-00	.3150-00
6.50	-.1938-00	-.4414-00	-.8338-00	.2922-00
7.00	-.2141-00	-.4172-00	-.9738-00	.2710-00
7.50	-.2308-00	-.3938-00	-.1108+01	.2520-00
8.00	-.2438-00	-.3723-00	-.1231+01	.2350-00

CASE 2c

$\gamma^2 = 0.25$

$\lambda_1^2 = 1.00$

$\lambda_2^2 = 2.50$

$\Psi_H = 1.299$

FREQUENCY	F	G	K	C
.50	.9456-00	-.2723-00	.9766-00	.5624-00
1.00	.8001-00	-.4896-00	.9093-00	.5564-00
1.50	.6114-00	-.6211-00	.8049-00	.5451-00
2.00	.4266-00	-.6753-00	.6700-00	.5278-00
2.50	.2741-00	-.6813-00	.5082-00	.5053-00
3.00	.1473-00	-.6611-00	.3211-00	.4804-00
3.50	.4511-01	-.6239-00	.1153+00	.4556-00
4.00	-.3260-01	-.5759-00	-.9799-01	.4327-00
4.50	-.8622-01	-.5258-00	-.3037-00	.4116-00
5.00	-.1213+00	-.4818-00	-.4913-00	.3904-00
5.50	-.1461-00	-.4468-00	-.6611-00	.3676-00
6.00	-.1667-00	-.4188-00	-.8206-00	.3435-00
6.50	-.1855-00	-.3942-00	-.9773-00	.3195-00
7.00	-.2019-00	-.3708-00	-.1133+01	.2972-00
7.50	-.2148-00	-.3484-00	-.1282+01	.2773-00
8.00	-.2241-00	-.3284-00	-.1418+01	.2597-00

TABLE 3.3 CONTINUED

## CASE 3c

$\gamma^2 = 0.333$

$\lambda_1^2 = 1.00$

$\lambda_2^2 = 2.50$

$\Psi_H = 1.382$

FREQUENCY	F	G	K	C
.50	.9401-00	-.2823-00	.9758-00	.5860-00
1.00	.7824-00	-.5010-00	.9064-00	.5805-00
1.50	.5843-00	-.6237-00	.7999-00	.5693-00
2.00	.4007-00	-.6663-00	.6629-00	.5511-00
2.50	.2508-00	-.6643-00	.4974-00	.5270-00
3.00	.1294-00	-.6401-00	.3033-00	.5003-00
3.50	.3144-01	-.6007-00	.8690-01	.4744-00
4.00	-.4237-01	-.5507-00	-.1389-00	.4513-00
4.50	-.9158-01	-.4993-00	-.3554-00	.4306-00
5.00	-.1222+00	-.4555-00	-.5494-00	.4096-00
5.50	-.1435-00	-.4218-00	-.7229-00	.3864-00
6.00	-.1617-00	-.3954-00	-.8860-00	.3611-00
6.50	-.1768-00	-.3723-00	-.1048+01	.3358-00
7.00	-.1941-00	-.3500-00	-.1212+01	.3122-00
7.50	-.2059-00	-.3285-00	-.1370+01	.2914-00
8.00	-.2142-00	-.3093-00	-.1513+01	.2731-00

## CASE 4c

$\gamma^2 = 0.50$

$\lambda_1^2 = 1.00$

$\lambda_2^2 = 2.50$

$\Psi_H = 1.632$

FREQUENCY	F	G	K	C
.50	.9195-00	-.3157-00	.9729-00	.6680-00
1.00	.7166-00	-.5330-00	.8978-00	.6658-00
1.50	.4954-00	-.6189-00	.7883-00	.6565-00
2.00	.3194-00	-.6226-00	.6523-00	.6357-00
2.50	.1920-00	-.5996-00	.4843-00	.6050-00
3.00	.9146-01	-.5691-00	.2753-00	.5710-00
3.50	.8354-02	-.5294-00	.2980-01	.5396-00
4.00	-.5433-01	-.4796-00	-.2332-00	.5146-00
4.50	-.9292-01	-.4292-00	-.4819-00	.4946-00
5.00	-.1140+00	-.3887-00	-.6947-00	.4738-00
5.50	-.1265-00	-.3599-00	-.8801-00	.4480-00
6.00	-.1427-00	-.3382-00	-.1059+01	.4184-00
6.50	-.1574-00	-.3184-00	-.1247+01	.3883-00
7.00	-.1704-00	-.2980-00	-.1446+01	.3612-00
7.50	-.1793-00	-.2781-00	-.1638+01	.3386-00
8.00	-.1846-00	-.2611-00	-.1805+01	.3192-00

TABLE 3.3 CONTINUED

## CASE 5c

$\gamma^2 = 0.00$

$\lambda_1^2 = 1.50$

$\lambda_2^2 = 2.50$

$\Psi_H = 1.073$

FREQUENCY	F	G	K	C
.50	.9543-00	-.2576-00	.9767-00	.5274-00
1.00	.8285-00	-.4740-00	.9093-00	.5203-00
1.50	.6550-00	-.6210-00	.8041-00	.5082-00
2.00	.4735-00	-.6955-00	.6688-00	.4912-00
2.50	.3111-00	-.7156-00	.5109-00	.4701-00
3.00	.1704-00	-.7022-00	.3365-00	.4465-00
3.50	.6941-01	-.6700-00	.1530-00	.4219-00
4.00	-.1242-01	-.6287-00	-.3141-01	.3975-00
4.50	-.7286-01	-.5859-00	-.2085-00	.3736-00
5.00	-.1107+00	-.5470-00	-.3730-00	.3497-00
5.50	-.1507-00	-.5141-00	-.5250-00	.3257-00
6.00	-.1791-00	-.4860-00	-.6675-00	.3019-00
6.50	-.2043-00	-.4608-00	-.8042-00	.2790-00
7.00	-.2264-00	-.4365-00	-.9364-00	.2579-00
7.50	-.2448-00	-.4130-00	-.1062+01	.2389-00
8.00	-.2593-00	-.3909-00	-.1178+01	.2221-00

## CASE 6c

$\gamma^2 = 0.25$

$\lambda_1^2 = 1.50$

$\lambda_2^2 = 2.50$

$\Psi_H = 1.279$

FREQUENCY	F	G	K	C
.50	.9454-00	-.2723-00	.9767-00	.5626-00
1.00	.8000-00	-.4893-00	.9097-00	.5564-00
1.50	.6119-00	-.6202-00	.8061-00	.5447-00
2.00	.4305-00	-.6745-00	.6724-00	.5267-00
2.50	.2772-00	-.6818-00	.5118-00	.5034-00
3.00	.1510-00	-.6634-00	.3261-00	.4777-00
3.50	.4822-01	-.6282-00	.1215+00	.4521-00
4.00	-.3079-01	-.5815-00	-.9081-01	.4287-00
4.50	-.8584-01	-.5320-00	-.2956-00	.4071-00
5.00	-.1221+00	-.4881-00	-.4822-00	.3856-00
5.50	-.1478-00	-.4530-00	-.6509-00	.3627-00
6.00	-.1692-00	-.4248-00	-.8092-00	.3386-00
6.50	-.1866-00	-.4000-00	-.9644-00	.3147-00
7.00	-.2055-00	-.3762-00	-.1118+01	.2925-00
7.50	-.2166-00	-.3535-00	-.1266+01	.2728-00
8.00	-.2262-00	-.3332-00	-.1399+01	.2554-00



TABLE 3.3 CONTINUED

## CASE 7c

$\gamma^2 = 0.333$

$\lambda_1^2 = 1.50$

$\lambda_2^2 = 2.50$

$\Psi_H = 1.389$

FREQUENCY	F	G	K	C
.50	.9375-00	-.2862-00	.9757-00	.5957-00
1.00	.7746-00	-.5042-00	.9068-00	.5903-00
1.50	.5742-00	-.6218-00	.8016-00	.5787-00
2.00	.3931-00	-.6596-00	.6668-00	.5593-00
2.50	.2475-00	-.6565-00	.5029-00	.5335-00
3.00	.1290-00	-.6337-00	.3085-00	.5051-00
3.50	.3186-01	-.5963-00	.8935-01	.4778-00
4.00	-.4235-01	-.5473-00	-.1406-00	.4541-00
4.50	-.9189-01	-.4959-00	-.3606-00	.4333-00
5.00	-.1219+00	-.4520-00	-.5561-00	.4125-00
5.50	-.1427-00	-.4187-00	-.7295-00	.3891-00
6.00	-.1608-00	-.3928-00	-.8926-00	.3635-00
6.50	-.1700-00	-.3700-00	-.1056+01	.3377-00
7.00	-.1934-00	-.3477-00	-.1221+01	.3136-00
7.50	-.2051-00	-.3262-00	-.1381+01	.2930-00
8.00	-.2131-00	-.3072-00	-.1525+01	.2747-00

## CASE 8c

$\gamma^2 = 0.50$

$\lambda_1^2 = 1.50$

$\lambda_2^2 = 2.50$

$\Psi_H = 1.822$

FREQUENCY	F	G	K	C
.50	.8971-00	-.3474-00	.9693-00	.7508-00
1.00	.6552-00	-.5555-00	.8880-00	.7529-00
1.50	.4200-00	-.6021-00	.7794-00	.7448-00
2.00	.2625-00	-.5779-00	.6516-00	.7172-00
2.50	.1579-00	-.5480-00	.4856-00	.6740-00
3.00	.7206-01	-.5212-00	.2603-00	.6275-00
3.50	-.4593-02	-.4863-00	-.1942-01	.5875-00
4.00	-.6376-01	-.4375-00	-.3262-00	.5595-00
4.50	-.9679-01	-.3869-00	-.6085-00	.5405-00
5.00	-.1119+00	-.3487-00	-.8341-00	.5200-00
5.50	-.1226+00	-.3237-00	-.1024+01	.4912-00
6.00	-.1350-00	-.3053-00	-.1212+01	.4566-00
6.50	-.1490-00	-.2874-00	-.1422+01	.4219-00
7.00	-.1610-00	-.2678-00	-.1649+01	.3919-00
7.50	-.1678-00	-.2487-00	-.1865+01	.3685-00
8.00	-.1710-00	-.2336-00	-.2040+01	.3484-00

TABLE 3.3 CONTINUED

CASE 9c

$\gamma^2 = 0.00$

$\lambda_1^2 = 2.00$

$\lambda_2^2 = 2.50$

$\psi_H = 1.043$

FREQUENCY	F	G	K	C
.50	.9553-00	-.2552-00	.9771-00	.5220-00
1.00	.8319-00	-.4705-00	.9107-00	.5151-00
1.50	.6606-00	-.6183-00	.8070-00	.5035-00
2.00	.4801-00	-.6944-00	.6736-00	.4872-00
2.50	.3177-00	-.7155-00	.5183-00	.4670-00
3.00	.1851-00	-.7026-00	.3474-00	.4442-00
3.50	.7677-01	-.6710-00	.1683-00	.4203-00
4.00	-.4497-02	-.6309-00	-.1130-01	.3962-00
4.50	-.6469-01	-.5897-00	-.1838-00	.3724-00
5.00	-.1092+00	-.5522-00	-.3447-00	.3485-00
5.50	-.1440-00	-.5204-00	-.4941-00	.3245-00
6.00	-.1734-00	-.4931-00	-.6345-00	.3008-00
6.50	-.1994-00	-.4685-00	-.7693-00	.2780-00
7.00	-.2225-00	-.4448-00	-.8997-00	.2569-00
7.50	-.2419-00	-.4216-00	-.1024+01	.2379-00
8.00	-.2575-00	-.3996-00	-.1139+01	.2211-00

CASE 10c

$\gamma^2 = 0.25$

$\lambda_1^2 = 2.00$

$\lambda_2^2 = 2.50$

$\psi_H = 1.278$

FREQUENCY	F	G	K	C
.50	.9447-00	-.2730-00	.9770-00	.5646-00
1.00	.7978-00	-.4892-00	.9110-00	.5586-00
1.50	.6093-00	-.6179-00	.8091-00	.5470-00
2.00	.4294-00	-.6703-00	.6777-00	.5289-00
2.50	.2784-00	-.6771-00	.5195-00	.5053-00
3.00	.1539-00	-.6596-00	.3354-00	.4793-00
3.50	.5183-01	-.6257-00	.1315-00	.4535-00
4.00	-.2724-01	-.5800-00	-.8081-01	.4301-00
4.50	-.8255-01	-.5310-00	-.2859-00	.4086-00
5.00	-.1189+00	-.4874-00	-.4726-00	.3873-00
5.50	-.1448-00	-.4525-00	-.6416-00	.3644-00
6.00	-.1664-00	-.4245-00	-.8004-00	.3403-00
6.50	-.1860-00	-.3997-00	-.9568-00	.3164-00
7.00	-.2031-00	-.3759-00	-.1112+01	.2942-00
7.50	-.2163-00	-.3531-00	-.1261+01	.2745-00
8.00	-.2258-00	-.3328-00	-.1396+01	.2572-00

TABLE 3.3 CONTINUED

CASE 11c

 $\gamma^2 = 0.333$  $\lambda_1^2 = 2.00$  $\lambda_2^2 = 2.50$  $\Psi_H = 1.437$ 

FREQUENCY	F	G	K	C
.50	.9328-00	-.2928-00	.9758-00	.6127-00
1.00	.7603-00	-.5094-00	.9078-00	.6081-00
1.50	.5553-00	-.6173-00	.8055-00	.5970-00
2.00	.3779-00	-.6457-00	.6750-00	.5768-00
2.50	.2392-00	-.6387-00	.5143-00	.5492-00
3.00	.1263-00	-.6163-00	.3192-00	.5191-00
3.50	.3205-01	-.5804-00	.9487-01	.4908-00
4.00	-.4074-01	-.5320-00	-.1431-00	.4672-00
4.50	-.8843-01	-.4806-00	-.3704-00	.4473-00
5.00	-.1166+00	-.4371-00	-.5698-00	.4271-00
5.50	-.1359-00	-.4048-00	-.7453-00	.4037-00
6.00	-.1530-00	-.3800-00	-.9118-00	.3774-00
6.50	-.1698-00	-.3580-00	-.1081+01	.3508-00
7.00	-.1647-00	-.3362-00	-.1255+01	.3264-00
7.50	-.1958-00	-.3150-00	-.1423+01	.3053-00
8.00	-.2032-00	-.2964-00	-.1573+01	.2869-00

CASE 12c

 $\gamma^2 = 0.00$  $\lambda_1^2 = 3.00$  $\lambda_2^2 = 2.50$  $\Psi_H = 0.998$ 

FREQUENCY	F	G	K	C
.50	.9562-00	-.2535-00	.9771-00	.5181-00
1.00	.8350-00	-.4688-00	.9106-00	.5112-00
1.50	.6653-00	-.6182-00	.8067-00	.4997-00
2.00	.4847-00	-.6963-00	.6734-00	.4837-00
2.50	.3213-00	-.7183-00	.5190-00	.4640-00
3.00	.1865-00	-.7052-00	.3505-00	.4418-00
3.50	.8079-01	-.6737-00	.1755-00	.4181-00
4.00	.5126-03	-.6345-00	.1273-02	.3940-00
4.50	-.5918-01	-.5949-00	-.1656-00	.3699-00
5.00	-.1040+00	-.5593-00	-.3212-00	.3457-00
5.50	-.1394-00	-.5289-00	-.4660-00	.3214-00
6.00	-.1696-00	-.5029-00	-.6020-00	.2975-00
6.50	-.1966-00	-.4794-00	-.7322-00	.2747-00
7.00	-.2207-00	-.4567-00	-.8578-00	.2536-00
7.50	-.2415-00	-.4344-00	-.9776-00	.2344-00
8.00	-.2586-00	-.4130-00	-.1089+01	.2174-00

TABLE 3.3 CONTINUED

## CASE 13c

$\gamma^2 = 0.25$

$\lambda_1^2 = 3.00$

$\lambda_2^2 = 2.50$

$\psi_H = 1.315$

FREQUENCY	F	G	K	C
.50	.9403-00	-.2796-00	.9771-00	.5810-00
1.00	.7842-00	-.4950-00	.9119-00	.5755-00
1.50	.5904-00	-.6150-00	.8124-00	.5641-00
2.00	.4131-00	-.6578-00	.6846-00	.5451-00
2.50	.2687-00	-.6600-00	.5291-00	.5199-00
3.00	.1499-00	-.6422-00	.3447-00	.4922-00
3.50	.5119-01	-.6097-00	.1367-00	.4653-00
4.00	-.2621-01	-.5649-00	-.8197-01	.4416-00
4.50	-.7988-01	-.5160-00	-.2930-00	.4206-00
5.00	-.1144+00	-.4729-00	-.4831-00	.3996-00
5.50	-.1387-00	-.4391-00	-.6540-00	.3765-00
6.00	-.1593-00	-.4123-00	-.8156-00	.3517-00
6.50	-.1786-00	-.3884-00	-.9771-00	.3270-00
7.00	-.1954-00	-.3651-00	-.1140+01	.3042-00
7.50	-.2081-00	-.3425-00	-.1296+01	.2843-00
8.00	-.2169-00	-.3225-00	-.1436+01	.2668-00

## CASE 14c

$\gamma^2 = 0.00$

$\lambda_1^2 = 4.00$

$\lambda_2^2 = 2.50$

$\psi_H = 0.996$

FREQUENCY	F	G	K	C
.50	.9567-00	-.2532-00	.9768-00	.5171-00
1.00	.8364-00	-.4690-00	.9096-00	.5101-00
1.50	.6669-00	-.6198-00	.8045-00	.4985-00
2.00	.4855-00	-.6992-00	.6701-00	.4825-00
2.50	.3209 00	-.7213-00	.5149-00	.4629-00
3.00	.1855-00	-.7077-00	.3467-00	.4407-00
3.50	.8022-01	-.6756-00	.1733-00	.4170-00
4.00	.7602-03	-.6365-00	.1876-02	.3927-00
4.50	-.5829-01	-.5977-00	-.1616-00	.3683-00
5.00	-.1028-00	-.5630-00	-.3139-00	.3438-00
5.50	-.1384-00	-.5336-00	-.4554-00	.3193-00
6.00	-.1587-00	-.5084-00	-.5879-00	.2953-00
6.50	-.1960-00	-.4858-00	-.7143-00	.2724-00
7.00	-.2206-00	-.4640-00	-.8356-00	.2511-00
7.50	-.2420-00	-.4426-00	-.9512-00	.2319-00
8.00	-.2601-00	-.4218-00	-.1059+01	.2147-00

APPENDIX C  
EXAMPLES OF DESIGN CALCULATIONS

The purpose of this appendix is to provide several examples indicating the procedure to determine the amplitude of vibration of a foundation subjected to harmonic forces. This will include an example where the soil properties coincide with one of the cases from Table 2.2 and the mass ratio with one of the values considered in Chapter 5 and so the curves from Chapter 5 are directly applicable. Examples will also be presented where the impedance coefficients are determined by using the results of an equivalent isotropic soil (having the same  $\gamma^2$  as the anisotropic soil) and the anisotropy is accounted for by using the correct expression for the static stiffness, as explained in Chapter 5.

C.1 VERTICAL VIBRATION PROBLEM

Consider a machine foundation, five feet in diameter ( $r_0 = 2.5$  feet) which has a total weight,  $W$  of 22500 lbs. This includes the dead weight of the machine and the concrete footing. Operation of the machine results in an unbalanced force with an amplitude of 5000 lbs. The soil underlying the foundation has the following properties:

$$C_{rr} = 24000 \text{ psi}$$

$$G = 6000 \text{ psi } (\gamma^2 = 1/4)$$

$$C_{zz} = 8000 \text{ psi } (\lambda_1^2 = 3.0)$$

$$\gamma_s = 120 \text{ pcf (soil unit weight)}$$

Determine the maximum amplitude of vibration and the frequency at which it occurs.

The factor  $\psi_v$  is first calculated from eqn. 3.11.

$$\psi_v = - \frac{\lambda_1(\phi - 2)}{\phi(1 - \lambda_1)} = \frac{-1.732(4.0 - 2)}{4.0(1 - 1.7321)} = 1.1831$$

where  $\phi$  was obtained from Table 2.2, since we note the soil properties above correspond to material case 13. The dimensionless mass ratio is now determined from eqn. 5.15a

$$B_v = \frac{\psi_v}{4} \frac{M}{\rho r_o^3} = \frac{1.183}{4} \frac{22500/386.4}{(120/386.4)(2.5)^3} = 3.549$$

Neglecting material damping, we obtain from Figure 5.16 a maximum dynamic magnification factor of 2.54 at a dimensionless frequency of 0.47. The circular frequency is then found from

$$\omega = a_o \frac{c_2}{r_o}$$

where  $c_2$  is the shear wave velocity in the distorted coordinate system,

$$c_2 = G/\rho = 6000 \times 144 \times 32.2/120 = 481 \text{ ft./sec}$$

thus  $\omega = 0.47 \cdot \frac{481}{2.5} = 90.8$  rad/sec (14.5 cps).

To determine the amplitude of vibration we also need the static stiffness from eqn. 3.19

$$K_v = \frac{4Gr_D}{\psi_v} = \frac{4 \times 6000 \times 2.5 \times 12}{1.183} = 608,622 \text{ lbs/in.}$$

Now from the definition of the DMF, eqn. 5.14,

$$\text{DMF} = \left| \frac{\Delta}{P/K} \right| = 2.54$$

where P is the unbalanced force. Thus

$$\Delta = \frac{5000}{608672} \times 2.54 = 0.0209 \text{ in.}$$

This vibration amplitude would now be compared with the acceptable criteria to determine if the foundation design is adequate.

## C.2 VERTICAL SINGLE - CYLINDER COMPRESSOR

This example is taken with slight modification, from page 360 of Richart et al., ref (25). A vertical single cylinder compressor develops periodic forces which can produce a vertical motion of the machine and its foundation block. The weight of the compressor plus the motor is 10,900 lbs. and it develops a periodic force of 11,400 lbs. at 450 rpm. The compressor is to be supported on a foundation resting on a silty clay with a shear wave velocity of 806 ft/sec. and a unit weight of 100 pcf. Thus G is

14000 psi. Poisson's ratio is 1/3. The maximum acceptable amplitude of vibration is 0.0021 in.

For initial sizing purposes, set the radius of the footing to yield a static displacement of 0.0021 in. when subjected to a force of 11400 lbs. Thus

$$\Delta = \frac{(1 - \nu)P}{4Gr_0} = 0.0021 = \frac{.667 \times 11400}{4 \times 14000 \times r_0}$$

or  $r_0 = 67.9 \text{ in} = 5.66 \text{ ft.}$

Use  $r_0 = 6.0 \text{ ft.}$

Richart et al. uses an equivalent SDOF representation for the machine-foundation-soil system where the mass is the total mass of the machine and foundation, the stiffness is the static stiffness of the soil and the percent critical damping (for vertical vibrations) is found from

$$\beta = \frac{0.425}{B_v}$$

This expression can be derived from eqn. 5.11 herein, by assuming a constant value for  $c$  of 0.85 and ignoring the virtual mass ratio,  $B_v^*$ .

Assuming a 3ft. thick foundation, the weight of the foundation is

$$W_f = \pi (6)^2 (3)(150) = 50,893 \text{ lbs.}$$



The total oscillating weight is

$$W = 50,893 + 10,900 = 61,793 \text{ lbs.}$$

The dimensionless mass ratio is then

$$B_v = \frac{(1 - \nu)}{4} \frac{M}{Pr_o^3} = \frac{(.667)}{4} \frac{61793/386.4}{(100/386.4)(6)^3} = 0.4768$$

The damping ratio is

$$\beta = \frac{.425}{B_v} = \frac{.425}{.4768} = 0.6155$$

To determine the material frequency, we first need the spring stiffness

$$K_v = \frac{4Gr_o}{1 - \nu} = \frac{4 \times 14000 \times 72}{.667} = 6.048(10)^6 \text{ lbs/in.}$$

Thus

$$\omega_n = \sqrt{\frac{K_v}{M}} = \sqrt{\frac{6.048(10)^6 (386.4)}{61793}} = 194.5$$

$$\text{therefore } f_n = \frac{\omega_n}{2\pi} = 30.95 \text{ cps}$$

The operating frequency is

$$f = 450 \text{ rpm} = 7.5 \text{ cps}$$

$$\text{or } \omega = 2\pi f = 47.12 ; \omega/\omega_n = .242$$

The DMF is from eqn. (5.14)

$$DMF = \frac{1}{[1 - (\omega/\omega_n)^2]^2 - 4\beta^2(\omega/\omega_n)^2}$$

$$DMF = \frac{1}{[1 - (.242)^2]^2 - 4(.6155)^2(.242)^2} = 1.1197$$

or  $\frac{\Delta}{P/K_v}$

$$\Delta = \frac{11400}{6.048(10)^6} = 0.0021$$

This is equal to the allowable value and therefore the motion satisfies the criterion.

The problem will now be repeated for an anisotropic soil. For comparison purposes assume the shear modulus,  $G$  is the same and the value of  $\gamma^2$  is the same ( $\gamma^2 = 1/4$  for Poisson's ratio of  $1/3$ ). Take  $\lambda_1^2 = 2.0$  thus

$$C_{rr} = G/\gamma^2 = 56000 \text{ psi}$$

$$C_{zz} = C_{rr}/\lambda_1^2 = 28000 \text{ psi}$$

Calculate  $\psi_v$

$$\psi_v = -\frac{\lambda_1(\phi - 2)}{\phi(1 - \lambda_1)} = \frac{-1.414(2.73 - 2)}{2.73(1 - 1.414)} = 0.9133$$

The value of  $\phi$  was taken from Table 2.2, case 10. Sizing

the footing again by static considerations,

$$\Delta = \frac{\psi_v P}{4Gr_o} = 0.0021 = \frac{0.9133 \times 11400}{4 \times 14000 \times r_o}$$

or  $r_o = 88.53 \text{ in.} = 7.38 \text{ ft.}$

Use  $r_o = 7.5 \text{ ft.}$

Assume the footing must be 3 ft. thick for simplicity, thus the weight of the foundation block is

$$W_f = \pi(7.5)^2(3)(150) = 79,522 \text{ lbs.}$$

The total oscillating weight is

$$W = 79,522 + 10,900 = 90,422 \text{ lbs.}$$

The dimensionless mass ratio is then

$$B = \frac{\psi_v}{4} \frac{M}{Pr_o^3} = \frac{(.9133)}{4} \frac{90422}{100(7.5)^3} = 0.4894$$

The damping ratio is

$$\beta = \frac{.425}{B_v} = 0.6075$$

The static spring constant is found from

$$K_v = \frac{4Gr_o}{\psi_v} = \frac{4 \times 14000 \times 7.5 \times 12}{.9133} = 5.518(10)^6 \frac{\text{lbs}}{\text{in.}}$$

Then 
$$\omega_n = \sqrt{\frac{K_v}{M}} = \sqrt{\frac{5.518(10)^6 (386.4)}{90422}} = 153.56 \frac{\text{rad.}}{\text{sec.}}$$

therefore  $f_n = \frac{\omega_n}{2\pi} = 24.4 \text{ cps.}$

Recall the operating frequency is

$$\omega = 47.12 \text{ rad/sec., therefore}$$

$$\omega/\omega_n = 0.307$$

The DMF is

$$\text{DMF} = \frac{1}{[1 - (.307)^2]^2 - 4(.6075)^2(.307)^2} = 1.212$$

or  $\frac{\Delta}{P/K_v} = 1.212$

$$\Delta = \frac{11400 \times 1.212}{5.518(10)^6} = 0.0025 > 0.0021$$

Thus the design is inadequate.

Repeating the computations above using  $r_0 = 10.0 \text{ ft.}$  yields:

$$W_f = 141,372 \text{ lbs.}$$

$$W = 152,272 \text{ lbs.}$$

$$B_v = 0.3477$$

$$\beta = 0.7208$$

$$K_v = 7.357(10)^6 \text{ lbs/in.}$$

$$\omega_n = 136.64 \text{ rad/sec.}$$

$$\omega/\omega_n = 0.3449$$

$$\text{DMF} = 1.3748$$

$$\Delta = 0.0021 = \text{the design allowable,}$$

OK.

Thus for the vertical vibration problem considered here, where the anisotropy can be measured by  $\lambda_1$ , a significant difference is noted between the isotropic and anisotropic designs.

### C.3 ROCKING OF A RADAR TOWER

This example is again taken from Richart et al., ref (25), page 376. The rotation of a certain radar antenna induces transient pulses in the tower which may cause the tower to rock at its natural frequency because of the flexible connection to the soil. The tower is considered rigid. The supporting soil has a shear modulus,  $G = 20,000$  psi, and if considered isotropic, a Poisson's ratio of  $1/3$ , and a unit weight,  $\gamma_s$  of 100 pcf. The foundation diameter is 60 ft. and the mass moment of inertia of the entire system about a diameter through the base is  $I = 80.545(10)^6 \text{ lb-ft-sec}^2$ . Consider a constant moment excitation of  $P_M = 212,000 \text{ ft-lbs}$ .

Determine the amplitude of vibration for this system for several degrees of anisotropy (as measured

again by  $\lambda_1$ ). The value of  $\gamma^2$  will be taken as 1/4 in all cases (in the isotropic case this is equivalent to a Poisson's ratio of 1/3).

The following formulas will be required.

Mass ratio:

$$B_R = \frac{3\psi_v}{8} \frac{I}{\rho r_o^5} \text{ anisotropic}$$

$$B_R = \frac{3(1 - \nu)}{8} \frac{I}{\rho r_o^5} \text{ isotropic}$$

Percent damping (from references 2 and 25):

$$\beta = \frac{0.15}{(1 + B_R)\sqrt{B_R}}$$

Static stiffness:

$$K_R = \frac{8Gr_o^3}{3\psi_v} \text{ anisotropic}$$

$$K_R = \frac{8Gr_o^3}{3(1 - \nu)} \text{ isotropic}$$

Natural frequency:

$$f_n = \frac{1}{2\pi} \sqrt{\frac{K_R}{I}}$$

Frequency for max. amplitude (25):

$$f_{max} = f_n \sqrt{1 - 2\beta^2}$$

Maximum amplitude of vibration (25):

$$\Delta = \frac{P_M}{K_R} \frac{1}{2\beta \sqrt{1 - \beta^2}}$$

With the given data and the above formulas the following table is easily prepared.

TABLE C.1  
Results for Sample Problem C.3

	isotropic $\nu = 0$	$\lambda_1^2 = 1.5$	$\lambda_1^2 = 2.0$	$\lambda_1^2 = 3.0$
$B_R$	.2665	.3165	.365	.4729
$\beta$	.2294	.2025	.1819	.1481
$K_R = \frac{ft - K}{rad.}$	$3.11(10)^8$	$2.619(10)^8$	$2.27(10)^8$	$1.75(10)^8$
$f_n, cps.$	9.89	9.08	8.45	7.42
$f_{max}, cps.$	9.355	8.7	8.17	7.26
$\Delta, rad.$	$1.526(10)^{-6}$	$2.041(10)^{-6}$	$2.61(10)^{-6}$	$4.135(10)^{-6}$

As the anisotropy increases, the mass ratio  $B_R$  increases and the radiation damping  $\beta$  decreases which leads to a significant increase in the amplitude of the response. The acceptable rocking amplitude for radar towers is approximately  $5(10)^{-5}$  rad. and so all the cases shown in Table C.1 would be satisfactory. However, for certain designs the degree of anisotropy could be the determining factor.



## LIST OF REFERENCES

- 1) Supplement to the (Draft for Trial Use and Comment) Manual of Engr. Practice in Structural Analysis and Design of Nuclear Plant Facilities, Ad Hoc Group on Soil-Structure Interaction, Nuclear Structures and Materials Committee of the Structural Division of the American Society of Civil Engineers.
- 2) Saada, H. S., Bianchini, G. F., Shook, L., "The Dynamic Response of Normally Consolidated Anisotropic Clay", Proc. of the ASCE Geotechnical Engr. Div. Specialty Conf. on Earthquake Engr. and Soil Dynamics, Pasadena, CA, June, 1978.
- 3) Salamon, M.D.G., "Elastic Moduli for a Stratified Rock Mass", Int. Jnl. Rock Mech. Min. Sci., 5, pp. 519-527, 1968.
- 4) Wardle, L. J., and Gerrard, C. M., "The Equivalent Anisotropic Properties of Layered Rock and Soil Masses", C.S.I.R.O. Aust., Unpubl. Rept.
- 5) Brekhovskikh, L. M., "Waves in Layered Media", Academic Press, New York, 1960.
- 6) Lysmer, J., Seed, H.B., Udaka, T., Hwang, R. N., Tsai, C. F., "Efficient Finite Element Analysis of Seismic Structure-Soil-Structure Interaction", Report No. EERC 75-34, Nov. 1975, Univ. of Cal., Berkeley.
- 7) Waas, G., "Linear Two-Dimensional Analysis of Soil Dynamics Problems in Semi-infinite Layered Media", Ph.D. dissertation, Univ. of Cal., Berkeley, 1972.
- 8) Kausel, E., "Forced Vibrations of Circular Foundations on Layered Media", Ph.D. dissertation, Massachusetts Institute of Technology, 1974.
- 9) Gazetas, G., "Dynamic Stiffness Functions of Strip and Rectangular Footings on Layered Media", M. S. thesis, Mass. Inst. of Tech., 1975.
- 10) Wong, H.L., Luco, J. E., "Dynamic Response of Rigid Foundations of Arbitrary Shape", Earthquake Engineering and Structural Dynamics, Vol. 4, pp. 579-587 (1976).

- 11) Dasgupta, G., Chopra, A.K., "Dynamic Stiffness Matrices for Homogeneous Viscoelastic Halfplanes", Report No. UCB/EERC - 77/26, Nov. 1977, Univ. of Cal. - Berkeley.
- 12) Luco., J. E., Westmann, R. A., "Dynamic Response of Circular Footings", UCLA - ENG - 7113, April 1971, Univ. of Cal. - Los Angeles.
- 13) Veletsos, A. S., Wei, Y. T., "Lateral and Rocking Vibration of Footings", Jnl. of the Soil Mechanics and Foundation Division, American Society of Civil Engineers, SM9, Sept. 1971.
- 14) Wei, Y. T., "Steady State Response of Certain Foundation Systems", Ph.D. dissertation Rice University, 1971.
- 15) Kashio, J., "Steady State Response of a Circular Disc Resting on a Layered Medium", Ph.D. dissertation Rice University, 1970.
- 16) Luco., J. E., "Impedance Functions for a Rigid Foundation on a Layered Medium", Nuclear Engineering and Design 31, 1974, pp. 204 - 217.
- 17) Luco., J. E., "Vibrations of a Rigid Disc on a Layered Viscoelastic Medium", Nuclear Engineering and Design 36, 1976, pp. 325 - 340.
- 18) Karasudhi, P., Keer, L. M., and Lee, S. L., "Vibratory Motion of a Body on an Elastic HalfPlane", Jnl. of Applied Mechanics, Vo. 35, Series E. No. 4, Dec. 1968, pp. 697 - 705.
- 19) Reissner, E., "Stationare, axial symmetrische durch eine SchutteInde Mass erregte Schwingungen eines homogeneous elastischen Halbraumes", Ingenieur-Archiv, Vol. 7, December, 1936, pp. 381-396.
- 20) Lamb, H., "On the Propagation of Tremors over the Surface of an Elastic Solid", Philosophical Transactions of the Royal Society of London, Ser. A, Vol. 203, pp. 1-42.
- 21) Sung, T. Y., "Vibrations in Semi-Infinite Solids due to Periodic Surface Loadings", Symposium on the Dynamic Testing of Soils, ASTM-STP No. 156, pp. 35-64, 1953.

- 22) Quinlan, P. M., "The Elastic Theory of Soil Dynamics", Symposium on the Dynamic Testing of Soils, ASTM-STP, No. 156, pp. 35-64, 1953.
- 23) Bycroft, G. N., "Forced Vibrations of a Rigid Circular Footing on a Semi-infinite Elastic Space and on an Elastic Stratum", Philosophical Transactions of the Royal Society of London, Vol. 248, Ser. A, No. 948, January, 1956.
- 24) Parmalee, R. A., Perelman, D. S., Lee, S. L., and Keer, L. M., "Seismic Response of Structure-Foundation Systems", Jnl. of Engineering Mechanics, ASCE, Vol. 94, No. EMG, Dec. 1968, pp. 1295-1315.
- 25) Richart, F. E., Hall, J. R., and Woods, R. P., "Vibrations of Soils and Foundations", Prentice-Hall, Inc., 1970.
- 26) Robertson, I. A., "Forced Vertical Vibration of a Rigid Circular Disc on a Semi-infinite Elastic Solid", Proceedings of the Cambridge Philosophical Society, Vol. 62, Sec. A, pp. 547-553, 1966.
- 27) Sneddon, I. N., "Mixed Boundary Value Problems in Potential Theory", North-Holland Publishing Co., 1966.
- 28) Gladwell, G.M.L., "Forced Tangential and Rotatory Vibration of a Rigid Circular Disc on a Semi-Infinite Solid", Int'l. Jnl. of Engineering Science, Vol. 6, pp. 591-607, 1968.
- 29) Sezawa, K., "Further Studies on Rayleigh Waves Having Some Azimuthal Distribution", Bull. Earth. Res. Inst., Tokyo, Vol. 6, No. 2, 1929.
- 30) Shah, P. M., "On the Dynamic Response of Foundation Systems", Ph.D. thesis, Rice University, 1968.
- 31) Love, A. E. H., "Treatise on the Mathematical Theory of Elasticity", Dover Press.
- 32) Carrier, G. F., "Propagation of Waves in Orthotropic Media", Quarterly of Applied Mathematics, 4, 1960 pp. 160 - 165.
- 33) Cameron, N. and Eason, G., Quarterly Jnl. of Mechanics and Applied Mathematics, 20, (1967) pp. 23.

- 34) Payton, R. G., "Green's Tensor for a Constrained Transversely Isotropic Elastic Solid", Quarterly Jnl. of Applied Mathematics, Vol. XXVIII, pt. 4, 1975, pp. 473-481.
- 35) Bachelushvili, M. O., "The Basic Solutions of Differential Equations for an Anisotropic Elastic Body" (in Russian), Soobshch. Akad. Nauk. Greg SSR. 19, 4, 393-400, 1957.
- 36) Morse, P. M., and Feshbach, H., "Methods of Theoretical Physics", McGraw-Hill, 1953 Vol. I, II.
- 37) Synge, J. L., "Elastic Waves in Anisotropic Media", Proceedings of the Royal Irish Academy 5.
- 38) Deresiewicz, H., and Mindlin, R. D., "Waves on the Surface of a Crystal", Journal of Applied Physics, Vol 28, No. 6, June 1957, pp. 669-671.
- 39) Stoneley, R., "The Propagation of Surface Waves in Anisotropic Media", in Partial Differential Equations and Continuum Mechanics", University of Wisconsin Press, 92, 1961, pp. 81-93.
- 40) Paulos, H. G. and Davis, E. h., "Elastic Solutions for Soil and Rock Mechanics", Appendix B By Gerrard, C. M., and Harrison, W. J., John Wiley and Sons, Inc.
- 41) Ewing, W. M., Jardetsky, W. S., and Press, F., "Elastic Waves in Layered Media", McGraw-Hill Book Co., 1957.
- 42) Abramovitz, M., and Stegan, I., (ed.), "Handbook of Mathematical Functions with Formulas, Graphs and Mathematical Tables," U. S. Department of Commerce, National Bureau of Standards Applied Mathematical Series, 55, 1964.
- 43) Watson, G. N., "A Treatise on the Theory of Bessel Functions", Cambridge University Press, 1944.
- 44) Bland, D. R., "The Theory of Linear Viscoelasticity Pergamon Press, 1960.
- 45) Veletsos, A. S., and Verbic, B., "Vibration of Viscoelastic Foundations", Earthquake Engineering and Structural Dynamics, Vol. 2, 87-102 (1973).
- 46) Biot, M. A., "Theory of Stress-Strain Relations in Anisotropic Viscoelasticity and Relaxation Phenomena", Journal of Applied Physics, Vol. 25, No. 1 (1954).

- 47) Dobry, R., "Damping in Soils: It's Hysteretic Nature and the Linear Approximation", MIT Research Report R70-14, (1970).

